Computational Investigation of Flow over Gabion Spillways

Zuhaira, Ali A A.

Swansea University
Prifysgol Abertawe

Computational Investigation of Flow over Gabion Spillways

Ali Adel Abdulwahed Zuhaira

Submitted to Swansea University in Fulfilment of the Requirements for the Degree of Doctor of Philosophy in Engineering

Swansea University 2018

Abstract

A spillway is a hydraulic structure that is used to pass high discharges in flood seasons in a controlled way and also to release surplus water that cannot be safely stored in the reservoir to downstream. Stepped spillways and gabion stepped spillways have been used for centuries as an effective and efficient way of dissipating the energy of overflowing water. The steps of the spillway's surface increase its roughness and therefore can generate high turbulence levels. Three main flow regimes can be identified over stepped spillways; namely nappe, transition and skimming flow depending on step size and water discharge. Under skimming flow conditions, the aerated and non-aerated flow regions can be clearly recognised over the chute slope depending on the air content.

Investigation of the hydraulics of skimming flow conditions over gabion stepped spillways have been exclusively experimental to date, and have concentrated on the aerated zone under skimming flow conditions. Our knowledge of the flow properties in the non-aerated flow region over gabion steps is lacking and further research is required to improve the hydraulic structure design. This thesis describes the research undertaken to address this need.

It is primarily a computational study but includes some experimental work for model validation. The numerical code is initially validated against different laboratory experimental data. The results indicated that the numerical code is robust in predicting flow field variables over gabion stepped spillways. The validated code is then applied to different cases of gabion stepped spillways, to explore the behaviour of the skimming flow with various step heights, chute slopes and step shapes. This work provides new insights into the hydraulics of skimming flow conditions in the non-aerated flow region over gabion stepped spillways. The computational results of this study have important implications for designing gabion stepped chutes, such as determining the position of free surface aeration and optimum step configuration.

Declaration and statements

Declaration

This work has not previously been accepted in substance for any degree and is not being concurrently submitted in candidature for any degree.

Signed: . . . . . (candidate)

Date: . . . . . .

Statement 1

This thesis is the result of my own investigations, except where otherwise stated. Where correction services have been used, the extent and nature of the correction is clearly marked in a footnote(s). Other sources are acknowledged by footnotes giving explicit references. A bibliography is appended.

Signed: . . . . . (candidate)

Date: . . . . . .

Statement 2

I hereby give consent for my thesis, if accepted, to be available for photocopying and for inter-library loan, and for the title and summary to be made available to outside organisations.

Signed: . . . . . (candidate)

Date: . . . . . .

Contents

Acknowledgments

I would like to express my special appreciation and thanks to my supervisor Prof. Dominic Reeve, for the patient guidance, encouragement and advice he has provided throughout my time as his student. I have been very fortunate to have a supervisor who cared so much about my work, and who provided such valuable insights and perspectives whilst giving me the freedom to do what I wanted. I would also like to thank Prof. Harshinie Karunarathna for providing fresh observations and recommendations throughout my studies.

I thank our engineering group for all of the motivating discussions, the shared moments of stress, and for all the fun and laughter we have had over the last four years. I would also like to present my appreciation to Dr. Jose Horrillo-Caraballo for his effort during different stages of the work, especially during the experimental work. Many thanks to my friends and colleagues across Swansea University who have supported me and often provided much needed escape from my studies, to help me regain focus.

The scholarship provided by the Higher Committee of Education in Iraq (HCED) is gratefully acknowledged. Without it, I could not have carried out my work.

Further gratitude is due to the academic and administrative staff of the College of Engineering at Swansea University who shared with me their valuable expert advice and supported me in managing various issues throughout the course of this research.

I would like to thank my parents, brothers and sisters for their continuous support and encouragement. I wish I could write a chapter to express my deepest gratitude and appreciation to them; without their continuous love, overwhelming support, unlimited patience and motivational talks this study would not have been possible. I hope one day I can offer them at least a small fraction of what they have offered me throughout all stages of this study. Special thanks go to my uncles, Ridha Al-Zuhairi and Subhi Al-Zuhairi for their supporting during my stay in the United Kingdom. I deeply thank my friends for their love, support and understanding.

List of Figures

List of Tables

List of Symbols

D_{50}	Particle diameter
di	Water depth at the inception point
ε	Turbulence dissipation rate
hs	Step height
k	Turbulence Kinematic Energy
ks	Roughness height measured perpendicular to the pseudo bottom
Li	Length of the non-aerated zone
ls	Step width
P	Porosity of the porous media
v	Eddy Viscosity ($m^2.s^{-1}$)
v_n	Numerical viscosity
v_t	Kinematic Viscosity ($m^2.s^{-1}$)
y	Water depth
Yc	Water depth at the critical section
α	Coefficient of the kinetic energy Parameter
δ	Thickness of the boundary layer (m)
θ	Chute slope (degree)
σ	Cavitation index number
τ_{ij}	Viscous stress
μ	Dynamic viscosity = $1*10^{-3}$ ($N.s/m^2$) for water at 20° C
ρ	Fluid mass density (Kg/m^3)

Other symbols are defined within the text.

Abbreviations

CFD	Computational fluid dynamics
CFL	Courant number
Fr	Froude number
F_*	Roughness Froude number
$F_{*,\theta}$	Modified roughness Froude number
FFT	Fast Fourier Transformation
ICOLD	International commission on large dams
LES	Large eddy simulation
LLS	Laser light sheet
NSE	Navier-Stokes-equation
NSEs	Navier-Stokes equations
NWT	Numerical wave tank
PIV	Particle image velocimetry
RANS	Reynolds-averaged Navier Stokes-equations
RNG	Re-Normalisation Group
SPH	Smoothed particle hydrodynamics
TKE	Turbulent kinetic energy
VOF	Volume of fluid
2D	Two dimensional flow condition
3D	Three dimensional flow condition

Chapter 1 : Introduction

1.1. Hydraulic structures

The essential purpose of hydraulic structures is to modify the natural behaviour of the water body in rivers, lakes and seas by controlling its flow fall. This modification can lead to many economic benefits like generating the electric power and protecting the environment during the flooding seasons (flood control). Many other benefits can be achieved like improved water supply, silt mitigation, navigation, irrigation, draining, fish handling and farming, and ecologic protection as well as the recreational benefits (Chen, 2015).

Hydraulic structures can be either fully or partially submerged structures. These structures can be used for different purposes, such as to divert, disrupt, or stop the natural flow completely. Considering the construction purposes and the feature of actions, hydraulic structures can be divided into three types: water retaining structures, water conveying structures and special-purpose structures (Chen, 2015).

Dams are the archetypal water retaining structures. Dam construction is one of the earliest examples of civil engineering. Water is a vital natural resource; thus the great civilisations considered the control of water as an important parameter. Many aimed to build up a structure that can save water during the rainy seasons in order to use it during drought seasons. The ancient civilisations used basic concepts to construct dams; hence, dam construction was the first investment in such facilities. Some countries such as China, Turkey and India have had high rates of annual completion of dams (Novak et al., 2007).

Saving water is the main aim of dam construction; however, ancient people have used dams for other objectives such as raising water levels for irrigation purposes and controlling flooding during the rainy season (Novak et al., 2007). In the past, dam design

differed from case to case depending on the topography of the location and on the facilities available at the time (Chen, 2015).

1.2. Dam classification

Dams can be classified according to their essential purpose. Some categories include irrigation, water supply, hydroelectric power generation, river regulation and flood control. Classification can also be based on the construction material, whether it is concrete, steel, earth embankment or masonry. Alternatively, dams may be classified by their shape: gravity, arch, buttress, and multiple. Chen (2015) notes that hydraulic characteristics can be used to classify dams: such as overflow dams and non-overflow dams which have been constructed in many places around the world.

Many physical factors can affect the selection process of dams like topography, geology, foundation construction, material available, hydrology, spillway types and earthquakes. Some other factors can be considered such as the economic impact, statutory restriction, benefit-cost relation and appearance. For example, Figure 1.1 shows the Urft dam in Germany which is constructed as a curved gravity dam due to the site topography. The Urft Dam was built between 1900 and 1905. The Urft Dam was also the highest in Europe until the construction of the Bober Dam in the Giant Mountains of Silesia in 1912.

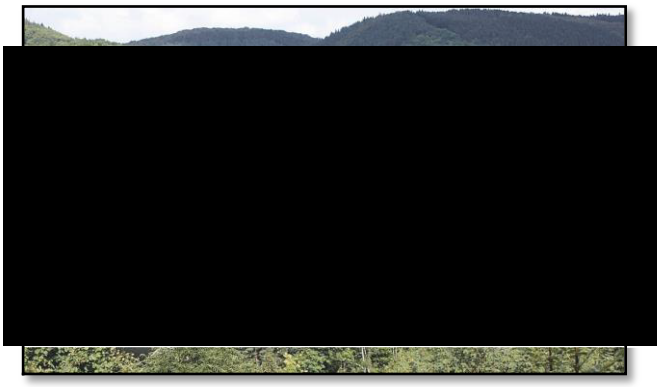

Figure 1.1 Stepped spillway of the Urft dam: Completed in 1905; curved gravity dam with a height of 58.5m; spillway with 33 steps with height h=1.5m (Germany) (Felder and Chanson, 2013).

1.3. Embankment Dams

Embankment dams are constructed by using the natural ground materials which are composed of fragmented particles, graded and compacted, in order to prevent flow through the dam body (i.e. seepage). The friction and the interlocking between the particles can bind the materials all together to resist sliding inside the body and also to give a stable mass without using a cementitious substance, known as a binder, (Chen, 2015). As a generalisation, most modern embankments designs have trapezoidal cross-sections. The top edge of the slope is normally called the crest, while the lowermost edge of the slope is called the toe or heel. Depending on the material which can be used for the construction purposes, embankment dams can be classified into two main types: earth fill dams which can be constructed by compressing fine-grained soils and rockfill dams when coarse-grained materials are used instead of fine-grained materials. Figure 1.2 depicts a rock-filled embankment dam in California in the United States. The dam supplies irrigation water, generates hydropower, controls flooding and has recreational benefits.

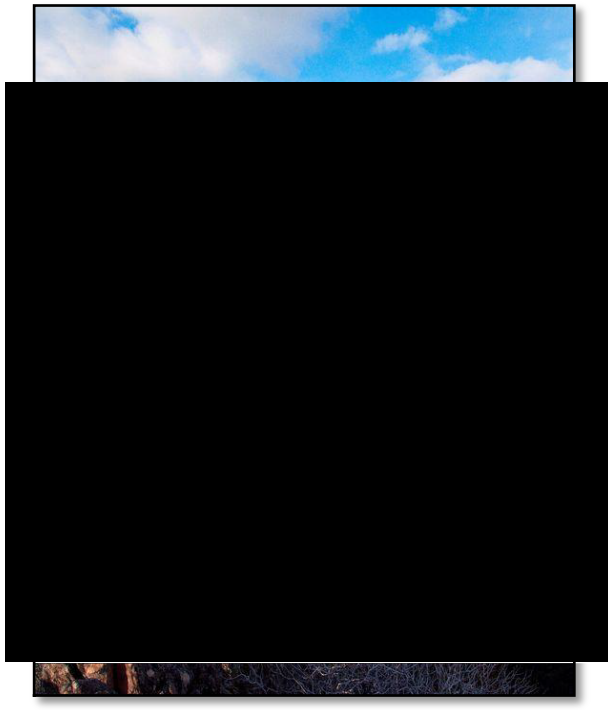

Figure 1.2 New Melones Embankment dam
(https://uk.pinterest.com/andrzejdudek/dams/).

Embankment dams can be classified by their height. Dams under 30m considered to be small dams, while above 30m, they are considered to be large dams. ICOLD reported that in 1995 that there were around 145000 embankment dams around the world, 93% of them were small dams, and 90% were earth fill dams. The reason for the preference of small-sized dams may be related to the construction costs.

André (2004) highlighted that the first embankment dams were built over 2000 years ago. However, many modern dams were constructed in the 1950's when detailed hydrological studies were just beginning; many limitations on the measurement techniques were identified at that time. A full appreciation of the hydraulic processes revealed that many spillway capacities were under-designed and therefore this can lead to overtopping problems. In turn, excessive overtopping can lead to erosion of the back face, damage to the spillway and scour in the stilling basin, all of which act to reduce the integrity of the structure. Failure modes for embankment dams fall into three general categories:

1. Hydraulic failures, such as overtopping failure. Overtopping can lead to many serious problems such as erosion on the downstream slope and breach formation which can cause a complete failure of the dam (Figure 1.3). The failure is caused by high flow rates as the loss of head is converted to kinetic energy;
2. Seepage failure, such as piping through the dam's body (Figure 1.4);
3. Structural failures, such as sliding in the body of the dam (Figure 1.5).

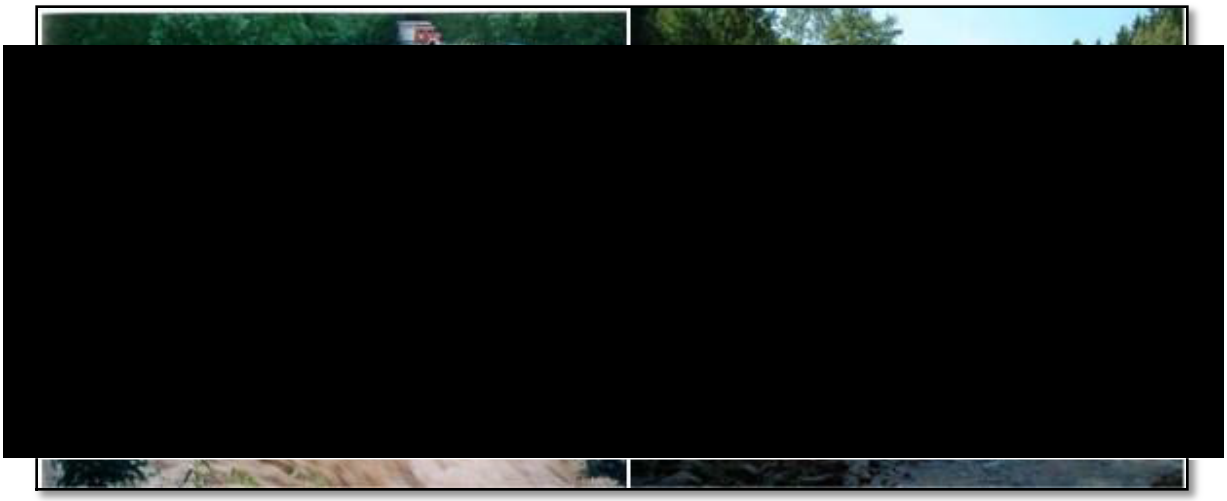

Figure 1.3 The overtopping and breaching of the Glashütte embankment dam in Germany on August 23, 2002 (http://damfailures.org/wp-content/uploads/2015/07/Design-Flood-2.jpg).

Figure 1.4 Seepage failure in the Teton dam in the United States (https://upload.wikimedia.org/wikipedia/en/7/71/Teton_Dam_Sequence_13.jpg).

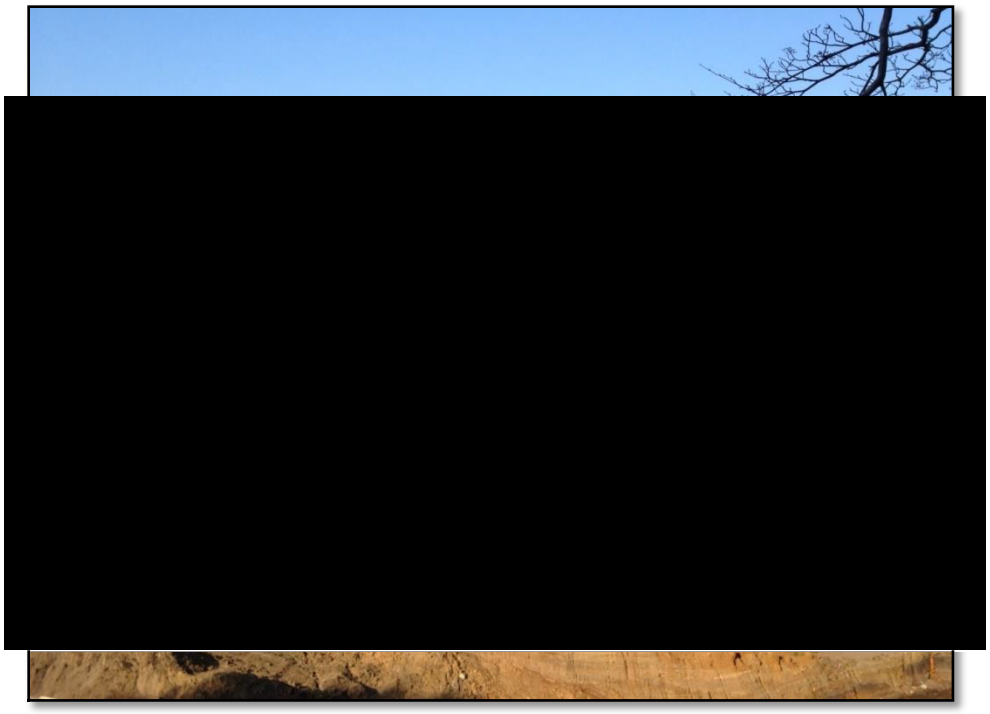

Figure 1.5 Earth dam failure due to land slide (http://www.seismoblogs.com/2014/06/analysis-of-earth-dam-failure-during.html#sthash.HLIcujC3.dpbs).

André (2004) claimed that about 40% of embankment dams around the world, not including China, with heights less than 30m, are damaged due to overtopping. All dams, especially embankment dams need structures to discharge the overtopping flow during the flooding seasons to the downstream safely and effectively, which was the main reason to construct spillways. Normally, spillways are uncontrolled and work automatically when the level of the water increases, however, some types of spillway can be controlled by gates.

Cavitation damage is one of the main problems which can be observed over spillway chutes. Cavitation is the formation of vapor cavities in a liquid. Cavitation occurs in high velocity flow, where the water pressure is reduced locally because of an irregularity in the flow surface. As the vapor cavities move into a zone of higher pressure, they collapse, sending out high pressure shock waves. If the cavities collapse near a flow boundary, there will be damage to the material at the boundary.

Due to the high kinetic energy of overtopping water, a number of protection systems have been suggested to protect the downstream slope of spillways and embankment dams against any damages like erosion, cavitation and breaching; the advantages of using these systems are that they:

- resist erosion,
- dissipate more energy along the slope to reduce the scour at the downstream of the chutes,
- enhance the flow turbulence so that the flow will be highly aerated, thereby reducing the risk of cavitation.

Some of these techniques have been used to resist erosion, such as riprap and pre-cast concrete blocks. However, stepped spillways and gabion stepped spillways have been used to dissipate more energy along the slope and to reduce the risk of cavitation. These techniques will be defined and discussed individually in details in the next section.

- Riprap can be described as two or more layers of armour and filter which are placed on the downstream slope. Using poorly-graded riprap can have more stability for overflows than well-graded riprap; however, well-graded riprap can resist sudden failures better than poorly-graded riprap. The process of riprap selection depends mainly on the expected conditions in the construction area. A benefit of using riprap is that it dissipates more energy due to the rough surface of riprap. Also, it is an easy structure to apply maintenance (Figure 1.6). However, the drawbacks of using riprap are:
    - It requires large sizes of rocks so riprap could be difficult to implement in some places,
    - Water could accumulate between the blocks, which can lead to some issues regarding stability,
    - Finally, there are few studies about design guidelines under turbulent aerated flow available (André, 2004).

Figure 1.6 Riprap (Bureau of Reclamation http://www.andersondragline.com/Projects/Derby-Dam-Spillway/).

- Pre-cast concrete blocks which can be achieved by setting up solid concrete blocks or open cells blocks on the downstream slope of the embankments. Concrete blocks can efficiently dissipate the energy rate and can also provide a good level of stability in the downstream. However, this type of protection is expensive to construct. Furthermore, floating debris can be accumulated between the blocks or in the cells if open cells blocks are used. That can lead to many problems in terms of block stability and it can impact the energy dissipation rate as well (André, 2004).

- Stepped spillways

  Stepped spillways are used initially to increase the energy dissipation and to reduce the cost and size of the downstream stilling basin (Chanson, 2001). Stepped chutes have been used for centuries. Applications can be found in the ancient dams in the Khosr River (Iraq), in the Roman Empire, and in the Inca Empire among other cultures. According to Chanson (2001), the Greek engineers were the first people to design the stepped chute spillway over 3500 years ago.

Stepped spillways are one of the most important solutions used to dissipate the energy of overtopped water over embankment dams. They also stabilise the downstream slope of embankments. However, stepped spillways have many problems which need be solved to optimise their work. Cavitation damage over the steps is one such problem; it is due to negative pressure. The negative pressure over the steps can create air bubbles in the zone where the air entrainment is absent. These air bubbles could face differences in the values of the flow velocity or the flow pressure over the steps. That difference in the velocity and the pressure can blast air bubbles which could affect the shape of the steps and its performance in terms of energy dissipation rate (Figures 1.7 and 1.8). Over the past three decades, stepped spillways have been employed in the design of a number of embankment dam spillways (Chanson, 2002). Additionally, stepped spillways were designed to perform as a secondary spillway for approximately two-thirds of the dams constructed in the USA during the 1990s (Husain, 2013).

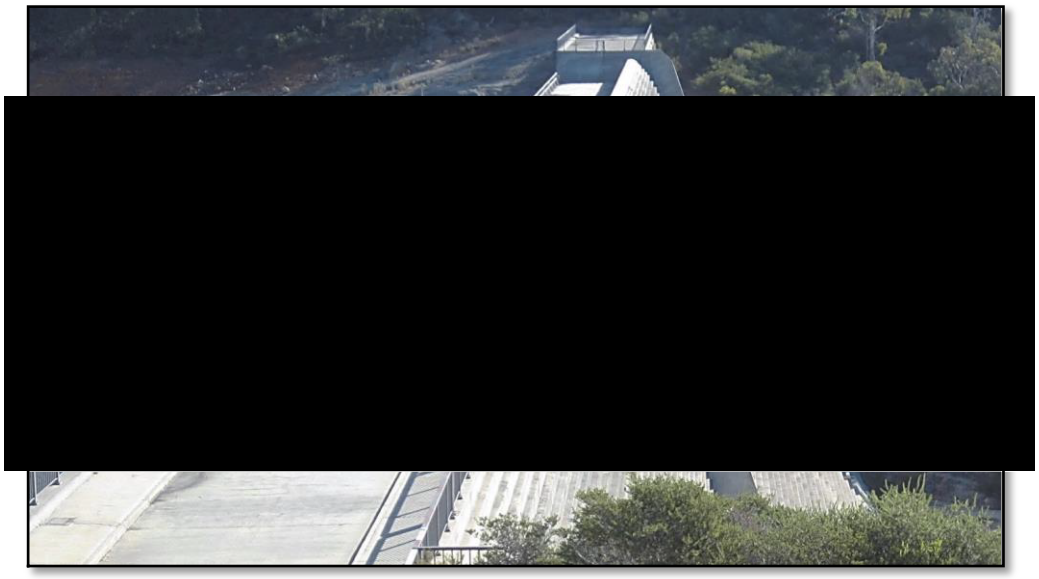

Figure 1.7 Stepped spillway of New Victoria dam; Completed in 1991; RCC arch-gravity dam with height of 52m; Changing slope of spillway in Western Australia (downstream stepped face θ=51.3º, h=0.325m; upstream face with steeper slope) (Felder and Chanson, 2013).

Generally, using stepped spillways can provide many benefits which are summarised below (André, 2004)

- Stepped spillways can be applied over the embankment dams to increase the capacity of the water.
- Reduce the slope erosion as the steps will reduce the bottom velocity.
- Increase the energy dissipation due to the high level of turbulence that can diminish the scouring problem at the downstream and reduce the dimensions of the stilling basin.
- Increase the stability of the downstream slope.
- Reduce the cavitation risk as a result of the flow's high aeration.
- Improve the water quality through the re-aeration.

The largest overflow stepped spillway, the Puentes Dam, was built in Lorca by the Spanish in 1791; however, as a result of the foundation failure, it washed out in 1802. Due to the structural failure of the dam, a 12m high wave was created; this damaged everything in its path. According to Calitz (2015), this failure killed more than 600 people.

In the nineteenth century, designers started to conduct studies on stepped spillways which led them to use stepped spillways for energy dissipation purposes. The New Croton Dam was the first dam that constructed to use the stepped spillway as an energy dissipater. Nevertheless, in the early twentieth century, stepped spillways started to lose favour due to the energy dissipation problems. As a result of that, more investigations were applied at that period of time to understand the principles of energy dissipation and the interaction between the flow and hydraulic jump. Stilling basins were a good solution to dissipate the high flow energy, but since 1970, studies started to pay more attention to stepped spillways again due to many reasons, including the high cost of constructing stilling basins (Calitz, 2015).

Figure 1.8 Hinze dam stepped spillway (Australia) in operation on 29 January 2013 (shutter speed: 1/8,000s) - Flow conditions: $q=14m^2/s$, Yc/h=2.3, Spillway geometry: θ=51.3°, h=1.2m, Rockfill dam wall with conventional concrete spillway (Felder and Chanson, 2013).

- Gabions

  Gabions are baskets that can be filled with gravel, cobble, stone and rock depending on the purpose of construction. Over 7000 years ago, the Ancient Egyptians used gabions; they were also used in China since 1879. The word gabion comes from the Latin ‘cavea’ or cave which refers to a container with box-shaped made of wire mesh. Gabions have also been used for different purposes such as riverbed protection, bank stabilisation and retaining walls. There are three different types of gabion: gabion basket, gabion mattress and sack gabion. All of these types are filled with the gravel and/or cobble materials. Depending on the purpose of the construction, the most suitable type of the gabion should be selected. For instance, the basket gabion is commonly used, for stability purposes and to protect the bed and the stream bank (Freeman and Fischenich, 2000).

There are two ways to use gabions in the embankment dams: as a lining layer parallel to the embankment slope or as steps over the downstream slope. Stepped gabions can deliver more rates for the energy dissipation than the lining gabions and also can provide more structural stability as well. There are many advantages for using stepped gabions such as the availability of the material at many places, light construction techniques, cheap construction cost and easy to maintain as baskets can be replaced easily. The only issue is that gabions require regular maintenance.

The porosity and permeability of gabions can be considered as main benefits of using gabions due to the vital role in decreasing the uplift pressure. The typical dimensions of the stepped gabion are 0.5 or 1 m height, which is equal to the width. The length to height ratio should be between 1.5 and 4. In the case of long gabions steps, gabions should be subdivided into many cells using diaphragms which are made from mesh panels to increase the gabion strength (Wüthrich and Chanson, 2014).

It is worth to mention that for practical purposes, the quality of the mesh and the wire should be extremely strong to increase gabion's durability. Normally, the wire is made of soft steel with a zinc coating. The stone size should be between 1 or 1.5 times of the mesh size but not larger than 2/3 of the minimum dimension of the gabion. Using stone size with 1.5 times of the mesh size can show the best performance to resist the deformation of the gabion boxes (Chanson, 2000b). Attention needs to be paid for stone selection with respect to:

- Grading and cleaning before packing;
- A hard non-weathering type of stone is required;
- The stones in contact with the mesh should be rounded to reduce the possibility of cutting the wire;
- Gabion filling cannot be done by hand unless a certain finish is required.

The main two hydraulic parameters which can control the design of the gabion stepped spillways are: gabion dimensions and the flow rates over the crest. Regarding the dimensions, ideally the height of the step should be equal to the gabion's height. However, it can be twice or three times of the gabion height in some cases. The main difference between the concrete stepped spillways and the gabion stepped spillways can be characterised by the interaction between the surface overflow and seepage flow and also by the rough surface which is provided by gabion steps (Figure 1.9).

(a) Diversion stepped channel at Duralie Coal project (Australia) on 23 March 2005 (Courtesy of Tony Marszalek).

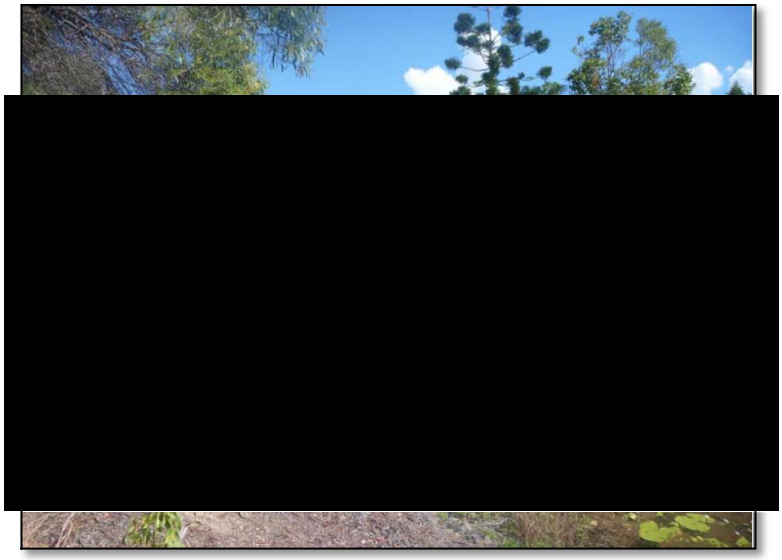

(b) Gabion stepped weir, Robina, Gold Coast (Australia)

Figure 1.9 Gabion stepped spillways Wüthrich and Chanson (2014).

1.4. Classification of flow over stepped chute spillway

Three different flow regimes can be identified in stepped spillways: nappe flow, transition flow and skimming flow. Chanson (2007) showed that these types of flow have a direct relationship with the amount of the discharge and the geometry of the steps. For example, for a given step geometry, the flow could be nappe flow if the discharge is low, it could be skimming flow if the discharge is high. A transition flow can be achieved when the flow rate is higher than the maximum limit for the nappe flow and lower than the minimum limit for the skimming flow (Chanson, 2001).

1.4.1. Nappe flow regime

The nappe flow regime appears when the flow rate is small and the step width is large (Chanson, 2001). This type of flow regime can be recognised by three features; first, by free falling nappe at each step, this is also called series of free falling (Figure 1.10). Secondly, air bubbles can appear in the pool step when the water is recirculating (André, 2004). Finally, a partially or fully hydraulic jump may be noticed in some cases at the downstream of the impacting point of the jet on each step (Toombes, 2000).

At this type of regime, air could enter at the point of intersection between the overfalling water and the recirculating water which is located on the pooled step (Chanson et al., 1994). Cavitation is therefore a low risk under nappe flow. Nappe flow is appropriate for the low dams or flat spillway which is available at the water treatment plant (Husain et al., 2013). Many equations have been suggested by the previous researchers in Table 1.1 in order to determine the limitation to achieve nappe flow conditions over spillways.

Table 1.1 Nappe flow equations

The authors	The equations	Validity	Comments
Chanson (1994)	$\frac{Yc}{hs} \leq 0.0961 \left(\frac{hs}{ls}\right)^{1.276}$	$0.2 \leq hs/ls \leq 0.6$.	Yc: Critical water depth hs: Height of the step ls: Length of the
Yasuda and Ohtsu (1999)	$\frac{hs}{Yc} = 1.4(1.4 - \tan\theta)^{-0.26}$	-	-
Chanson (2001)	$\frac{Yc}{hs} = 0.89 - 0.4\frac{hs}{ls}$	$3.4^o \leq \theta \leq 60^o$	Accuracy of 10%
Yasuda et al. (2001)	$\frac{hs}{Yc} = 0.57\left(\frac{hs}{ls}\right)^3 + 1.3$	$0.1 \leq hs/ls \leq 1.43$ $0 \leq hs/Yc \leq 1.3$	-
Chinnarasri (2002)	$\frac{Yc}{hs} = 0.98\,(0.55)^{hs/ls}$	-	-
Chanson and Toombes (2004)	$\frac{Yc}{hs} = 0.9174 - 0.381\frac{hs}{ls}$	$0 \leq hs/ls \leq 1.7$	-
Chinnarasri and Wongwises (2004)	$\frac{Yc}{hs} = 0.927 - 0.005\theta - 0.388\frac{hs}{ls}$	$0.1 \leq hs/ls \leq 1.73$	-

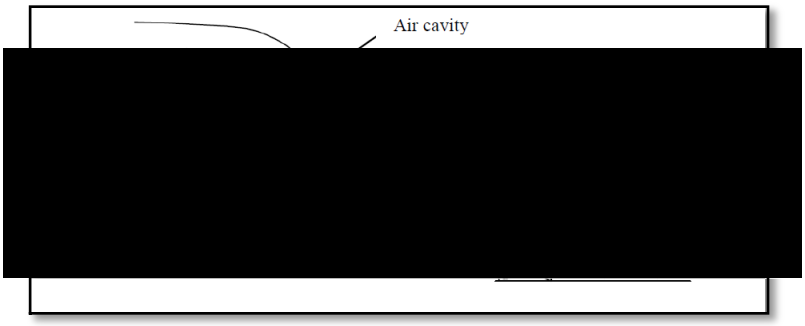

Figure 1.10 Nappe flow (Kositgittiwong, 2012).

1.4.2. Transition flow

The transition flow regime was firstly found by Elviro and Mateos (1995) and Othsu and Yasuda (1997). Spray and splashing near the free surface, moderate discharge and strong hydrodynamic fluctuations are the main properties of transition flow. The free surface appearance is different from the skimming flow and nappe flow as both air cavities and air bubbles can be observed (Kavianpour and Musoumi, 2008). Chanson and Toombes (2004) showed that if the water splashing is 3-8 times greater than the step height, it can be clearly seen at the downstream of the inception point. According to André (2004), this type of flow needs a gradual increase in the discharge from the nappe flow regime; therefore, it is very rare to catch this type of flow in particular cases (Figure 1.11).

Figure 1.11 Transition flow (Kositgittiwong, 2012).

1.4.3. Skimming flow

Skimming flow can be noticed when the rate of discharge per unit width is very high. When the water flows down over stepped spillway and all of the cavities are filled by

water, the water flow will appear as a coherent stream above the pseudo-bottom which is formed by the external edge of the steps; thus, skimming flow can be identified (Rajaratnan, 1990). Cavities can be present beneath the flow; these vortices are maintained through the transmission of shear stress from the flow over steps edges. Skimming flow plays a vital and significant role in the energy dissipation where the dissipation might happen because of the cavities (Kositgittiwong, 2012).

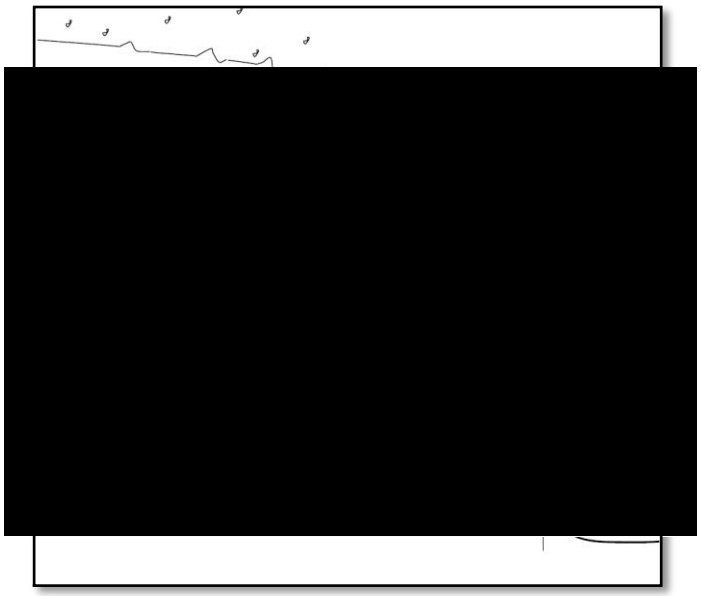

Figure 1.12 Skimming flow (André, 2004).

A skimming flow regime can be divided essentially into two zones depending on the air availability. In the first zone which is located on the early steps near the crest, the water has a smooth free surface (clear water) and also no air entrainment can be observed (Figure 1.12). However, in the second zone, the free surface of the water will have air entrainment and the flow of the water will become turbulent (André, 2004).

The non-aerated zone is sometimes called the black water zone due to the absence of air. Thus, the aerated zone can be termed the whitewater zone because of the presence of air which may mix with the water flow. That kind of mixing between water flow and air can lead to providing a white colour for the water flow that can easily observe over the chute steps. Normally, both of the zones can be clearly seen across the chute width. The point

which separates the non-aerated zone (water zone) and the aerated zone (air-water zone) called the inception point (André, 2004). According to Murillo-Munoz (2006), in the air-water zone and after the inception point, the fluid produces a rapidly varied flow region, and then a gradually varied flow region can be noticed. At the end of the downstream, the water is defined as the uniform flow (Figure 1.13).

Determining the onset of skimming flow is one of the most important facets for design of stepped spillways. Many studies have been conducted to show the boundary for each type of flow (nappe, transition and skimming). However, all of these studies have shown different empirical formulas to determine the upper and the lower limits for each type. Many of these studies have been conducted experimentally. There is scope for many uncertainties in experimental work, and variation in results might be observed from different experimental studies.

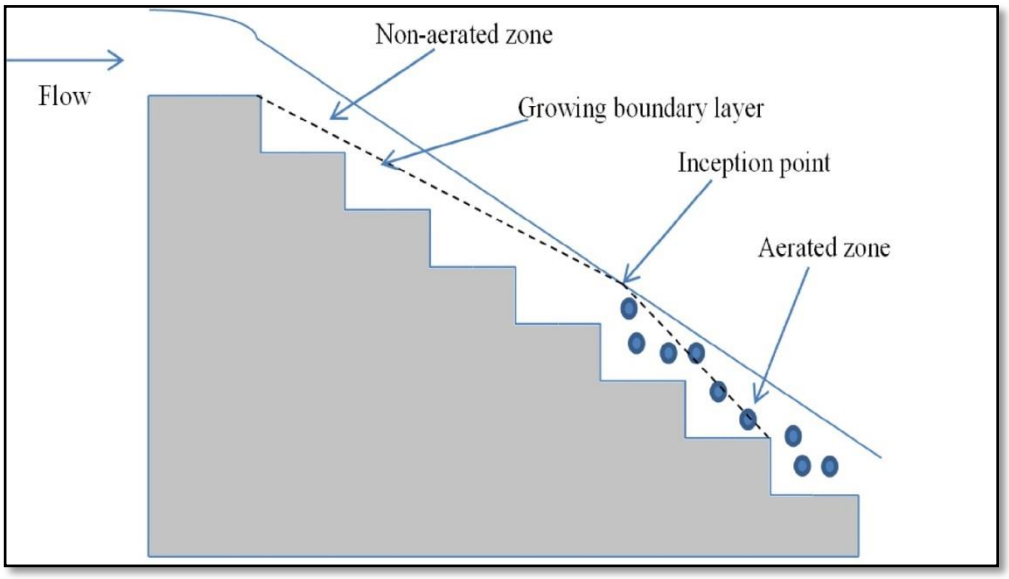

Figure 1.13 2D schematic view of flow over stepped spillways.

Skimming flow is the most critical type of flow regimes for design. This is demonstrated by the high number of spillways which have been designed and constructed around the world based on the skimming flow regime. For skimming flow, dimensional analysis has been used to predict the limitations which mainly depend on the discharge, the step height and step length (Murillo-Munoz, 2006). On the other hand, Peyras et al. (1992)

showed that it depends on the discharge and the slope of the spillway. Table 1.2 shows the previous equations which have been suggested in the literature to predict the limitations of the skimming flow regime over the spillways where

Yc: Critical water depth

hs: Height of the step

ls: Length of the

Table 1.2 Skimming flow equations

The authors	The equations	Validity
Rajaratnun (1990)	$Yc/hs > 0.8$	-
Chanson (1994)	$\frac{Yc}{hs} = 1.06 - 0.465 \frac{hs}{ls}$	$0.2 \leq hs/ls \leq 1.25$
James et al. (1999)	$\frac{Yc}{hs} = 0.541 (\frac{hs}{ls})^{-1.07}$	$hs/ls < 0.84$
Yasuda and Ohtsu (1999)	$\frac{Yc}{hs} = 0.826 (\frac{hs}{ls})^{-0.165}$	$\theta < 55^o$
Chamani and Rajaratnum (1999)	$\frac{hs}{ls} = \sqrt{0.89((\frac{Yc}{hs})^{-1} - \left((\frac{Yc}{hs})^{-0.34} + 1.5\right) - 1}$	
Ohtsu et al. (2004)	$\frac{Yc}{hs} = \left(\frac{6}{7}\right) (\tan\theta)^{-1/6}$	$5.7^o \leq \theta \leq 55^o$
Chanson (2002)	$\frac{Yc}{hs} = 1.2 - 0.328 \frac{hs}{ls}$	
Boes and Hager (2003)	$\frac{Yc}{hs} = 0.9 - 0.14 \frac{hs}{ls}$	$30^o \leq \theta \leq 50^o$

1.5. Problem statement and the motivation

Cavitation damage can be considered as one of the most important issues of skimming flows over gabion stepped spillways, especially when the air is entirely absent or insufficiently present over the upstream part of the bottom chutes. Therefore, air entrainment could play an important role in protecting the surface of gabion stepped spillways against cavitation damage. Cavitation damage is most often observed in the upstream part of the bottom chutes. That is, in the non-aerated zone. The length of the

non-aerated zone over the steps depends mainly on the value of the flow discharge (Figure 1.14). It could cover all the steps under the highest flow discharges. The non-aerated regime starts at some distance from the spillway crest and extends to the location of the inception point where the free surface intersects with the turbulent boundary layer. The next section after the inception point and down to the last step is called the aerated zone. In the aerated zone, the turbulence level of the flow is very high and that can make the air enter and mix with the flow which is known as self-aeration.

Figure 1.14 Cavitation damage on spillway profile of Nagarjunasagar Dam (https://www.ecronicon.com/ecag/agriculture-ECAG-01-00004.php).

In small embankment dams, investigating the skimming flow characteristics is extremely important as its length along the downstream slope may not be long enough to capture the self-aeration portion. Therefore, in such cases and especially in high flow rate conditions, the entire chute length along the downstream slope might be subjected to cavitation damage. Generally, a small number of studies have been carried out to investigate the flow properties over gabion stepped spillways; however, no attention has been paid before to the cavitation damage in the non-aerated zone over gabion stepped spillways under skimming flow conditions. Understanding the behaviour of hydraulic parameters is important for improving the design for such kinds of structures. For instance, investigating the pressure pattern on the step faces is significantly important in order to

avoid or reduce the cavitation damage. All of the previous studies of gabion stepped spillways have been conducted experimentally. Consequently, the current work focuses on numerical investigation of gabion stepped spillways which describe the features of the pressure flow field on the horizontal and vertical faces of steps situated in the non-aerated flow region for a wide range of slopes typical of moderate slopes. In addition, the inception point location, velocity flow fields, turbulent boundary layer thickness and energy dissipation upstream of the inception point for embankment dams are all examined as they are of direct interest for design. Also, the current work estimates the effects step height and chute slope have on the skimming flow in the non-aerated flow region over moderate slope of gabion stepped spillways. Finally, different kinds of geometries are examined to explore their ability to modify the energy dissipation rate.

1.6. Objectives of the present study

The current examination is a numerical study conducted on gabion stepped spillways having three different bottom slopes 1V:2H, 1V:2.5H, and 1V:3H typical of embankment dams. Furthermore, three-step heights of 0.06, 0.09 and 0.12m are used to give different numbers of steps for each slope. Four different porosities 0.25, 0.3, 0.35 and 0.4 and four different particle sizes 0.005, 0.01, 0.015 and 0.02m for each case have also been tested. All of these numerical runs are examined in the non-aerated flow region under a range of typical discharges of skimming flow conditions. It is important to mention that the scale effect should be considered during the numerical investigations of the current work, especially for the cavitation assessment. The main objectives of the present work are:

1- To investigate the effect of the step height and chute slope on the behaviour of skimming flow over gabion steps, in terms of the position of free surface and velocity profiles at different sections, turbulent boundary layer thickness, the position of the inception point, pressure pattern over the horizontal and vertical faces of steps, cavitation damage and the energy dissipation rate;

2- To investigate the effect of the gabion porosity on the behaviour of skimming flow over gabion steps, in terms of the position of free surface and velocity profiles at different sections, turbulent boundary layer thickness, the position of the inception point, pressure pattern over the horizontal and vertical faces of steps, cavitation damage and the energy dissipation rate;

3- To investigate the effect of the gabion particle sizes on the behaviour of skimming flow over gabion steps, in terms of the position of free surface and velocity profiles at different sections, turbulent boundary layer thickness, the position of the inception point, pressure pattern over the horizontal and vertical faces of steps, cavitation damage and the energy dissipation rate;

4- To use the numerical results of the present investigation to formulate appropriate design formulae and compare these with existing formulae;

5- To test different geometries of gabion stepped spillways in terms of energy dissipation rate.

1.7. Thesis outline

This thesis is divided into ten chapters. The first chapter presents the concept of stepped spillways and states the main objectives of the present investigation. Chapter Two reviews the published experimental and numerical research in this. It also explains the main features of the numerical code and shows the various numerical techniques implemented in this work. The validation of the numerical code is illustrated in Chapter Three. Chapter Four describes the experimental setup with the PIV (Particle image velocimetry) measurements and validate them with the numerical results. Chapter Five presents and discusses the main results obtained in the present study in terms of the position of the free surface elevation. The calculations of the location of the inception point are presented in Chapter Six. Chapter Seven deals with the computational velocity distribution and energy dissipation rates over gabion stepped spillways. The pressure distribution on both steps faces and evaluates the potential of cavitation damage on

moderate slope stepped spillways discussed and presented in Chapter Eight. Chapter Nine investigates different kinds of step shapes of gabion stepped spillways and also different geometries of gabion stepped spillways have been tested in terms of energy dissipation rate. Finally, the main conclusions and suggestions for further investigations are summarised in Chapter Ten.

Chapter 2 : Literature Review

2.1. Introduction

Many experimental and numerical studies have been conducted on stepped spillways. The studies included the geometry of the spillway which contains the number of steps, the shape of the steps and the slope of steps in addition to the slope of spillways. The main reason for conducting this kind of research is to understand the effect of these parameters on the hydraulic properties such as flow regime, water pressure, water velocity, the location of the inception point and the energy dissipation. Therefore, the review of the previous studies will be divided into five parts: experimental studies of energy dissipation, experimental studies of inception point, experimental studies of pressure values over stepped spillways, numerical studies of stepped spillways and previous studies of gabion stepped spillways.

2.2. Experimental studies of energy dissipation

Energy dissipation represents the main problem of stepped spillways. The overtopped water can have a high level of energy at the downstream of stepped spillways; this can cause dangerous issues such as scour and erosion at the downstream. Consequently, increasing the energy dissipation can help to reduce the cost of stilling basin constructions in the downstream of spillways. Sorensen (1985) conducted an experimental study to investigate the design of steps to increase the energy dissipation. It was a new concept in the dam construction. Sorensen showed that stepped channel can be constructed from RCC or gabions. A physical model was built to test if the steps can eliminate the deflecting water jet. Results showed that using stepped spillway can increase the energy dissipation more than the ogee spillway. The primary objectives were to make the water flow smoothly from the crest to the downstream to increase the water dissipation and define the characteristics of the flow over the steps. The results indicated that smooth flow from the crest of the spillway to the steps can be achieved easily.

Moreover, Christodoulou (1993) found that energy dissipation could be influenced by the number of steps and the ratio of the critical depth to the step height. Chanson (1994) studied energy dissipation in nappe and skimming flows. Although there are differences between nappe flow regime and skimming flow regime, energy dissipation has been observed for both of them. Results showed that the amount of the energy dissipation for the long chutes in skimming flow regime is more than nappe flow, on the other hand, in short chutes channels; the nappe flow produced more energy dissipation than skimming flow. A uniform flow regime has been noticed at the end of the spillway. However, Chanson (2002) reports that greater energy dissipation has observed under the nappe flow condition. Therefore, the flow conditions such as the flow rates and the flow regimes can show different results in terms of the energy rate.

Other studies revealed that the number of steps can play a significant role in the energy dissipation rate over stepped spillways. For instance, increasing the height of the steps on relatively flat slopes might be useful to achieve more energy dissipation. According to Chanson (1995), Boes (1999), Matos (2000), Chatila and Jurdi (2004) and Hunt and Kadavy (2010) energy dissipation values may decrease when the discharge is increased as the steps will be less effective and the performance of stepped and smooth spillways will be similar.

Furthermore, Fratino and Piccini (2000) conducted a study to examine and improve the energy dissipation efficiency at the downstream of the spillway with different geometric configurations such as height of the steps, the number of the steps and the slope of the spillway. All of these studies were conducted experimentally. The results showed that a reduction in the energy dissipation can be noticed when the discharge increases, also, there is a reduction in the energy dissipation when the spillway slope increases. Researchers such as Chamani and Rajaratnam (1994), Boes (1999), André et al. (2004) and Chanson and Gonzalez (2004) found that the number of steps is more important than their size; therefore, when the number of steps increases, the energy dissipation will also increase. This happens as the spillway steps can perform as macro-roughness which can increase the kinetic energy as a result of the increase of friction.

To assess the slopes of stepped spillways on the energy dissipation rate, Chanson, Yasudu and Ohtsu (2002) investigated the flow resistance of the skimming flow for wide slopes ranging from 5.7° up to 55°. Laboratory and prototype data was used in comparison with the experimental data. The authors used a simple analytical model to analyse the results in order to understand the mechanisms of flow resistance which is related to the shear stress and the recirculating cavity ejection. Therefore, the analysing process was carried out on more than 38 models and 4 prototypes which are more than 700 points in total. They concluded that the flow resistance is a combination of the skin friction on the horizontal faces and the form drag on the flat chutes ($\theta<20$); however, for the steep chutes ($\theta>20$), the form drag must be used to analyse the flow resistance.

As mentioned earlier, the step heights can be considered as one of the main parameters which can impact the energy dissipation; hence, investigate the shape of the steps could be essential to examine its impact. To do that, Barani, Rahnama and Sohrabipoor (2005) created a physical model to investigate the energy dissipation over stepped spillways for different types of steps such as plain step, inclined step and end sill step. The experimental tests of inclined steps have been conducted by using different adverse slope like 15°, 26°, 36° and 45°. The results showed that end sill steps and inclined steps can dissipate more energy than plain steps. The comparison was obtained between end sill steps and inclined steps and it showed that inclined steps can dissipate energy better than end sill steps. Therefore, large spillways with a high flow rate will be better if inclined steps are used instead of an end sill step. Also, Khademi and Shirvani (2014) researched different shapes of steps of stepped spillways. A physical model was employed to examine the effect of step shapes on energy dissipation. Experimental work was conducted by using three types of steps, these types were adverse slope inclined steps, end sill and plain steps. They concluded that the adverse inclined steps and end sill steps have more ability to dissipate energy compared to plain steps. Under different flow regimes such as nappe, transition and skimming, EL-Jumaily and Al-Lami (2009) carried out a research about different inclined upward slopes (42˚, 28˚, 14˚ and 0˚). The study was conducted by building a physical model with scale 1:20. They concluded that

increasing the slope of the inclined steps might not impact the flow properties; however, it could have a strong effect on energy dissipation by increasing the adverse slope.

To consider the air entrainment effect on the hydraulic performance over stepped spillways, Felder and Chanson (2013) experimentally investigated the characteristic of air-water flows and the energy dissipation for flat and pooled stepped spillways with slopes of 8.9° and 26.6° respectively. They studied different types of flow such as nappe flow, transition flow and skimming flow with different spillway slopes. Moreover, an investigation about the velocity distribution was conducted to observe more details about the waves with different flows. The results showed that pooled steps are better than flat steps in terms of energy dissipation but there are some other issues in terms of the stability so more studies need to apply to understand the properties of water over stepped spillways. For design purposes, it is important to highlight that many people preferred to use flat steps rather than the inclined steps for normal stepped spillways because of the stability issues, although inclined steps can dissipate more energy compared to the flat slopes. Therefore, testing different shapes for the steps of gabion stepped spillways is one of the objectives of this study to assess their performance with the presence of the porous media in terms of energy dissipation rate.

2.3. Inception point and air entrainment

The inception point represents the point where the non-aerated zone is finished and the aerated zone starts. Boes and Hager (2003) defined the inception point as the point where the air concentration is 1%. The position of the inception point is extremely important for designers for its use in determining the non-aerated zone where there is no air entrainment. The inception point can be determined in experimental work by visual observation where the white water starts to appear due to air entrainment. However, attention needs to be paid for this matter as determining the location of the inception point visually could have some uncertainties issues due to the difficulties of determining the location accurately.

Generally, due to viscous shearing action over solid surfaces, fluid can be affected when it flows over them. The velocity at the surface is equal to zero. The boundary layer can be defined by a layer of fluid which is adjacent to a surface where the viscous effects can be observed (Webber, 1979).

Figure 2.1 Development of boundary layer on a solid surface (Atencio, 2011).

As shown in Figure 2.1, the development of the boundary layer over solid surfaces can be divided into three different stages. First, a laminar boundary layer is developed along solid surfaces because of the laminar flow which has parabolic velocity distributions. Then, the laminar flow becomes unstable and may also start to have some eddies at the transition point. Finally, the fully turbulent flow will be established after a short transitional zone.

For the numerical work, the location of the inception point can be positioned depending on the definition of the inception point (Chanson, 2002). Chanson's definition has represented the inception point as being a point between the free surface of the water and the developed turbulent boundary layer from the upstream face of the weir. Therefore, it is significantly important to determine the boundary layer thickness. The boundary layer thickness (δ) for stepped spillways is defined as the perpendicular distance from the pseudo-bottom to where the velocity is equal to 99% of the maximum velocity (Chanson, 2002).

Matos (2000) and Chanson (2002) reported that the length of the non-aerated zone might be affected by three important factors: discharge, step height and chute slope. André (2004) claimed that increasing the roughness of the spillway can be considered as one of the important benefits of using steps. Consequently, the turbulent boundary layer growth will be accelerated which could increase the opportunity to intersect with the free surface much earlier than using a smooth step-free surface.

Many empirical equations have been suggested by researchers to find the location of the inception point and the water depth at the inception point. While some of those equations are applicable for the smooth spillway, some can be used for stepped spillways (Table 2.1). If the slope of stepped spillways is less than 22° ($\theta<22°$) then it will be considered as a flat stepped spillway; in contrast, if the slope is equal or higher than 22° ($\theta\geq22°$) then it will be considered as a steep stepped spillway (Hunt and Kadavy, 2010).

Keller and Rastogi (1977) reported that the position of the inception point is the primary function of the discharge and the roughness of spillway; they suggested

$$\frac{Li}{ks} = f(F_*, \sin\theta)$$

$$\frac{di}{ks} = f(F_*, \sin\theta)$$

where Li is the distance from the start of growth of the boundary layer to the inception point, di is the water depth normal to the free surface measured at the inception point. F_* is the Froude number which can be defined by

$$F_* = \frac{q}{\sqrt{g*\sin\theta*ks^3}} \qquad (2.1)$$

where

ks is the roughness height measured perpendicular to the pseudo bottom ;

ks=hs*cosθ

hs: step height and

θ: angle of the slope of the spillway

q: the unit discharge of the water

g: the gravitational acceleration

Table 2.1The equations of location and the water depth of the inception point

The authors	The equations	Validity
Wood et al. (1983)	$\frac{Li}{ks} = 13.6 * (\sin\theta)^{0.0796} * (F_*)^{0.713}$ $\frac{di}{ks} = \frac{0.223}{(\sin\theta)^{0.04}} * (F_*)^{0.643}$	smooth concrete spillways
Chanson (1994)	$\frac{Li}{ks} = 9.8 * (\sin\theta)^{0.08} * (F_*)^{0.71}$ $\frac{di}{ks} = \frac{0.4}{(\sin\theta)^{0.04}} * (F_*)^{0.64}$	stepped spillways with ogee crest $27° \le \theta \le 52°$
Chanson (1996)	$\frac{Li}{ks} = 9.719 * (\sin\theta)^{0.0796} * (F_*)^{0.713}$ $\frac{di}{ks} = \frac{0.4034}{(\sin\theta)^{0.04}} * (F_*)^{0.592}$	stepped spillways $27° \le \theta \le 59°$.
Chamani (2000)	$\frac{Li}{ks} = 8.29 * (F_*)^{0.85}$	ogee crest spillways $50° \le \theta \le 60°$
Boes and Hager (2003)	$\frac{Li}{ks} = \frac{5.9 * (\cos\theta)^{1/5}}{\sin\theta} * (F_*)^{4/5}$ $\frac{di}{hs} = 0.40 * (F_s)^{0.6}$	Gated stepped spillways $26° \le \theta \le 55°$ $F_s = \frac{q}{\sqrt{g*\sin\theta*hs^3}}$
André (2004)	$\frac{Li}{ks} = \frac{8.0}{\tan\theta} * (F_{*,\theta})^{0.730}$	$18.6° \le \theta \le 30°$ $F_{*,\theta} = \frac{q}{\sqrt{g*\cos\theta*ks^3}}$
Meireles and Matos (2009)	$\frac{Li}{k} = 5.25 (F_*)^{0.95}$ $\frac{di}{k} = 0.28 (F_*)^{0.68}$	θ=26.6°
Hunt and Kadavy (2011)	$\frac{Li}{ks} = 6.1 * (\sin\theta)^{0.08} * (F_*)^{0.86}$	$\theta \le 22°$ $1 < F_* < 100$
Hunt and Kadavy (2013)	$\frac{Li}{ks} = 5.19 * (F_*)^{0.89}$	$\theta \le 26.6°$ $0.1 < F_* < 28$
Hunt and Kadavy (2013)	$\frac{Li}{ks} = 7.48 * (F_*)^{0.78}$	$\theta \le 26.6°$ $28 < F_* < 10^5$

Chanson (2002) claimed that the development of the turbulent boundary layer is considered as the main factor to predict the location of the inception point. However, other factors are likely to play minor roles such as the step geometry, including the height, slope and shape, the upward inclined steps and the pooled end sill steps. Finally, the construction materials used in the gabions can significantly impact the location of the inception point, especially due to the flow through the porous media.

2.4. Pressure distribution over spillway steps

As aforementioned, there are two regimes over stepped spillways under skimming flow conditions, non-aerated zone or black water region where the air entrainment is absent and the aerated regime or the white water where air enters the flow. For the whitewater region, air entrainment plays a significant role in reducing the damage from the cavitation. Peterka (1953) reported that the presence of 5%-8% of the air in the flow over stepped spillways can eliminate any damage associated with cavitation. The upstream region (non-aerated zone) is more prone to cavitation than the downstream region (aerated zone) due to the lack of the air content. The flow velocity increasing in the non-aerated zone can cause drops in the pressure values: near the outer edge of the steps, it can reach zero or negative pressure values. The next section reviews the previous experimental studies about the pressure distribution over stepped spillways.

Frizell and Mefford (1991) conducted an experimental study to investigate whether cavitation can occur due to the drop in the pressure values over stepped spillways. Two stepped spillways models were built-up to examine the pressure under different heads. The slope of the first model was 1V:2H while the slope for the second one was 0.8V:1H. The results showed that the area which is near to the top of the return eddy may have cavitation depending on the pressure value. Sanches-Juny et al. (2000) built up a physical model to characterise the pressure field of the skimming flow over stepped spillways using a pressure transducer and flow visualising technique. The main finding was that the mean pressure values are positive along the stepped spillways and both maximum and minimum pressures occur upstream of the inception point location.

Generally, over the horizontal face of steps, the flow hits the downstream half of the horizontal face; therefore, the maximum discharge and the lowest pressure can be observed in the upstream half of the horizontal face where this zone can be characterised by a boundary separation of the flow (Frizell, 1992). Over the vertical face, the pressure value could be negative in the region which is closer to the outer edge of the step where the boundary separation of the eddy can be found. Pressures might be less negative for the higher discharge. The mean pressure will be positive in the area nearer to the continuous horizontal faces which receive the impact of recirculating flow, that positive pressure will be lower than the pressure in the impact zone of the horizontal face (Sanches Juny et al., 2000).

André (2004) carried out laboratory experiments to study the effect of the microroughness elements on the pressure distribution over the horizontal and vertical faces for a wide range of discharge and different flow conditions like nappe, transition and skimming flow. No negative pressure was achieved during the measurements because they were recorded in the uniform flow regime where the flow is fully aerated.

Amador et al. (2004) studied flow characterisation under skimming flow in the non-aerated zone experimentally by using the particle image velocimetry technique to measure the velocity and pressure transducers for the pressure measurements. They reported that the pressure variations can show the flow effects in the downstream half of the horizontal face as the mean pressure is higher in the upstream half. They also showed that there is a separation flow zone and negative pressure near the outer edge of the vertical face of steps. They concluded that pressure over the vertical faces might be influenced by the cavity's recirculation zone and the separation of the shear layer.

Amador et al. (2009) studied the mean and the fluctuated pressure of steeply stepped spillways with 1V:0.8H bottom slope. The measurements have recorded in the non-aerated zone for both faces and near to the inception point location under skimming flow conditions. The main point in this research was to determine the allowable discharge

value; above this value, the extreme negative pressures could be observed which can lead to cavitation appearing in the non-aerated zone. The result showed that the maximum value for the velocity is 15m/s; this should be enough to avoid the occurrence of cavitation in the non-aerated flow.

Frizell et al. (2011) conducted an experimental work to study the potential of cavitation damage over stepped spillways for two different prototypes; the first one was with a moderate slope (1V:2.48H), while the second was with a steep slope (2.48V:1H).The results were collected in the low ambient pressure chamber; they claimed that cavitation could occur in the absence of the aeration. The cavitation index was used in this study to characterise the potential of cavitation along the chute slope.

$$\sigma = \frac{2(P_\circ - P_v)}{\rho V_\circ^2} \qquad (2.2)$$

where σ is the cavitation index, $P_\circ$ and P_v are respectively the reference pressure and the vapour pressure of water at a given temperature, ρ is the density of water and $V_\circ$ is the reference velocity. It is crucial to mention that if the cavitation index between 0.6-0.7, cavitation bubbles could occur along the pseudo-bottom; moreover, if the cavitation index decreases below than 0.6, cavitation damages can take place on stepped spillways. Thus, the value of the cavitation index (0.6) can be considered as the inception cavitation index.

However, Frizell et al. (2013) performed an experimental study to assess the cavitation potential on stepped spillways with two-step angles θ=21.8° and θ=68.2°, with two step heights each. Various discharges have been tested for each configuration. A critical cavitation index of 0.60–0.65 was obtained for θ=68.2° and 0.30–0.40 for θ=21.8°. Generally, the designer needs to pay more attention to the non-aerated zone that is located upstream of the inception point and below the pseudo-bottom as that area can be prone to cavitation.

2.5. Numerical studies of stepped spillways

As described in the earlier sections of this chapter, the complex phenomenon of flow over stepped spillways has been studied experimentally. Physical models have been used in the design of stepped spillways for many reasons such as the accurate estimation of the discharge capacity, local flow pattern, discharge coefficient, free surface profile, pressures, velocities, investigation of cavitation risk and friction losses. However, there are many issues with using physical models such as the cost, time-consuming and the uncertainties associated with scaling effects. Therefore, the recent developments in the technology start to provide a solution for the hydraulic problems by using different mathematical models. The numerical method to solve, analyse and simulate the fluid flow problems is called Computational Fluid Dynamics (CFD). In addition to the main benefits from using numerical work like the relatively low cost and the lesser time requirements compared to experimental work, any changes in the model's design can be easily adopted in the numerical work to the existing model in contrast to the experimental work as changing the model consumes a lot of time and money. Also, CFD can be considered as a virtual laboratory as CFD may provide very good results if high capacity computers and efficient CFD codes are used together. It is clear that there are many advantages for using numerical models to simulate the hydraulic problem; however, it is important to mention that all of the numerical models need to be validated against experimental data (Usta, 2014). In the next section, a review of some important numerical studies of spillways which have been applied during last years will be provided and briefly discussed.

Mehdi (1997) used a 2D numerical model which solves Bernoulli's equation based on the finite element method in order to calculate the positions of the free surface flow over an ogee crest of stepped spillways. The results revealed that the model can predict accurate results in the uniform flow region in the downstream of the structure. That was due to the implemented formula which well-known U.S. Army Corps of Engineering formula as it has the ability to show the effect of air entrainment on the flow. However, Unami et al. (1999) presented a study about verifying a 2D numerical model can be applied to

practical design. Finite element and finite volume methods were used to resolve free surface flow equations. Also, an unstructured triangular mesh system was applied in the code. For the two-phase flow, a model of the air entrainment was added to the system. The results showed that the numerical model can be used as a primary analysis tool for hydraulic design of spillways. They claimed that the finite volume method needs less effort than the finite element. Unlike Unami et al. (1999), Tabbara et al. (2005) studied the characteristics of flow over stepped spillway such as vortices, energy dissipation and water surface by using computational fluid dynamic module, the ADINAA software. This software used finite element technique to discretise the equation and k-ε flow model was used to solve turbulence problem. Two phases were used to increase the solution accuracy which is the first solution was used as initial condition for the second solution. A good agreement was achieved between the results from numerical and experimental works.

More studies have been conducted numerically such as Dong and Lee (2006) who used FLUENT 6.1 software, which is based on VOF, k-ε standard and unstructured mesh to simulate the flow over stepped spillway and to study the different flow regimes such as nappe, transition and skimming. FLUENT 6.1 provided good information about flow characteristics; therefore, it is used to estimate the velocity profile, clear water and bulked depth, friction factor and static pressure. Also, air concentration was calculated. However, Lobosco et al. (2011) paid more attention for the self-aerated zone. Lobosco et al. (2011) used a numerical simulation (CFD) to investigate the bubbles in the self-aerated zone and wave description. They used Open Foam and Salome software for mesh generation. k-ε model and VOF model were used for turbulence and free surface water problems respectively. A validation of the software was made by comparing the results with experimental work which was taken from the previous researchers.

Generally, computational software has started to be more reliable as many researchers have validated it with different kinds of experimental data. As a result, numerical models have started to be used commonly to investigate the geometries of stepped spillways, energy dissipation rates and the location of the inception point over the steps. Abbasi and

Kamanbedast (2012) created a new numerical model which is based on turbulence Navier-Stokes equation to find the influence of dimension varying on energy dissipation, such as the changing in steps height, steps width and numbers of steps and all investigations have been done with different discharges. The researchers solved the governing equation by using finite volume discretisation method (3D). The k-ε model was applied to simulate the flow turbulence. The structured grid method was employed for the irregular boundary problems. The numerical model implemented the volume of fluid technique (VOF) for tracking and locating the free-surface. They concluded that if the number of steps increases, the energy dissipation will decrease. They also found that if the dimension of the steps increases, it could cause an increase in the energy dissipation rate.

Moreover, Sarfaraz et al. (2012) used a commercial programme called Flow-3D to study the location of the inception point for steeply sloping stepped spillway. Flow-3D was implemented for solving Reynolds-averaged Navier-Stokes equation in combination with two eddy-viscosity closure models. Flow-3D uses the finite volume approximation to discretise the domain. To investigate turbulence, two models could be used for calculations: the RNG k-ε model and the large eddy simulation (LES). A physical model with steep slope equal to 50 degrees has been conducted for comparison purposes with the Flow-3D programme. Generally, the results exposed a good level of agreement between the numerical result and the experiment result. Additionally, the LES showed more accurate solution compared to the RNG as the maximum relative error of the LES model was 4.1376%; however, it was 13.5046% for the RNG k-ε model. Furthermore, Rassaei and Rahbar (2014) conducted a study to investigate the effective parameters over stepped spillways like the number of steps, the height of steps and the flow velocity. This study was conducted numerically using the Fluent software. In this software, the governing equation has been solved by using the finite volume method. For the turbulence requirement, a standard k-ε model was employed. A regular mesh was used to determine boundary condition in addition to the VOF technique which is used to solve free surface flow. The results from the numerical model were compared with the

experimental results of different research. The results showed that when the number of steps increases, the energy dissipation rate will also increase.

Additionally, Chakib (2013) examined a method developed by Chanson to determine the location of inception point and to compare the velocity distribution with 1/6 law. These comparisons were carried out by using a numerical method named Fluent Computation Fluid Dynamic. In this method, VOF was used to simulate air-water interaction and k-ε standard turbulence method used for turbulence problem. The results showed that there is a good agreement between numerical method and experimental method.

To improve the results of the computational codes, a comparison between the finite element meshes and the finite volume meshes have been made by Shoja et al. (2013). The results from the numerical methods were compared with measured values. The error percentage of the finite element and the finite volume was 2.85% and 1.26% respectively. Therefore, the finite volume has shown more ability to provide more accurate information compared to the finite element. For the finite volume meshes, the Fluent software was used to conduct the simulation. It is important to mention that Fluent has used k-ε models which include RNG model for the turbulence modelling, in addition to the VOF technique that applied to simulate the two-phase flow. Mesh generation has been done by using GAMBIT software. For the finite element model, a code that developed in Fortran 90 was employed. The code was based on the discretisation and solving the poisson equations of stream and pressure through the Galerkin method.

To assess different numerical techniques, Kositgittiwong et al. (2013) analysed the velocity profiles over spillways by using a large-scale physical model and by using a CFD code. Five different types of turbulence model were used such as standard k-ε, realisable k-ε, renormalization group k-ε, standard k-w and shear stress transport k-w model. A comparison has been done between the results from experiment work and numerical work. Generally, the results showed that the five types of the numerical models worked well because all of them have provided good agreement with the experimental results. The k-w model was more accurate in simulating the lower regions of the velocity

profile while in the upper part of the velocity profile, the realisable k-ε model showed more accurate results. Furthermore, Vosoughifar et al. (2013) developed a CFD code called V-Flow by using Matlab. This code can model unsteady flow over stepped spillways in two-dimensions. The V- Flow code was coupled with GAMBIT software to model different spillways geometries using Voronoi mesh elements (unstructured meshes); they also used Finite Volume (FVM) to discretise the governing equation. The flow was considered to be in the laminar state without turbulence effect. The results validated with other results which were established from FLUENT software. Results showed good agreement in terms of velocity vectors, static pressures, streamlines, dynamic pressures and total pressures.

The Smoothed Particle Hydrodynamics (SPH) technique has been widely used to investigate many applications of hydraulics. Husain et al. (2013) carried out a numerical study to investigate the pressure distribution and cavitation damages over stepped spillways in the non-aerated zone under skimming flow conditions. An open source code called 2D SPHysics has used for this purpose by using Smoothed Particle Hydrodynamics (SPH) technique. The code was validated against the laboratory data of a broad crested weir and with a stepped spillway; the results showed good agreement between them in terms of water surface and velocity profiles at different sections, then the code was applied to observe the pressure variation over spillways steps. Cavitation index number for stepped spillway with 1V:2.5H slope was found between 0.6 and 0.7. The main finding of this study was that the close area to the outer step edge of the vertical face of the step can have cavitation due to the negative pressure.

Finally, Zindovic et al. (2014) used three different methods to investigate flow properties over stepped spillways. This study established a comparison between a scaled model, an empirical equation and a numerical model (Ansys Fluent Model). The results showed that there are acceptable agreements between the empirical and the numerical methods. However, there are considerable differences with the scaled model. The review revealed that many types of numerical models have been used to simulate flow over stepped spillways by using different equations and techniques. Some of these models were able to

give accurate results; however, some of the models could not achieve a good level of accuracy. That's probably due to the limitations of using specific equations or techniques. Therefore, the numerical models need to be selected with caution. To achieve that, the important issues which can impact the results significantly need to be considered such as the governing equation, the technique of solving the free surface, the turbulence model, the boundary conditions and the stability of the model.

2.6. Gabion stepped spillways

Gabions are one of the most common construction types for spillways in the African Sahel (Peyras et al., 1992). Gabions have been used widely in hydraulic structures like small earth dams, retaining walls, intakes and soil conservation work. Salmasi et al. (2012) state that there are many benefits of using gabions, such as ease of construction, structurally stable, flexibility and resistance to water load. The reason for these advantages could be related to flow through porous media; its porosity also could help the water to drain faster which can reduce the water load behind the structure.

Permeability has been neglected in many engineering applications; hence, many studies have considered turbulent flows over porous beds as equivalent to standard rough-wall turbulent boundary layers over impermeable beds (Manes et al., 2009). However, that might be not accurate as there is a significant difference between flow over permeable and impermeable obstacles.

It is important to mention that generally, non-slip conditions apply to solid surfaces. However, that might not be applicable for porous beds as the flow can go inside and between the particles. Thus, the interaction with the interstitial fluid can be observed. That kind of interaction includes mass, momentum and energy exchange between surface and subsurface flows (Zhang and Chanson, 2016a).

Many experimental and numerical studies have reported that permeability can affect significantly flow properties of the free surface (Manes et al., 2009). They claimed that

flow mechanism can play a vital role in increasing or decreasing friction factors and that could be linked to the shear penetration within the permeable bed which essentially can affect the boundary layer. Hence, increasing the flow resistance may increase the energy dissipation due to the momentum exchange between the surface and subsurface flows. The next section outlines the few studies which have been conducted about gabion spillways and all of these studies were accomplished experimentally.

Stephenson (1979) performed a study about energy dissipation over stepped gabions. Different geometries have been studied such as a stepped gabion with two to four steps and with four different slopes 1/1, 1/2, 1/3 and 2/3. The energy dissipation was calculated using the differences in depths between the upstream and the downstream. The result revealed that the relative energy dissipation could range from 25% to 85%; also, the outcome showed that the energy dissipation can increase with using more steps up to 3 but then it could reduce with increasing the number of steps. Moreover, Peyras et al. (1992) conducted an experimental study to investigate the energy dissipation over stepped gabion weirs. A one fifth scale ratio was selected to construct different models with 1/1, 1/2 and 1/3 downstream slope. Four configurations were tested: plain gabion, horizontal impervious concrete slabs, adverse impervious concrete slabs and end sills for different types of flow over the steps such as nappe flow and skimming flow. The results showed that gabion stepped weirs can withstand floods up to $3m^2/s$ without any damage. Kells (1994) studied the energy dissipation over a stepped gabion weir experimentally with different values for the critical depth over the crest. This study was done for two downstream slopes 1/1 and 1/2; the main finding was that 20% of energy can be dissipated due to the through-flow. No significant differences were noticed in the energy dissipation when the slopes change.

Chinnarasri et al. (2008) established an experimental study to investigate the hydraulic characteristics of gabion stepped weirs. Three stone types were used, i.e., (1) Stone I: crushed stone of about 25–35mm diameter; (2) Stone II: rounded stone of about 25–35mm diameter; and (3) Stone III: crushed stone of about 50–70mm diameter. Two components of flow were identified, base flow through the void between filled stones and

overflow on the gabions. The results showed that the energy dissipation ratios over gabion stepped weirs were greater than those in the corresponding horizontal stepped weirs by nearly 7%, 10%, and 14% for weir slopes of 30, 45, and 60°, respectively. Consequently, the outlet velocity was lower. Moreover, the results revealed that both stone size and stone shape had a small effect on the energy loss and flow velocity compared to the weir slope effect. The pressure on the step face of the gabion-stepped weirs was less than those in the horizontal steps due to the dampening influence of filled stones. The average pressure difference was approximately 29%.

Shafai-Bajestan and Kazemi-Nasaban (2011) conducted a study about the energy dissipation over gabion stepped spillways to assess the scour hole at the end of the spillway. The authors revealed that more energy dissipation will be expected when gabion stepped spillways use instead of concrete stepped spillways. Therefore, there is no need for using the stilling basin. It is crucial to mention that this kind of cases can be happened only when the stilling basin at the end of spillway is eliminated. Three different types of gabions spillway were used in the testing. Three different equations were suggested to calculate the local scour hole at the end of the spillway.

Salmasi et al. (2012) showed that over-flow and through–flow represent the essential two types of flow over gabion stepped spillways. In order to investigate energy dissipation over gabion stepped spillways, eight physical models were constructed. Some of these models were built up with permeable vertical and horizontal faces. However, some of them have impermeable faces. The gabion stepped spillway was one of the models that have vertical and horizontal permeable faces. The results showed that energy dissipation over gabion stepped spillways are more than those with impermeable vertical or horizontal faces. However, it was smaller compared to the energy dissipation over that stepped spillway with two impermeable faces. Steps with impervious vertical face have more energy dissipation from the horizontal impervious face. It is concluded that the energy dissipation might increase when the slope of gabion stepped spillways decreases which is opposite to the finding of Chinnarasri et al. (2008).

Wüthrich and Chanson (2014) carried out a laboratory study to investigate the hydraulic characteristics of flow such as flow patterns, air-water flow properties and energy dissipation over gabion stepped spillways and normal stepped spillways with 1V:2H slope and 0.1m step height. This study was conducted with a wide range of flow rates in order to investigate nappe, transition and skimming flow. The results showed that high velocities can be observed at the downstream end of gabion stepped spillways, and also small rates of energy dissipation can be achieved compared to smooth impervious steps. Moreover, friction factors for the gabions chute are lower than its magnitude for the impervious steps. Finally, Zhang and Chanson (2014) conducted a physical model to study the effect of the air entrainment on the steps cavity of gabion stepped spillways. A phase-detection probe, complemented by some videos was used to observe the air-flow characteristics. The results showed that there is a strong interaction between the steps cavity flow and the seepage through the gabion. Bubbly flowmotions were observed inside and over the gabion boxes which is why low levels of turbulence, velocity and aeration can be detected in the mainstream flow.

As mentioned above, the experimental studies have produced general and simple design guidelines for gabion stepped chutes. Key characteristics of practical engineering applications have been identified for normal stepped spillways which include guidelines for the inception point of air entrainment, pressures, cavitation damages, velocities, energy dissipation and flow depths. The same key characteristics will be investigated in this study for gabion stepped spillways.

It is well established that both of normal stepped spillways and gabion stepped spillways have great advantages in terms of prevention of cavitation damage, amount of entrained air and energy dissipation performance. Although there is a good understanding of the performance of normal stepped spillways, gabion stepped chutes with more complex designs are not well understood. Finding an optimum gabion stepped spillway design could improve the future designs of gabion stepped spillways.

While stepped spillways have been extensively studied using computational models, detailed numerical modelling studies on gabion spillways have not been recorded. This can be considered as one of the main objectives of this work as it could be challenging to simulate water flows over the porous media and inside the porous media at the same time. Therefore, in order to choose the numerical model for the current work, a full review has been established for most of the numerical models which are mentioned in section 2.5. Considering the capability to simulate the flow over and inside the porous media, NEWFLUME model has been selected to conduct the investigation for gabion stepped spillways.

As gabion porosity and grain size can affect the flow over gabion stepped spillways, both of them need to be investigated in detail in order to demonstrate their impact on the other important parameters such as pressure, inception point location, the growth of the boundary layer and energy dissipation. Different shapes of steps and different geometries of the spillways body will be tested with gabion. Finally, three different slopes with three different steps height will be tested to be able to optimise the design of gabion stepped spillways.

Chapter 3 : Numerical Model

3.1. Numerical model

Hydrodynamics studies have been conducted for many years experimentally by using water flumes or the wave tanks; however, due to advances in computer technology, numerical modelling has become a viable alternative. Ohyama and Nadaoka (1991) were the first researchers to introduce the terminology of numerical wave tank (NWT). The idea was to build up a virtual tank and a set of governing equations which can be solved using a computational method to get an accurate numerical model that can describe the flow phenomena. From the numerical results, flow quantities such as free surface, velocity and pressure and the other derived variables like vorticity, strain, stress and turbulence intensity could be directly collected. There are two types of NWT, the first for viscous fluids and the second for inviscid fluids. The second one is based on potential flow theory and can only be used for irrotational flows. The former NWT can solve Navier-Stokes equations (NSE) and Reynolds-Averaged Navier-Stokes (RANS) equations. Lin and Liu (1998) developed a two-dimensional RANS model for simulating breaking waves. They undertook extensive verification of their numerical results against experimental data. That model has passed through various stages of development since then. Lin and Xu (2006) developed a general-purpose model after combining all the previous works together. The new model which can simulate the interaction between the turbulent free surface flows with different structures. The model is called NumErical Water FLUME and is termed NEWFLUME in the following.

NEWFLUME has the ability to simulate different types of flows such as turbulent flows with rapidly changing free surface, breaking waves, dam break flows, tidal bores and hydraulic jumps. NEWFLUME solves Reynolds-averaged Navier-Stokes equations as governing equations in two dimensions. The Reynolds-averaged Navier-Stokes equation has been implemented in the numerical models because of its ability to simulate many applications like fluid-structure interaction and that can be conducted with permeable and

impermeable structures (Lin and Liu, 1998). This represents the main reason for selecting this model in the current work. Additionally, NEWFLUME model has not been used previously to simulate water flow over gabion stepped spillways under dam break conditions.

The model has been validated against many different problems including breaking waves overtopping a seawall with a porous armour layer, flow forces on submarine pipelines, dam break, jets (plane and submerged), hydraulic jumps and water exiting from a circular cylinder, (Lin and Xu, 2006). All the results showed very good agreement with experimental data, providing reassurance that the code will be able to simulate the flow over stepped spillways. The technical description of the model follows that of Lin and Xu (2006) and is reproduced here for completeness 'sake'.

The velocity field and the pressure field for the full flow can be divided into two parts

1. The mean velocity and pressure, $\langle u_i \rangle$ and $\langle p \rangle$.
2. The turbulent velocity and pressure, $\grave{u}_\imath$ and $\grave{p}$.

$$u_i = \langle u_i \rangle + \grave{u}_\imath \tag{3.1}$$

$$p = \langle p \rangle + \grave{p} \tag{3.2}$$

in which i = 1, 2 for a two-dimensional flow. Reynolds equations for an incompressible fluid have been used as the governing equation of the mean motion of turbulent flows.

$$\frac{\partial \langle u_i \rangle}{\partial x_i} = 0 \tag{3.3}$$

$$\frac{\partial \langle u_i \rangle}{\partial t} + \langle u_j \rangle \frac{\partial \langle u_i \rangle}{\partial x_j} = -\frac{1}{\rho}\frac{\partial \langle p \rangle}{\partial x_i} + g_i + \frac{1}{\rho}\frac{\partial}{\partial x_j}\left(\mu \frac{\partial \langle u_i \rangle}{\partial x_j} - \rho \langle \grave{u}_\imath \grave{u}_j \rangle\right) \tag{3.4}$$

where,

$\langle u_i \rangle$ the mean velocity in the i directions ($m.s^{-1}$)

$\langle p \rangle$ mean pressure ($KN.m^{-2}$)

$\boldsymbol{\rho}$ fluid density ($Kg.m^{-3}$)

g_i gravitational acceleration in the i direction ($m.s^{-2}$)

$\boldsymbol{\mu}$ molecular viscosity ($m^2.s^{-1}$)

$\langle \grave{u}_\imath \grave{u}_j \rangle$ Reynolds stress ($KN.m^{-2}$)

It is worth mentioning that the mean viscous stress can be given as

$$\langle \tau_{ij} \rangle = \mu \frac{\partial \langle u_i \rangle}{\partial x_j} + \mu \frac{\partial \langle u_j \rangle}{\partial x_i} \quad (3.5)$$

Reynolds stress has been calculated by using nonlinear eddy viscosity model. This model uses mean velocity, turbulence kinematic energy (k) and dissipation rate of turbulence (ε). k-ε transport equation has been used to calculate the last two parameters k and ε (Lin and Xu, 2006).

$$\frac{\partial k}{\partial t} + \langle u_j \rangle \frac{\partial k}{\partial x_j} = \frac{\partial}{\partial x_j}\left[\left(\frac{v_t}{\sigma_k} + v\right)\frac{\partial k}{\partial x_j}\right] - \langle \dot{u_i}\dot{u_j} \rangle \frac{\partial \langle u_i \rangle}{\partial x_j} - \varepsilon \frac{\partial \varepsilon}{\partial t} + \langle u_j \rangle \frac{\partial \varepsilon}{\partial x_j} \quad (3.6)$$

$$\frac{\partial \varepsilon}{\partial t} + \langle u_j \rangle \frac{\partial \varepsilon}{\partial x_j} = \frac{\partial}{\partial x_j}\left[\left(\frac{v_t}{\sigma_\varepsilon} + v\right)\frac{\partial \varepsilon}{\partial x_j}\right] - c_{1\varepsilon}\frac{\varepsilon}{k}\langle \dot{u_i}\dot{u_j} \rangle \frac{\partial \langle u_i \rangle}{\partial x_j} - c_{2\varepsilon}\frac{\varepsilon^2}{k} \quad (3.7)$$

where,

v and $v_t = \frac{c_{d*}\, k^2}{\varepsilon}$ Kinematic and eddy viscosity respectively ($m^2.s^{-1}$)

$c_d = \frac{2}{3}\left(\frac{1}{7.4+s_{max}}\right)$ where $s_{max} = \frac{k}{\varepsilon}$ max $\left[\left|\frac{\partial \langle u_i \rangle}{\partial x_i}\right|\right.$ (indices not summed)].

The recommended values for the empirical coefficients are $\sigma_k = 1.0, \sigma_\varepsilon = 1.3, c_{1\varepsilon} = 1.44$ and $c_{2\varepsilon} = 1.92$ (Rodi, 1980).

The mean flow in porous media is governed by

$$\frac{\partial \bar{u}_i}{\partial x_i} = 0 \quad (3.8)$$

$$\frac{1+C_A}{n}\frac{\partial \bar{u}_i}{\partial t} + \frac{\bar{u}_j}{n^2}\frac{\partial \bar{u}_i}{\partial x_j} = -\frac{1}{\rho}\frac{\partial \bar{p}}{\partial x_i} + g_i + \frac{\nu}{n}\frac{\partial^2 \bar{u}_i}{\partial x_j \partial x_i} - g a_p \bar{u}_i - g b_p \sqrt{\bar{u}_k \bar{u}_k}\bar{u}_i \quad (3.9)$$

where,

$\bar{u}_i$ is the i-th component of the mean velocity

n porosity of the porous medium

C_A, a_p and b_p coefficients of the porous medium

Subscript k refers to the summation of velocities in two directions

The coefficients in above equations are found to be

$C_A = \gamma_p \frac{1-n}{n}$

$a_p = \alpha \frac{(1-n)^2}{n^3}\frac{\nu}{g D_{50}^2}$

$b_p = \beta\left(1 + \frac{7.5}{KC}\right)\frac{1-n}{n^3}\frac{1}{g D_{50}}$

where $\gamma_p = 0.34, \alpha = 200, \beta = 1.1, KC = \frac{\sqrt{\bar{u}_k \bar{u}_k}\, T}{n D_{50}}$

The initial conditions for the mean flow and pressure distribution are required by the model across the whole computational domain. These initial conditions can be taken from the initial stationary flow at the start of the test with zero mean velocity and hydrostatic pressure. Also, from the analytical solutions and laboratory measurements, mean velocities could be determined along with initial free surface displacements. The mean flow is treated like still water with no waves or current motions in the initial conditions.
The model has the normal different types of boundary conditions. No-slip boundary condition and free-slip boundary condition are imposed on the solid boundary of the mean flow field. However, by neglecting the effect of the air flow, the zero-stress condition can be imposed on the mean free surface.

The no-slip boundary conditions can be used when the viscous boundary layer is resolved while the free-slip condition might apply when the viscous boundary layer is not resolved; the latter condition could be more fitting for the solid boundary, therefore, the log-law distribution of mean tangential velocity in the turbulent boundary layer can be used for the turbulence field near the solid boundary. The values of k and ε can be shown as functions of distance from the boundary and the mean tangential velocity outside of the viscous sublayer.
For the free surface, the gradients of k and ε can be set to zero

$$\frac{\partial \mathrm{k}}{\partial \mathrm{n}} = 0$$

$$\frac{\partial \varepsilon}{\partial \mathrm{n}} = 0$$

where n is the unit normal on the free surface. The assumption behind these conditions is that there is no turbulent exchange between the water and the air.
If the k value is equal to zero then the production term and the dissipation term for ε will be singular; moreover, the model will not be able to produce turbulent energy as there is no initial turbulent kinetic energy. Therefore, it is very important to set the initial k-value to a small non-zero value:

$$\mathrm{k} = \frac{1}{2}\mathrm{u_t^2}$$

with $\mathrm{u_t} = \delta_c\, \mathrm{c_r}$ where $\mathrm{c_r}$ is the wave celerity at the inflow boundary and $\delta_c = 2.5 \times 10^{-3}$.

The value of ε in the model can be found from $\varepsilon = c_\mu \frac{k^2}{v_t}$ with $v_t = 0.1v$ and $c_\mu = 0.09$.

For free surface tracking, the NEWFLUME model uses the volume of fluid method (VOF).The method was established originally by Hirt and Nichols (1981) and subsequently adjusted by Kothe et al. (1991). The VOF equation for incompressible flow is

$$\frac{\partial F}{\partial t} + \langle u_j \rangle \frac{\partial F}{\partial x_j} = 0 \tag{3.10}$$

where

F is the volume of fluid function. This refers to the fraction of fluid in the cell. Thus,

F=1 means that the cell is completely full

F=0 means that the cell is empty

F between 1 and 0 means that the fluid surface lies within the cell

There are two main benefits from using VOF, firstly, it needs the minimum storage for the computations, and secondly, the VOF can avoid issues with the intersecting surfaces due to its ability to follow the regions rather than boundaries.

Finite difference technique is employed to approximate all partial differential equations. It is crucial to mention that the earlier Navier-Stokes equation solver RIPPLE which was developed by Kothe et al. (1991) has been used to do the calculation for the mean flow outside the porous media. A finite difference technique involving a two-step projection method is used to solve the momentum equations, which reads,

$$\frac{u_i^{n+1} - u_i^n}{\Delta t} + u_j^n \frac{\partial u_j^n}{\partial x_j} = -\frac{1}{\rho^n} \frac{\partial p^{n+1}}{\partial x_i} + g_i + \frac{\partial \tau_{ij}^n}{\partial x_j} \tag{3.11}$$

into two steps, i.e., step 1:

$$\frac{\tilde{u}_i^{n+1} - u_i^n}{\Delta t} = -u_j^n \frac{\partial u_j^n}{\partial x_j} + g_i + \frac{\partial \tau_{ij}^n}{\partial x_j} \tag{3.12}$$

and step 2,

$$\frac{u_i^{n+1} - \tilde{u}_i^{n+1}}{\Delta t} = -\frac{1}{\rho^n} \frac{\partial p^{n+1}}{\partial x_i} \tag{3.13}$$

In this method, the code can estimate the velocity in the first step without the pressure gradient term; however, the velocity will be corrected in the second step by using the updated pressure field.

$$\frac{\partial}{\partial x_i}\left(\frac{1}{p^n}\frac{\partial p^{n+1}}{\partial x_i}\right) = \frac{1}{\Delta t}\frac{\partial \tilde{u}_i^{n+1}}{\partial x_i} \tag{3.14}$$

The Poisson pressure equation could be derived from combined equations 3.13 and equation 3.3,

$$\frac{\partial \langle u_i{}^{n+1}\rangle}{\partial x_i} = 0 \tag{3.15}$$

The governing equations for the flow through the porous media have the same structure as RANS equations; however, Reynolds stresses are replaced by the linear and nonlinear friction. The two-step projection technique can be used also for the flow calculation through the porous media. On the interface between the porous media and outside flow, the continuity of the pressure and the velocity is satisfied. The central difference method is applied to discretise all the pressure and stress gradient in the projection method. The upwind scheme is combined with the central difference to discretise the advection terms and for the k-ε transport equations.

The default set up is to use a fixed rectangular mesh system (m cells by n cells) to discretise the computational domain. All the scalar quantities such as pressure, eddy viscosity and turbulence intensity are specified at the cell centres while the vector quantities like velocities are given at the cell nodes. Also, the model has the ability to utilise both uniform and non-uniform meshes. A uniform mesh is normally applied when accurate results are required, however, in terms of computational cost, non-uniform meshes can reduce the running time. Here, accuracy of calculations is paramount and uniform grids are used.

As a result of the discretisation of time derivative and convection terms, numerical errors arise. Other errors may come from the VOF method. All the numerical errors caused by convection terms and the discretisation of time derivative can be determined analytically. The numerical viscosity v_n in two dimensional problems with $\Delta x \approx \Delta y$ and $|\langle u\rangle| \approx |\langle v\rangle|$

can be estimated from equation (3.16). The reason is that the leading errors have the same effect as momentum diffusion by the molecular viscosity.

$$v_n \approx \frac{|\langle u \rangle| \Delta x}{2}\left(\alpha - \frac{|\langle u \rangle| \Delta t}{\Delta x}\right) \approx \frac{|\langle v \rangle| \Delta y}{2}\left(\alpha - \frac{|\langle v \rangle| \Delta t}{\Delta y}\right) \quad (3.16)$$

where α is the weighting function between the central difference method and the upwind method and it normally set to 0.3. The flow dissipation rate due to the numerical viscosity is proportional to the product of the numerical viscosity v_n and squares of mean velocity gradients. The order of both the magnitude of v_n and velocity gradients need to be estimated to be able to find how numerical errors can affect the true solutions. The Courant number should be less than or equal to 0.3 for all computational cells in order to achieve numerical stability.

$$C_r = \max\left[\frac{|\langle u \rangle| \Delta t}{\Delta x}, \frac{|\langle v \rangle| \Delta t}{\Delta y}\right] \quad (3.17)$$

The Courant number depends on velocity, cell-size and time step.

$$\text{CFL} \equiv \frac{V \Delta t}{\Delta x} \quad (3.18)$$

where v is the characteristic speed, Δt is the time-step of the numerical model, and Δx is the spacing of the grid in the numerical model. A flowchart showing the NEWFLUME model key routines is shown in Figure 3.1.

To be able to measure the water depth, horizontal velocity and vertical velocity at different locations during the numerical simulations, a simple development has been applied to the NEWFLUME code. This development is conducted by implanting gauges to measure and record the water depth and the velocity values with time.

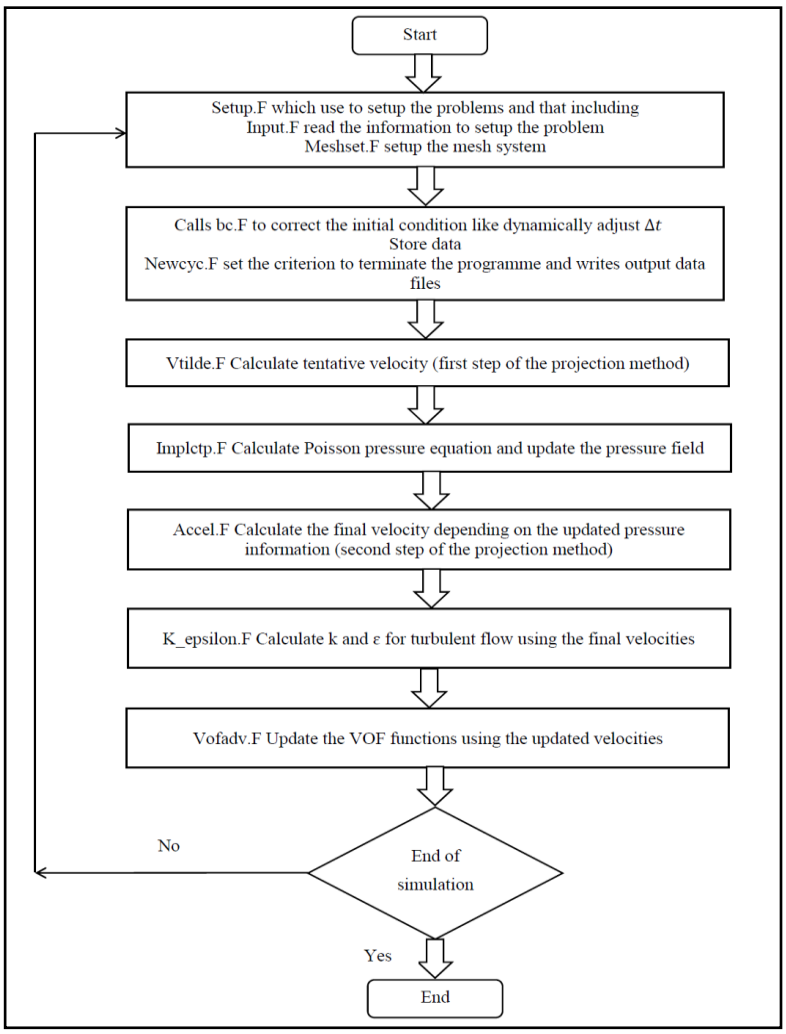

Figure 3.1 Sketch of the numerical process.

3.2. Broad crested weir validation

Since the main purpose of this investigation is to determine the characteristics of flow over gabion stepped spillways such as discharge, velocity, and free surface depth, an initial validation test has been conducted against the laboratory model study for flow over a broad crested weir reported by Hager and Schwalt (1994). The experimental set up of Hager and Schwalt (1994) has been recreated in the computational model to allow a direct comparison for free surface profiles, pressure distributions and velocity profiles.

Broad-crested weirs are one type of hydraulic structure which is used for measuring the flow rate. Over the crest of the weir, three different types of flow can be observed (Chow, 1959):

1) Subcritical flow found when the depth of the water is high and normally occurs on the upstream side of the weir where the Froude Number, (Fr), is less than 1;
2) Supercritical flow found when the depth of the water is small and often observed at the downstream end of the weir (Fr>1);
3) Critical flow, found where Fr=1, and represents the transition flow from subcritical to supercritical.

Hager and Schwalt (1994) conducted experiments in a rectangular flume of length 7m, width 0.499m, and height 0.7m. The broad crested weir dimensions were 0.5m (length), 0.401m (height) and 0.449m (width). The upstream water depth above the crest varied between 0.0509m and 0.2047m.

For validation purposes, the same dimensions were set up in the computational model. The weir was placed after 4.82m of the domain from the left solid wall with initial water depth equals to 0.375m (Figure 3.2). Non-slip conditions were imposed on the top, bottom and left sides of the domain while the right-hand side of the domain was set to be an open boundary condition to allow the water to leave the domain. The fluid was initially at rest and the first time step was set to 10^{-4} seconds according to the Courant stability criterion. The model was set to simulate a period of 19 seconds. Uniform mesh size was used in the x-direction and y-direction with resolution 0.01m and 0.004m respectively. The water upstream of the weir was held in place by a virtual barrier. At t=0 the barrier is removed and the water begins to move over the crest weir due to water head and gravitational acceleration.

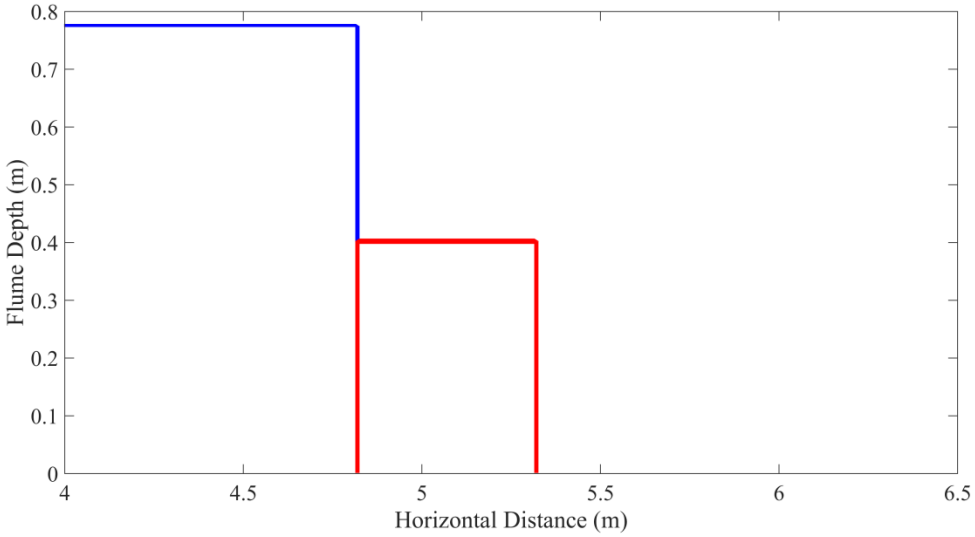

Figure 3.2 Broad crested weir set-up

At 0.52s, the water reaches the floor at the downstream end of the weir. As some particles of water moved towards the weir body, nappe flow started to form. It is crucial to mention that nappe flow condition was achieved when the non-slip condition used in the setup of the numerical model, however, it was not achievable with free slip conditions. Therefore, non-slip condition results were selected to be compared with the experimental results. Snapshots of flow over the broad crested weir at different times are shown in Figure 3.3.

To compare the computational and experimental results, the relative error index is used, which can be calculated by

$$R = \frac{q_{num.} - q_{exp.}}{q_{exp.}} * 100\% \qquad (3.19)$$

where $q_{num.}$ is the numerical discharge and $q_{exp.}$ is the experimental discharge.

To compute the discharge over the broad crested weir, the critical section needs to be determined by testing where the Froude number equals one. The discharge was calculated by multiplying the water depth by the velocity at the critical section. The results showed very good agreement between the experiment and the numerical result with a maximum relative error of 3.43% (Table 3.1). The free water surface for different discharges has been compared from the numerical and experimental work. Points for comparison have

been selected at the upstream side and also on the crest of the weir. The results showed acceptable relative error on the upstream side. The maximum relative error of the free surface profile at the upstream side has been observed when the discharge equals to $0.1364 m^2 s^{-1}$. The relative error was 4.8%. For the same discharge, there were very good agreements on the downstream side of the weir with a maximum relative error of 1.7% (Figure 3.4).

Table 3.1 A comparison between experimental and numerical values of discharge.

Measurement Number	Time(s)	$q_{exp}(m^2s^{-1})$	$q_{num}(m^2s^{-1})$	Relative error (%)
1	4.48	0.1364	0.1352	-0.88
2	4.78	0.1099	0.1091	-0.73
3	5.43	0.0753	0.0771	2.39
4	9.18	0.0521	0.0509	-2.30
5	13.26	0.0357	0.0358	0.28
6	16.90	0.0218	0.0226	3.43

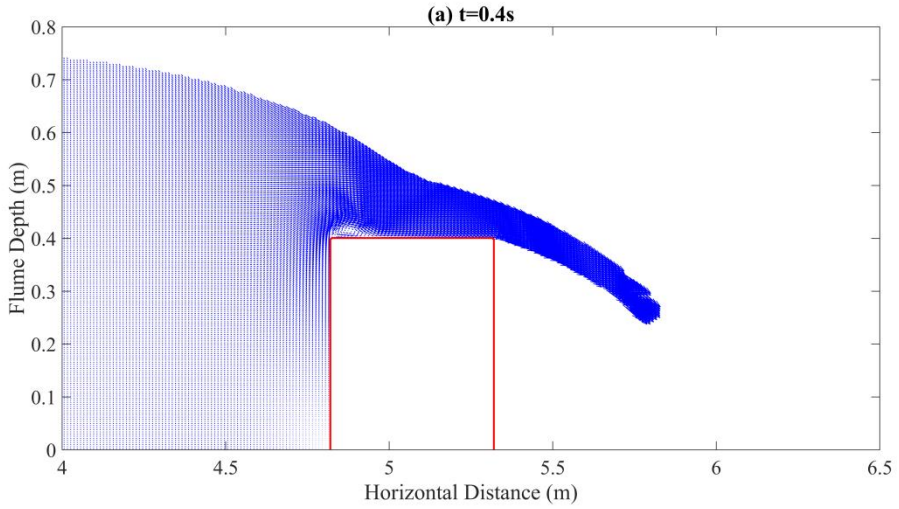

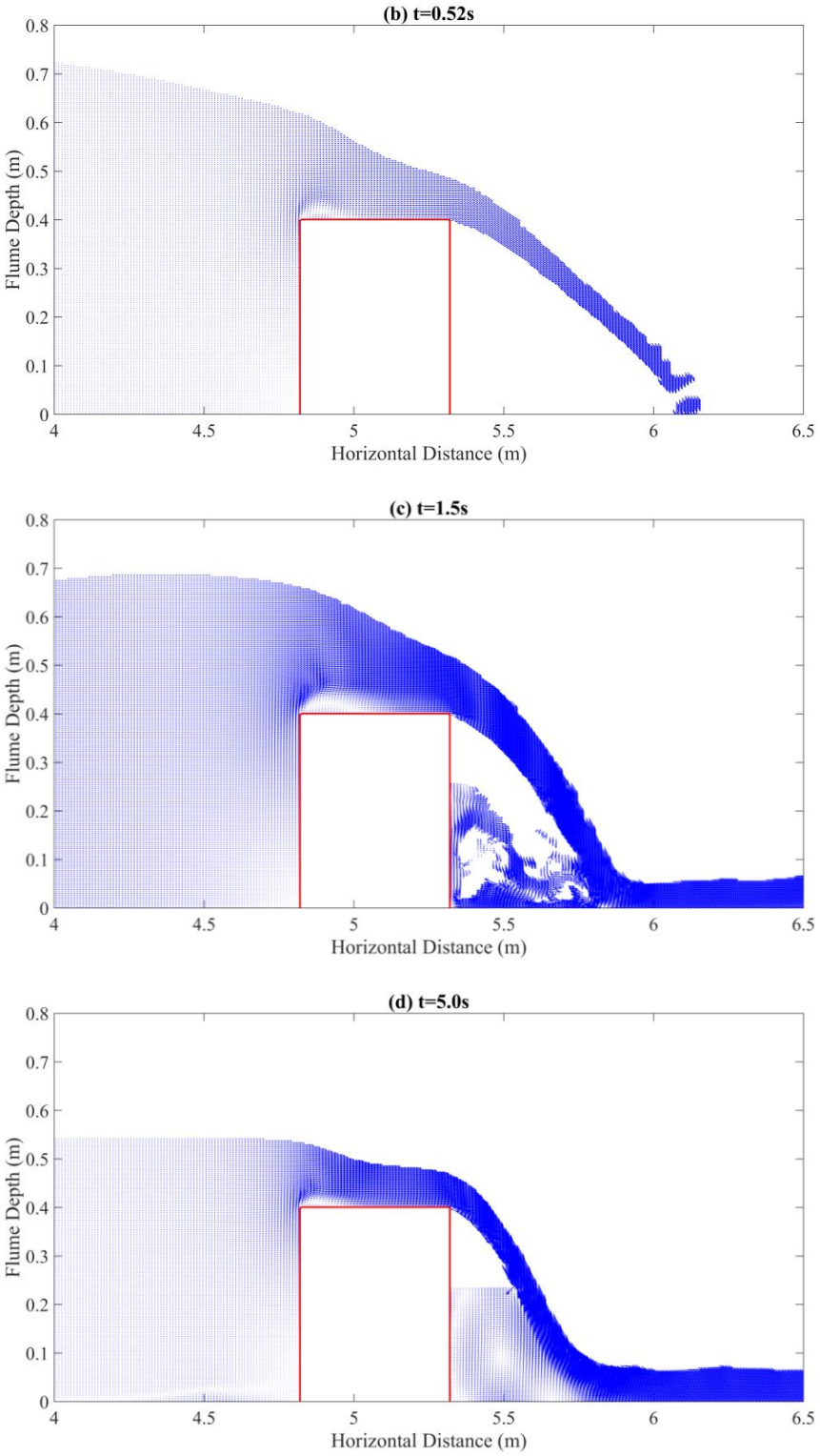

Figure 3.3 Snapshots of velocity vectors to show the free surface over the broad crested weir at: (a) t=0.4s; (b) t=0.52s; (c) t=1.5s; (d) t=5s.

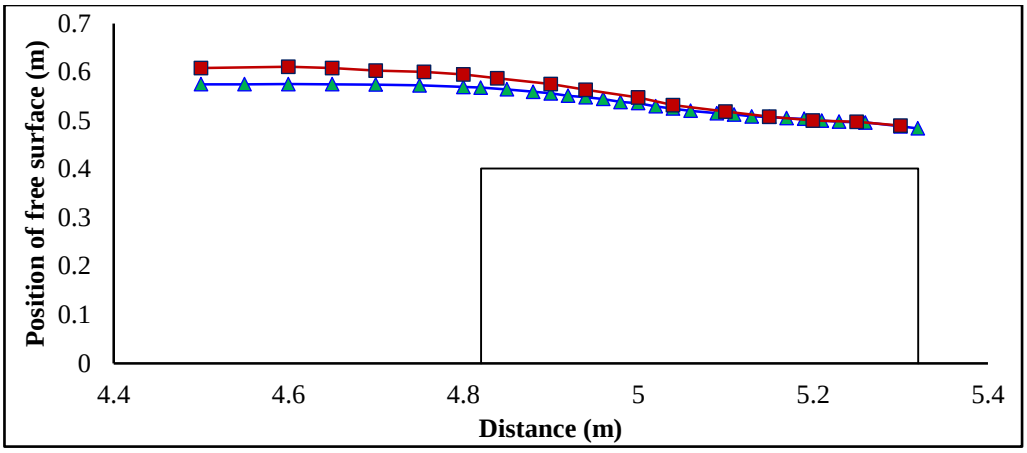

(a) $q=0.1364 m^2 s^{-1}$

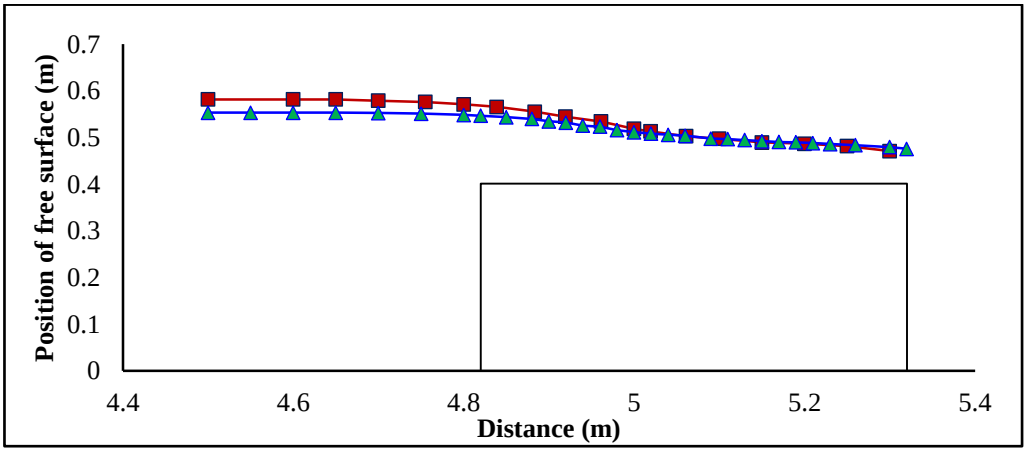

(b) $q=0.1099 m^2 s^{-1}$

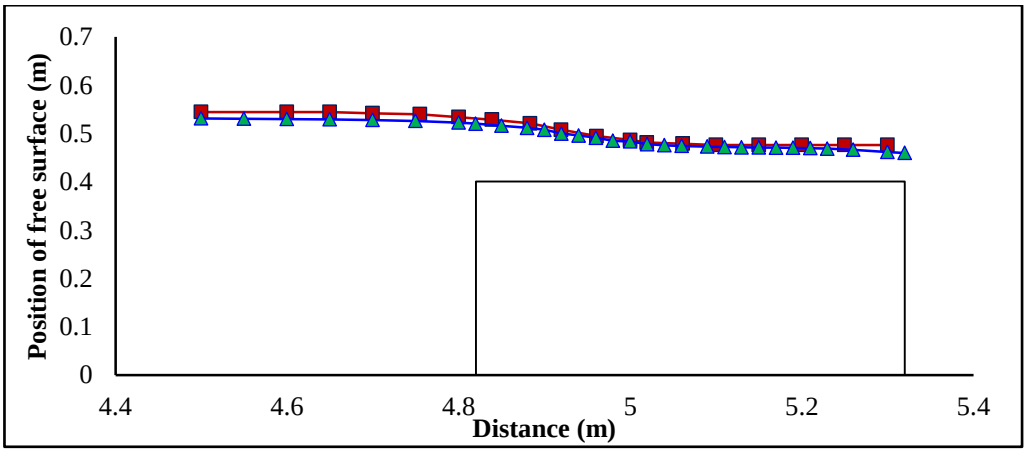

(c) $q=0.0753 m^2 s^{-1}$

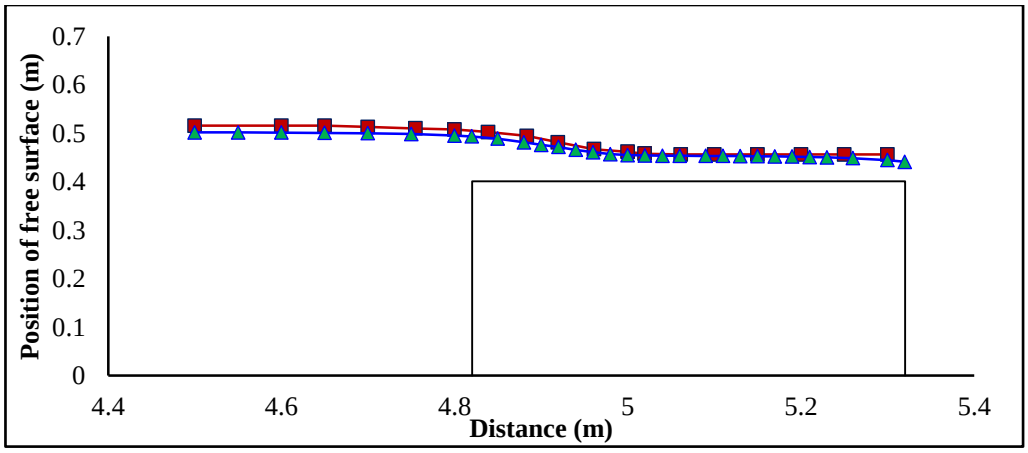

(d) $q=0.0521 m^2 s^{-1}$

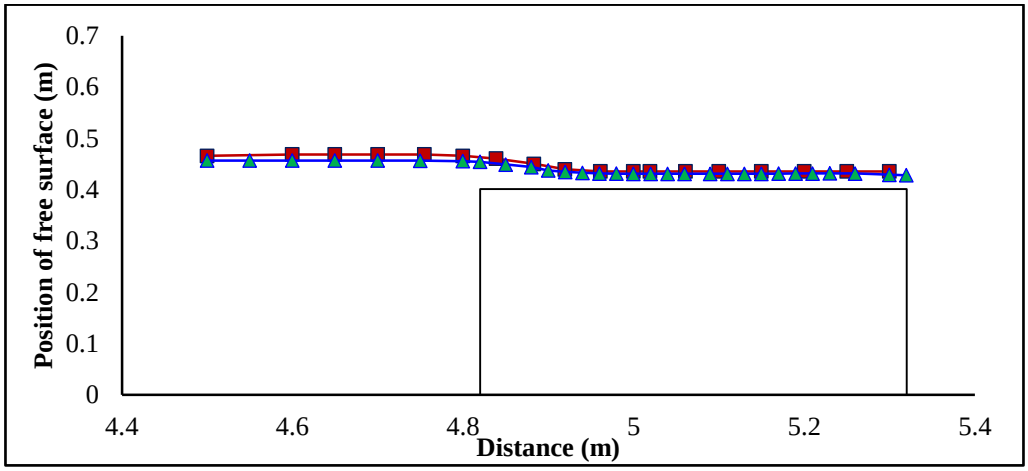

(e) $q=0.0218 m^2 s^{-1}$

Figure 3.4 A comparison between experimental work (square) and numerical work (triangle) for different discharges.

Hager and Schwalt (1994) measured the pressure over the crest of the weir and presented results in the form of normalised pressure heads calculated as $p/\sqrt{\rho g H}$ where p represents the pressure, $\boldsymbol{\rho}$ water density and H represents the total head at the upstream side. The numerical results again showed very good agreement with the experiment results with the relative error being less than 1% for the maximum pressure and approximately 6% for the minimum pressure. The good level of agreement between the computational and experimental results for this case provided reassurance that the numerical flume could simulate the flows over a stepped spillway (Table 3.2).

Table 3.2 A comparison between experimental and numerical values of the pressure at different places over the broad crested weir

x/H	Pressure values (Exp.)	Pressure values (Num.)	Relative error (%)
0.8766	0.7383	0.698	-5.463
0.9314	0.7394	0.714	-3.441
0.9862	0.7355	0.725	-1.433
1.0410	0.7310	0.73	-0.147
1.0958	0.7255	0.725	-0.067
1.1506	0.7182	0.716	-0.310
1.2053	0.7098	0.7025	-1.035
1.2601	0.7031	0.689	-2.012
1.3149	0.6909	0.6755	-2.223
1.3697	0.6802	0.662	-2.683
1.4245	0.6691	0.6485	-3.076
1.4793	0.6585	0.635	-3.564
1.5341	0.6467	0.6215	-3.904
1.5889	0.6350	0.608	-4.254
1.6437	0.6233	0.5945	-4.618
1.6984	0.6088	0.581	-4.560
1.7532	0.5976	0.5675	-5.035
1.8080	0.5864	0.554	-5.529
1.8628	0.5697	0.5405	-5.120
1.9176	0.5602	0.527	-5.922
1.9724	0.5417	0.5135	-5.213
2.0272	0.5306	0.5	-5.762

Hager and Schwalt (1994) measured the velocity profile at different four points over the weir crest under the maximum discharge condition. These profiles were compared with two different results of two different sizes of the mesh grids. In order to investigate the sensitivity of the results on the mesh size, the same run was conducted with mesh size of 0.008m in the x-direction and 0.02m in the y-direction. Hager and Schwalt (1994) conducted their calculation based on the normalised velocity head (V) which is calculated by $^{v}/_{\sqrt{2gH}}$ where u represents the velocity parallel to the flow and H represents the total head at the upstream side. The results showed good agreement with the experimental work for both of the grids; especially at the second point where negative velocities occur due to the eddy circulation near the upstream corner of the weir. However, Figure 3.5 clearly shows that the smaller grid size which is titled numerical data 2 (0.01m in x-direction and 0.004m in y-direction) has more points closer to the experimental velocity profile than the bigger grid size which titled numerical data 1 (0.02m in x-direction and 0.008m in y-direction).

The maximum relative error has been achieved at x/H=0. The relative error was around 34% for the coarse meshes; conversely, it was around 20% for the small grids. The results showed good agreement at x/H=0.5 and x/H=2 with maximum relative errors of 8% and 16% for the small and coarse grids respectively. The relative error was less than 5% in many points when the small mesh size applied instead of the coarse grid. Therefore, using small mesh sizes can remove the potential errors which can come from using coarse resolution.

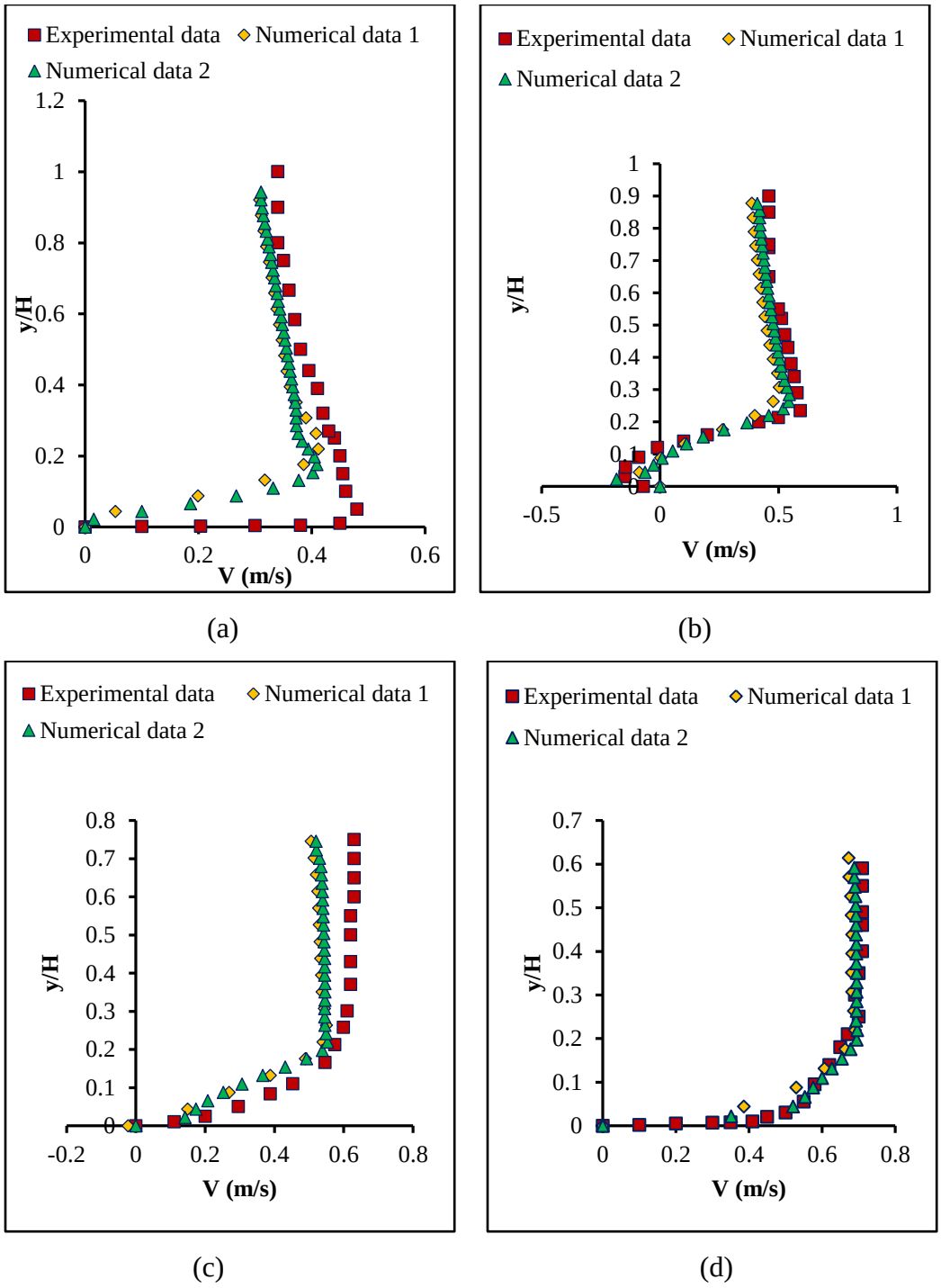

Figure 3.5 A comparison between the experimental and numerical velocity profiles triangle at sections: (a) x/H=0; (b) x/H=0.5; (c) x/H=1 and (d) x/H=2.

3.3. Skimming flow over stepped spillways

The simulation of skimming flow over stepped spillways presents a significant challenge for computational models because of many issues including:

- Complicated structural geometry;
- The flow accelerates very quickly and therefore can transition from subcritical to supercritical;
- A growth in the turbulent boundary layer thickness as the water flow accelerates down the spillway.

To test the performance of the numerical flume under these complex conditions, laboratory data from three different spillways configuration and flow regimes have been used. In each case, attempts to recreate the experimental set-up of the laboratory experiment in the numerical flume have been established.

The locations of the inception point and the discharge values have been selected as key parameters to compare the numerical and experimental work. Both parameters provide a good level of testing for the numerical model. It is important to have accurate representation for complicated flows over stepped spillways. Also, it is crucial to capture the development of the turbulent boundary layer when the flow accelerates down the spillway so that the location of the inception point can be determined accurately (see e.g, Hunt and Kadavy, 2010; Meireles and Matos, 2009 and Hunt and Kadavy, 2013).

The three comparison tests are the experiments reported by Meireles and Matos (2009), Chanson and Toombes (2002), and Hunt and Kadavy (2013). These three studies have a range of different conditions that provide a rigorous test of the model's performance. Specifically, the three cases vary in terms of discharge and spillway geometry, including the slope as well as the number and width of steps.

3.3.1. Stepped spillways of 1V:2H slope

Meireles and Matos (2009) used a stepped spillway of height 0.5m and 1V:2H slope for a wide range of flow rates. A broad crested weir was installed before the spillway chute

with 0.5m length and 0.5m height to measure the flow rate at the critical sections. The weir had a semi-circular edge at the upstream corner of the weir to prevent flow separation. From hydraulic considerations, the broad crested weir has sufficient length to determine the critical sections (Chow, 1959).

To maintain calm conditions and to achieve the required discharge, the area for the upstream tank was set to be 7.0m of length and 0.85m of depth. Thus, the initial water elevation over the crest was fixed to 0.35m. A uniform mesh size was used to discretise the domain with a grid size of 0.005 m in the horizontal, (x-direction), and 0.0025m in the vertical, (y-direction). The total time for the simulation was 16 seconds and the initial time step is 0.0001 seconds to achieve the stability requirement (Figure 3.6).

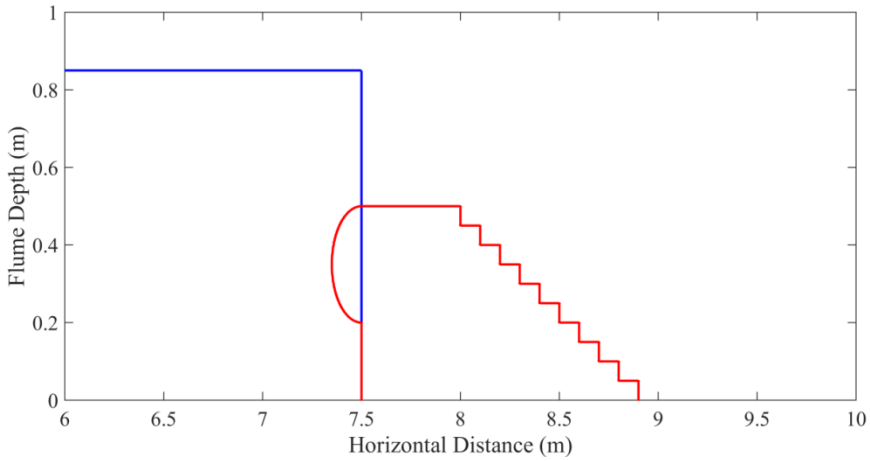

Figure 3.6 The initial conditions of Meireles and Matos (2009) spillway.

In order to investigate the sensitivity of mesh sizes on the result, another mesh size has selected to compare the velocity distribution over steps; the second mesh size is 0.01m in the x-direction and 0.005m in the y-direction. As can be seen in Figure 3.6, the numerical data 1 which represents the smaller mesh size has shown better results compared to the numerical data 2 at all positions where velocity distribution has been measured. Figure 3.6 also illustrates that the velocity profiles showed very good agreement near the free surface where most of calculations are conducted. The results showed that the maximum relative error for the small mesh size was around -1.8% near the free surface; however, it was around 9% for the coarse mesh size.

The small mesh size has been selected to conduct more comparison with the experimental data although it required long time of computation. More comparisons of different parameters like discharge values and inception point location are investigated later by using the numerical results of the small mesh size. It is worth to mention that depending on the sensitive study of the mesh size, the number of grids in both directions would be preferred to be around 35 grids to be able to capture good results. Furthermore, as the mesh size is decreased smaller time steps are required, particularly for the initial time steps, in order to achieve the Courant stability condition.

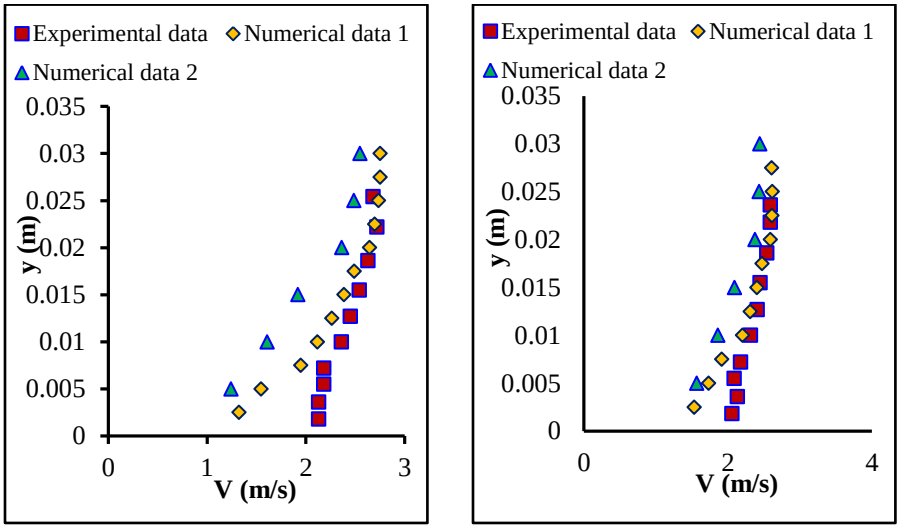

(a) $q=0.06982 m^2 s^{-1}$ (b) $q=0.06006 m^2 s^{-1}$

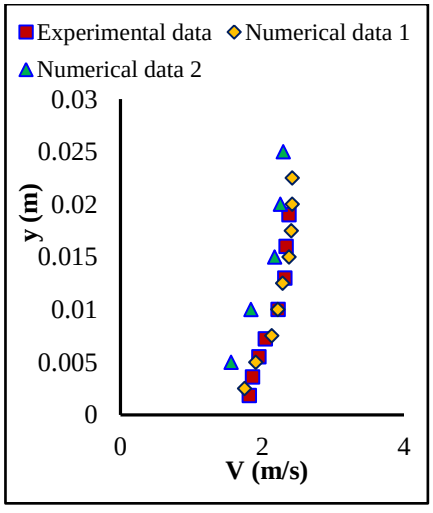

(c) $q=0.050137 m^2 s^{-1}$

Figure 3.7 A comparison between the experimental data and the numerical data at the inception point.

Skimming flow was achieved after 5.48 seconds. Figure 3.8 shows snapshots at different selected times. In Figure 3.8d, skimming flow was not established because of air pockets present on the first step; however, in Figure 3.8e, the skimming flow was established. In Figure 3.8f, the results showed that velocities near the steps are small because of the circulation phenomenon. To show that in the visualisation, light colours are used for small velocities and dark colours for high velocities. The initial water depth over the crest is fixed to 0.35m in order to achieve the required values of discharge to conduct the comparison with the experimental results. However, using a small value for the initial water depth might not be sufficient to achieve the required discharges as huge amount of the upstream water can be wasted before attaching the skimming flow conditions.

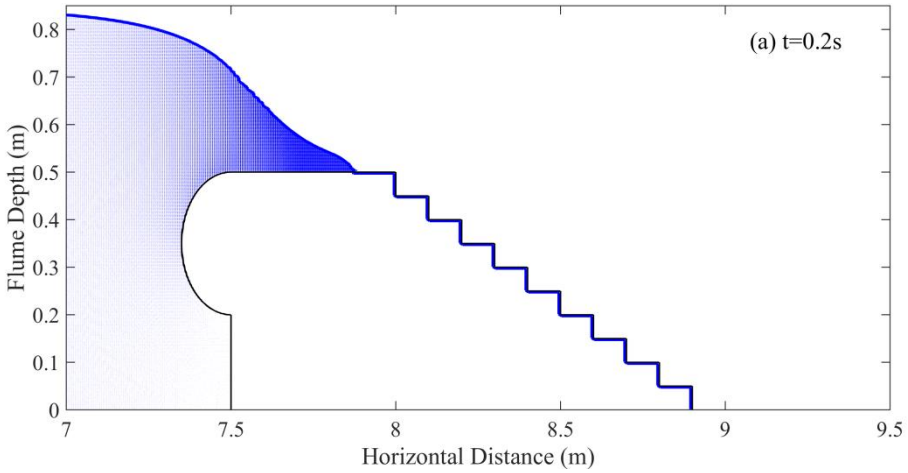

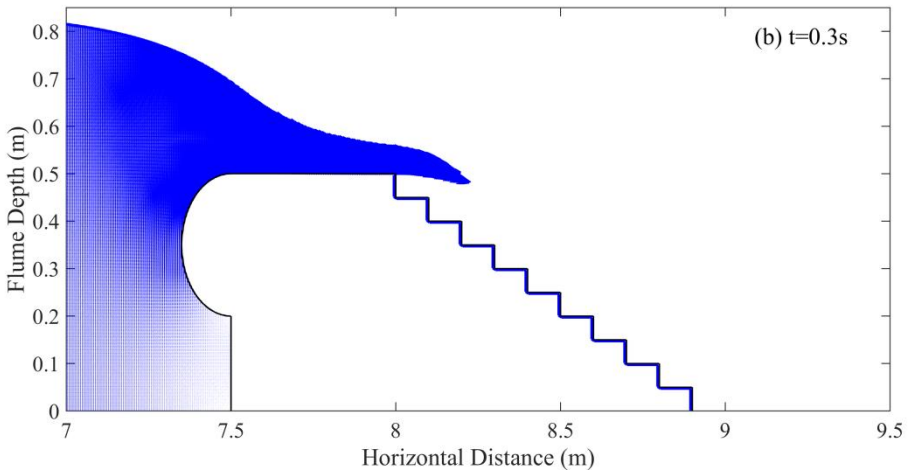

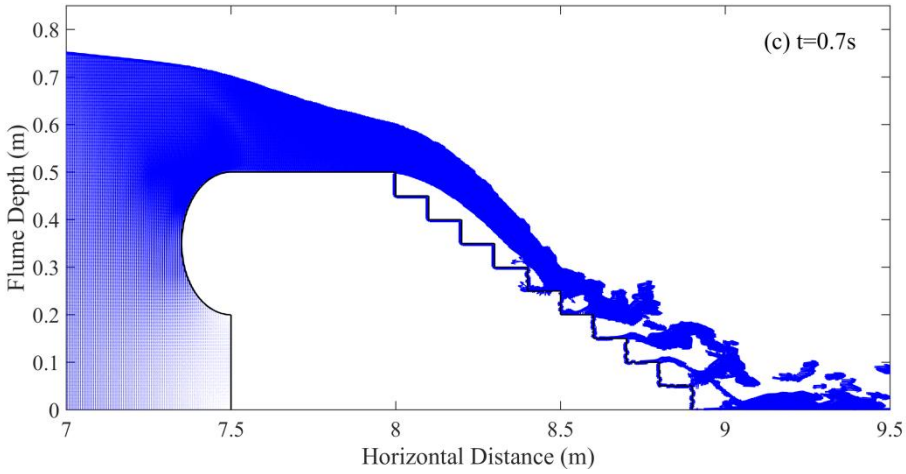
(c) t=0.7s
Flume Depth (m)
Horizontal Distance (m)
0
0.1
0.2
0.3
0.4
0.5
0.6
0.7
0.8
7
7.5
8
8.5
9
9.5

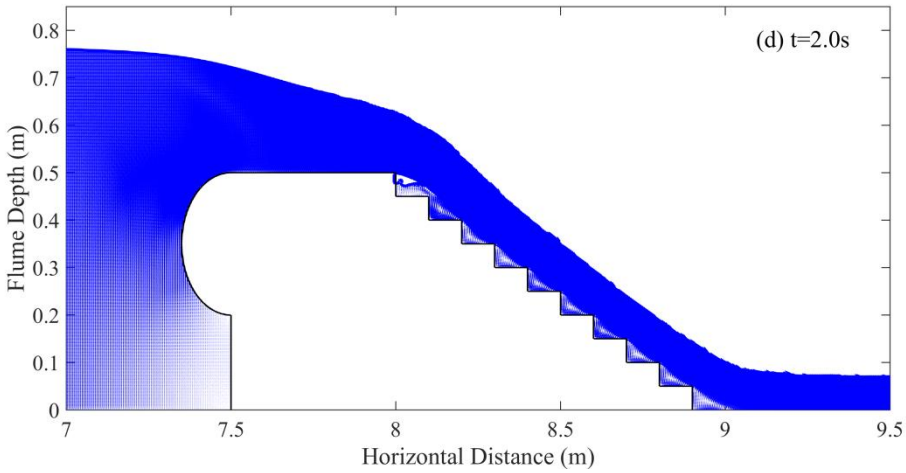
(d) t=2.0s
Flume Depth (m)
Horizontal Distance (m)
0
0.1
0.2
0.3
0.4
0.5
0.6
0.7
0.8
7
7.5
8
8.5
9
9.5

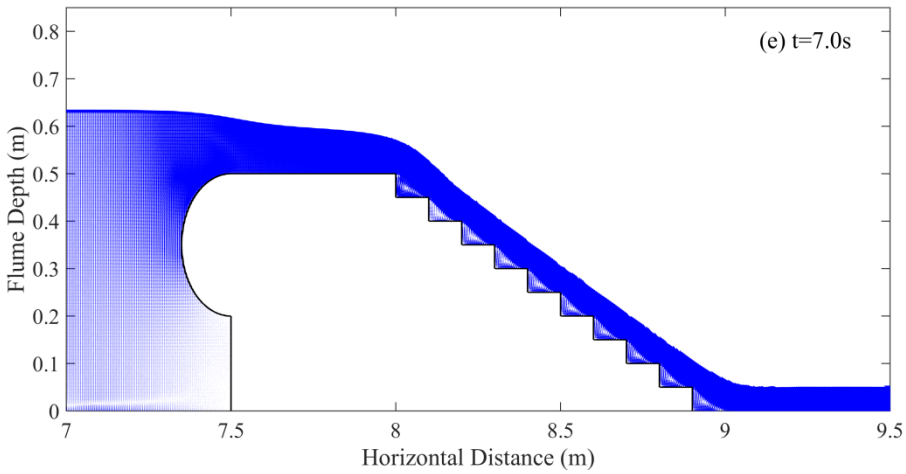
(e) t=7.0s
Flume Depth (m)
Horizontal Distance (m)
0
0.1
0.2
0.3
0.4
0.5
0.6
0.7
0.8
7
7.5
8
8.5
9
9.5

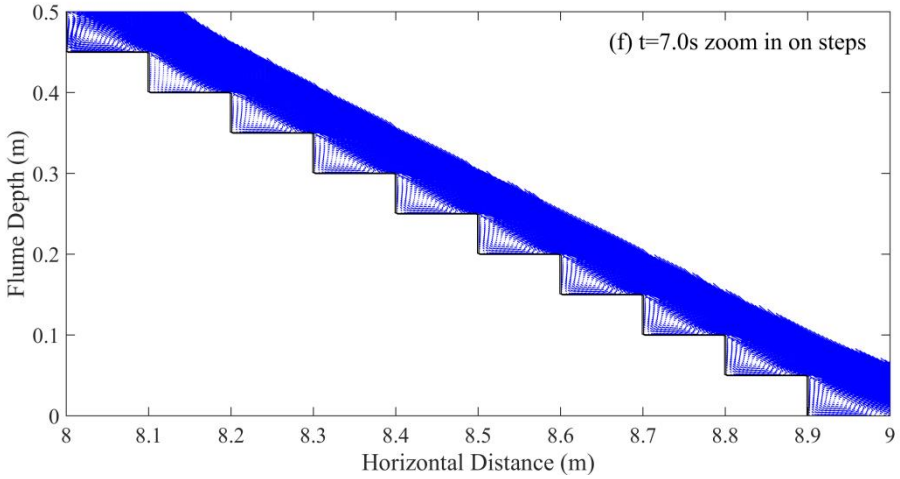

Figure 3.8 Snapshots of velocity vectors to show the free surface over the steps at: (a) t=0.2s; (b) t=0.3s; (c) t=0.7s; (d) t=2s; (e) t=7.0;(f) zoom in on the steps at t=7.0s.

The water depth at the critical section over the broad crested weir has been calculated using Equation 3.20 with the experimental discharge value:

$$q = \sqrt{Y_c^3 * g} \tag{3.20}$$

where Yc is the water depth at the critical point (m).

Depending on water depth, the Froude number is used to determine the correct placement of the critical section, (Fr=1). Then the numerical discharge has been calculated by multiplying the velocity by the water depth at the critical section. A comparison between the numerical results and the experimental results of four discharge values has shown very good agreement with maximum relative error of 2.61% (Table 3.3).

Table 3.3 A comparison between experimental and numerical values of discharge for 26.56° slope spillway.

Measurement Number	Time(s)	$q_{exp.}(m^2s^{-1})$	$q_{num.}(m^2s^{-1})$	R (%)
1	7.16	0.08	0.08209	2.61
2	7.74	0.07	0.06982	-0.257
3	12.52	0.06	0.06006	0.1
4	12.80	0.05	0.050137	0.274

Another validation was conducted between the numerical and experimental results of free surface profiles. This evaluation has obtained in the non-aerated zone for different values of flow rate. The results exposed good agreement between both of the numerical and experimental data with a maximum relative error of less than 2.0% (Figure 3.9).

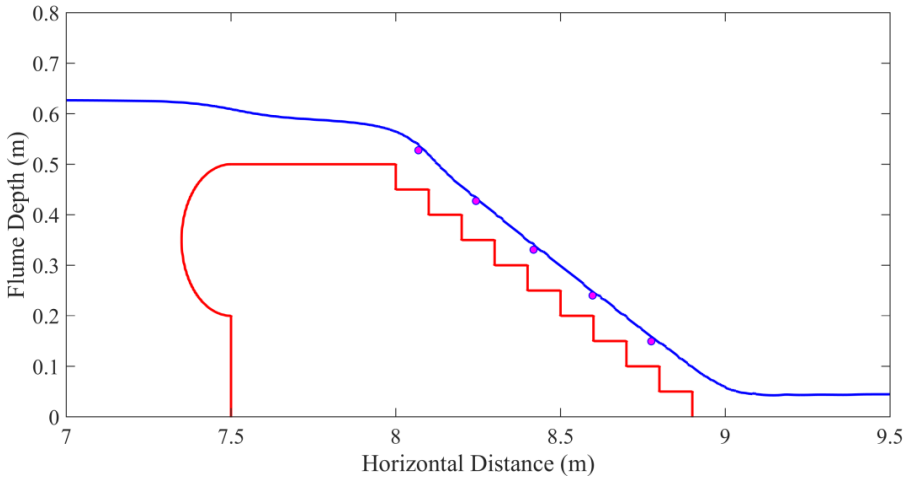

(a)

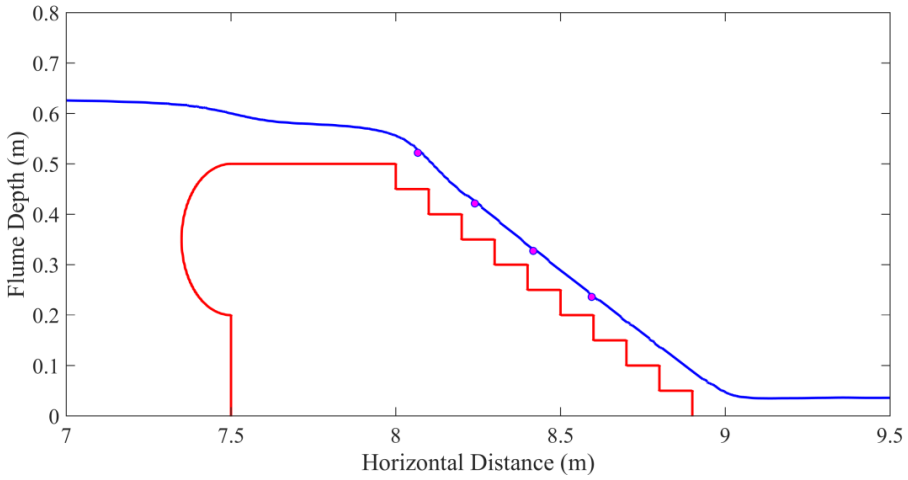

(b)

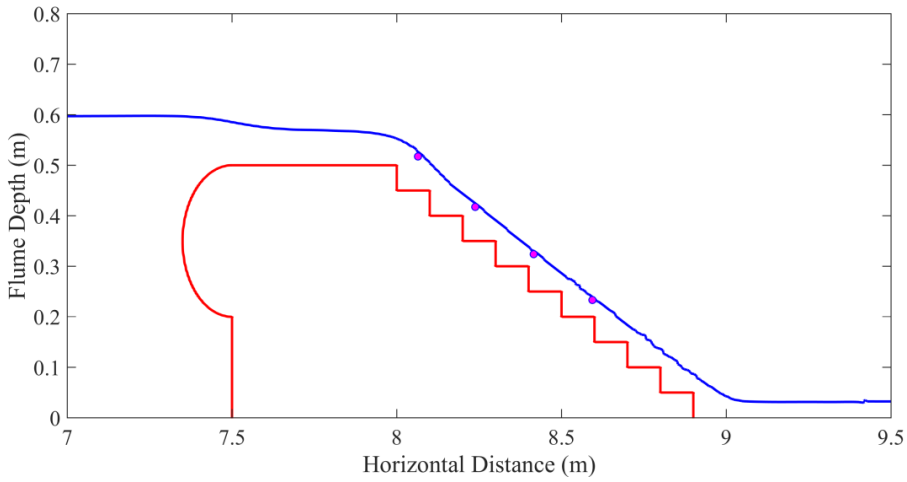

(c)

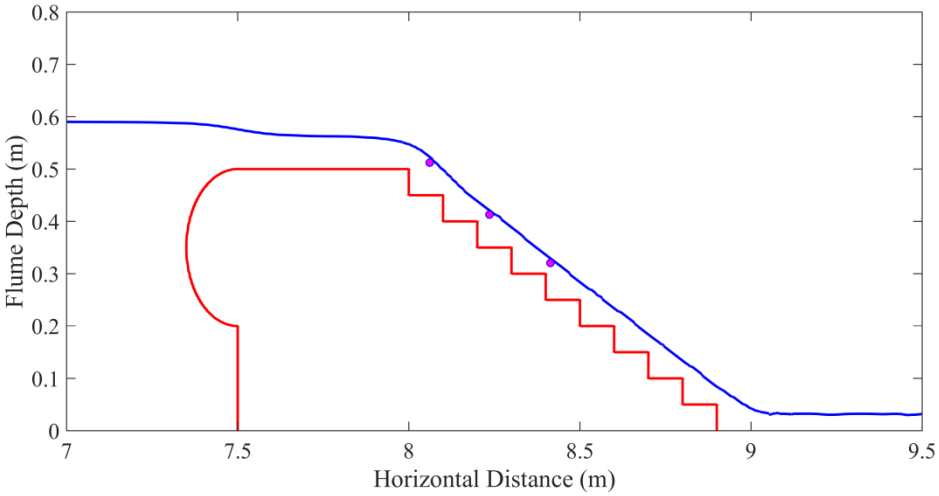

(d)

Figure 3.9 Comparisons between the experimental (circles) and numerical free surface profiles along the chute slope of different discharges at: (a) q=0.08m^2/s, (b) q=0.07m^2/s, (c) q=0.06m^2/s and (d) q=0.05m^2/s.

The location of the inception point of the experimental study has been located by using the following equations, (Meireles and Matos, 2009)

$$\frac{Li}{k} = 5.25\ (Fr_*)^{0.95} \tag{3.21}$$

$$\frac{di}{k} = 0.28\ (Fr_*)^{0.68} \tag{3.22}$$

where:

Li is the downslope distance measured from the downstream edge of the crest to the inception point location.

di is the water depth at the inception point.

Fr_* is the roughness Froude number and $Fr_* = \frac{q}{\sqrt{g \sin\theta \, k^3}}$;

k is the roughness height measured perpendicular to the pseudo-bottom;

$k = hs * \cos\theta$

hs: step height and

θ: the angle of the slope of the spillway

In Figure 3.10, the location of the inception point of the numerical work has been determined based on the definition of the inception point where the boundary layer intersects with the free surface of the water. The boundary layer thickness is predicted by determining the point where the velocity is 99% of its maximum value in the velocity distribution profile at any particular point down the spillway following Husain, (2013). Thus, the depth of the water at that point could be estimated easily by measuring it perpendicularly to the pseudo-bottom. The relative error in the location of the inception point varied from 1.28% to 8%; however it ranged from 3% to 15% for the water depth at the inception point (Table 3.4).

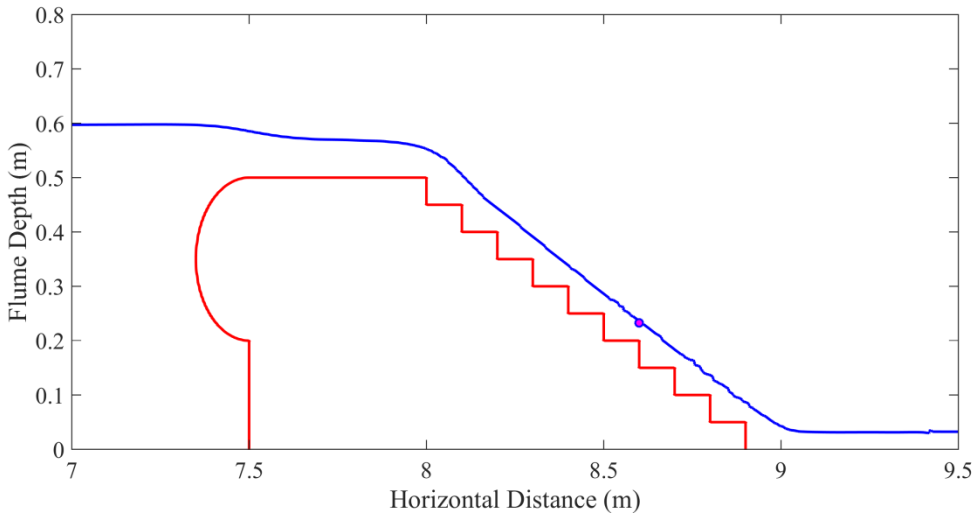

Figure 3.10 Inception point location at discharge 0.06006 (m^2s^{-1}) for 25.56° spillway.

Overall, the results show good agreement, given that the parameters chosen for the comparison provide a very stringent test. Some discrepancies are to be expected due to the limited accuracy of measuring equipment, the empirical formula used to identify the inception point and numerical rounding errors arising in the computational solution.

Table 3.4 Comparisons between experimental and numerical values of inception point location and the water depth at that point.

Measurement Number	Li_{exp}(m)	Li_{num}(m)	R (%)
1	0.906	0.875	-3.42
2	0.777	0.767	-1.82
3	0.673	0.655	-2.65
4	0.567	0.521	-8.11
Measurement Number	di_{exp}(m)	di_{num}(m)	R (%)
1	0.0329	0.0368	11.8
2	0.0295	0.0304	3.05
3	0.0266	0.0284	6.76
4	0.0235	0.0272	15.74

3.3.2. Stepped spillways of 1V:2.5H slope

In the experiment of Chanson and Toombes (2002), a stepped spillway with 21.8° slopes and length of 2.7m was subjected to different flow rates. A broad crested weir, with 0.9m height and 0.6m length, was installed before the spillway steps with an upstream rounded corner of r=0.057m. They used the broad crested weir before the spillway steps to measure flow rates. The spillway has had nine identical steps with 0.1m height and 0.25m depth.

For the comparison purposes, the same dimensions of experiment details were recreated in the numerical model. To achieve the required values for the discharges and calm upstream conditions, the area of the upstream tank was 1.5m deep and 4.9m long. The

initial water elevation above the crest was set to 0.6m. A uniform mesh was used to discretise the domain with resolution 0.01m in the x-direction and 0.004m in the y-direction (Figure 3.11). The initial time step fixed to 0.0001 seconds for stability purposes. The total simulated time period was 20 seconds. The same procedure of the flow rates calculations over the weir crest that used in the previous case was applied again in the current test. Also, a comparison of the flow rates results was conducted between the numerical model results and the experimental results. The results showed very good agreement between the numerical and experimental work with a maximum relative error of 2.19%, as tabulated in Table 3.5.

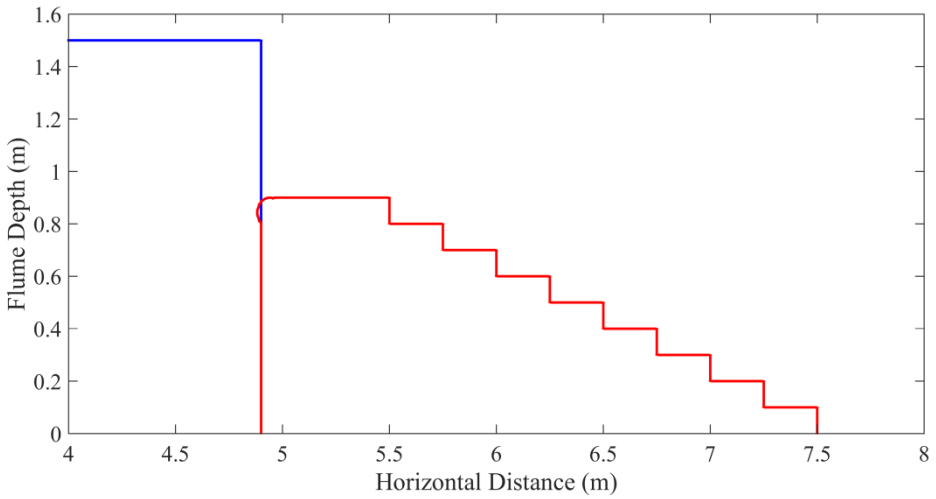

Figure 3.11 The initial setup of Chanson and Toombes (2002) experiment.

Table 3.5 A comparison between experimental and numerical values of discharge for 21.8° slope spillway.

Measurement Number	Time(s)	$q_{exp.}(m^2s^{-1})$	$q_{num.}(m^2s^{-1})$	R (%)
1	4.11	0.182	0.1834	0.769
2	6.24	0.164	0.16205	-1.189
3	6.33	0.147	0.1467	-0.2
4	6.52	0.124	0.125	0.806
5	6.64	0.114	0.1115	-2.19

Regarding the inception point location (Figure 3.12), the numerical results were compared with two values:

- The first one is determined from the equation that proposed by Chanson (1995) on the basis of regression against experimental observations:

$$Li = 9.719 * ks * \sin\theta^{0.0796} * Fr^{0.713} \quad (3.23)$$

  where the symbols have the same meaning as in the previous subsection.

- The second one comes from the equation of Chanson and Toombes (2002), again it is based on the regression of their experimental observations:

$$\frac{s}{ks} = \frac{12.34}{\sin\theta^{0.0796}} Fr^{0.465} \quad (3.24)$$

where S is the distance from the upstream edge of the weir (after the round edge) to the inception point.

The results of the comparison are shown in Table 3.6 and 3.7. These tables demonstrate that the computational results are in good agreement with Equation 3.23. Equation 3.23 is based on a larger database of experiments compared to Equation 3.24, thus it is likely to provide more robust results. On this basis the better agreement of the computational results with Equation 3.23 is satisfactory.

For the water depth at the inception point, just one empirical equation is available and is reported in Chanson (1995). This equation is used in the current work to carry out a comparison with the numerical computations. The results showed reasonable agreement with a maximum relative error of about 13%.

The formula proposed by Chanson (1995) is:

$$di = 0.4034 * ks * \sin\theta^{-0.04} * Fr^{0.592} \quad (3.25)$$

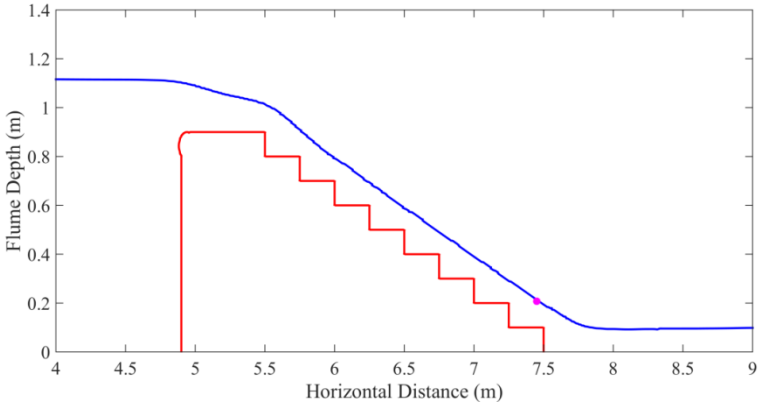

Figure 3.12 Inception point location at discharge 0.1834 (m^2s^{-1}).

Table 3.6 Comparisons between experimental (Chanson equations, 1995) and numerical values of inception point location and the water depth at that point.

Measurement Number	Li_{exp}(m)	Li_{num}(m)	R (%)
1	2.526	2.593	2.65
2	2.368	2.261	4.51
3	2.233	2.134	-4.87
4	2.061	2.072	0.53
5	1.942	1.993	2.62
Measurement Number	di_{exp}(m)	di_{num}(m)	R (%)
1	0.0803	0.0806	0.334
2	0.07468	0.06501	-13.16
3	0.0704	0.0607	-2.13
4	0.06407	0.0593	-12.94
5	0.05988	0.0586	-7.3

Table 3.7 A comparison between experimental (Chanson and Toombes, 2002) and numerical values of inception point location.

Measurement Number	Li_{exp}(m)	Li_{num}(m)	R (%)
1	2.189	2.593	18.4
2	2.066	2.261	9.43
3	1.973	2.134	8.16
4	1.832	2.072	13.1
5	1.7373	1.993	14.7

3.3.3. Stepped spillways of 1V:3H slope

The last comparison is against the experiments reported by Hunt and Kadavy (2013) which were conducted for water flow over a large scale stepped spillway. The large-scale spillway has a height of 5.642m and a 18.4 degree slope and was tested under a wide range of discharges ranging from 1.79 to 0.33m^2/s. A broad crested weir of 3.05m length was installed before the spillway. All of the steps had the same height and length of 0.305m and 0.914m respectively except the last step which had 0.152m height.

The same details were recreated in the numerical model. The initial upstream water depth was 4.358m and the length of the tank equalled to 15m. The initial time step set to 0.0001 seconds and the total simulation time fixed to 30 seconds. Skimming flow was achieved after 6.78 seconds. A fix mesh was used with a grid size of 0.04 m in the x-direction and 0.015m in the y-direction (Figure 3.13). The same procedures as in the previous comparisons are used to estimate the flow rates values and the location of the inception point in the computational model. The comparison of the discharge results showed very good agreement between the experimental and numerical work with maximum relative errors being 1.06% as shown in Table 3.8.

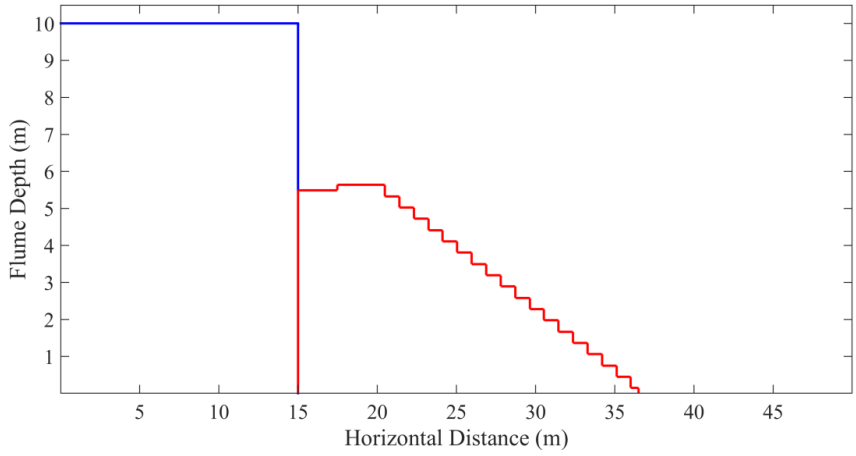

Figure 3.13 The initial setup of Hunt and Kadavy (2013) experiments.

Table 3.8 A comparison between experimental and numerical values of discharge for 18.4° slope spillway.

Measurement Number	Time(s)	$q_{exp.}(m^2s^{-1})$	$q_{num.}(m^2s^{-1})$	R (%)
1	7.29	1.79	1.7998	0.547
2	7.49	1.58	1.5935	0.854
3	7.95	1.24	1.23	-0.806
4	10.19	0.948	0.9432	-0.506
5	10.58	0.799	0.8002	0.15
6	11.74	0.619	0.6177	-0.21
7	14.01	0.461	0.4659	1.06
8	17.01	0.33	0.3284	-0.484

For the inception point position (Figure 3.14), the computational results are compared with two values from the experimental work. The first one has been determined by the equation proposed by Hunt and Kadavy (2013) on the basis of the full set of their experiments:

$$\frac{Li}{ks} = 5.19 * Fr^{0.89} \quad (3.26)$$

However, the second value represents the direct observation, as reported by Hunt and Kadavy (2013).

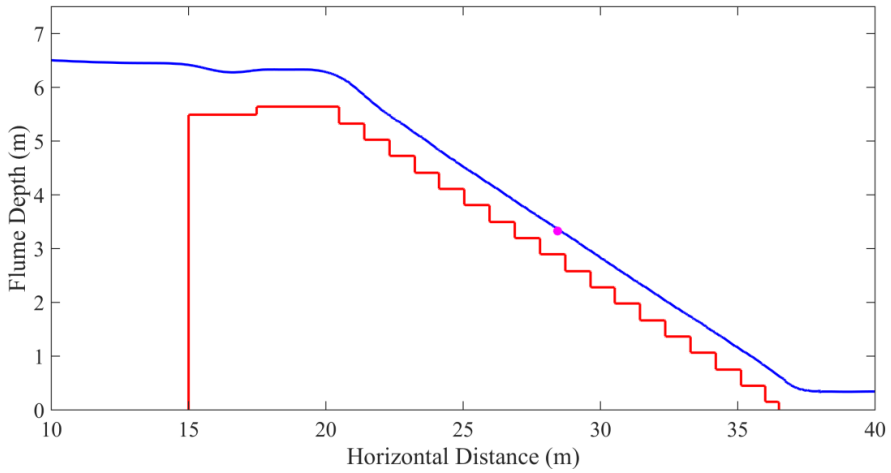

Figure 3.14 Inception point location at discharge 1.7998 (m^2s^{-1}).

As shown in Table 3.9, the comparison of the inception point location for the numerical results with the empirical formula provided smaller relative errors than the direct observations. The larger discrepancies found with the directly measured observation can be attributed to the difficulty of making such readings in strongly turbulent flow and differences between the direct observation results and the empirical formula results are to be anticipated.

Table 3.9 A comparison between experimental and numerical values of inception point location.

Measurement Number	Li_{num}(m)	$Li_{exp.equation}$(m)	R (%)	$Li_{exp.direct\ observation}$(m)	R (%)
1	8.255	8.017	2.986	6.74	22.40
2	8.09	7.2	12.36	6.28	28.80
3	6.24	5.717	9.14	5.30	17.70
4	4.722	4.514	4.603	4.82	-2.03
5	3.759	3.899	-3.59	3.87	-2.87
6	2.844	3.077	-8.18	2.90	-1.93
7	2.599	2.409	7.88	2.40	8.26
8	1.773	1.765	0.447	1.70	4.29

3.3.3.1. Pressure distribution over stepped spillways with 1V:3H slope

Pressure investigations over stepped spillways in the non-aerated zone have been conducted to describe the pressure variation in terms of positions and magnitudes. Pressures can have a significant effect on the flow characteristics in the non-aerated zone. Therefore, it is necessary to design stepped spillways to reduce or eliminate cavitation formation in the non-aerated zone during the skimming flow conditions. That could be achieved by giving more information about the pressure distribution over the vertical and horizontal faces in the non-aerated region. André (2004) claimed that the maximum fluctuation of the pressure has been measured for the skimming flow rather than nappe

and transition flow as result of interference between the oscillating jet impacts and the recirculating vortices.

In the experimental work of Hunt and Kadavy (2013), pressure distributions in the non-aerated zone were not measured; thus, computational results are used to analyse the pressure distribution rather than comparison. Four different discharges have been picked to study the pressure variation over the horizontal faces and the vertical faces for the skimming flow in the non-aerated zone. Although the slopes of Hunt and Kadavy (2013) spillway is 1V:3H, the results show the same trend of the experimental result of Frizell and Renna (2011) where the pressure variation over the horizontal steps shows an approximately S-curve shape with a positive peak value at the boundary points (Figure 3.15). The positive peak value for the pressure has been achieved where the mainstream hits the horizontal step face.

Over the vertical face, the peak value of the positive pressure has been observed in the lower half of the steps at the corner point with the horizontal step. The reason for that could be related to the formation of small eddies as a result of the reverse flow inside the step cavity. Also, in certain conditions, negative pressure might be achieved in the upper half of the vertical face.

It is worth mentioning that it is not necessary to get negative pressure in the non-aerated zone in all conditions. However, it might depend on many reasons like velocity distribution and discharge values. Therefore, no significant negative values of the pressure have been observed under three different flow rates. These results agree with the result of Amador et al. (2009) which claimed that there are no extreme values for the negative pressure if the discharge less than $11.5 m^2/s$.

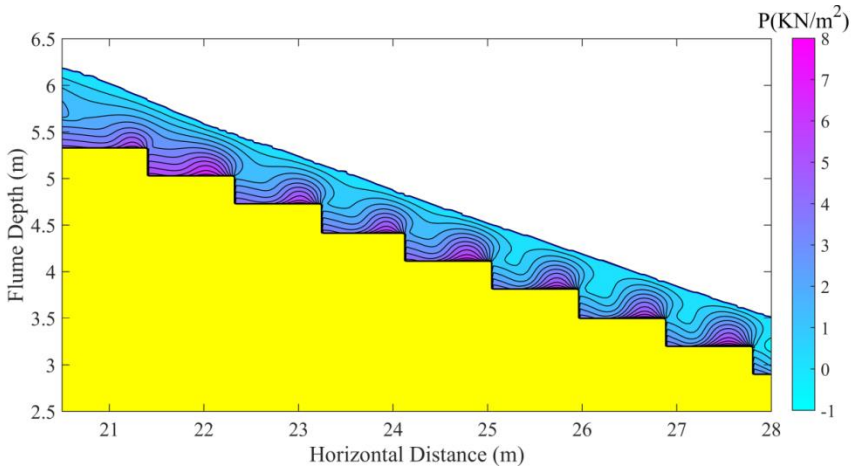

(a)

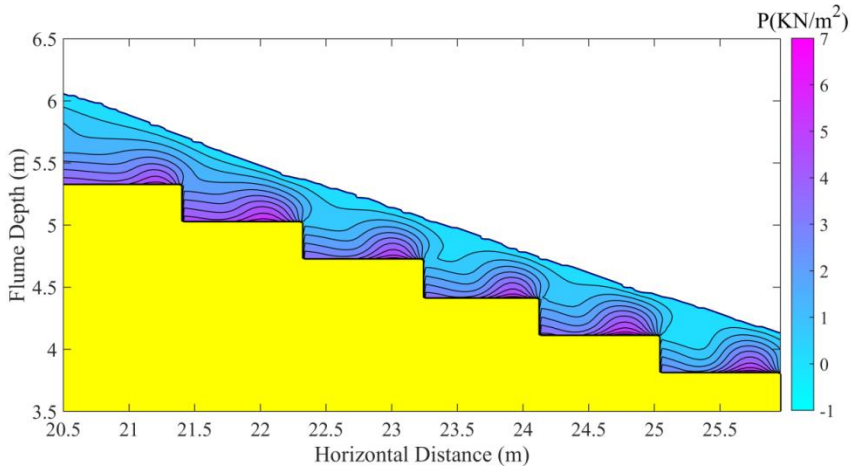

(b)

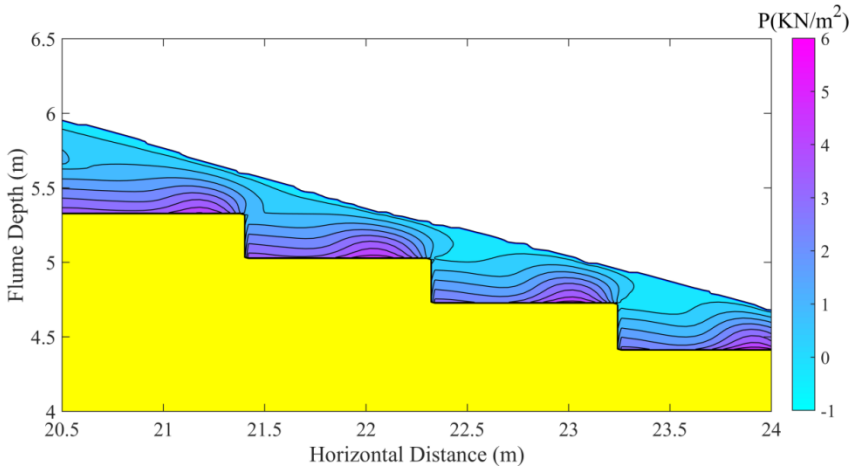

(c)

Figure 3.15 Pressure distribution over the non-aerated zone for different flow rates at: (a) $q=1.79 m^2/s$, (b) $q=1.23 m^2/s$ and (c) $q=0.8 m^2/s$.

3.4. Gabion validation

Since the main task of this work is to simulate flow over gabion stepped spillways, a validation was conducted against the experimental work of Wüthrich and Chanson (2014). The test section consisted of a broad crested weir with length 1.01m and height 1.0m, followed by ten identical impervious steps with height 0.1m and length 0.2m. Gabion steps were installed over the impervious steps, which are made from marine plywood, with 0.1m height and 0.3m length. The gravel inside the gabions had a D_{50} of 0.01m. The porosity ranged from 0.35 to 0.4.

The same experimental details were established in the numerical model and the mesh size set to 0.01m and 0.005m in the x-direction and y-direction respectively. The depth of the initial water was set to 1.4m in order to achieve the required discharge. The discharge was calculated by determining the critical section over the broad crested weir from estimation Froude number value. To ensure numerical stability, the initial time step was set to 0.001s and the total time of the simulation was 24s. As in the experimental work, all of the boundaries were closed except the right boundary which was opened. Finally, the porosity of the gravel particles was fixed to 0.375 which represented the average value in the experimental work (Figure 3.16).

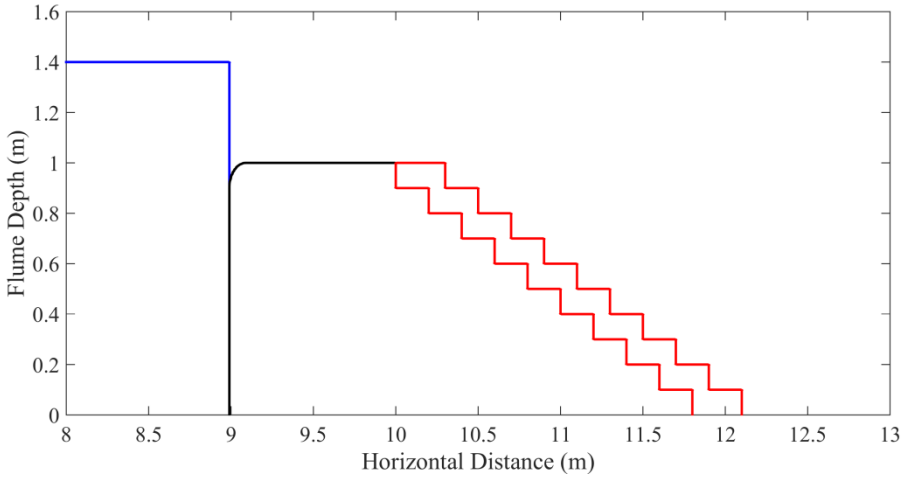

Figure 3.16 Gabion setup

The fluid initially was set at rest. The barrier at x=9m was removed instantaneously at t=0s and the resulting flow computed. The time needed to establish the skimming flow was more than 4.0s (Figure 3.17). Four different discharges were used for the comparison. The discharge value was calculated by multiplying the water depth at the critical section over the broad crested weir by the velocity at that point, (Chow, 1959). To determine the critical section, the Froude Number needs to be calculated as it should be equal to 1 at the critical section. During the process of skimming flow establishing over gabion stepped spillways, some air pockets are observed inside and outside the porous media (Figure 3.18).

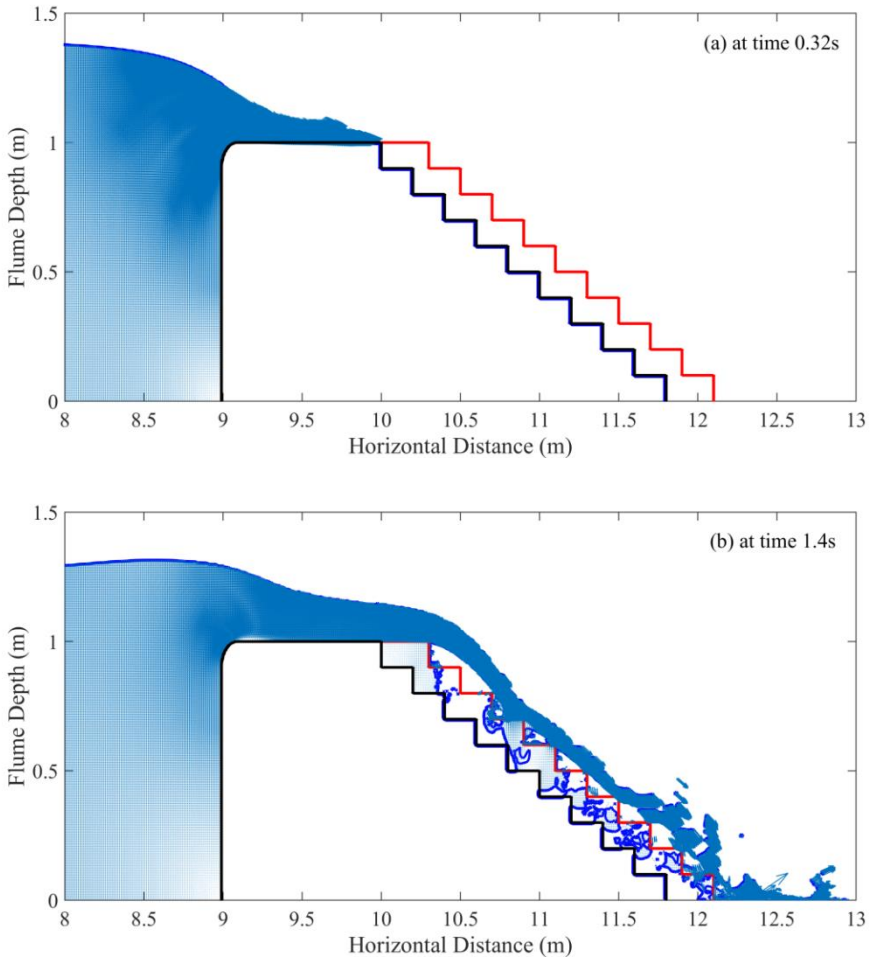

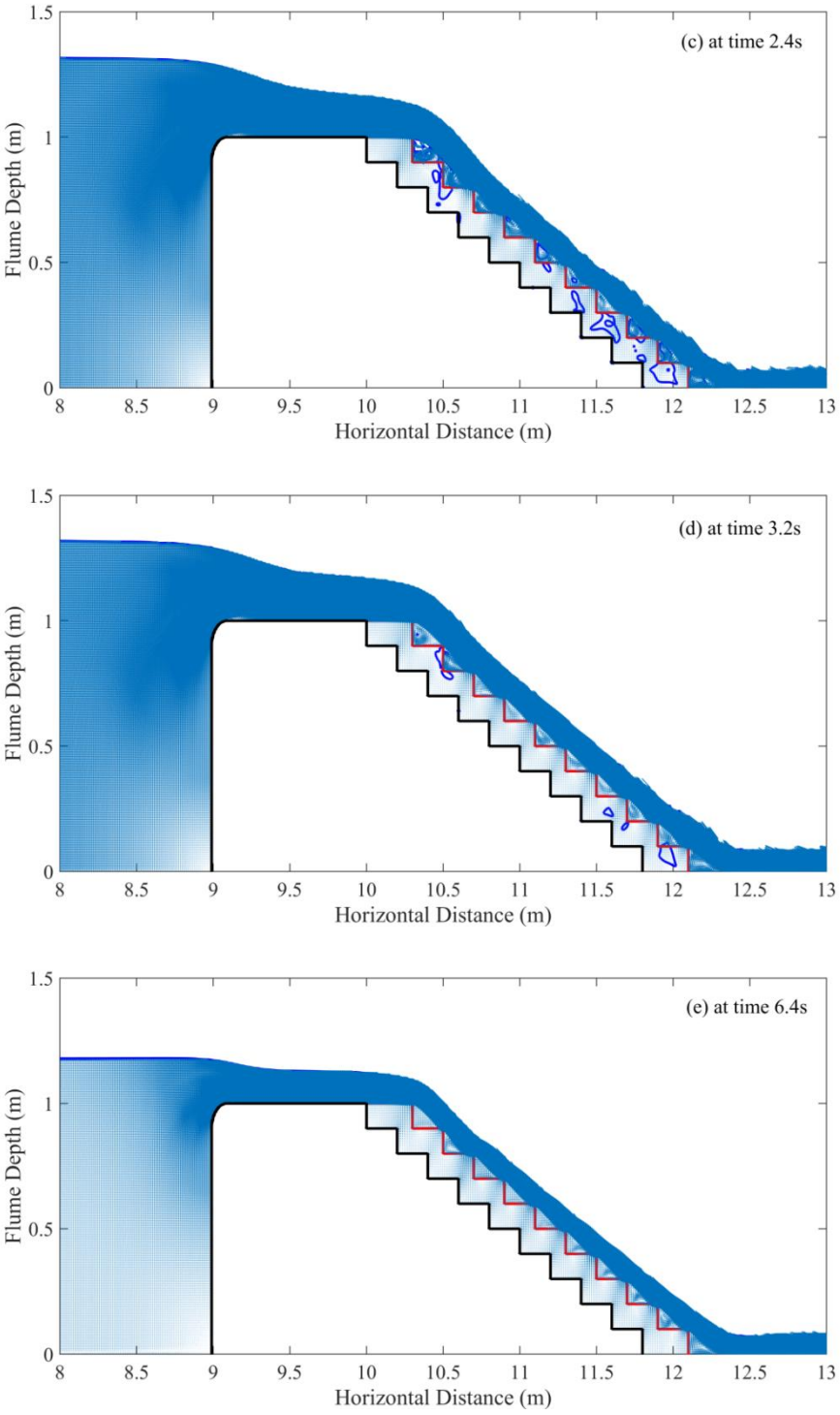

Figure 3.17 Flow over gabion stepped spillway at different times.

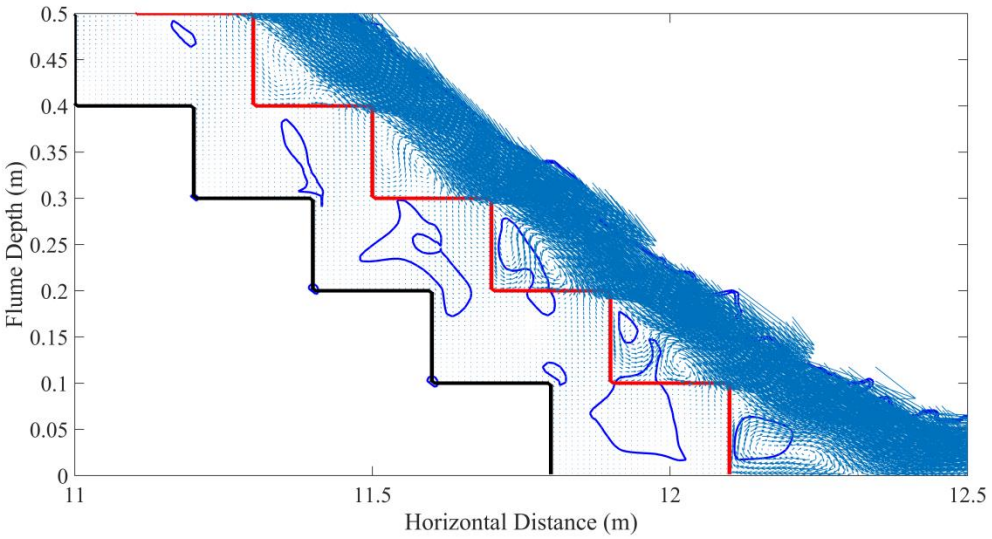

Figure 3.18 The air pockets inside the porous media at t=2.56s.

According to Husain et al. (2013), the location of the inception point may be estimated from the assumption that the inception point represents the intersection point between the free surface water and the point where the velocity is equal to 99% of the maximum velocity over the pseudo-bottom (Figure 3.19). Results from the four experiments are summarised in Table 3.10; where a good agreement between the numerical and experimental work is revealed. As can be seen in Table 3.10, the experimental results were reported in a fairly vague way; therefore, the opportunity to apply qualitative comparison was limited.

Table 3.10 A comparison between the inception point location in the experiment and numerical results.

Experiment Number	Time(s)	Discharge (m^2s^{-1})	Inception point location (Wüthrich and Chanson, 2014)	Inception point location (Computed)
1	5.568	0.114	Step 8 to step 9	At the end of step 8
2	5.984	0.095	Step 7 to step 8	At the end of step 7
3	6.432	0.076	Step 5 to step 6	At the end of step 5
4	7.008	0.059	Step 5	At the middle of step 5

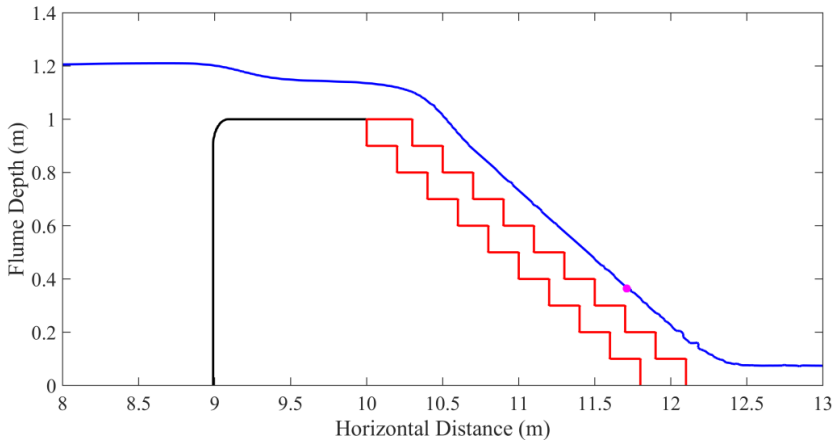

Figure 3.19 Inception point location for the second experiment at 5.984s.

A comparison of the measured and computed velocity profiles is shown in Figure 3.20 for the third experiment. This show the velocity profiles on steps 8 to 10, all the values of velocity profiles have been divided by Vc and Yc to present them in dimensionless form, Vc and Yc represent the velocity and the depth of the water at the critical section. There are differences in the velocity values near the gabion surface, however, the results agree closely towards the top of the velocity profile where the maximum velocity is achieved.

The average value of the root means square error and the correlation coefficient of the three profiles was 0.32 and 0.991 respectively which is fairly good. The discrepancies at the bottom of the profile are not entirely unexpected. They could arise from the intrinsic limitation of the measurement methods and equipment and also from the limitations of the computational model which simulates single-phase flow.

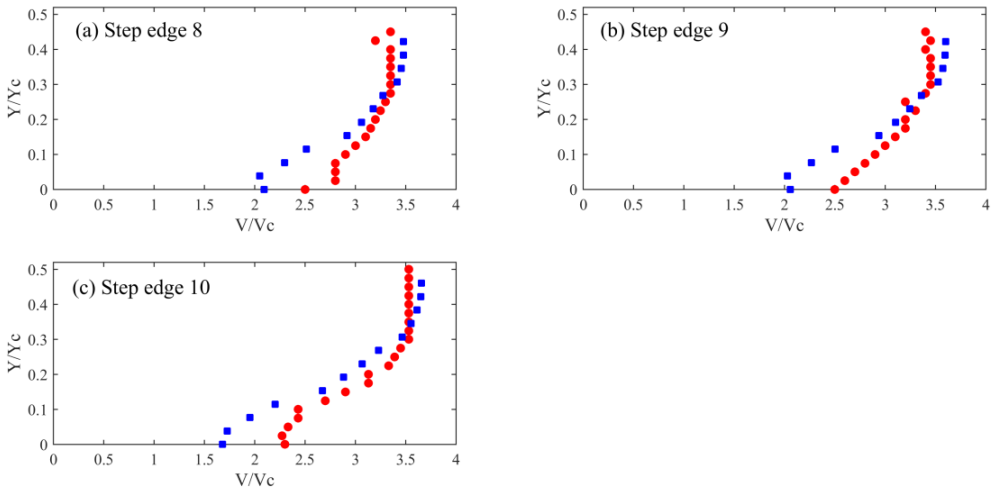

Figure 3.20 A comparison between the velocity profiles of the experimental results (red circles) and numerical results (blue squares) of the second discharge.

It should be noted that due to the lack of the experimental data of velocity profiles in the non-aerated zone over gabion stepped spillways, the comparison with the numerical results has been conducted against velocity profiles in the aerated zone. Therefore, discrepancies are expected in the profile as the numerical model simulates single phase flow where air entrainment is not considered while the velocity profiles were measured where air entrainment is presented.

Liu et al. (1999) showed that the interface boundary between the porous media and the outside flow field can represent a crucial issue compared to the other issues in the numerical work. This is because the outside mean (ensemble-averaged) flow is not equivalent to the averaged (spatially averaged) flow in porous media. Thus, the latter may still have turbulent fluctuations in principle. Although the studies showed that the maximum turbulence length scale in the porous media is limited to the pore size and the length scale that used in the spatial averaging process, Losada et al. (1995) revealed that limited turbulent fluctuations should be observed in the resulting averaged flow quantities. This phenomenon was confirmed experimentally in their work. Therefore, it is assumed that the outside mean and the averaged flow in porous media represent the same flow system which is free of turbulence. Hence, across the interface of porous media and outside flow, the continuity of the pressure, mean velocity and averaged velocity can be

applied. It is noted that with that implementation of the continuity across the interface, the realistic velocity characteristics outside of the porous media is not well captured to obtain. In reality, as a result of the presence of a porous surface, the flow just outside of the porous media can create numerous jets or wakes. The jets and wakes are turbulent and will be quickly mixed within a short distance.

The detailed information of the mixing of jets and wakes is neglected and only the average momentum flux is captured in order to solve that issue. As the energy dissipation in porous media is the main point in the NEWFLUME code which is not significantly influenced by the approximation of the flow field outside the porous media, the simplified treatment suggested above is acceptable. However, when the detailed velocity information outside the porous media is needed, particularly at the position which is very close to the porous media surface, the explanation of the modelling result must be made with caution (Liu et al., 1999).

Moreover, Kálal et al. (2014) found that the k-ε model underestimates the turbulent quantities, which results in an underestimation of the power number computed from the integral of the turbulent dissipation rate. However, current design uses the peak value of the velocity, normally located near the top of velocity profiles, and the numerical results reproduce the observed maximum velocities with a relative error of less than 5%. Due to the scarcity of experimental studies about gabion stepped spillways, a series of physical experiments are undertaken in the next chapter.

Chapter 4 : Physical Modelling of Stepped Spillways

4.1. Model setup

The experiments were conducted over a stepped spillway model in the Coastal Laboratory at Swansea University. As a result of the experimental data lack in the non-aerated zone for stepped spillways, especially gabion stepped spillways, a physical model has been built to run some experiments. The model was installed inside a wave flume that has a paddle to produce a different type of waves. The dimensions of the flume are 1.2m height, 0.8m width, and 30m length. The 'flume' is a wave tank and was never designed to be a hydraulic flume. However, it was adapted to simulate dam break problems and therefore dam break conditions were selected to run experiments.

The stepped spillway model was positioned at 12.9m with 0.7m height and 1.5m length of broad-crested weir followed by ten identical steps with 0.05m height and 0.1m length thus the slope of the spillway is 1:2 (V:H). The eleventh step height was 0.2m in order to assure that the water flow will not submerge the last two steps when the gate lifted up as the downstream side of the flume is closed. In other words, when the water flow hits the downstream wall, it would come back towards the model. The model was constructed by using a ply marine wood. In order to increase the resistance of wood against water, the entire model was varnished (Figure 4.1).

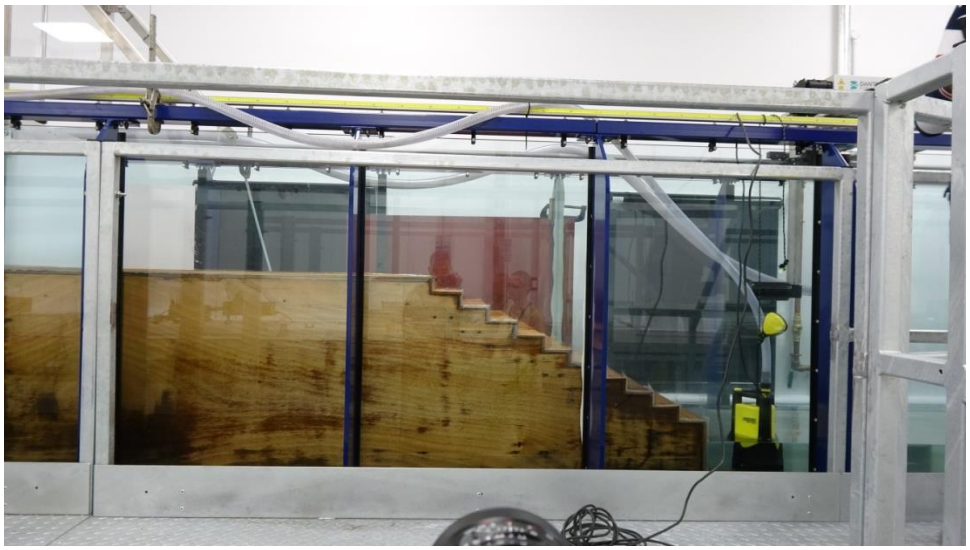

Figure 4.1 Normal stepped spillway model

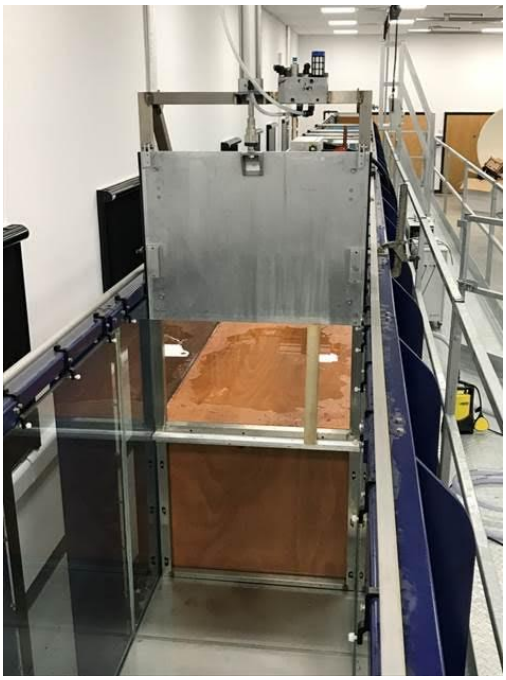

Figure 4.2 Guillotine-type gate

A guillotine-type mechanism was used to lift the gate; this was achieved by using a cylinder with an air compressor to lift the gate very fast. The gate was installed with a frame to increase the stability (Figure 4.2). According to the dam break conditions, the time to open the gate should be very fast depending on the initial water depth at the upstream. The mechanism was designed to lift the gate up in less than 0.3s.

Two baffles were installed behind the gate to reduce the wakes and vortices over the crest. These two baffles are connected to the frame of the guillotine gate which is already connected to the model. The connection between the parts of the whole system increased the stability of the model as well. Another two baffles were installed over the crest with 0.4m length to help reduce downstream wakes and vortices induced by the frame of the guillotine.

The experimental studies were divided into two stages: flow measurements over normal stepped spillways and flow measurements over gabion stepped spillways. The initial water depth in the first stage is fixed to be 0.4m above the crest elevation so that the volume of water in the upstream side above the crest is 4.128m^3. On the other hand, 0.35m was the initial water depth over the crest in the gabion test stage (Figure 4.3). The second stage of the experimental work tested the water flow over gabion stepped spillways by using PIV (Particle image velocimetry) measurements. Thus, the gabion steps were installed over the impermeable steps. Square mesh wires (chicken wire) with size of 13mm*13mm have been used to construct the cages into which gravel was loaded. The gravel particle size ranged between 14-20mm (Figure 4.4).

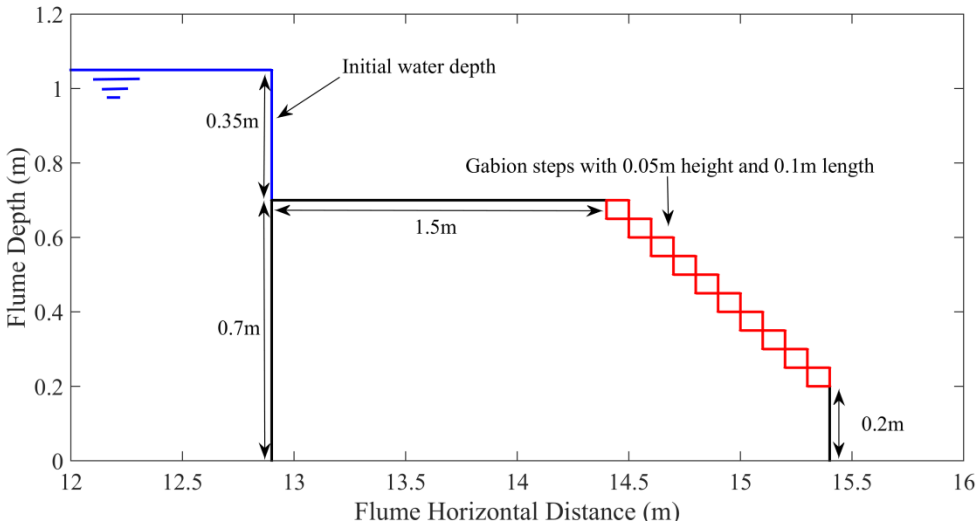

Figure 4.3 Schematic diagram of the experimental set-up.

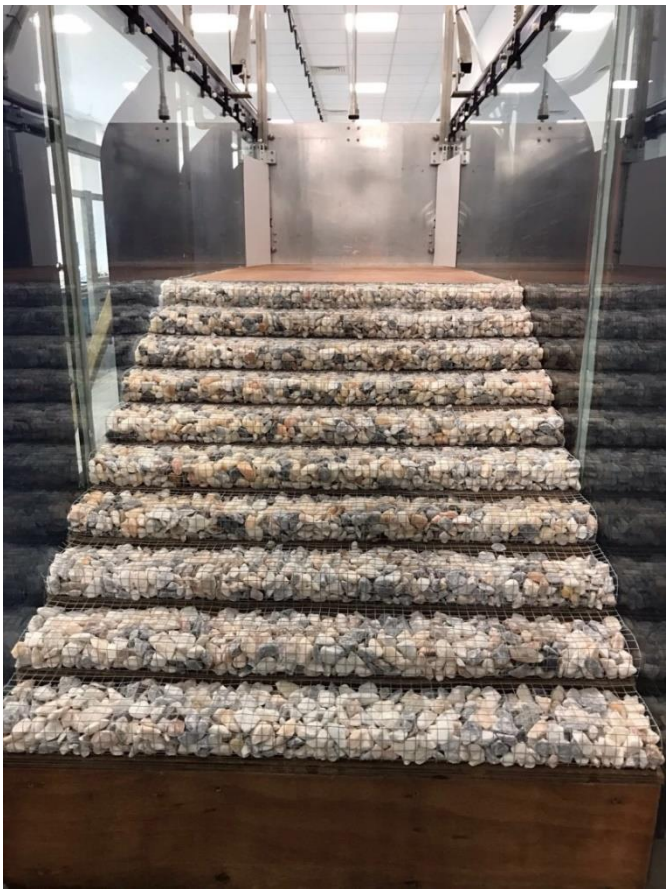

(a)

(b)

Figure 4.4 Gabion stepped spillway model.

4.2. PIV measurements

Particle image velocimetry (PIV) was used to measure the velocity and the water depth over the steps. PIV measures flow parameters by mixing seeding particles such as polystyrene within water together with a laser light sheet (LLS). Flow parameters such as velocity can be calculated by following some patterns of particles by using a cross-correlation function between a pair of digital images in a narrow interrogation window (Nezu and Sanjou, 2011). Velocity vectors can be observed by PIV through tracing particles which are illuminated by planar laser light. The PIV system is comprised of dual cavity flash-pumped Nd-Yag lasers using a cylindrical lens (DualPower lasers), with a maximum energy output of 700 mJ and capability of providing various wavelengths range from the fundamental wave of 1064nm, and including 532, 355 and 266nm harmonics. Nd-Yag can provide light pulses of short duration like 4ns which can capture rapid movements typical of turbulent flow. A high sensitivity speed camera, CCD camera, of 2320×1726 pixel resolution has been used to capture frames. A Nikkor 50mm 2.8, together with a narrow bandwidth filter that passes the 532 nm light from the Nd-Yag laser, is mounted on the CCD camera. The camera and laser pulses are synchronised with an electronic sequencer, (Figure 4.5).

(a)

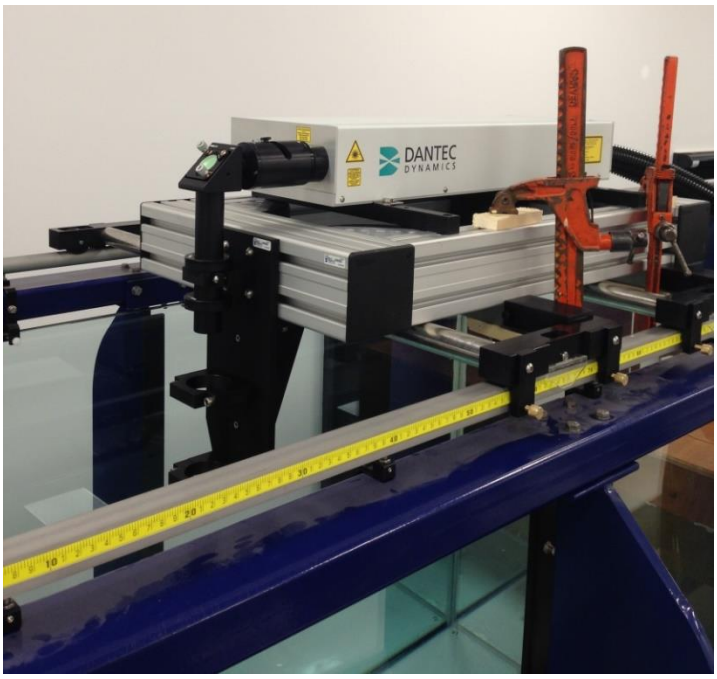

(b)

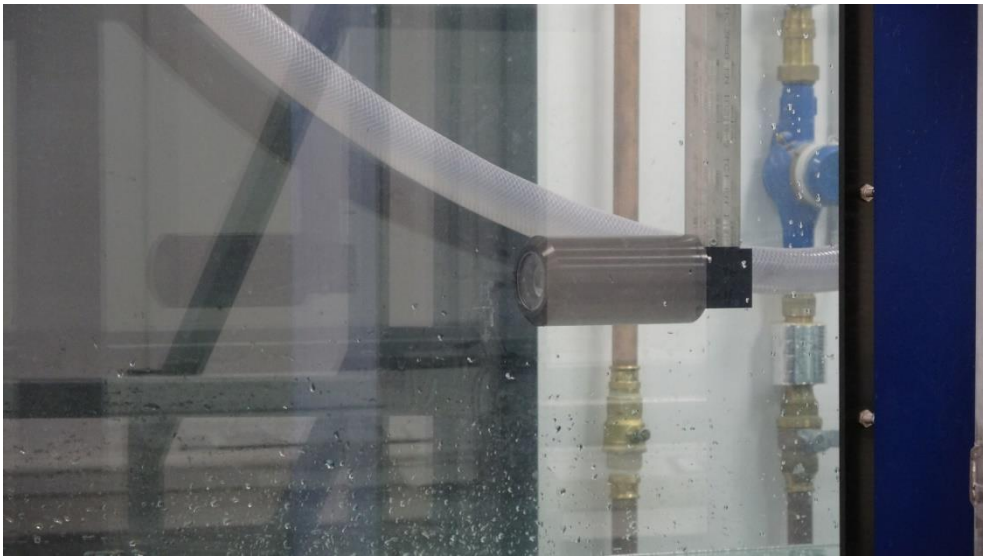

(c)

Figure 4.5 PIV equipment: a) camera b) laser shutter and c) laser lens.

PIV has become one of the most important techniques in hydro-sciences nowadays, for instance, PIV has been used to measure different types of flow such as mixing flow and open channel flow (Nezu and Sanjou, 2011). A high capacity computer has been used to check the connections between the laser and the camera and also to set the parameters like the time between two pulses and the trigger rate (number of images per second). The

single frame mode has to be selected through the calibration process while the double frame mode should be selected for the acquisition.

The size of the PIV seeds which used in the experiments is 50**μ**s ceramic micro spheres. In order to get a maximum particle image displacement of eight pixels, the separation time between two lasers pulses should be between 200-250**μ**s. Trigger rate is the number of frames per second of the camera and it represents an important parameter that can affect the measurement accuracy. As the flow moves very fast over the steps, the trigger rate should be set carefully to be able to capture a good number of frames in each second so that particle movements can be captured unambiguously from the sequence of PIV images (Figure 4.6). Different trigger rates have been tested in order to demonstrate the suitable rates for this study. For the normal stepped spillways, 20 frames per second was enough to capture the details of establishing skimming flow, However, 30 frames per second was selected in the gabion case due to the presence of flow through porous media.

It is important to mention that the PIV should be always calibrated before running the experiments. Generally, the calibration process should be establishing once the position of the camera is changing. Hence, to conduct the calibration, an object with known dimensions should be located in front of the camera. As mentioned earlier, the single frame mode has to be selected before the acquisition. Then, after the acquisition and saving the snapshots, one snapshot should be selected to run the calibration. The real dimensions between two points, the edges of the object, should be applied through the calibration window of the software. Once the calibration is done, the acquisition can be applied normally after selecting the double frame mode.

After the acquisition and saving of data, results are analysed. To do this, a suitable tracking method and interrogation area within the full images must be defined. The size of the interrogation area is required in order to determine velocity vectors. Obviously, that could be significantly vital because the interrogation area size can change the values of the velocity vectors. Generally, selecting a small size for the interrogation area within

the PIV post-processing analysis will lead to better results. However, if the interrogation area is too small then the accuracy of the velocity vectors may be degraded (Nezu and Sanjou, 2011). Therefore, selecting the correct size of the interrogation area is extremely important.

Adaptive PIV method was used to analyse the data, it can be defined by an automatic method for calculating velocity vectors based on particle images. It is adaptive because the velocity vector calculation adjusts the shape and the size of the individual interrogation areas depending on the seeding density (the amount of the seeds in one image) and flow gradients. The Grid Step Size parameter has been used to control the number of the interrogation areas and the spacing between their centres and can be determined as the number of pixels from one area to the next. It is important to mention that the adaptive PIV has the ability to change the size of the interrogation areas during the process of the analysis depending on the solution. However, the maximum and the minimum sizes need to be specified. The largest size of interrogation areas will be used in the first iteration and then with more iteration, the size will reduce until reach that size where the particle density is high enough to get the vectors.

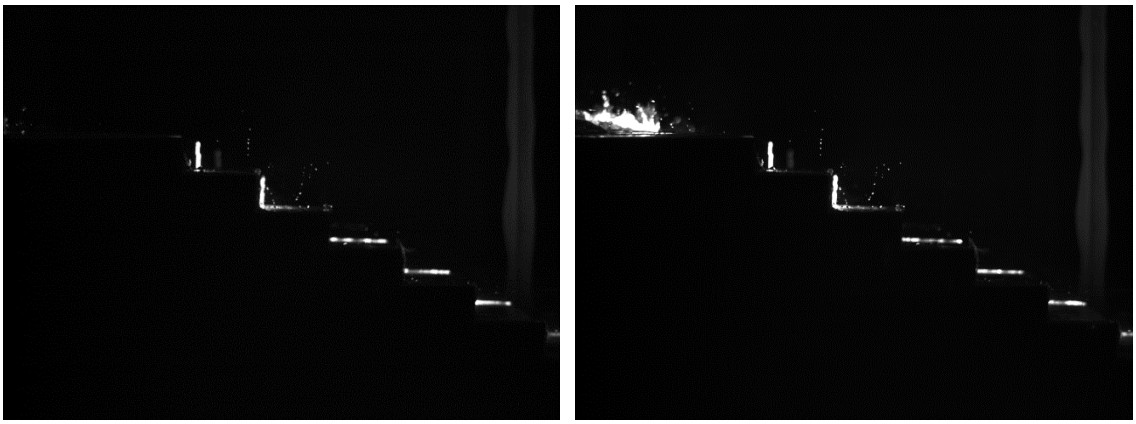

(a) at 0.3s (b) at 0.35s

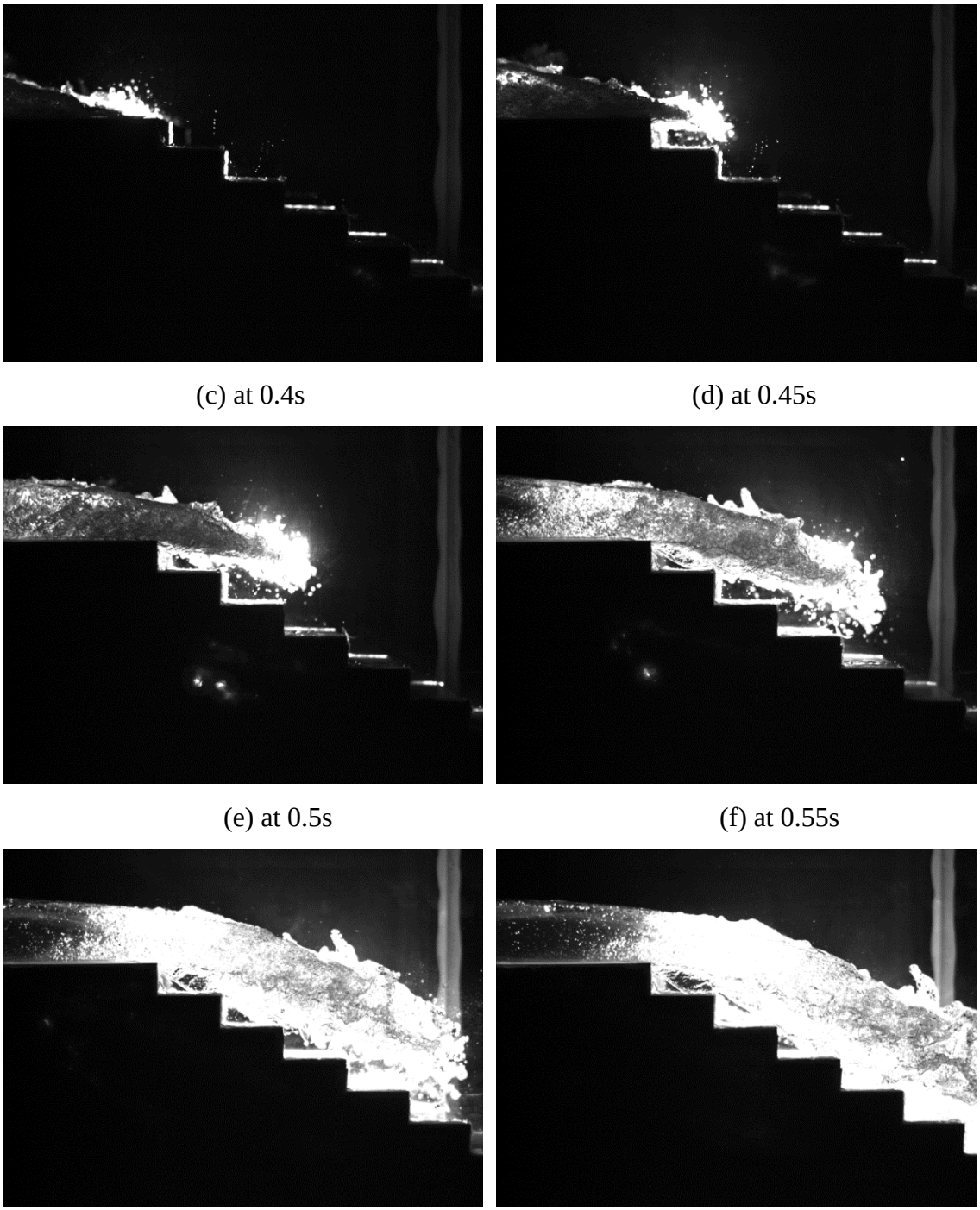

(c) at 0.4s (d) at 0.45s

(e) at 0.5s (f) at 0.55s

(g) at 0.6s (h) at 0.7s

Figure 4.6 Snapshots of flow over a normal stepped spillway at different time steps.

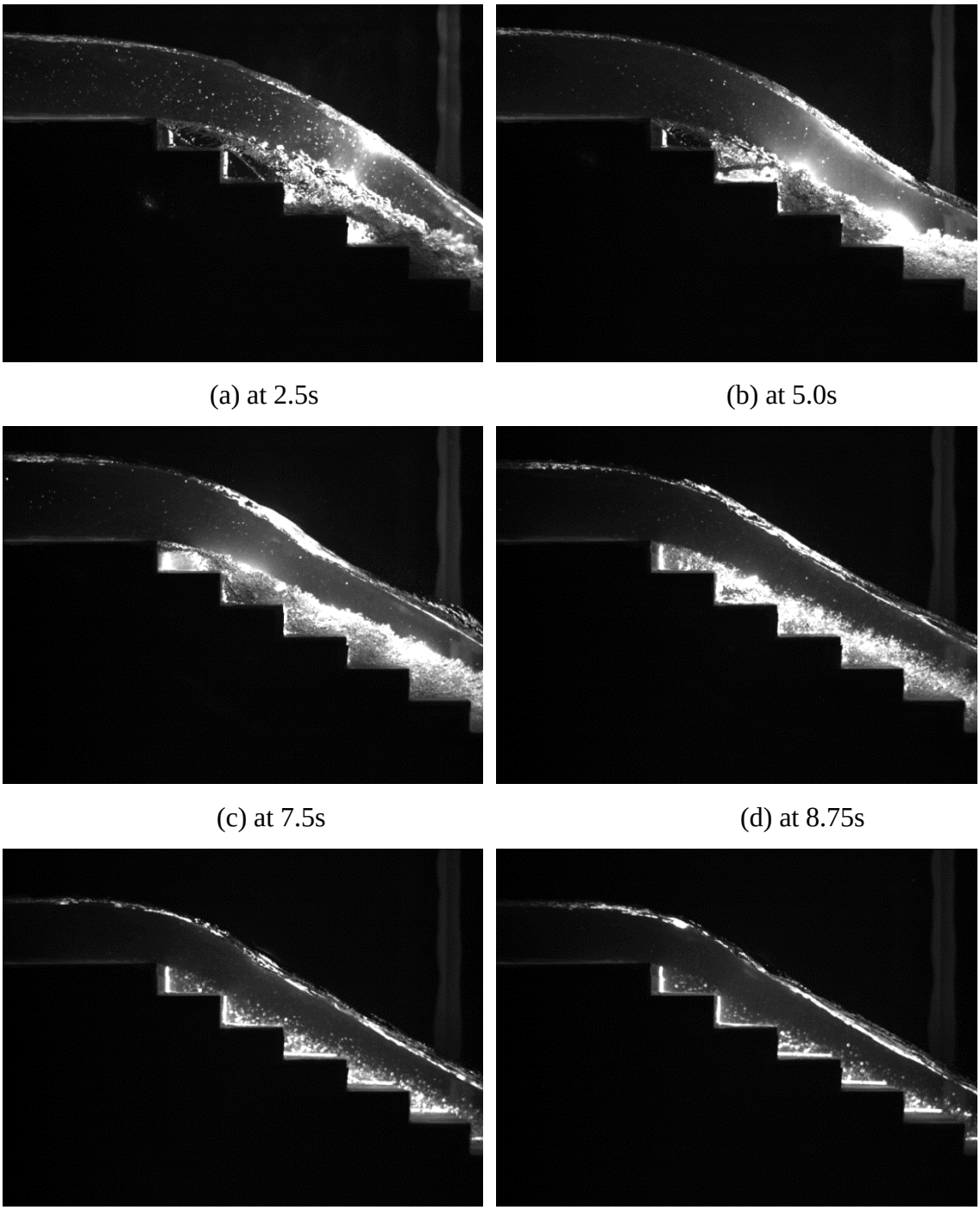

(a) at 2.5s (b) at 5.0s

(c) at 7.5s (d) at 8.75s

(e) at 10s (f) at 10.5s

Figure 4.7 Snapshots showing flow developing over a normal stepped spillway.

It is very important to mention that all tests have been conducted under skimming flow condition. That was the reason for waiting some time at the beginning of the experiment until the water fills all air pockets over steps. In Figure 4.7a, it is clear that water has not

filled the first two steps at that moment. However, after 6.25s, water starts to fill both of them (Figure 4.7d). Some cloudy patches can be observed at the early stage of the skimming flow where some tiny air pockets reflect the laser light. Therefore, it is better to wait longer to be sure that skimming flow conditions have established completely. Under skimming flow conditions, particles can be observed due to laser reflections (Figure 4.7).

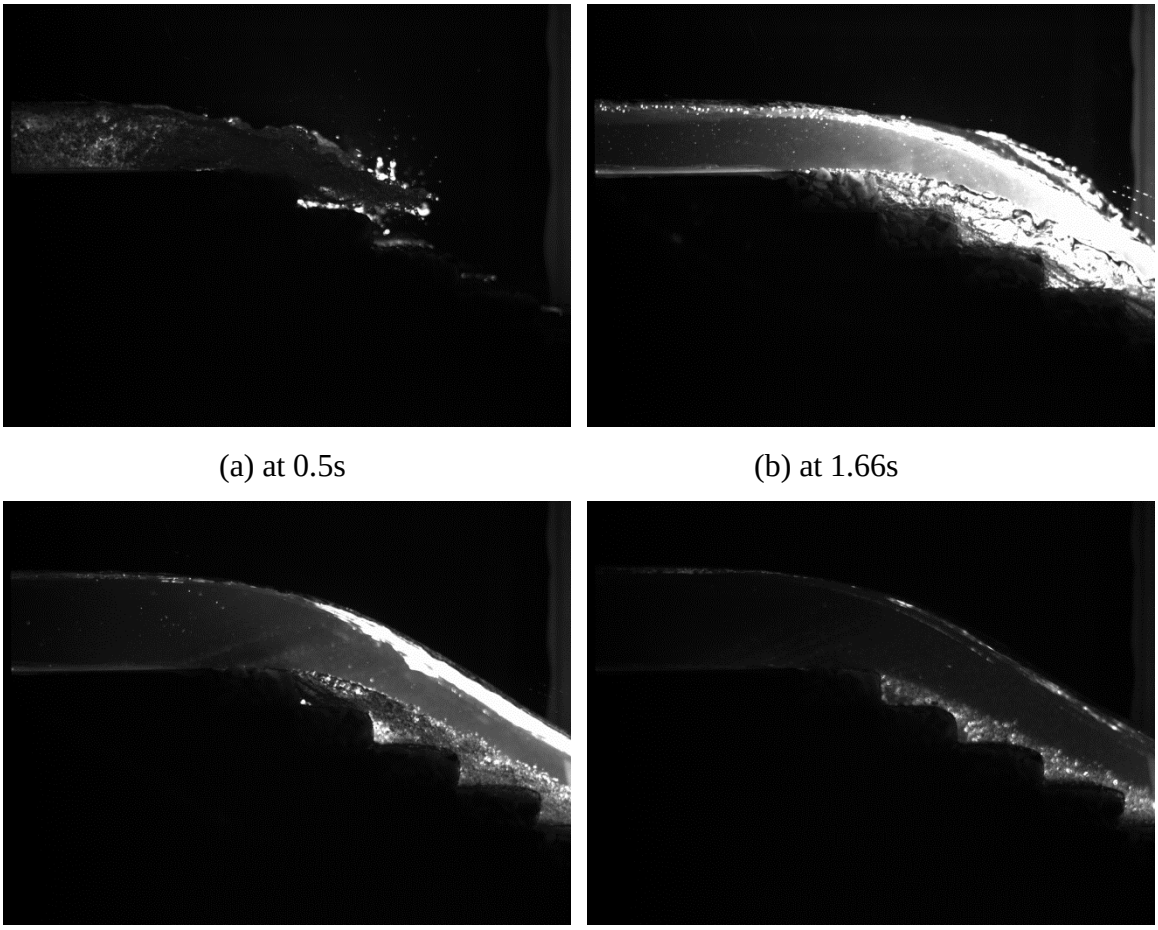

(a) at 0.5s (b) at 1.66s

(c) at 3.3s (d) at 5s

Figure 4.8 Snapshots show flow developing over the gabion steps.

For gabion stepped spillways, it can be concluded that the process to establish skimming flow is almost the same without gabions, however, gabion stepped spillways needs more time to establish skimming flow as some of the water goes through the porous media

(between the gravel); this is likely to be the reason for the delay in establishing skimming flow (Figure 4.8).

4.3. Post-processing of PIV measurement

The Dynamic Studio software of Dantec was used for the post-processing purposes. As mentioned earlier, the adaptive PIV method was applied to analyse the data. The Fast Fourier Transformation (FFT) was used to calculate the correlations within the adaptive method. The main reason for using this approach is due to its ability to give higher calculation speed compared to a direct implementation, however, this method has an inherent assumption that the input particle patterns are cyclic and the correlation can apply across the boundary of the interrogation area. In cases where the patterns are not cyclic, 'edge' effects are generated leading to a loss of accuracy near the boundaries

This assumption of the cyclic behavior can be an error source as the particles near the left-hand edge are assumed to be present just to the right of the furthest edge to the right of the interrogation area, and in the same way particles close the right-hand edge are assumed to be present also just left of the leftmost edge. However, if the sizes of the interrogation area and time between the two particle image recordings were set to be suitable enough, a dominant peak in the correlation map can be produced by the "true" particle displacement. These supposed phantom correlations can show small noise-peaks which can be removed by filtering for a smoother result.

It is possible to reduce or even eliminate the cyclic noise from the correlation map by using different window functions such as the top hat, Gaussian, Bartlett and Hamming window. The window's function is a preprocessing of data in the interrogation areas prior to the performing the correlation. For example, the top hat function can mask out the right, left, lower and upper 25% of the interrogation area, set all grayscale values here to zero and process further on the remaining central 50% of the interrogation area. Probably, drawbacks can be found due to these functions such as using the top hat function can reduce the signal strength to 25% by reducing both height and width of the effective interrogation area by 50% each. In order to avoid this, it is suggested to use larger interrogation areas, when applying a window function. Therefore, attention needs to be

paid when window functions are used to reduce the noise. The window functions normally run in the spatial domain by manipulating the interrogation areas prior to correlation, while the filter functions work in the frequency domain.

Particle images should be at least two pixels in diameter to fulfil the Nyquist sampling criterion; however, in the real PIV experiments that might not be possible as particle image diameters are often in the range of 1-2 pixels. Violating the Nyquist criterion can create 'pixel locking' where measured velocities are biased towards values that correspond to integer pixel displacements on the images. While it is difficult to completely avoid that, the effects can be reduced by using a Gaussian low-pass filter. This filter can damp the high-frequency components that correspond to the narrow peaks in the correlation plane, which is normally produced due to small particle images. However, using this filter can also lower correlation peaks. Damping the high-frequency components can lead to broadening the peaks. The broadening of the peaks may decrease the pixel locking influence, whereas reducing the peak corresponds to a decrease in signal strength. The low-pass filter can reduce the noise. Gaussain k-value can be used to control the filter width; Small k-values produce broad filters while large k-values produce narrow filters.

There are other filters such as the No-DC filter which can also remove DC-components from the signal besides to Phase only Gaussian filter that has the effect of removing all energy content from the cross spectrum. It is important to highlight that every filter has advantages and disadvantages. Filters must be chosen carefully if used at all. In the present study, no filters were applied for the normal stepped spillways as the noise was not high. However, for the gabion stepped spillways case, due to the reflection of the porous media, a low pass filter has been used to improve the results (Figures 4.9 and 4.10).

4.4. Results

A comparison between the numerical and experimental results was conducted in order to find out the differences between the PIV and computational results. The comparison included velocities over the spillway crest and also over the outer edges of some steps. In

order to avoid discrepancies in the results which might be observed in the aerated zone, this study was carried out for the non-aerated zone. It is noted that the main issue in the aerated zone that air bubbles act as reflectors and that would make PIV images much nosier and more difficult to process. Additionally, the numerical code has the capability to simulate the single phase flows in the non-aerated regime rather than the two-phase flow in the aerated zone and this is crucial to conduct the comparison between both results. Consequently, the flow velocity data of the experimental work was observed and measured over the spillway crest and over the first three steps in the non-aerated zone where no air entrainment is expected to be observed.

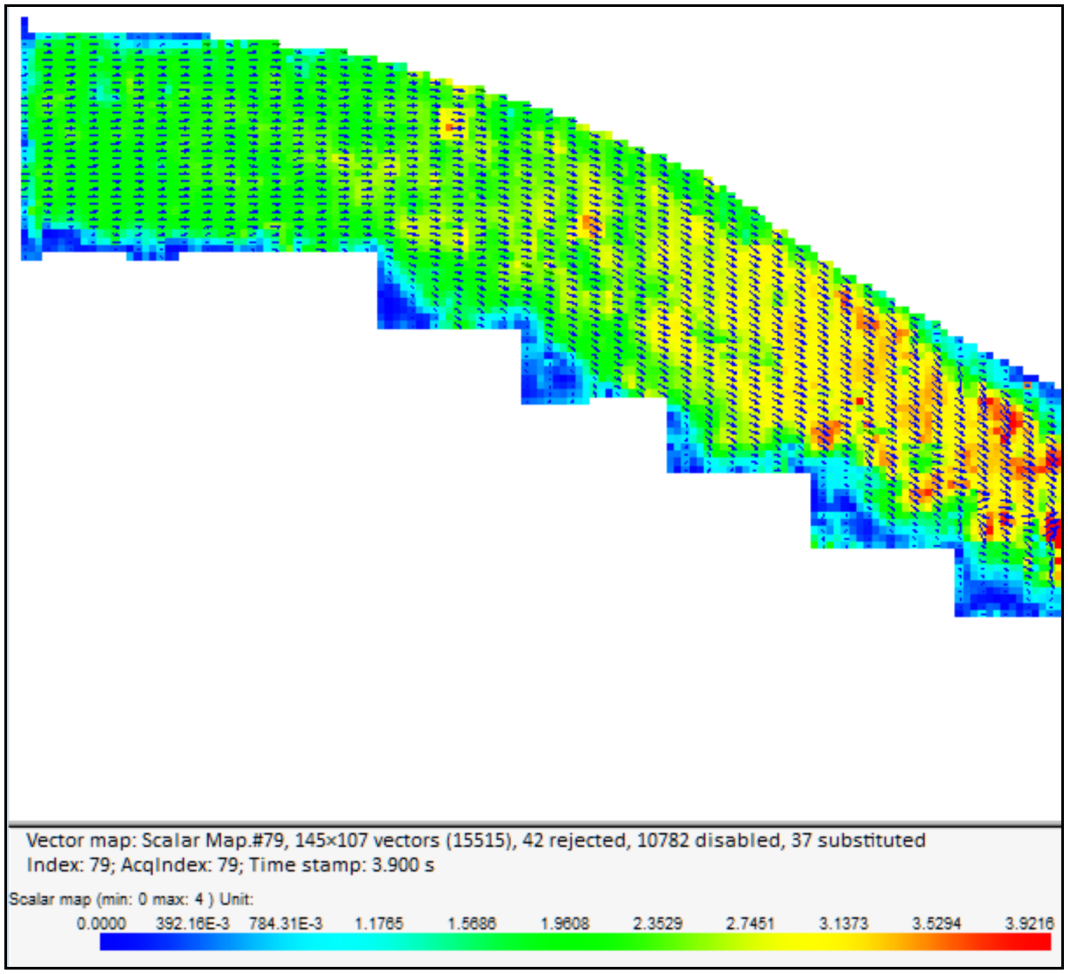

(a)

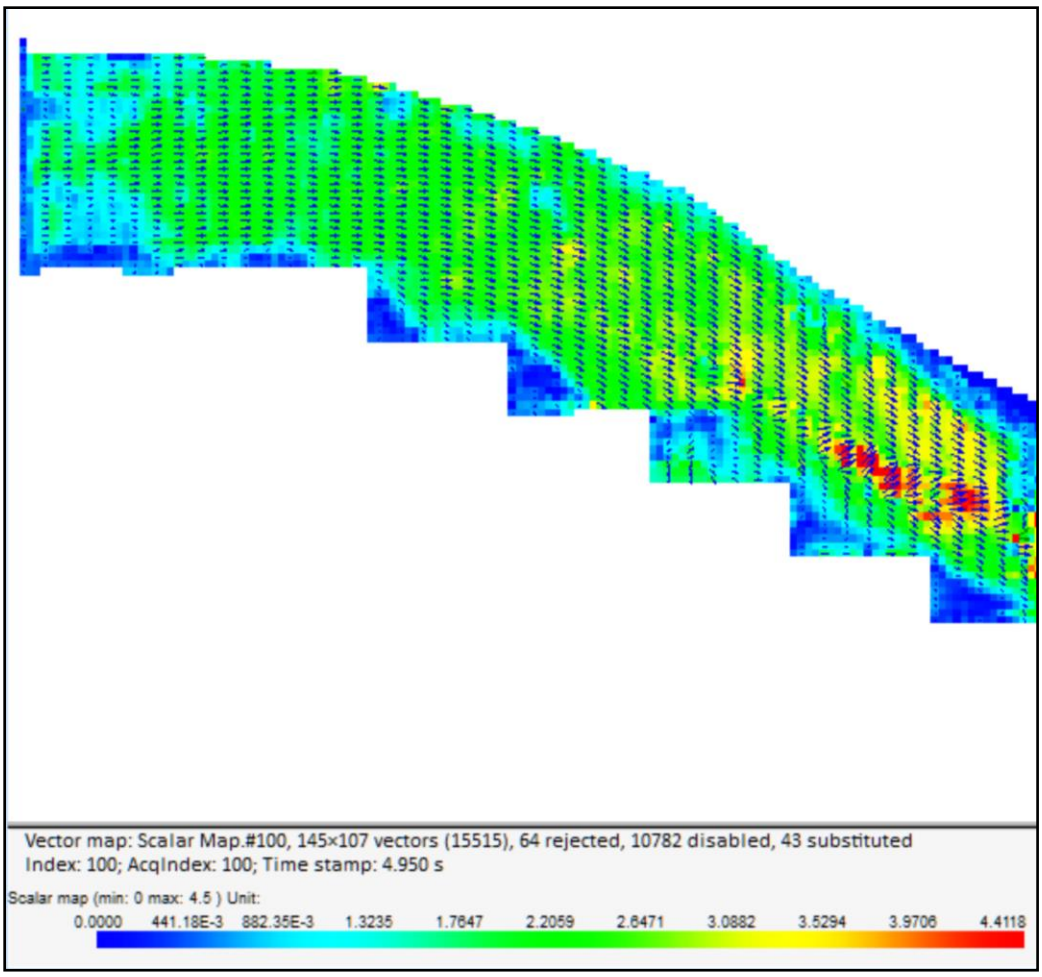

(b)

Figure 4.9 PIV scalar map with velocity vectors (m/s) of flow over normal stepped spillways at: (a) t=3.9s and (b) t=4.95s.

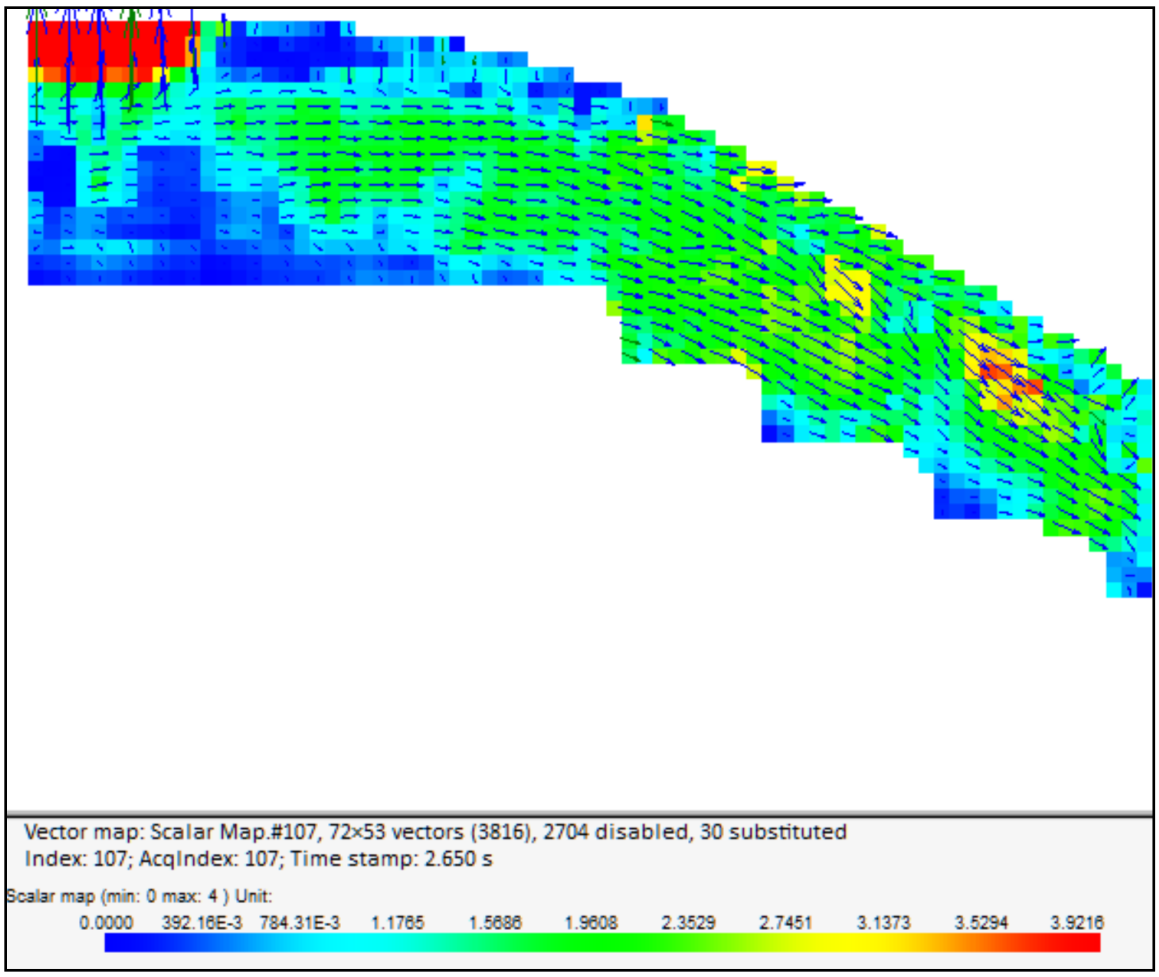
Vector map: Scalar Map.#107, 72×53 vectors (3816), 2704 disabled, 30 substituted
Index: 107; AcqIndex: 107; Time stamp: 2.650 s
Scalar map (min: 0 max: 4) Unit:
0.0000 392.16E-3 784.31E-3 1.1765 1.5686 1.9608 2.3529 2.7451 3.1373 3.5294 3.9216

(a)

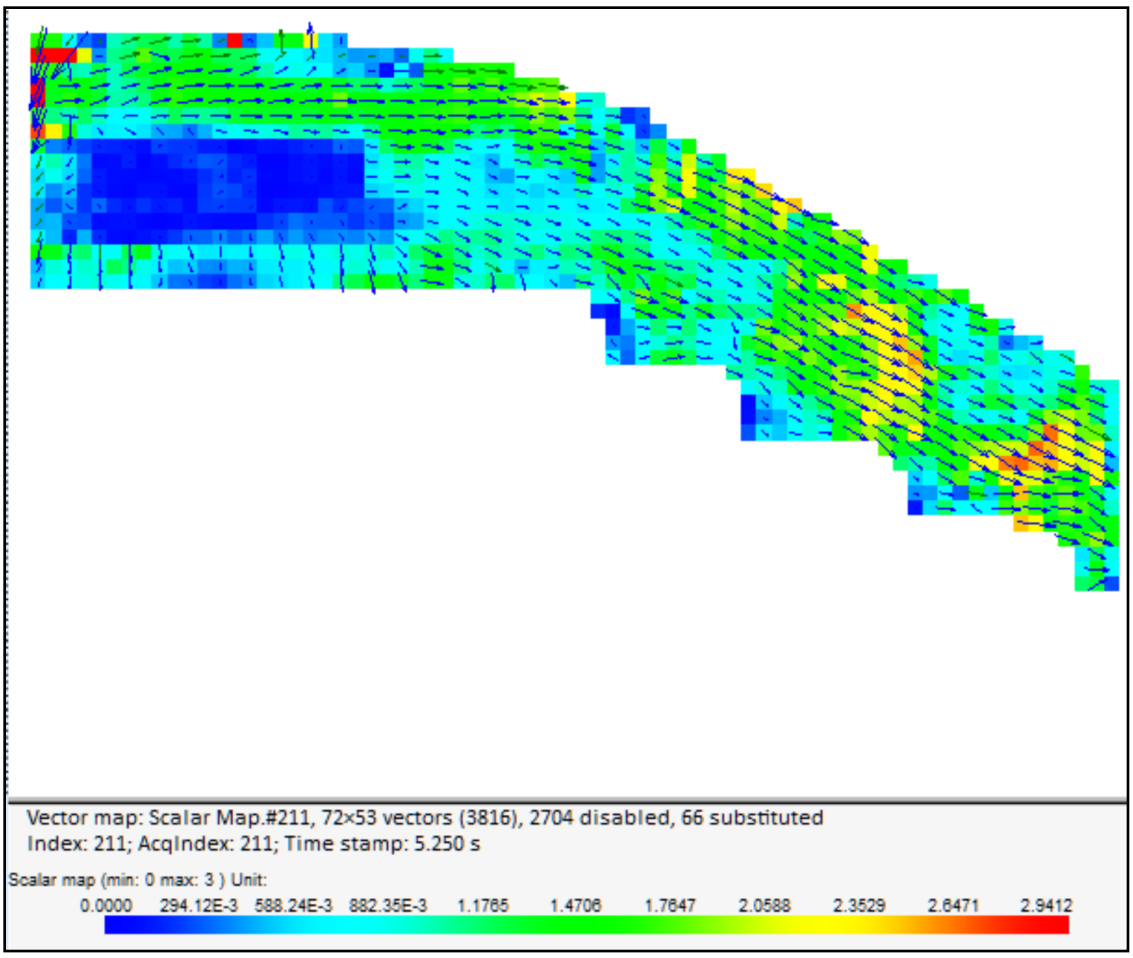

(b)

Figure 4.10 PIV scalar map with velocity vectors (m/s) of flow over gabion stepped spillways at (a) t=2.65s and (b) t=5.25s.

The first comparison was established for velocity distributions near to the end of the broad crest and at different vertical positions to be able to observe the velocity profile over time (Figure 4.11). Comparisons were also made at approximately mid-depth at the ends of step 3 and 4. The comparison between the velocity results of the experimental work and the numerical work is shown in Figure 4.12. Overall, the agreement between the results and over different points with time is good. It can be noticed that the numerical data is very close to represent the average value of the experimental data in some points. However, it is slightly different for the first three points and that probably due to the noise in the images. Also, the reason for having spikes in the experimental data could be related to the noise, and that may come due to the reflection of the laser when it

hits the turbulent flow. Generally, the level of the noise was light and therefore acceptable results were able to be achieved.

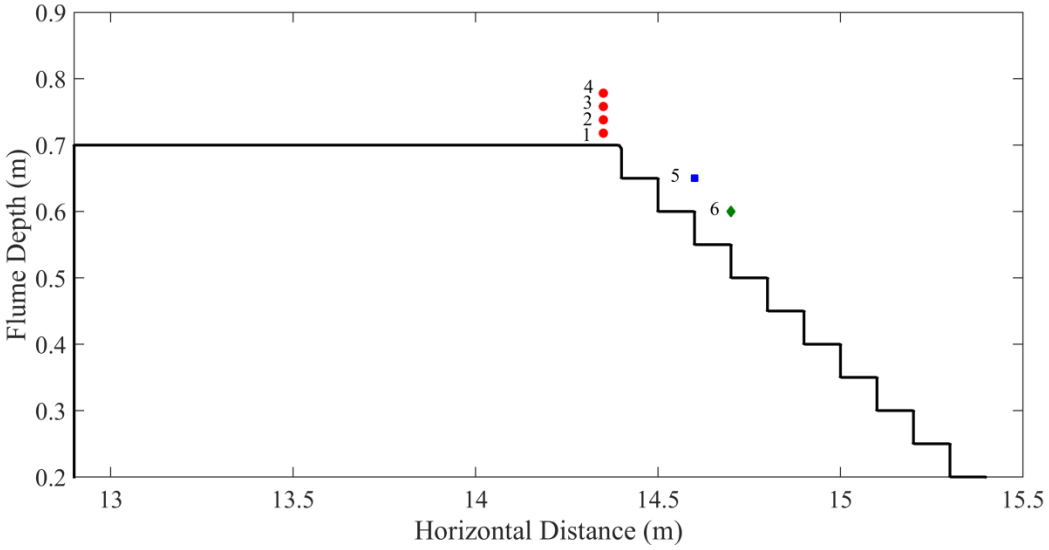

Figure 4.11 The locations of the validation points over the normal stepped spillway.

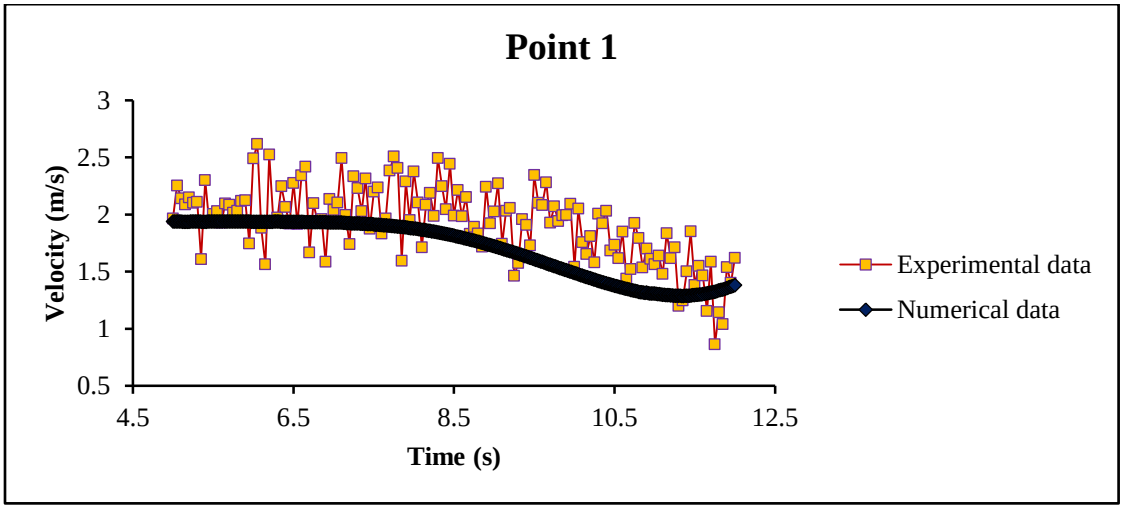

(a)

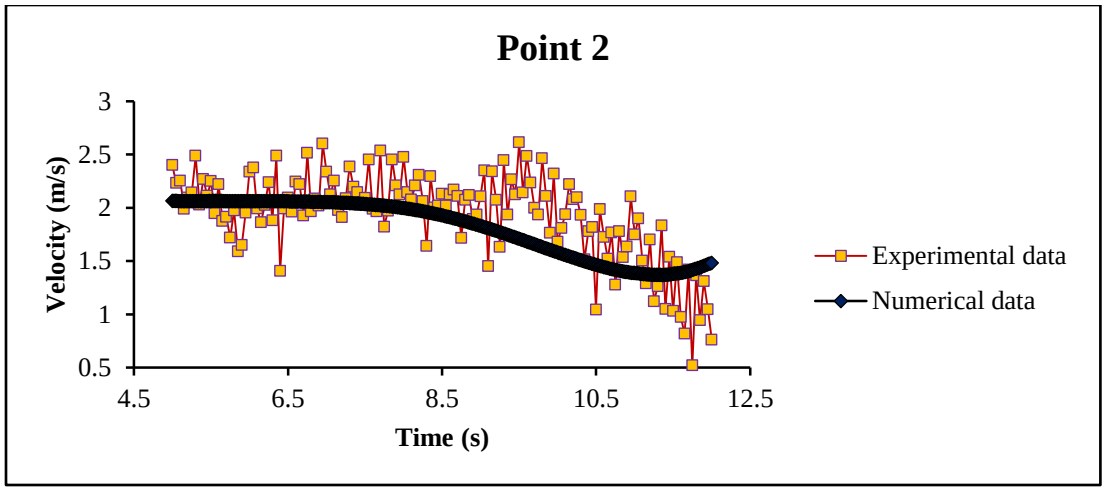
Point 2
Velocity (m/s)
3
2.5
2
1.5
1
0.5
4.5
6.5
8.5
10.5
12.5
Time (s)
Experimental data
Numerical data

(b)

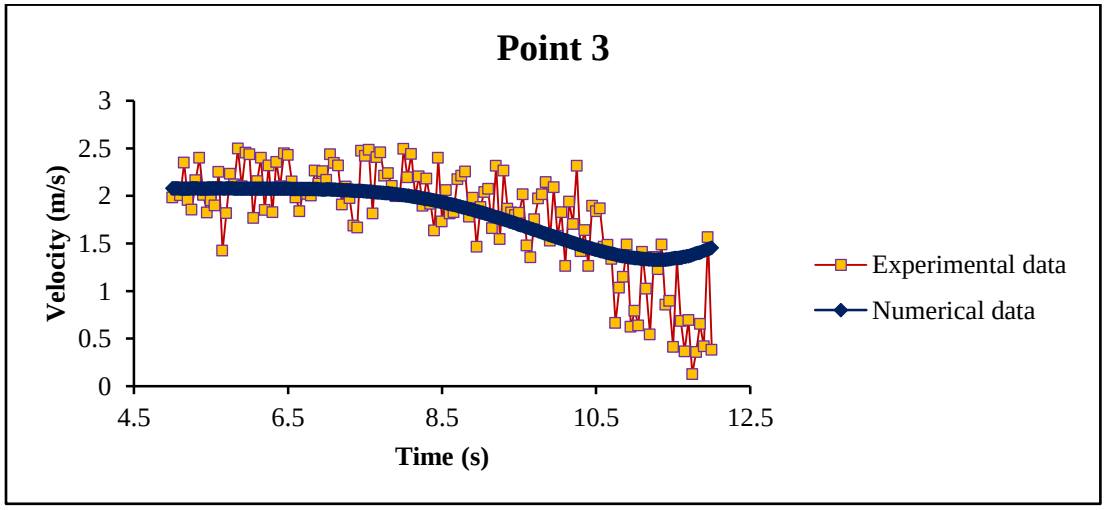
Point 3
Velocity (m/s)
3
2.5
2
1.5
1
0.5
0
4.5
6.5
8.5
10.5
12.5
Time (s)
Experimental data
Numerical data

(c)

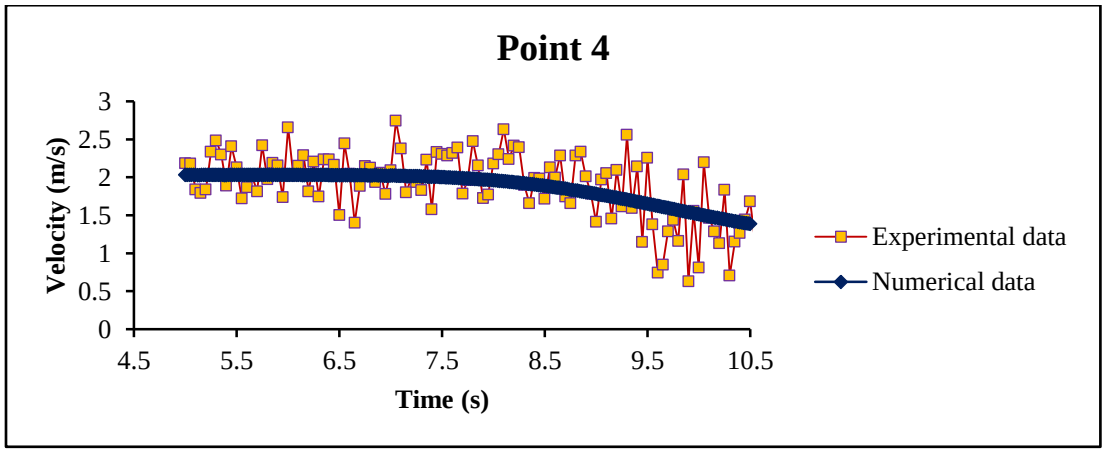
Point 4
Velocity (m/s)
3
2.5
2
1.5
1
0.5
0
4.5
5.5
6.5
7.5
8.5
9.5
10.5
Time (s)
Experimental data
Numerical data

(d)

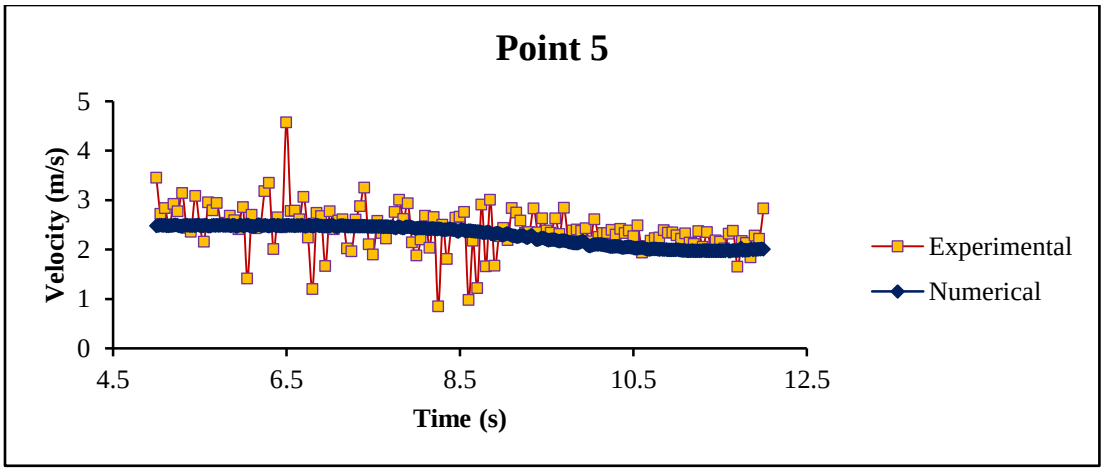

(e)

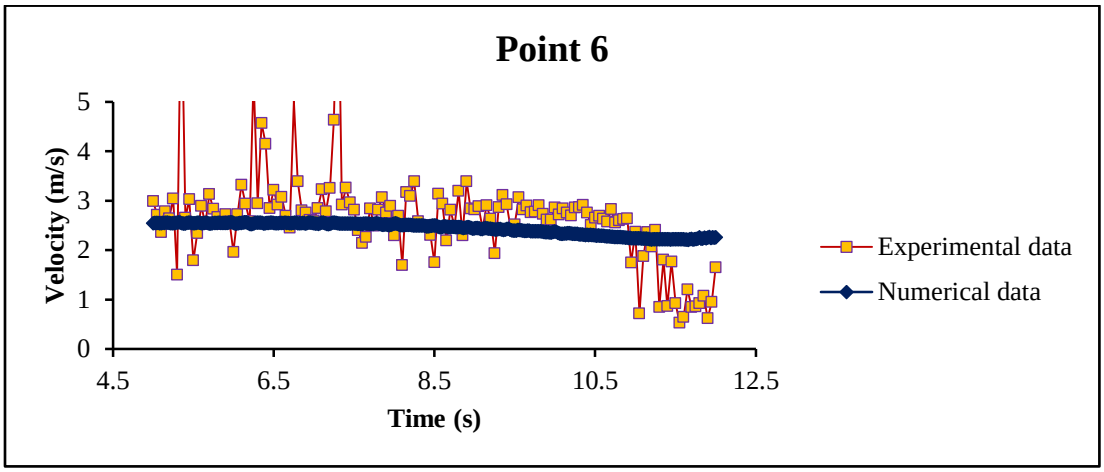

(f)

Figure 4.12 A comparison between the numerical and the experimental results of the velocity distribution over time at different locations over normal stepped spillway.

As shown in Figure 4.13, a second comparison was conducted also at different locations over the gabion stepped, similar to the earlier comparison of the normal stepped spillway. It is useful to highlight that the results of the gabion stepped spillways were not in good agreement with numerical results compared to the normal stepped spillways which showed good agreement with the numerical results. Although at certain positions and for certain times, good agreement has been achieved between the experimental and numerical results, few other points showed different levels of agreement between the results as can be seen in Figure 4.14.

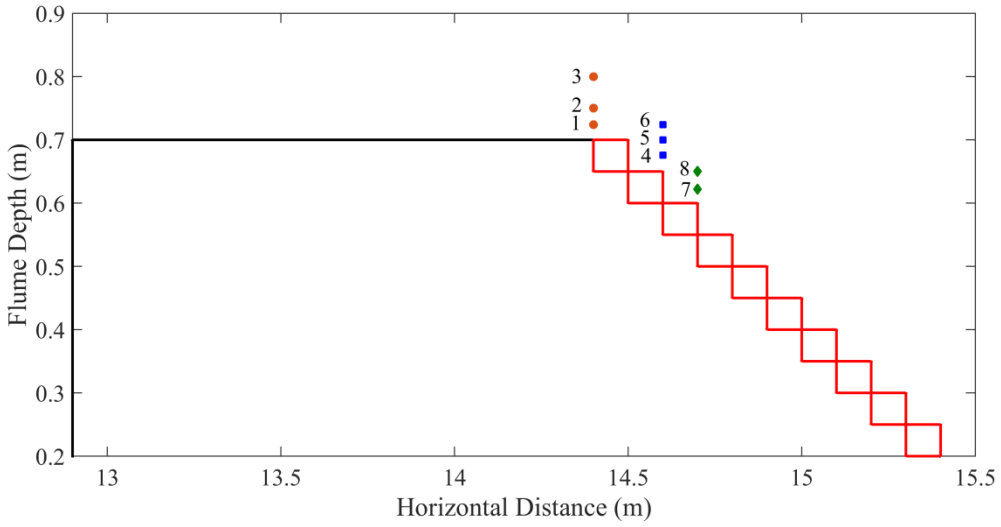

Figure 4.13 The locations of the validation points over the gabion stepped spillway.

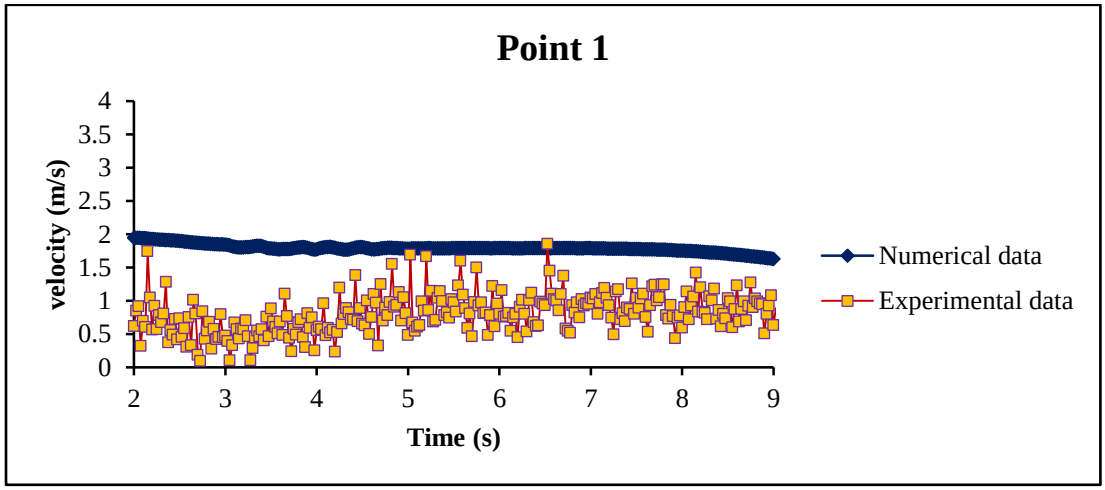

(a)

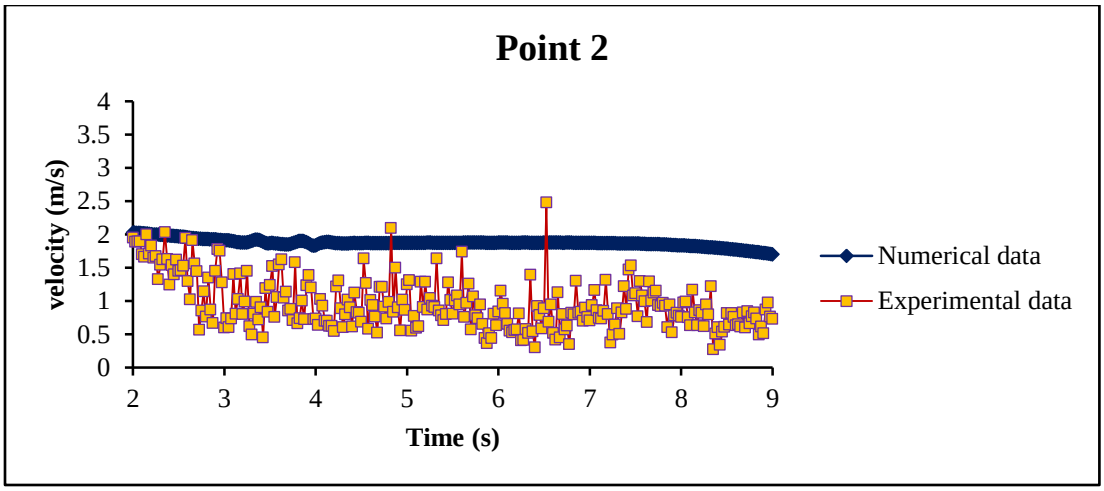
Point 2
velocity (m/s)
Time (s)
Numerical data
Experimental data

(b)

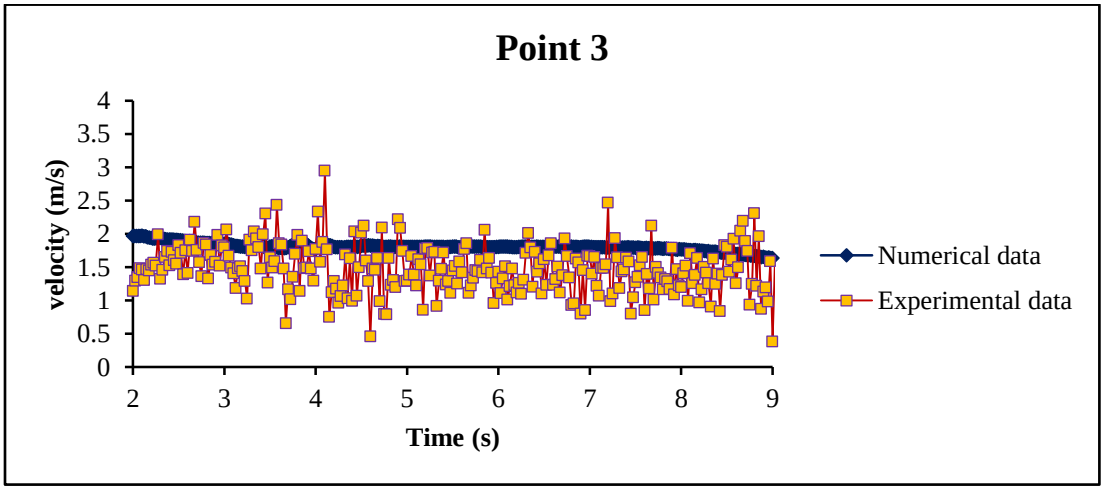
Point 3
velocity (m/s)
Time (s)
Numerical data
Experimental data

(c)

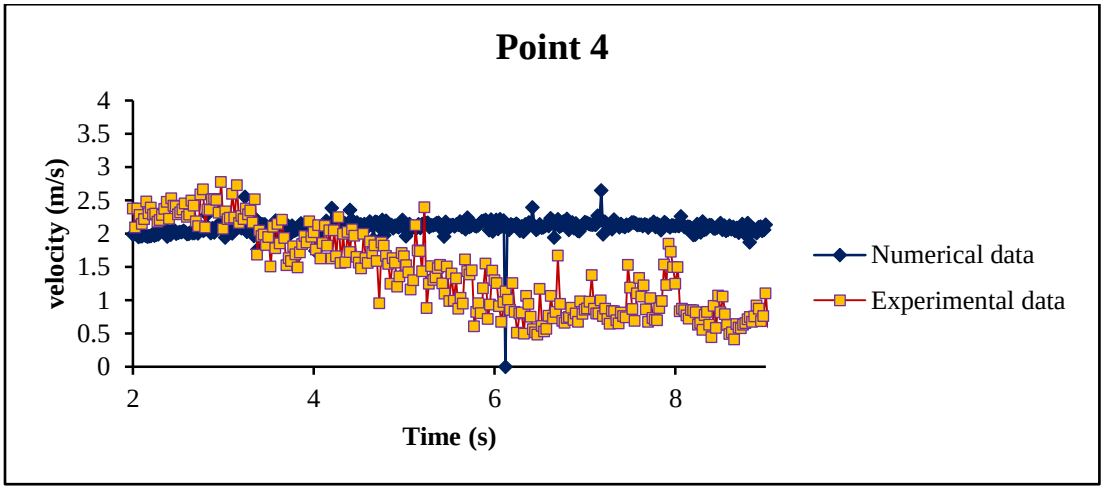
Point 4
velocity (m/s)
Time (s)
Numerical data
Experimental data

(d)

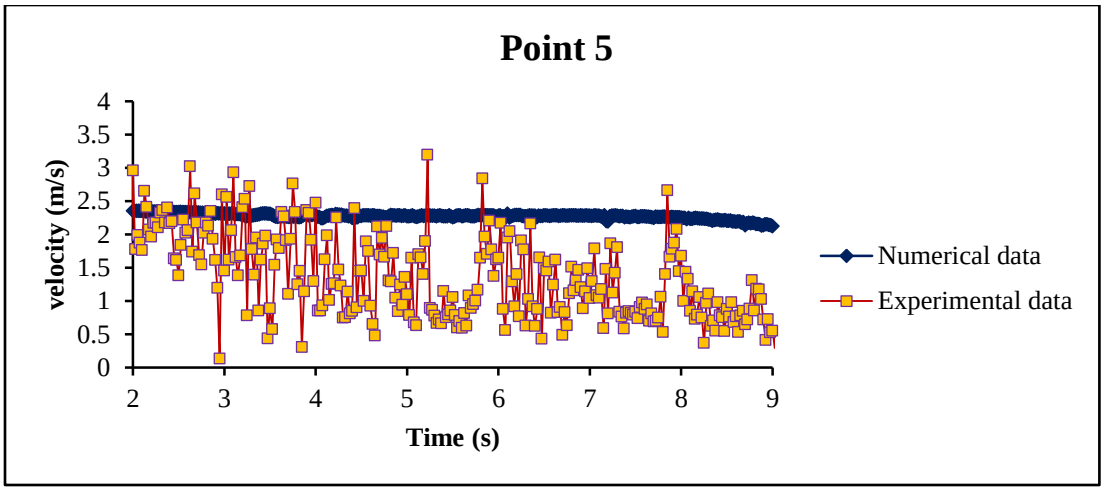
Point 5
velocity (m/s)
Time (s)
Numerical data
Experimental data

(e)

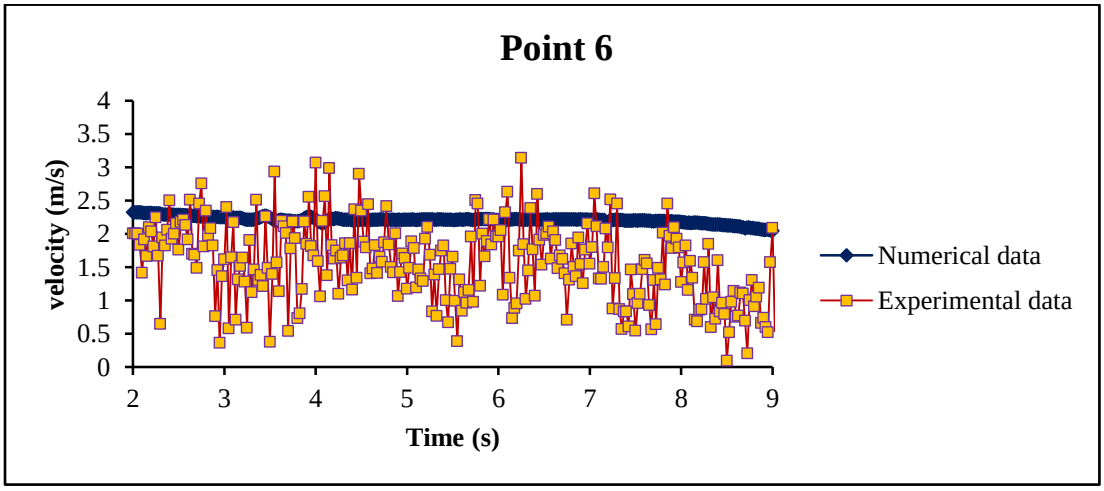
Point 6
velocity (m/s)
Time (s)
Numerical data
Experimental data

(f)

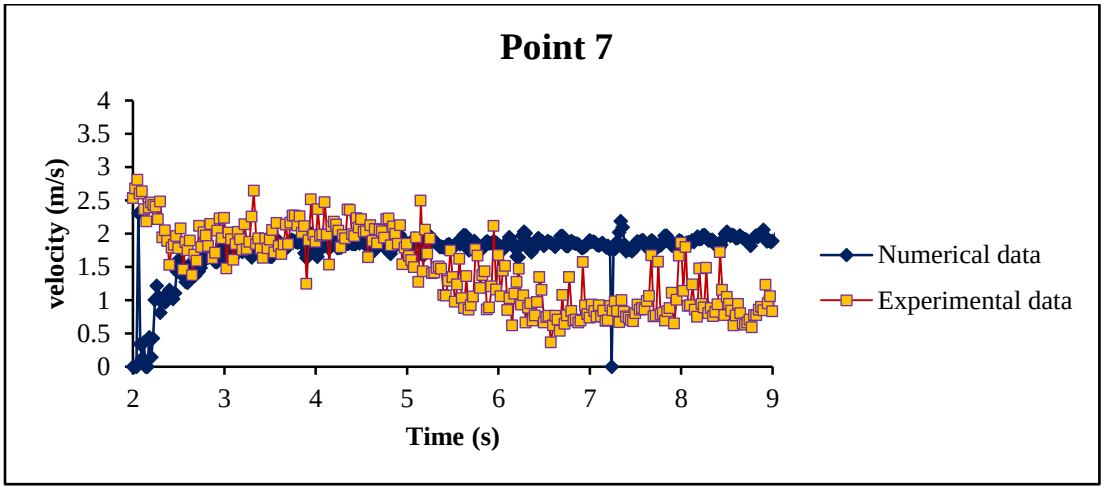
Point 7
velocity (m/s)
Time (s)
Numerical data
Experimental data

(g)

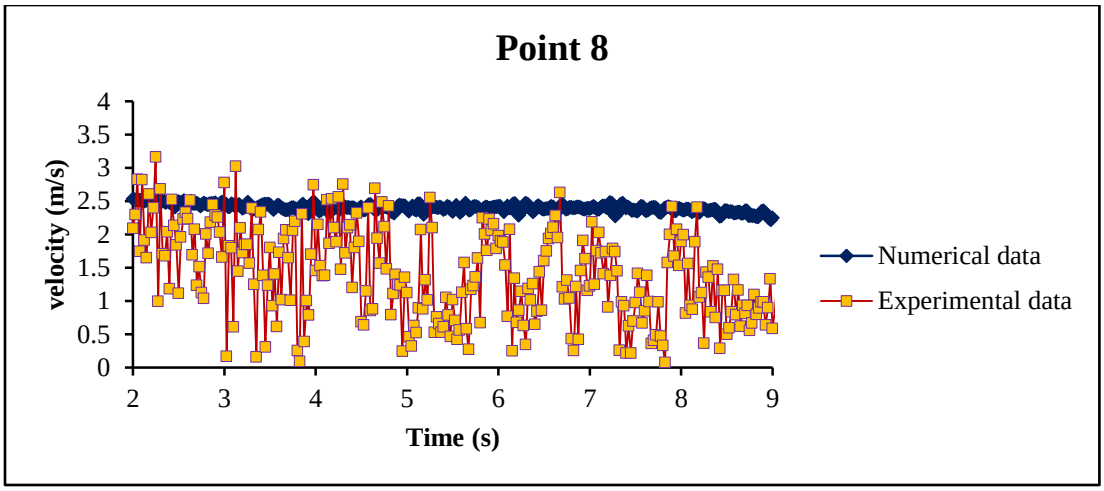

(h)

Figure 4.14 A comparison between the numerical and the experimental results of the velocity distribution over time at different locations over gabion stepped spillway.

The general trend of the results showed the computational results are higher than the experimental results. This relative overestimation for velocity values could be related to many reasons such as the fact of the unit length assumption in the 2D codes. Thus, the amount of the water volume on the upstream side will be affected, and that obviously an important reason. In other words, due to the difference in the volume of the water between the numerical and the experimental work, high velocity will be expected in the numerical results due to the high volume.

Although the same set up has been used for the normal stepped spillway in terms of the initial volume conditions, some discrepancies have been observed in the results. This is probably due to the noise level in the images of the PIV measurements which is slightly high as a result of the turbulent flow and the porous media effect. Furthermore, during the post-processing process of the images, the particle density was a bit low compared to the normal stepped spillways case so tracking the illuminate seeds was harder. The reflection in the gabion case was very high and that led to reduce the laser sheet inside the water, and therefore the noise level in the images was high.

The PIV setup in the present work in terms of the laser position and the model constructed material, which is made from the Marine Plywood, revealed that this kind of setup might be not ideal. Therefore, for the future work, many recommendations can be listed based on the experience of the current work. For instance, it would be better to build the model from a transparent material, in order to set the laser shutter beneath it, and therefore the effect of the reflection could be mitigated. Also, using other types of the gravel particles can allow the laser sheet to go through the gravel particles easily, in order to avoid the reflection problem. Furthermore, it might be better to use a flexible laser shutter which contains a flexible arm to modify its position as this kind of arms can give much more flexibility. Considering these issues may reduce the discrepancies in the results.

The results of this chapter showed that the numerical model is able to simulate the water flow over normal stepped spillways accurately. However, in the gabion case, the results showed some discrepancies at some points over the gabion boxes due to the noise issue. The next chapter will investigate the water profile over gabion stepped spillways with step heights of 0.06, 0.09 and 0.12m and chute slopes of 1V:2H, 1V:2.5H and 1V:3H. Additionally, different values for the porosity and the particle size of the porous media will be tested.

Chapter 5 : Results and Discussion of Free Surface Profiles

5.1. Introduction

This chapter focuses on the computational results provided by the numerical NEWFLUME code which is applied in the present work. First, a general description of the required parameters will be provided to establish the computational domain of numerical models that tested in the current work. Then the numerical results achieved in this study of the position of the water surface level will be presented and discussed. The present study was conducted to describe the skimming flow characteristics in the non-aerated zone over gabion stepped spillways. To achieve this, twenty-seven numerical cases were set and examined. The next section shows details of the physical parameters which are needed to create the geometry of the numerical models.

5.2. Chute slope

Stepped spillway generally can be named by a moderate spillway when the bottom slope is flatter than 27° and steeper than 16°. Moderate slopes are considered as the most common slopes used in the design of the downstream face of embankment dams (Chanson, 2002). Many moderate slopes have been tested by different researchers such as:

- Gonzalez (2005) tested the chute slopes of 16° and 21.8°,
- André (2004) examined the chute slopes of 30° and 18.4°
- Husain (2013) conducted a numerical study to investigate chute slopes of 18.4°, 21.8° and 26.6° which represents 1V:3H, 1V:2.5H and 1V:2H respectively.

All slopes were tested without gabion present; therefore, the last three slopes which are tested by Husain (2013) will be examined again in this study with the gabion steps. These

slopes represent a good range for the moderate slopes which may use regularly in the design of stepped spillways.

5.3. Step height

Since the numerical code has been validated against the reduced model scales, the numerical simulations of the current work are conducted in the same scale range and it will not be in the prototype scale. Therefore, three different step heights 0.06, 0.09 and 0.12m were tested in order to explore their impact on the flow properties under the skimming flow conditions. Step heights were selected in a way to fulfil the requirement of Froude similitude in stepped spillways. According to the construction techniques of placing roller compacted concrete, the step height in the real cases could be 0.3m, 0.6m, 0.9m or 1.2m (Boes and Hager, 2003). Chanson and Gonzalez (2005) showed that it is crucial to keep the step height bigger than 0.02m and make Reynolds number greater than 10^5 in order to apply Froude similitude satisfactorily in stepped spillways.

5.4. Scale effects

Unlike clear water open channel flow, highly turbulent air–water flow cannot be modelled without scale effects when using Froude similitude, because of the important role of viscosity and surface tension. For a true similarity of the aeration process between model and prototype, the Froude, the Reynolds and the Weber similarity laws would have to be fulfilled simultaneously. If Froude scaling is applied, air bubbles are proportionally too large in a scale model, resulting in a lower transport capacity and a higher detrainment rate as compared to prototype conditions. Therefore, care must be taken when upscaling model results to the prototype scale. Kobus (1984) proposed Reynolds numbers with flow depth as reference length of at least 10^5 to minimise viscous effects. Rutschmann (1988) and Speerli (1999), who investigated spillway aerators and bottom outlets, respectively, concluded that the Weber number, with the flow depth as the reference length, should be at least 110 for surface tension effects to be negligible.

The scale ratio can be defined as the ratio between the prototype and model dimensions. Pinto (1984) reported that model scales should not be less than1:15 for spillway aerators. However, Vischer et al. (1982) deduced that the scale factor should be equal to or less than 15 to achieve the correct aeration modelling. Pergram et al. (1999) reported that models with scale 1:20 can characterise the behaviour of stepped spillways, however, the results converge quicker when the scale is larger than 1:15. Boes and Hager (2003) claimed that in order to get the Froude model similitude in stepped spillways, the scale ratio needs to be no greater than 15. The step heights of 0.06m, 0.09m and 0.12m which are tested in the present study can give scale ratios of 10, 6.67 and 5 respectively and that considering 0.6m as the step height in the prototype structure. All the discharge values which are tested in the numerical models deliver Reynolds number higher than that recommended above. Therefore, the numerical results achieved in this study can be used in the design of moderate slope stepped spillways with three different heights 0.30m, 0.60m, 0.90m and 1.2m.

5.5. Discharge measurements over the crest

The discharge is calculated by the same way that conducted previously in the validation cases over the critical section on the broad crested weir. The critical section is located by testing the Froude Number. Therefore, when the Froude Number is equal to one then the corresponding location represents the critical section over the broad crested weir. The crest of the broad weirs needs to be long enough to allow the streamlines to flow parallel above the crest. The length of the broad crested weir needs to be greater than 1.75m of the total upstream head in order to localise the critical section of the required discharge. The total upstream head normally located at a distance from the upstream corner of the weir. It is important to locate that distance because it represents the distance where the flow is considered to be uniform. The Bernoulli's equation can be used to estimate the distance approximately by neglecting the head losses between that section and the critical section on the weir crest.

5.6. Run numerical model

In the present study, three different step heights and three different widths were tested with the numerical code to investigate the step configuration impact on the flow properties over gabion stepped spillways. Step widths were set to give spillway slopes of 1V:2H, 1V:2.5H and 1V:3H. The porosity of the gabion steps was varied from 0.25 to 0.4, while the grain size of the gabion steps (D_{50}) ranged between 0.005m and 0.02m. The selection of these values provides a good range of physical characteristics likely to be encountered in real schemes in order to investigate the effect of the gabion porosity, gabion particles size, spillway slopes and step heights on the flow characterisation (Table 5.1). It is essential to highlight that all the numerical runs have been conducted under the dam break conditions in order to achieve the typical high flow discharge that might be expected during the flooding seasons which represents the worst scenario.

In the numerical model, gabion stepped spillways with 0.06m step height were located at 7.5m and the weir was placed at 6.9m. The length of the weir crest is 0.6m, (Figure 5.1). Based on the recommendations which have mentioned earlier regarding establishing the critical depth over the weir crest, the crest length was set to 0.6m. Stepped spillways with 0.12m and 0.09m step height were positioned at a distance of 8m from the boundary edge, while the weir of 0.6m length was placed at a distance of 7.4m, (Figure 5.2 and 5.3). The initial water depths were 1.58m, 1.7m and 1.8m for 0.12m, 0.06m and 0.09m step height respectively; so the contents of the upstream tank was sufficient to achieve the required discharge and also to mitigate the effects of transients. The total simulation time was set to 15s for 0.12m step height, 16.5s for 0.09m step height and 18s for 0.06m step height. The time step was taken as 0.0001s to satisfy the stability criterion in all cases. The mesh sizes in the x- and in the y-directions were 0.01m and 0.005m respectively for 0.09m and 0.12m step height. However, for 0.06m step height, it was 0.0075m in the x-direction and 0.003m in the y-direction. The model domain has closed boundaries except the right-hand boundary which was set as an open boundary to let the water exit the flume (Figure 5.4).

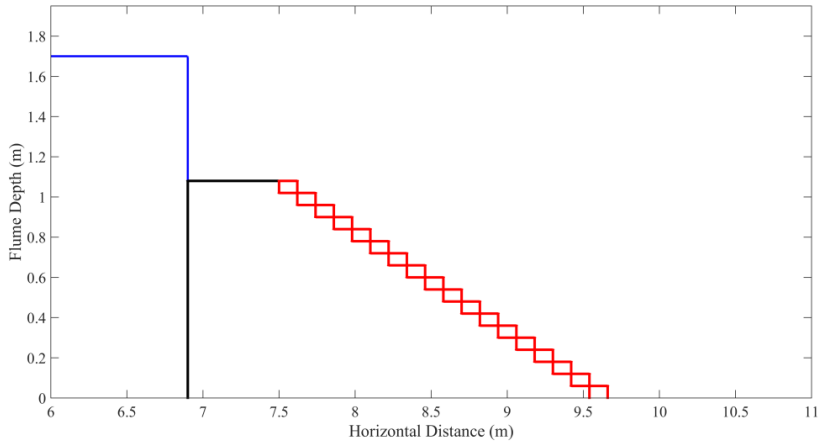

Figure 5.1 Gabion stepped spillway with 0.06m step height and 1V:2H slope.

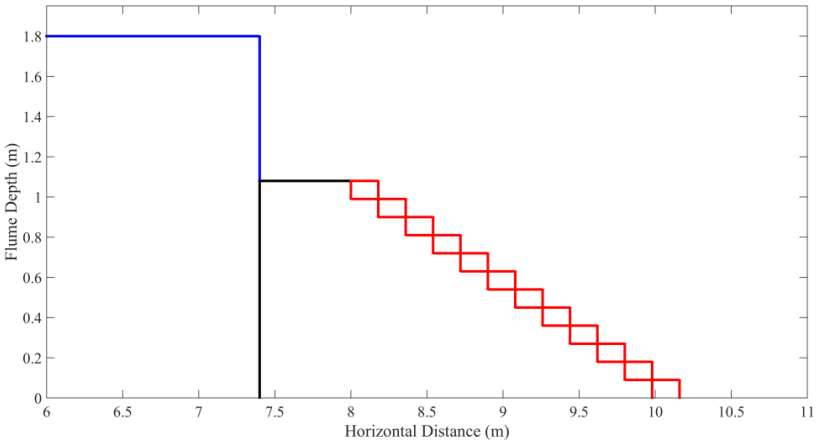

Figure 5.2 Gabion stepped spillway with 0.09m step height and 1V:2H slope.

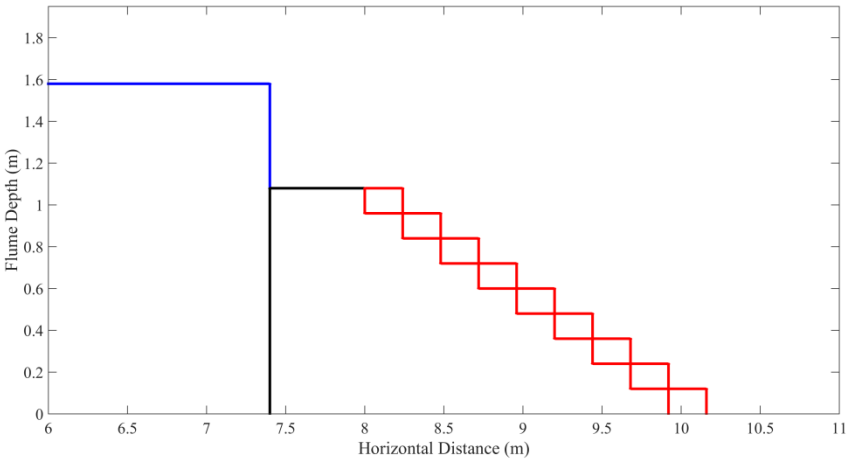

Figure 5.3 Gabion stepped spillway with 0.12m step height and 1V:2H slope.

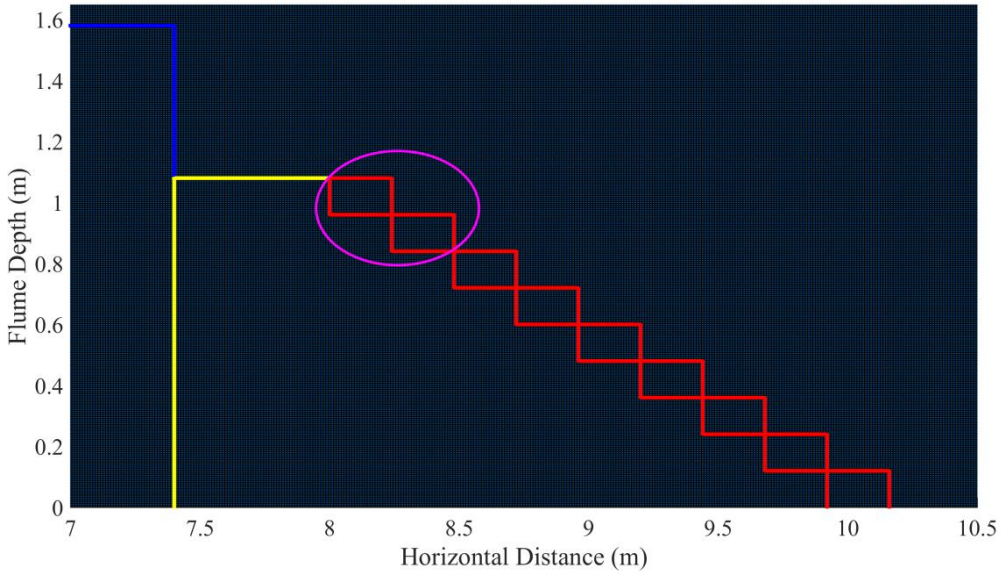

(a)

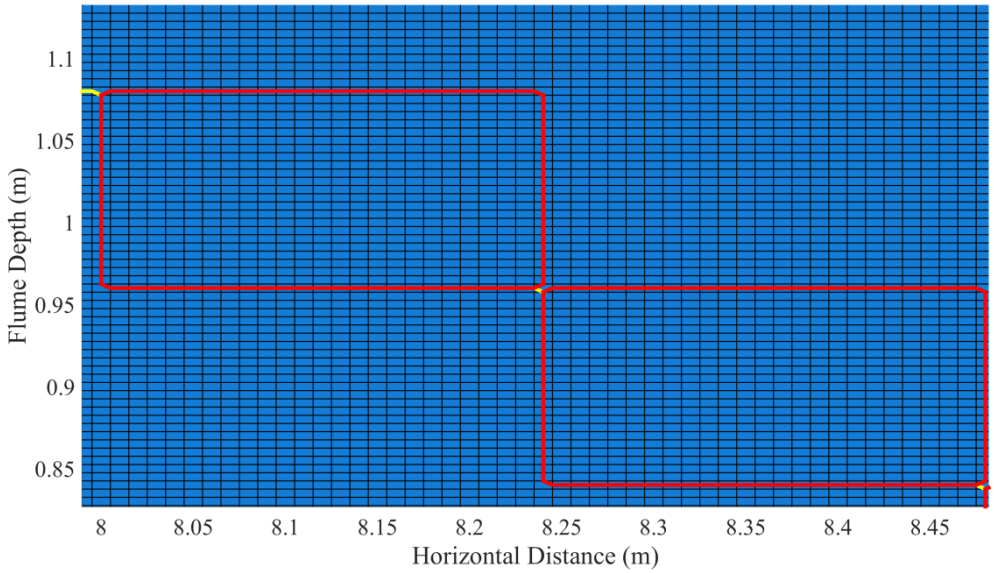

(b)

Figure 5.4 Grid distributions: (a) around the entire geometry area of gabion stepped spillway and (b) for the first two steps.

Overall, as planned in Table 5.1, twenty-seven gabion stepped spillways cases with different step heights, slopes, diameter sizes and porosity were set up to investigate the position of water surface level, the location of the inception point, velocity distribution, pressure distribution, cavitation damages and energy dissipation.

Table 5.1 The numerical cases of gabion stepped spillways.

Height (m)	No. of steps	Height of steps (m)	Slope	Step length (m)	Porosity	Particle size(m)
1.08	9	0.12	1V:2H	0.24	0.35	0.005
				0.24	0.30	0.005
				0.24	0.25	0.005
				0.24	0.4	0.005
				0.24	0.35	0.01
				0.24	0.35	0.015
				0.24	0.35	0.02
			1V:2.5H	0.3	0.35	0.005
				0.3	0.30	0.005
				0.3	0.25	0.005
				0.3	0.4	0.005
				0.3	0.35	0.01
				0.3	0.35	0.015
				0.3	0.35	0.02
			1V:3H	0.36	0.35	0.005
				0.36	0.30	0.005
				0.36	0.25	0.005
				0.36	0.4	0.005
				0.36	0.35	0.01
				0.36	0.35	0.015
				0.36	0.35	0.02
1.08	12	0.09	1V:2H	0.18	0.35	0.005
			1V:2.5H	0.225		
			1V:3H	0.27		
1.08	18	0.06	1V:2H	0.12	0.35	0.005
			1V:2.5H	0.15		
			1V:3H	0.18		

The total porosity of a porous medium is the ratio of the pore volume to the total volume of a representative sample of the medium. Porosity is a dimensionless quantity. Generally, the soil system is composed of three phases solid, liquid (water), and gas (air), thus

V_s is the volume of the solid phase,

V_l is the volume of the liquid phase,

V_g is the volume of the gaseous phase,

$V_p = V_l + V_g$ is the volume of the pores,

$V_t = V_s + V_l + V_g$ is the total volume of the sample,

Then the total porosity of the soil sample (p) is defined as follows:

$$P = \frac{V_p}{V_t} = \frac{V_l + V_g}{V_s + V_l + V_g} \quad (5.1)$$

Gravel has been used in the present study to represent the porous media component. According to the standards, the minimum diameter of the particles should be greater than 2mm in order to consider them as a gravel material. Therefore, the minimum value for the gravel in this study is set to 5mm. The porosity of the gravel normally ranges between 0.25 and 0.4, hence, four different values, including the minimum and the maximum values of the porosity, have been selected to test the effect of the porosity on the flow properties. It is worth mentioning that both porosity and gravel size are required to be specified to define the porous layer in the numerical model.

5.7. Position of free surface

The free surface profile of the water flow over moderate gabion stepped spillways is explored in the present study. In order to investigate the effects of bottom chute slopes, step heights and gabion parameters like particle sizes and porosity on the position of the free surface, some figures were obtained in the following sections. In the numerical model, as mentioned earlier, the tests have been conducted within an initial water depth over the crest in the upstream side; however, the downstream side is completely dry. That kind of set up is similar to the dam break conditions. Therefore, all the regimes of the

flow over the stepped spillways like nappe flow, transition flow and skimming flow might be captured. As the present study investigates the properties of flow over gabion stepped spillways under the skimming flow conditions, attention needs to be paid to the time steps to be able to determine the exact time when flow attaches skimming flow. From that time step and later on, all flow properties such as the critical depth over the crest and velocity profiles can be measured as the flow attached skimming flow conditions. It is important to highlight that skimming flow should be determined at the time when all of the air pockets vanish inside and outside the gabion under the water free surface.

The results showed that the required time to attach skimming flow can be significantly influenced by the bottom chute slopes, step heights, porosity and diameter sizes (Table 5.2). As can be seen in Table 5.2 and 5.3, the results can change dramatically with porosity and particle sizes. Consequently, many issues in terms of achieving specific discharges were taken place. These issues could impact the investigation process of flow characteristics as flow rates might need to be fixed in order to conduct comparisons. Therefore, that has generated many limitations in terms of achieving high discharge values as the initial water depth is always the same for all tests. In other words, due to the same initial water depth and also because of different required time to attach skimming flow, it was hard to achieve high values of flow rates for all cases as flow rates decrease with time due to dam break conditions. Apparently, in some cases, high values of flow rates were achieved as skimming flow conditions were reached quickly, especially, when porosity and particle sizes have high values. However, in other cases, normal values of flow rates were obtained as more time to attach skimming flow conditions was needed.

The results revealed that the time to attach skimming flow increases when the porosity and particle size decrease as the flow needs more time to flow inside the porous media and fill all the air pockets. Moreover, the results showed that skimming flow of gabion stepped spillways could be attached faster with 1V:2.5H compared to 1V:2.0H and 1V:3.0H under the same initial conditions.

Table 5.2 Time to attach skimming flow for different values of porosity for gabion stepped spillways with 0.12m step height and 1V:2H chute slope

Porosity	Time to attach skimming flow (s)
0.25	6.735
0.3	6.285
0.35	5.1
0.4	4.62

Table 5.3 Time to attach skimming flow for different values of particle size for gabion stepped spillways with 0.12m step height and 1V:2H chute slope

Particle size (m)	Time to attach skimming flow (s)
0.005	5.1
0.01	3.06
0.015	2.475
0.02	2.4

Figures 5.5 and 5.6 illustrate a number of snapshots of the flow development predicted by the numerical code during the simulation of skimming flow at different instants for 0.06m and 0.09m step heights.

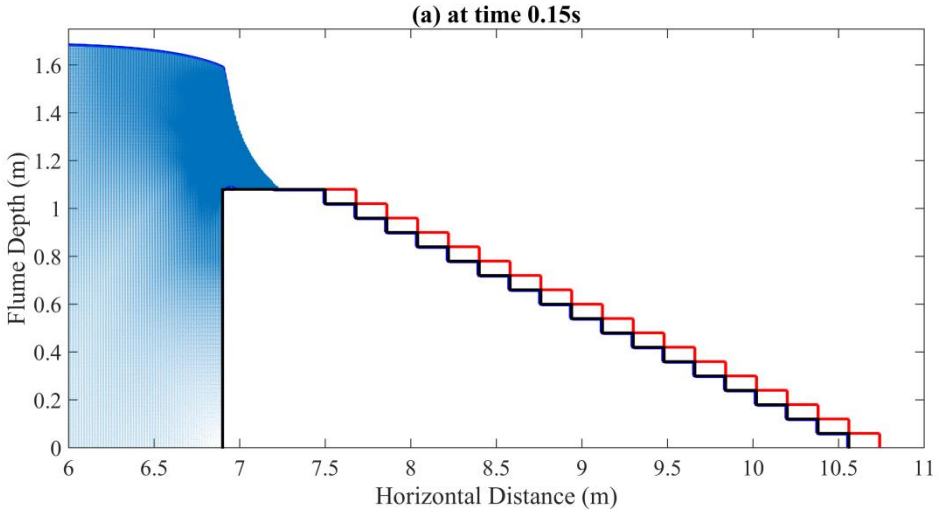

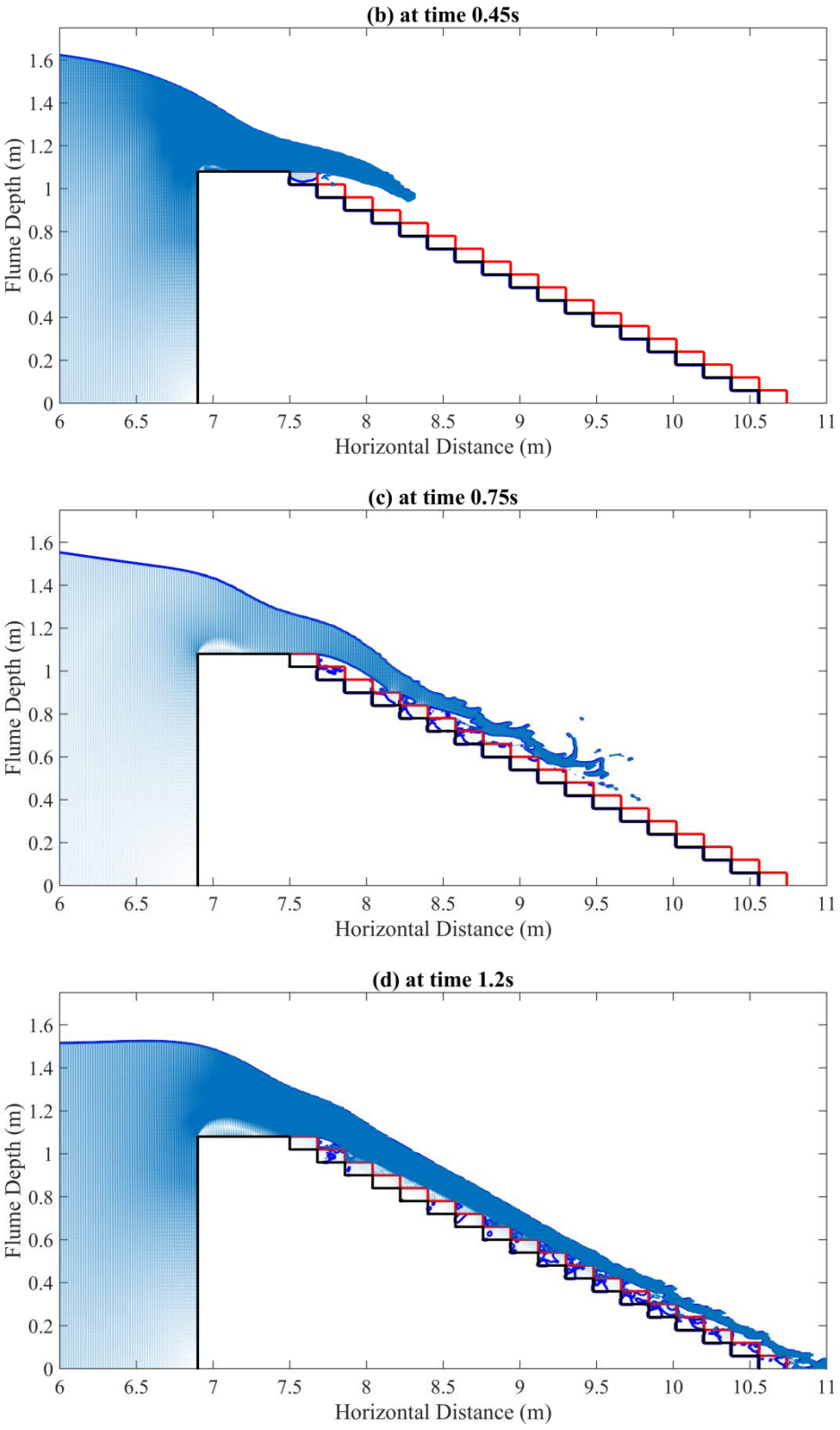
(b) at time 0.45s
Flume Depth (m)
Horizontal Distance (m)
(c) at time 0.75s
Flume Depth (m)
Horizontal Distance (m)
(d) at time 1.2s
Flume Depth (m)
Horizontal Distance (m)

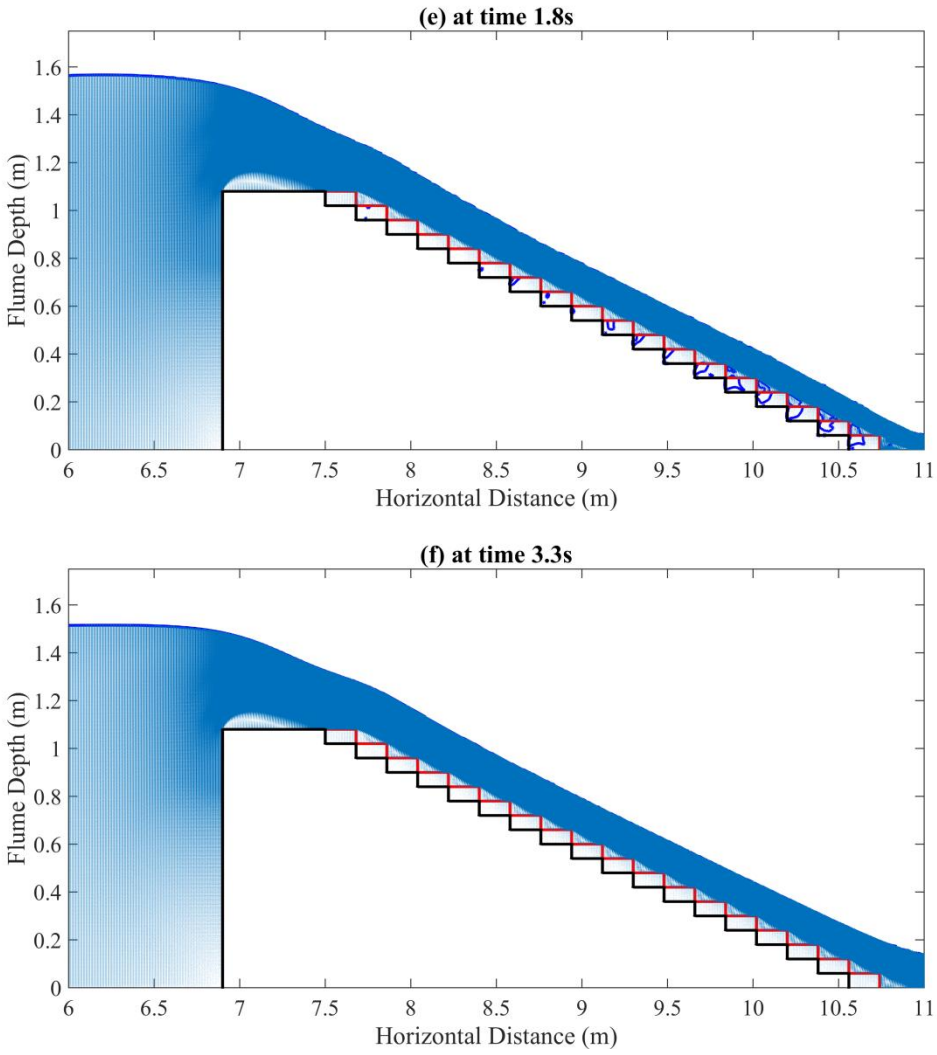

Figure 5.5 Snapshots of flow over gabion stepped spillway with 0.06m step height and 1V:3.0H chute slope.

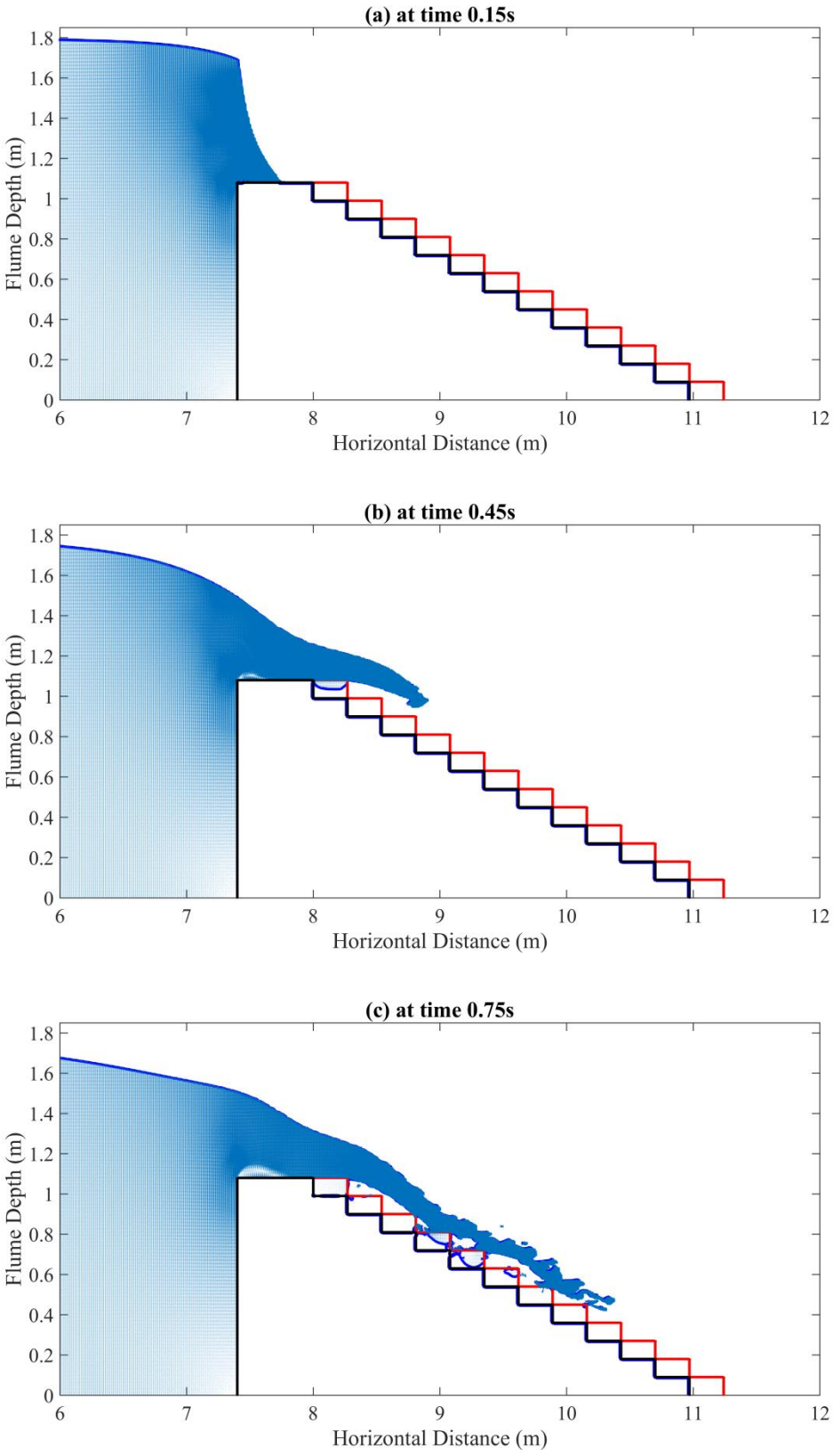
(a) at time 0.15s
(b) at time 0.45s
(c) at time 0.75s
Flume Depth (m)
Horizontal Distance (m)
0
0.2
0.4
0.6
0.8
1
1.2
1.4
1.6
1.8
6
7
8
9
10
11
12

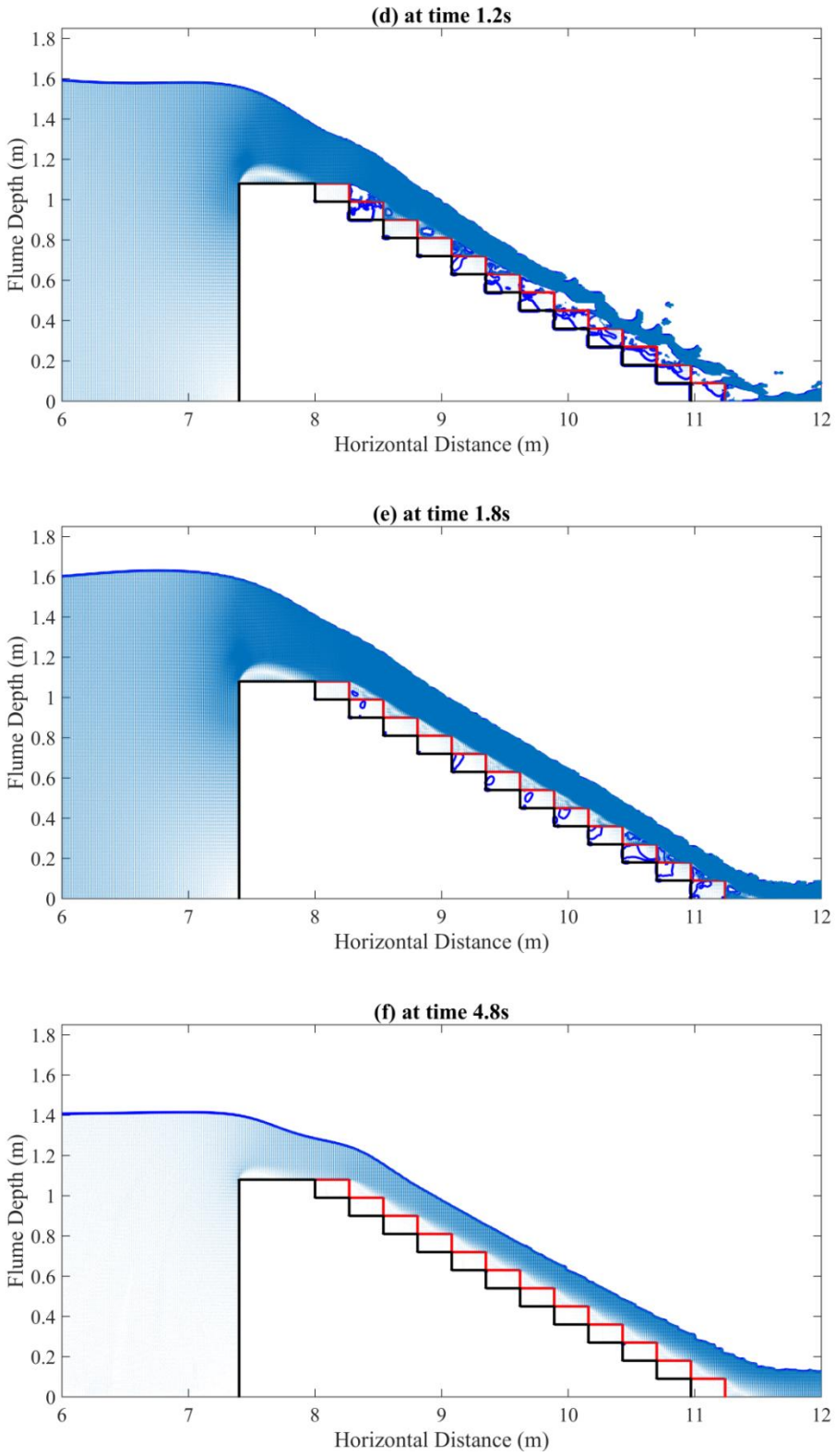

Figure 5.6 Snapshots of flow over gabion stepped spillway with 0.09m step height and 1V:3.0H chute slope.

As can be seen from these figures, jet forms could be noticed at the first stage as the water flows over the weir crest and then down the spillway slope. Having jet forms is related to the way the water flows which is driven by the upstream total head of water relative to the weir crest and also by the gravity. There is an additional influence of the lower mainstream jet on the horizontal face of the steps can be observed when the water flows down. This kind of flow can cause vortices over the horizontal steps and flow backwards against the step riser. However, the porous media can play a vital role here as the flow will try to seep inside the gabion between the particles and that can reduce the vortices significantly, and all of that depending on the size of the particles and the porosity which they can increase or decrease the seepage flow significantly. When the porous media is almost completely saturated in water, these vortices may rotate in a triangular area with a length of about one-third of the step length and that has been captured around the central part of the step length, while the height of the triangular area is approximately the same as the step height. Then, the vortices will be ejected back into the main flow due to the direction of the main flow stream and due to the flow which comes out from the porous media. It is very important to mention that rotation in vortices may start earlier depending on the properties of the porous media. This can be observed when the water cannot flow inside the porous media due to porosity and permeability parameters. The water flow over the steps looks like a coherent stream. These factors indicate the establishment of the skimming flow condition over the gabion stepped spillways. These observations are consistent with those reported by Wüthrich and Chanson (2014) during their experimental work on skimming flow conditions on moderate gabion stepped spillways.

In order to investigate the step height effects on the water surface level over moderate gabion stepped spillways, three-step heights of 0.06m, 0.09m and 0.12m are studied in the present study. Figure 5.7 shows the position of the free water surface along the non-aerated flow region, using three different step heights fitting the downstream face of a gabion stepped spillway of bottom slope 1V:2H. Three different unit discharges have been tested in each case. In these figures, d represents the highest point of the skimming layer and L represents the longitudinal distance along the chute slope to the point under consideration, measured from the downstream corner of the weir crest.

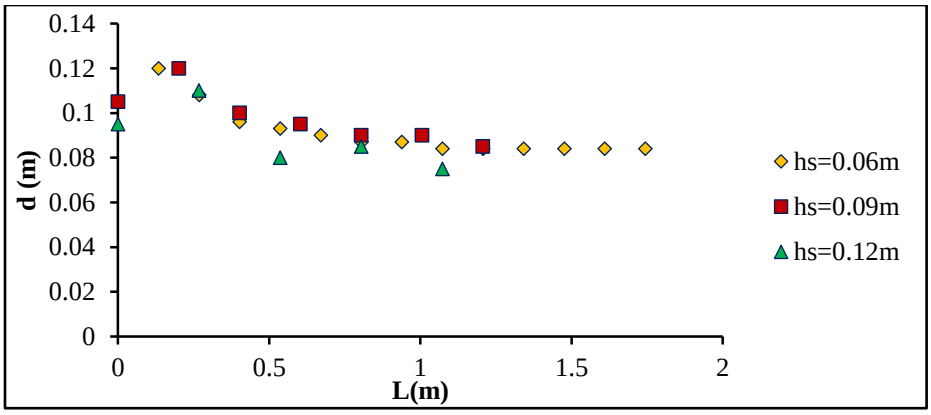

(a)

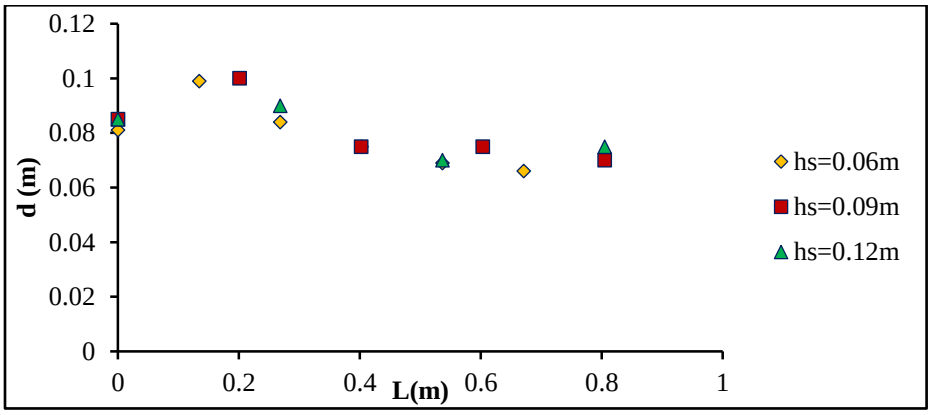

(b)

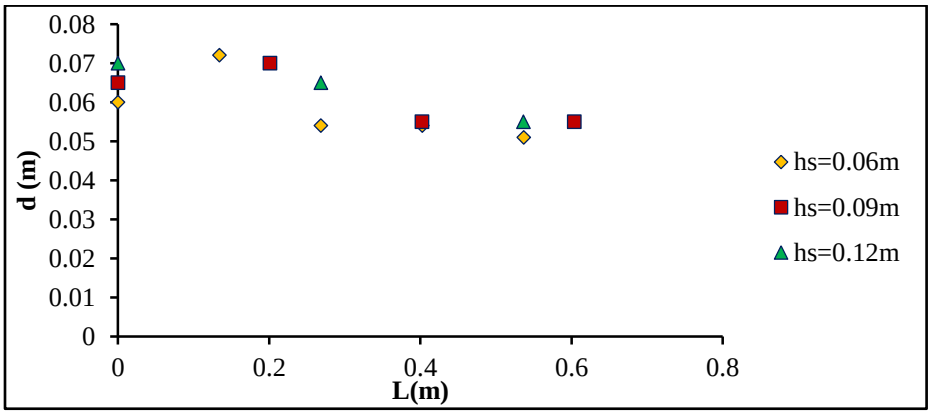

(c)

Figure 5.7 Free surface profile over along the gabion stepped spillway of bottom slope 1V:2H over identical steps of heights 0.06m, 0.09m and 0.12m, for unit discharges of: a) $q=0.20m^2/s$, b) $q=0.15m^2/s$ and c) $q=0.1m^2/s$.

The profiles of the free surface over the gabion steps are almost the same as they present a drop-down curve and wave-like surface (Chanson, 1994). In other words, the flow depth decreases along the chute slope in the non-aerated flow region. This is probably due to the gravity acceleration as the velocity of the water increases when water flows down until its reach the highest value close to the inception point (Chanson, 2002). As a result, a decreasing in the flow depth would be expected. Also, according to Boes and Hager (2003), the absence of air in the non-aerated zone can be considered as another reason, because the mixture of the water with the air can increase the flow depth.

Moreover, three different bottom slopes of 1V:2H, 1V:2.5H and 1V:3H were created to investigate the effect of the chute slope on the position of the free water surface. As can be seen in Figure 5.8, the free surface profile along the non-aerated flow region has been investigated for three different discharges q=0.25, 0.2 and 0.15m^2/s. This figure characterises the numerical free surface levels over steps with the step heights of 0.06m. It can be observed that the chute slope has an inverse influence on the position of the free water surface at the first point near the edge of the crest. In other words, when the chute slope is steep, low levels have been observed for the water surface profiles. This may be related to the flow velocity on the steep slopes, which is relatively higher than that on flatter slopes and therefore the flow depth can be decreased (Chanson, 2002). However, this relationship cannot be observed over the followed gabion steps as the level of the free surface is almost identical for the three slopes. Thus, no significant impact can be observed on the free surface of the water flows when the chute slope is flat or steep.

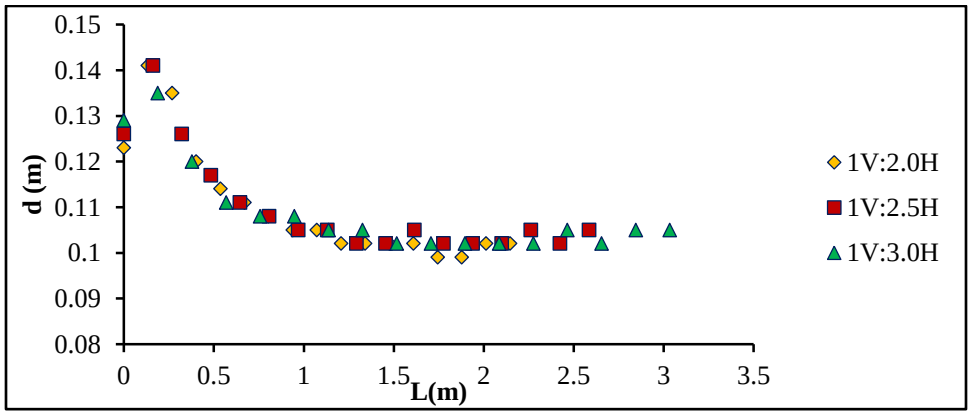

(a)

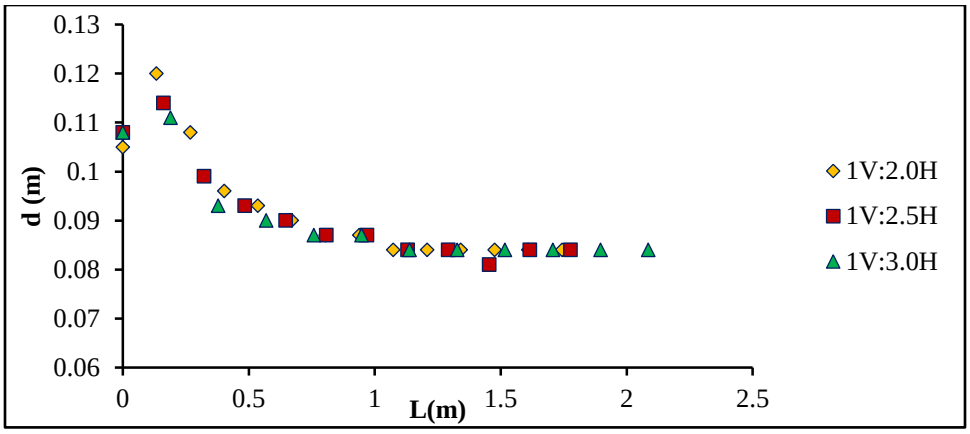

(b)

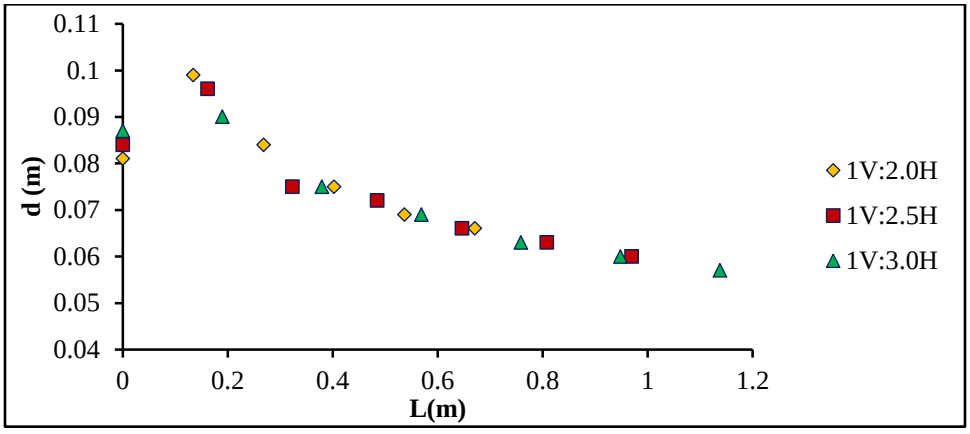

(c)

Figure 5.8 Free surface profile over the gabion stepped spillway of bottom slopes 1V:2H, 1V:2.5H and 1V:3H over identical steps having the height of 0.06m, for unit discharges of a) q=0.25m^2/s, b) q=0.2m^2/s and c) q=0.15m^2/s.

In order to investigate the effect of the gabion porosity on the flow surface profile, the water free surface profile in the non-aerated zone of a gabion stepped spillway with step height of 0.12m and 1V:2.5H bottom slope has been plotted for three different values of discharges q=0.30, 0.25 and 0.2m^2/s. Four different values for the gabion porosity were tested in Figure 6.9. These values are 0.25, 0.30, 0.35 and 0.4. As can be seen in Figure 5.9, the features of the free surface profile over the gabion steps are characterised by the wavy surface and the drop-down curve.

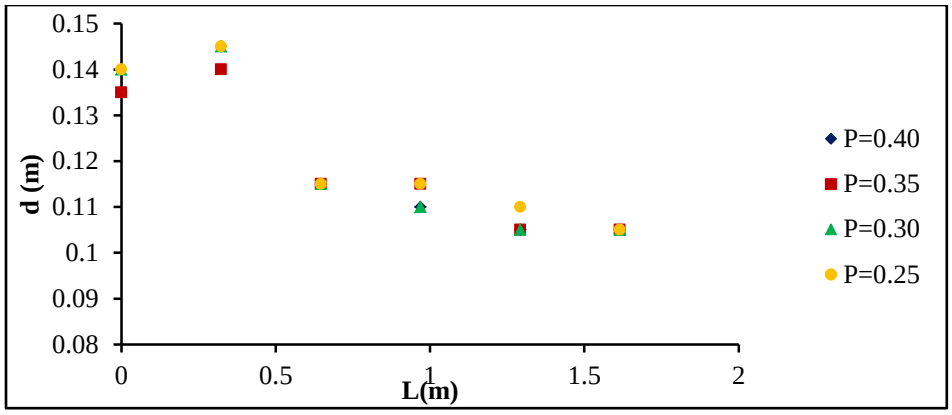

(a)

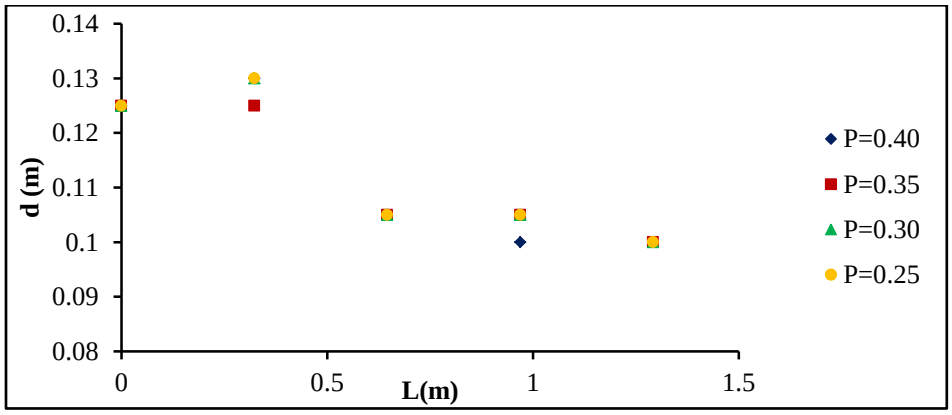

(b)

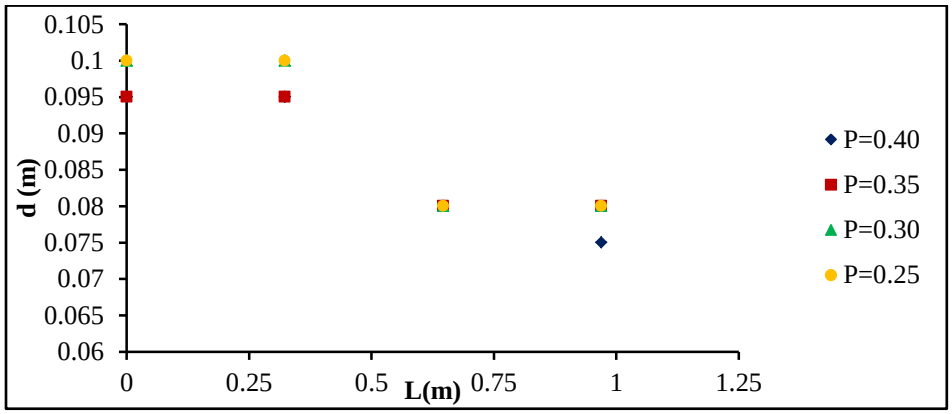

(c)

Figure 5.9 Free surface profile over the gabion stepped spillway of bottom slope 1V:2.5H with 0.12m step height and four different values for the porosity, for unit discharges of a) $q=0.3m^2/s$, b) $q= 0.25m^2/s$ and c) $q=0.2m^2/s$.

The porosity tests in the present study nearly showed the same trend as those obtained and discussed above, hence, no massive differences are observed when the porosity value is changed. However, the 0.25 value of porosity produces high free surface profile compared to the other values. This could be related to the fact that when the porosity decreases, it will be slightly hard for the water to go inside the gabion thus high levels for the free surface profiles could be achieved.

Moreover, the effect of four different sizes of the particles (D_{50}=0.005, 0.01, 0.015 and 0.02) on the free surface in the non-aerated zone has been investigated for three different values of discharge q=0.3, 0.25 and 0.20m^2/s. The investigation has been conducted for gabion stepped spillways of 0.12m step height with 1V:2.5H bottom slope.

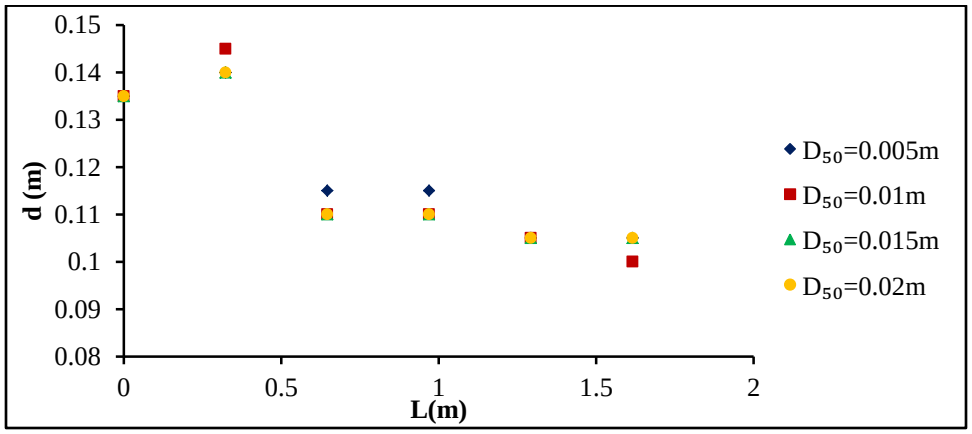

(a)

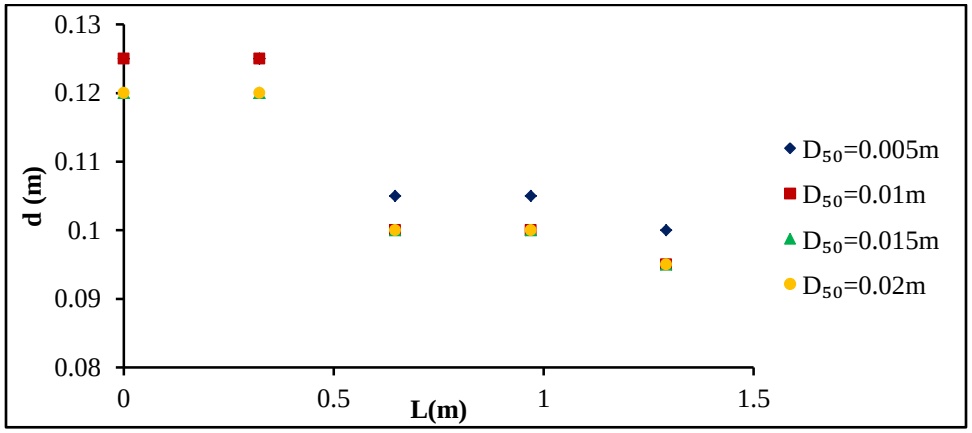

(b)

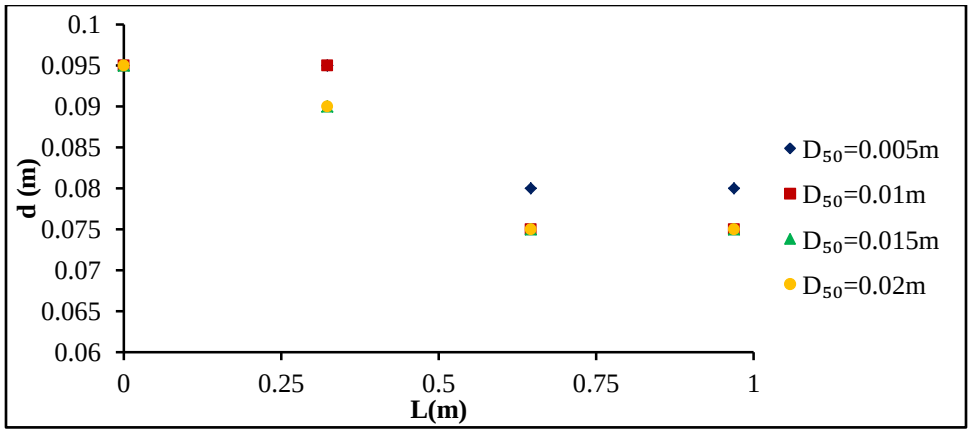

(c)

Figure 5.10 Free surface profile over the gabion stepped spillway of bottom slope 1V:2.5H with 0.12m step height and four different values for the particle size, for unit discharges of a) $q=0.3m^2/s$, b) $q= 0.25m^2/s$ and c) $q=0.2m^2/s$.

Similar to the porosity, changing the values of D_{50} did not significantly impact the profile of the free surface. However, as can be noted in Figure 5.10, the free surface profile of the water flow could be slightly higher when the particle size equals to 0.005m. This is due to the small spaces between the particles which can affect the water flow inside and between the particles. As a result of that, the water level could be increased considerably.

In conclusion, this chapter revealed that some parameters can impact the profiles of the free surface significantly such as the flow rates over steps. However, some parameters have very small effect such as the slope of the chute bottom. In the next chapter, the location of the inception point and the length of the non-aerated zone will be investigated numerically.

Chapter 6 : Results and Discussion of the Location of the Inception Point

6.1. Introduction

The upstream flow region in the skimming flow is characterised by developing the turbulent boundary layer. The inception point is located where the depth of the turbulent boundary layer equals the flow depth. In other words, it represents the point where the boundary layer thickness reaches the free surface of the water. The turbulent energy rate which is originally caused by the vortices could be slightly high at the inception point. Therefore, these vortices might exceed the surface tension and gravity effects which can lead to the natural air entrainment. The inception point determines the last point of the non-aerated zone; this point is immediately followed by the aerated zone. Air entrainment is one of the most important parameters that can protect the hydraulic structures from the cavitation damages due to the air-water flow. It can have high flow rates with high velocity values which may also increase the energy dissipation rate. The damage due to cavitation in the non-aerated zone should be considered in the design of the hydraulic structures as one of the essential parameters (Peterka, 1953; Falvey, 1990).

Generally, hydraulic structures are mostly built using concrete. Concrete has a low resistance against the impact of the vaporised bubbles when they collapse. Therefore, determining the inception point location is significantly important since the upstream part of this point is prone to cavitation damage (Boes and Minor, 2002; Amador et al. 2009). In severe flood conditions over embankment dams, self-aeration might not take place as the length of the downstream face is not enough to let the boundary layer developed (Chanson, 2002). The definition of the inception point will be used in the present study to determine the location of the inception point of air entrainment. This study aims to characterise the properties of the skimming flow conditions in the non-aerated flow region.

Moreover, studies have different conclusions about the impact of using different values of step heights, chute slopes and flow rates on flow characteristics over gabion stepped spillways. Three-step heights and three slopes typical of embankment dams are used to investigate their impact on the inception point location and the length of the non-aerated zone. Furthermore, different values of gabion porosity and gabion particle size are used to examine their effect on the inception point location (see Table 5.1). All of these cases are tested within a range of flow rates which are typical to the skimming flow conditions. It is worth to mention that there is a possibility that different adjustment time lags between the weir crest and spillway slope occur for different spillway configurations. In other words, the adjustment of inception points to changing flows may be slightly different for the geometries which have been tested. Therefore, that could be a reason for inconsistent parametric dependences for inception points between different spillway geometries.

Schlichting (1979) stated that the boundary layer is defined as that layer of the flow where the velocity is approximately 99% of the free stream velocity. This definition has been used in this study to determine the thickness of the turbulent boundary layer. In other words, the velocity distribution over the outer edge of the steps located within the non-aerated flow region, has been used to determine the inception point. Figure 6.1 shows the computed water surface level and thickness of the boundary layer.

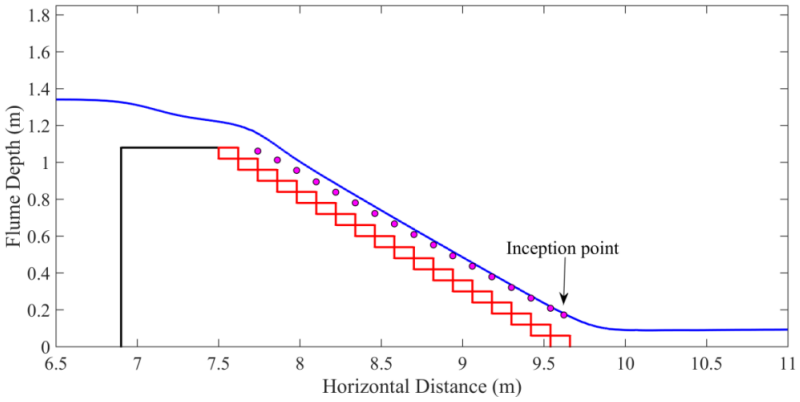

(a)

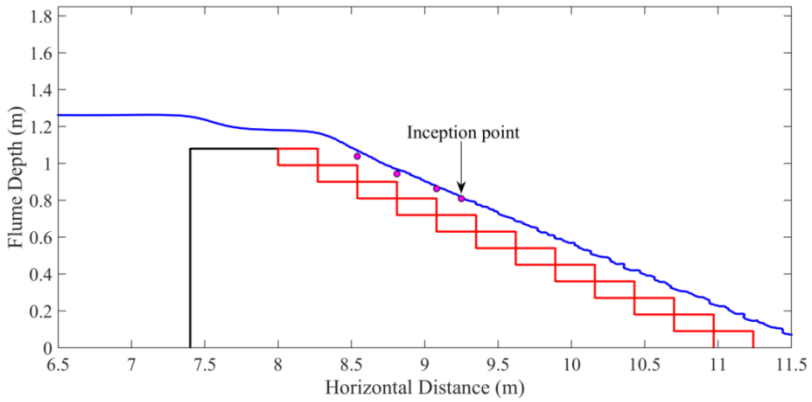

(b)

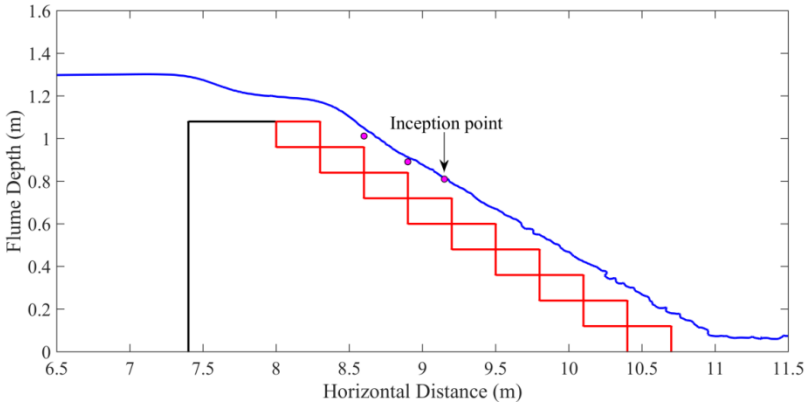

(c)

Figure 6.1 Estimation of the length of the inception point of air entrainment above the steps, based on the computed water flow depth and thickness of boundary layer: a) step height 0.06m, chute slope 1V:2H and unit discharge q=0.25m^2/s, b) step height 0.09m, chute slope 1V:3.0H and unit discharge q=0.15m^2/s, and c) step height 0.12m, chute slope 1V:2.5H and unit discharge q=0.20m^2/s.

The boundary layer thickness was found at the outer edge of each step. These outer edges of steps are located at different distances measured from the downstream face of the weir crest. As aforementioned, the length of the non-aerated flow region is supposed to be located at the intersection point of the water surface level and the boundary layer thickness (Chanson, 2002). It should be noted that for each value of step height, stepped spillway slope, gabion porosity and gabion particle sizes, this procedure is conducted for

different values of flow rates. It is important to highlight that the thickness of the boundary layer is small near the weir crest and the first step of the gabion, and then it starts to develop when water flows downwards (Figure 6.1). This relates to the uniform velocity distribution along the flow depth above the step outer edge. The thickness of the boundary layer developing due to the velocity distribution increasing over the outer edges of the steps until meets the free surface of the water at the inception point.

6.2. Steps configuration impact

Figures (6.2, 6.3 and 6.4) show the effect of the step height on the location of the inception point. The computational results of gabion stepped spillways of 1V:2H chute slope with three different flow rates 0.2, 0.15 and 0.1m^2/s revealed that step heights can affect the location of the inception point and the length of the non-aerated zone. It is important to highlight that gabion stepped spillways with 0.12m and 0.09m step height are positioned at a distance of 8m from the boundary edge, while the weir of 0.6m length was placed at a distance of 7.4m. However, gabion stepped spillways with 0.06m step height are located at 7.5m and the weir is placed at 6.9m as mentioned and discussed in Chapter 5.

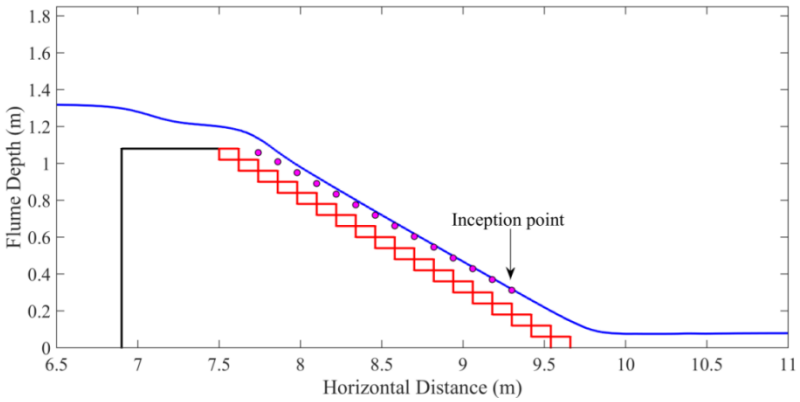

(a)

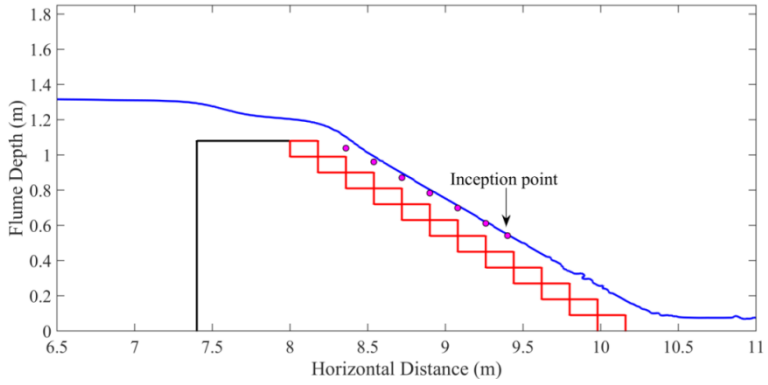

(b)

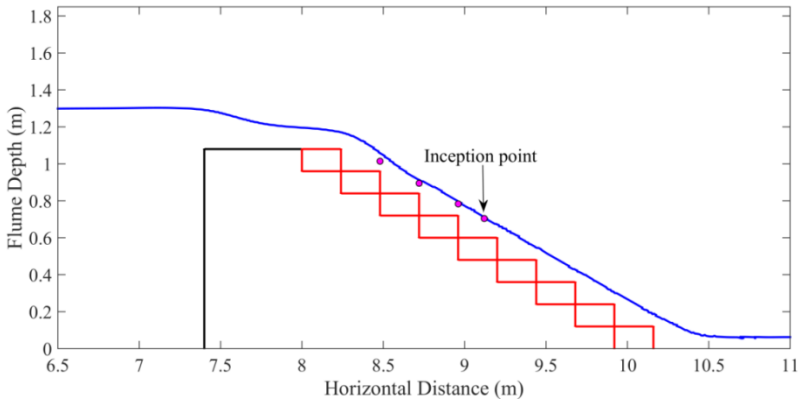

(c)

Figure 6.2 Estimation of the length of the inception point of air entrainment above the steps, based on the computed water flow depth and thickness of boundary layer of 1V:2H chute slope and unit discharge equals 0.2m^2/s: a) step height 0.06m, b) step height 0.09m, and c) step height 0.12m.

As shown in Figures 6.2, 6.3 and 6.4, the location of the inception point moves towards the downstream side of the weir crest when the discharge is increased. In other words, the length of the non-aerated zone is increased with increasing the unit discharge. This is because increasing flow rates could lead to an increase in the flow depth and velocity values of the water flow. Increasing the flow depth might increase the required length of the boundary layer developing to intersect with the free surface profile.

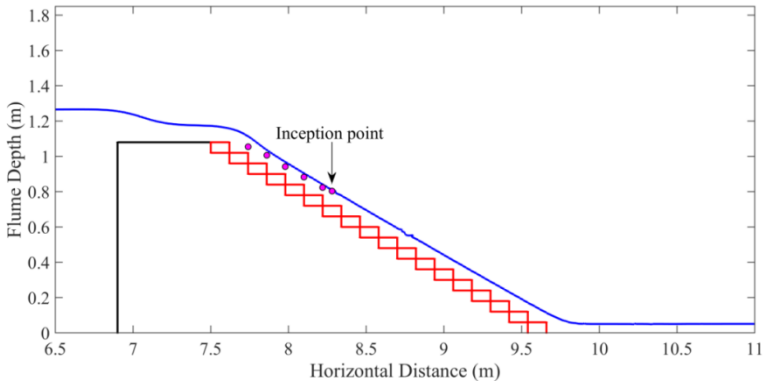

(a)

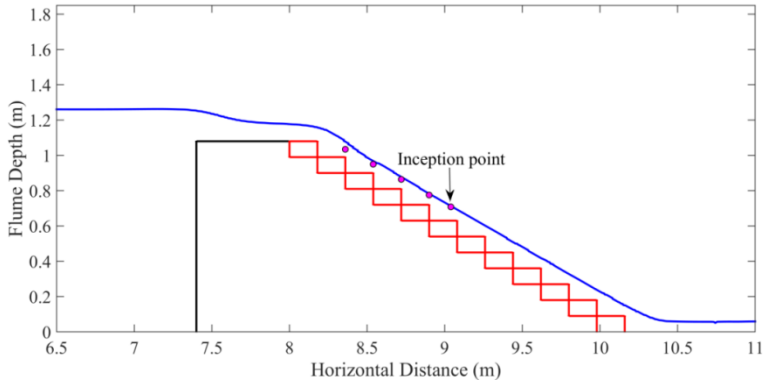

(b)

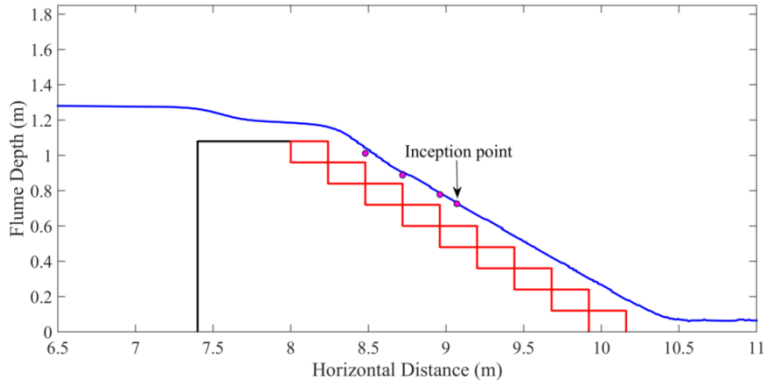

(c)

Figure 6.3 Estimation of the length of the inception point of air entrainment above the steps, based on the computed water flow depth and thickness of boundary layer of 1V:2H chute slope and unit discharge equals 0.15m^2/s: a) step height 0.06m, b) step height 0.09m, and c) step height 0.12m.

For a specific slope and discharge, it is observed that the location of the inception point moves to the upstream side towards the weir crest when the step height is increased. This can be attributed to the fact that large step height can have a positive impact on the location of the inception point compared to a small step height, as the velocity of the overflowing water is decelerated when it flows over the outer step edge and hits the horizontal face. However, the effect of the step height might not be very large with small discharges.

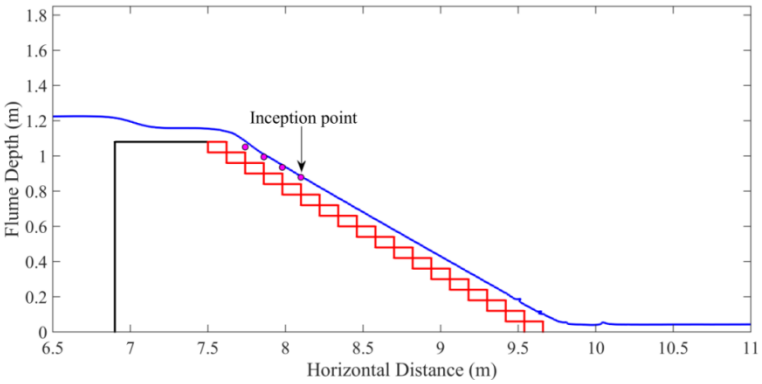

(a)

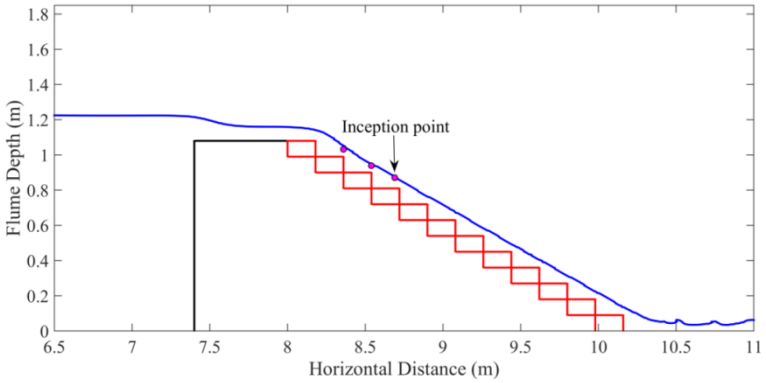

(b)

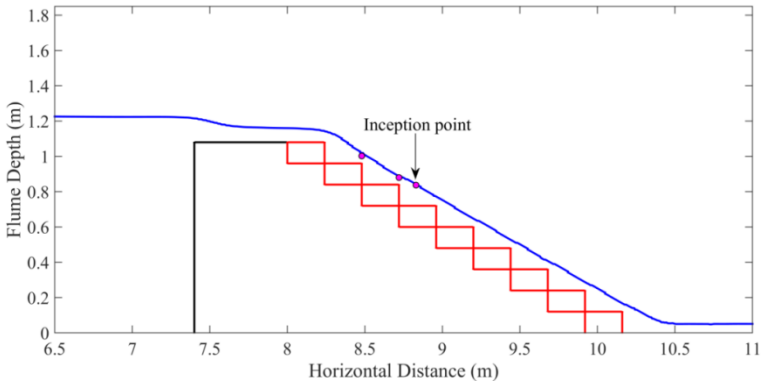

(c)

Figure 6.4 Estimation of the length of the inception point of air entrainment above the steps, based on the computed water flow depth and thickness of boundary layer of 1V:2H chute slope and unit discharge equals 0.10m^2/s: a) step height 0.06m, b) step height 0.09m, and c) step height 0.12m.

Following the past studies and to justify the previous conclusion about the step height impact. Figure 6.5 shows the computational results of Li/ks of the present work which is calculated with different values of step heights against to the corresponding values of the roughness Froude number (F_*) for three chute slopes 1V:2H, 1V:2.5H and 1V:3H. In this Figure, Li represents the length of the non-aerated zone measured from the outer edge of the first step up to the inception point, ks is the roughness which is calculated by hs*cosθ, hs as the step height and θ is the chute slope. The roughness Froude number can be calculated from

$$F_* = \frac{q}{\sqrt{g*\sin\theta*ks^3}}$$

where q is the discharge per unit width and g is the gravitational acceleration.

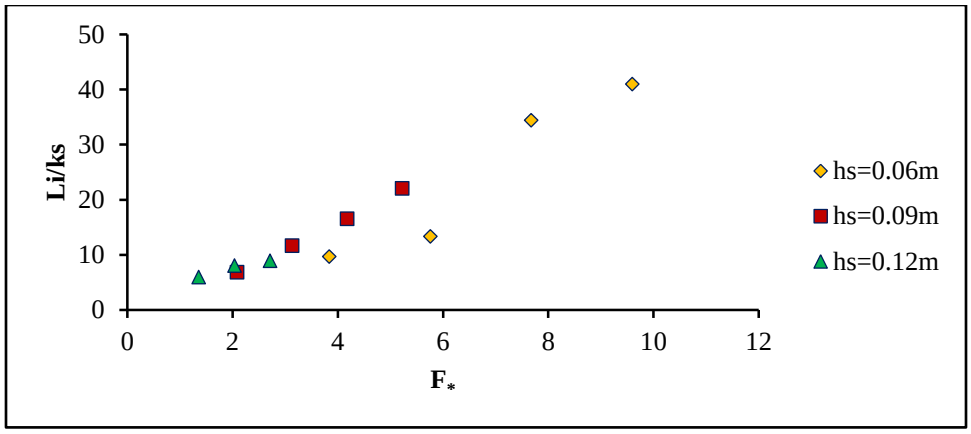

(a)

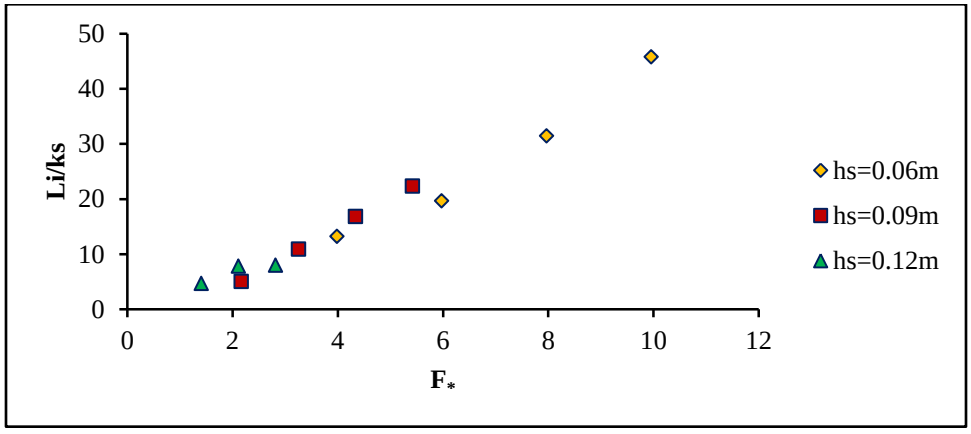

(b)

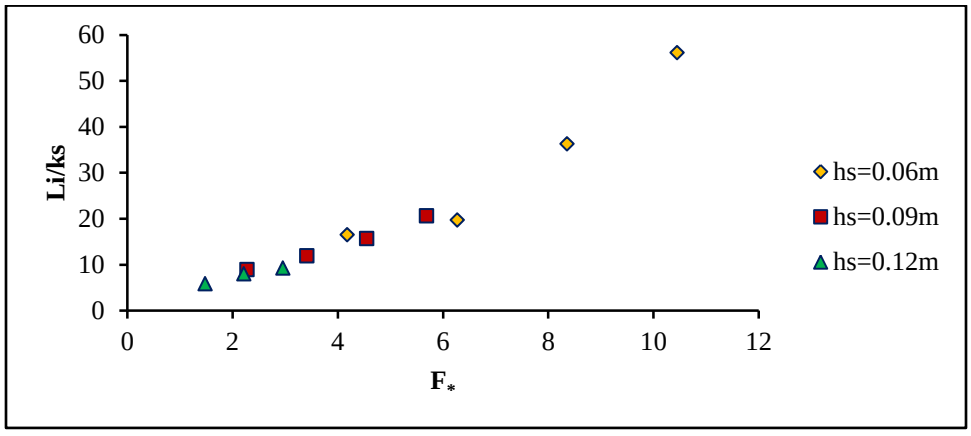

(c)

Figure 6.5 Computational results of the location of the free surface aeration on gabion stepped spillways for slopes: a) 1V:2H, b) 1V:2.5H and c) 1V:3H.

Figure 6.5 revealed that the length of the non-aerated zone increases with a decrease in step height as increasing the step height could move the location of the inception point towards the upstream side over gabion stepped spillways. The same behaviour has been achieved by most of the researchers for the moderate and steep normal stepped spillways like Chamani (2000) and Hunt and Kadavy (2009), thus, no differences in terms of the general trend of the location of the inception point between the normal stepped spillways and gabion stepped spillways when the step height is changed.

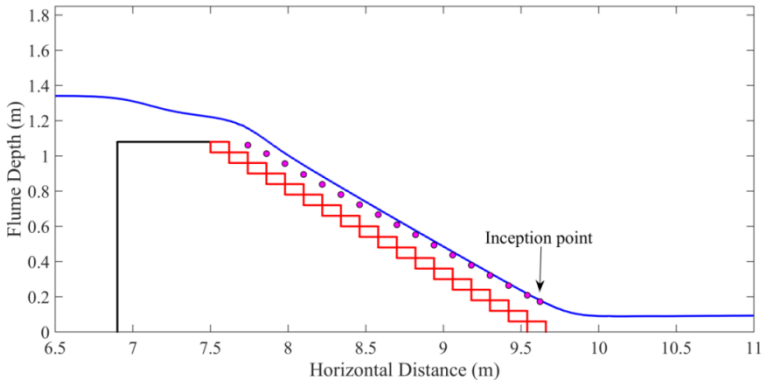

(a)

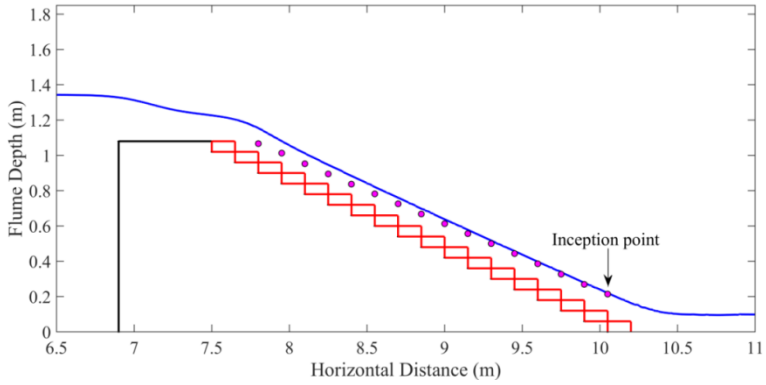

(b)

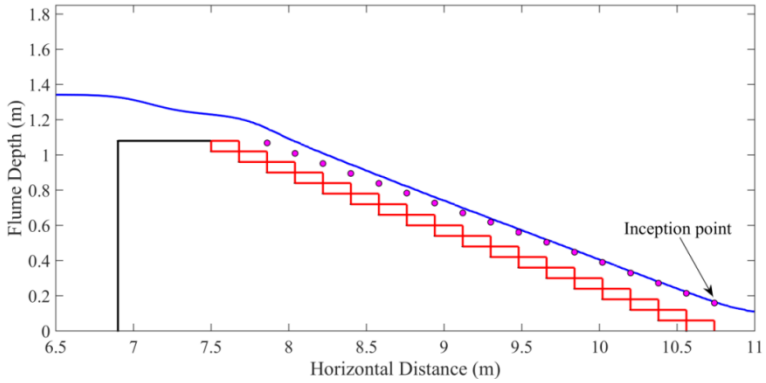

(c)

Figure 6.6 Estimation of the length of the inception point of air entrainment above the steps, based on the computed water flow depth and thickness of boundary layer of 0.06m step height unit discharge equals 0.25m^2/s: a) chute slope 1V:2H, b) chute slope 1V:2.5H and c) chute slope 1V:3.0H.

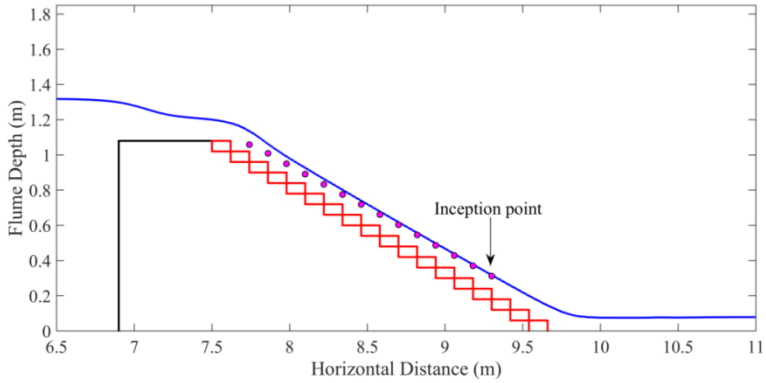

(a)

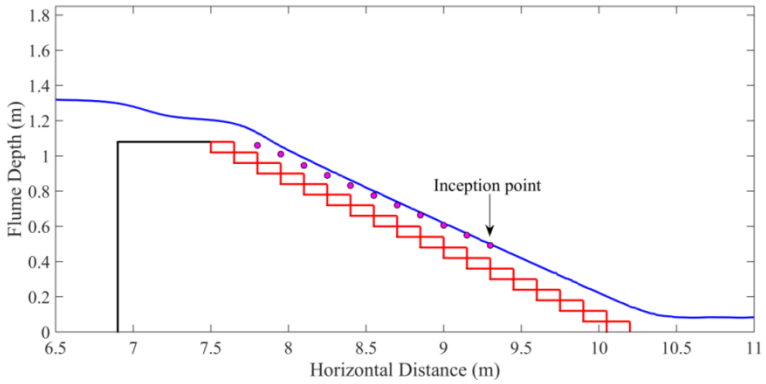

(b)

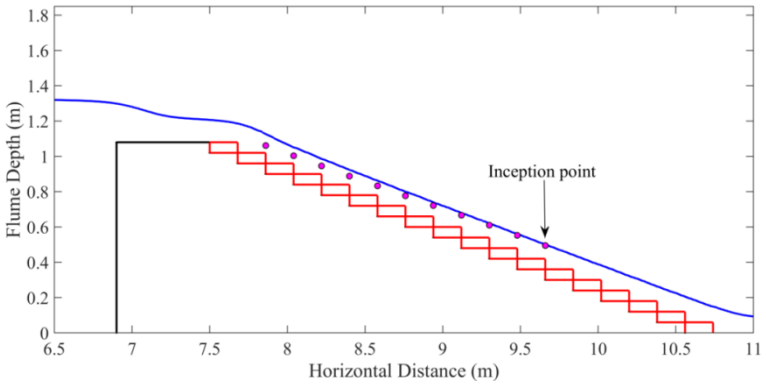

(c)

Figure 6.7 Estimation of the length of the inception point of air entrainment above the steps, based on the computed water flow depth and thickness of boundary layer of 0.06m step height unit discharge equals 0.20m^2/s: a) chute slope 1V:2H, b) chute slope 1V:2.5H and c) chute slope 1V:3.0H.

In order to investigate the effect of the chute slope on the location of the inception point and the length of the non-aerated zone, three different slopes1V:2H, 1V:2.5H and 1V:3.0H of gabion stepped spillways with step height of 0.06m have been tested and plotted in Figures 6.6, 6.7 and 6.8. Three different values of discharge 0.25 m^2/s, 0.2 m^2/s and 0.15m^2/s have used for comparison purposes to see how the discharge can impact the results.

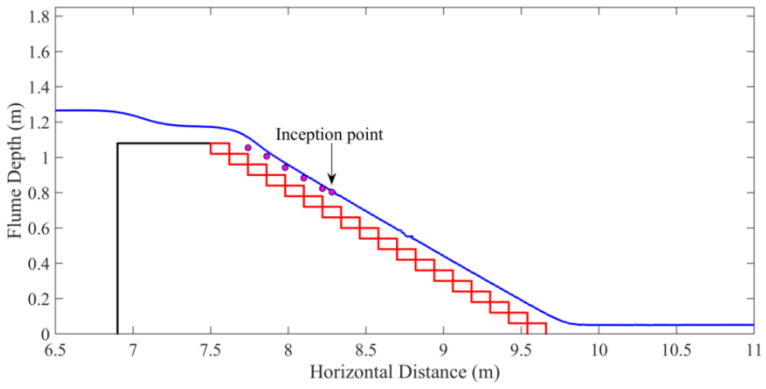

(a)

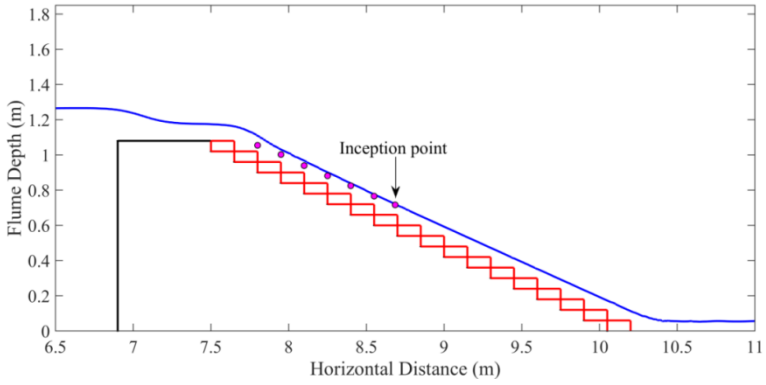

(b)

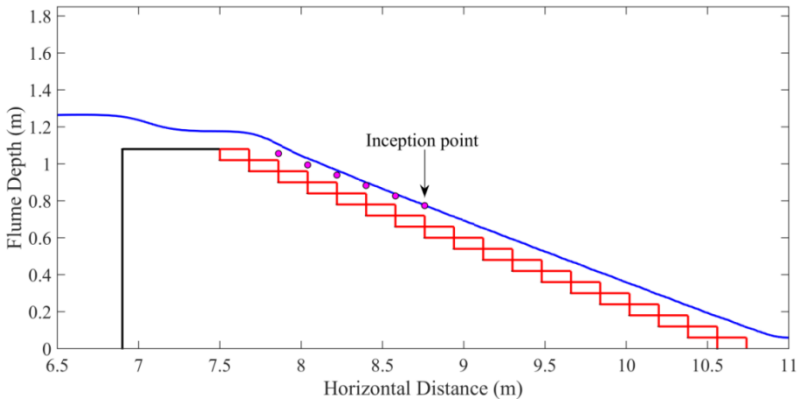

(c)

Figure 6.8 Estimation of the length of the inception point of air entrainment above the steps, based on the computed water flow depth and thickness of boundary layer of 0.06m step height unit discharge equals 0.15m^2/s: a) chute slope 1V:2H, b) chute slope 1V:2.5H and c) chute slope 1V:3.0H.

The general trend of the numerical results revealed that the location of the inception point may move towards the upstream side when slopes become steep. Therefore, it can be concluded that spillway slopes have a reciprocal dependence with the location of the inception point and the length of the non-aerated zone (Figure 6.9). In other words, a short length of the non-aerated zone will be expected for steep spillway slopes compared to flat spillway slopes. This is because the longitudinal velocity over steep slopes is higher than flat slopes. Therefore, water flow depth is lower in steep chute slopes, which

accelerates the development of the boundary layer and its expansion throughout the water column to meet the free surface.

All of the previous observations agree with the experimental observation of André (2004), who conducted a study on normal stepped spillways. However, over gabion stepped spillways, that kind of the relation cannot be achieved continuously. It can be noticed that for a given unit discharge and step height, no significant impact can be obtained on the location of the inception point (Figure 6.9).

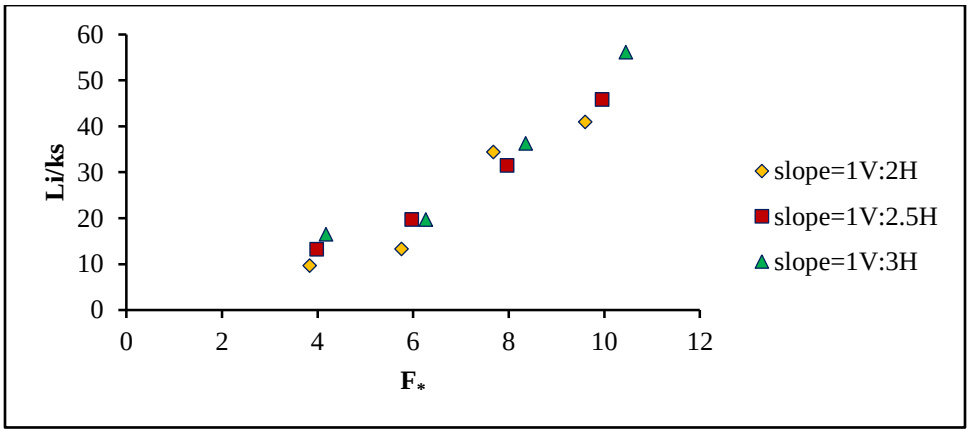

(a)

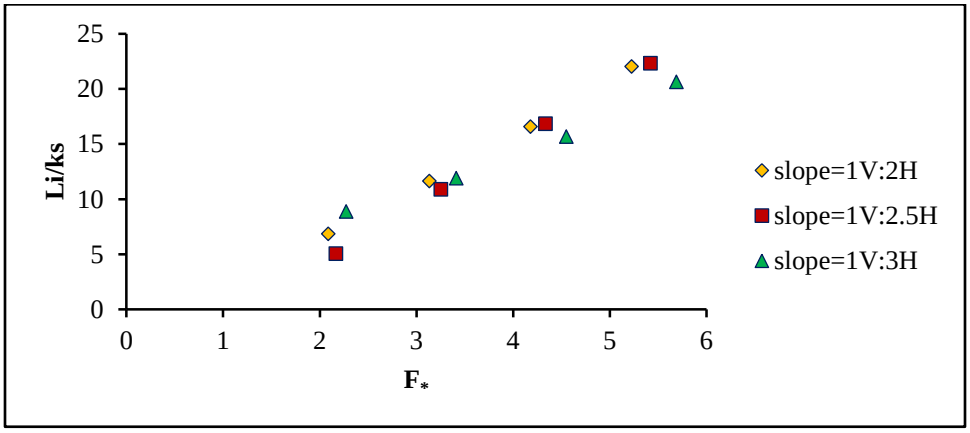

(b)

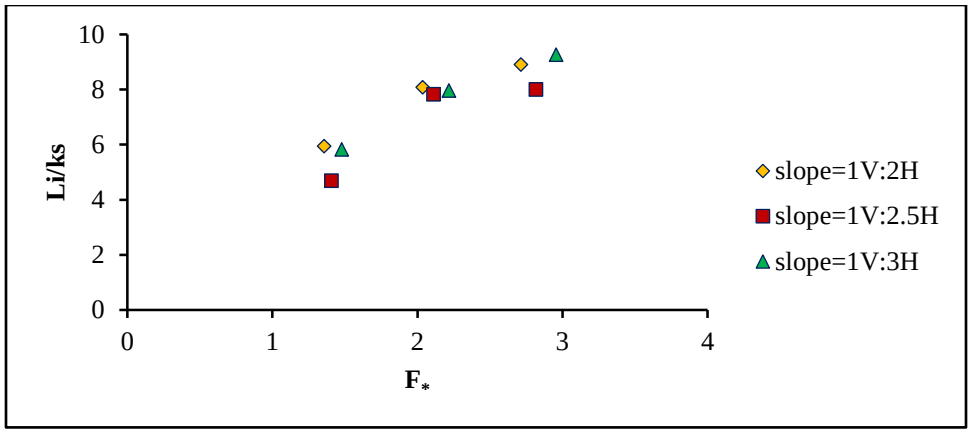

(c)

Figure 6.9 Computational results of the location of the free surface aeration on gabion stepped spillways for step height: a) 0.06m, b) 0.09m and c) 0.12m.

6.3. Gabion effect

This section discusses the effect of porosity and particle sizes on the location of the inception point for different three bottom slopes 1V:2H, 1V:2.5H and 1V:3H. To do so, the step height is fixed to 0.12m and four different values for the porosity 0.25, 0.3, 0.35 and 0.4 have been selected in addition to four different values for the particle size as well 0.005, 0.01, 0.015 and 0.2m. Figures 6.10 and 6.11 plot the numerical results of Li/ks against the porosity and the particle sizes with three chute slopes, to compare their effect on the location of the inception point and the non-aerated length.

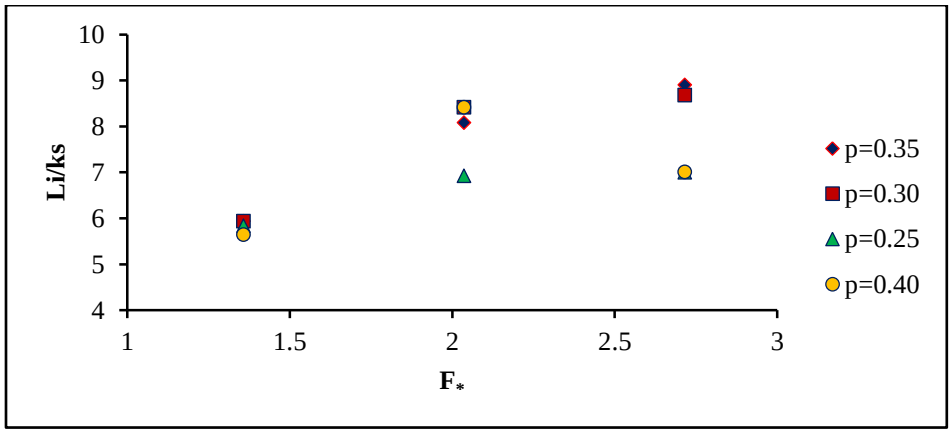

(a)

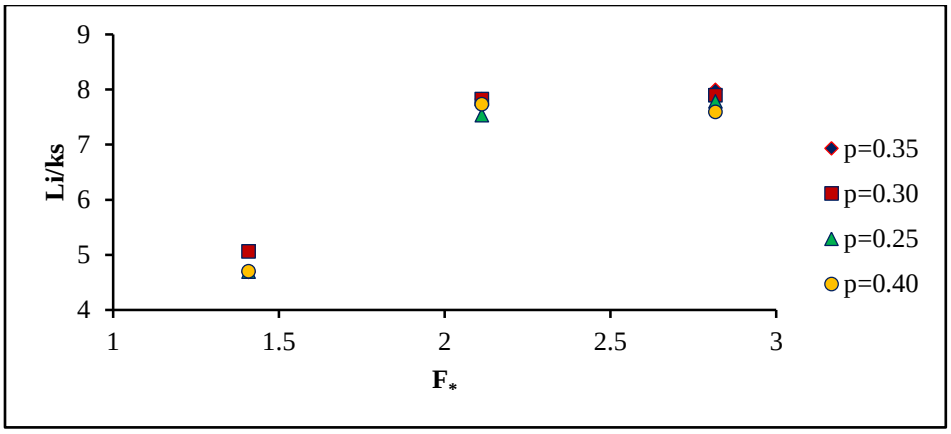

(b)

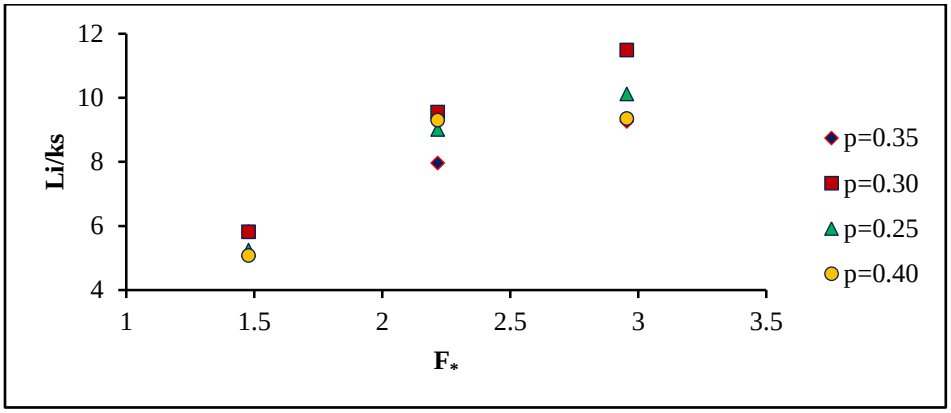

(c)

Figure 6.10 Computational results of the location of the free surface aeration with different values of porosity on gabion stepped spillways for chute slopes: a) 1V:2H, b) 1V:2.5H and c) 1V:3H.

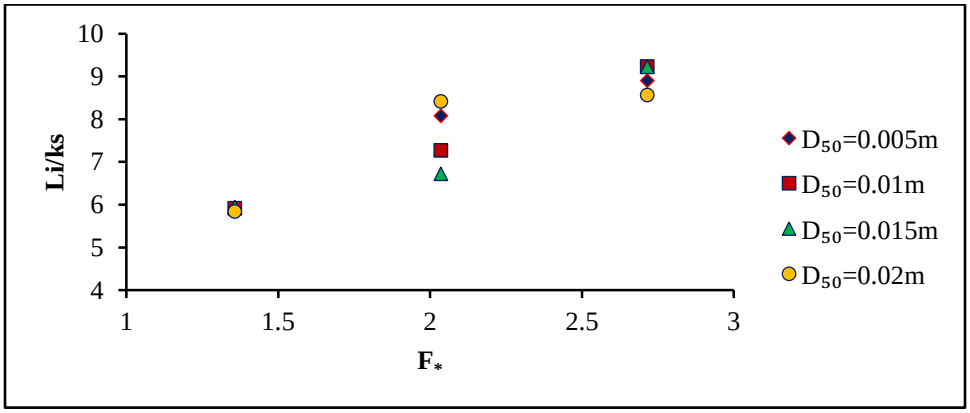

(a)

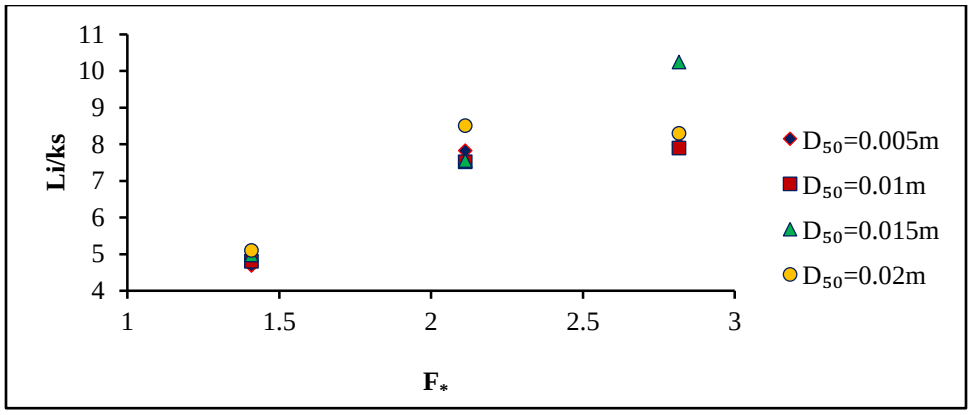

(b)

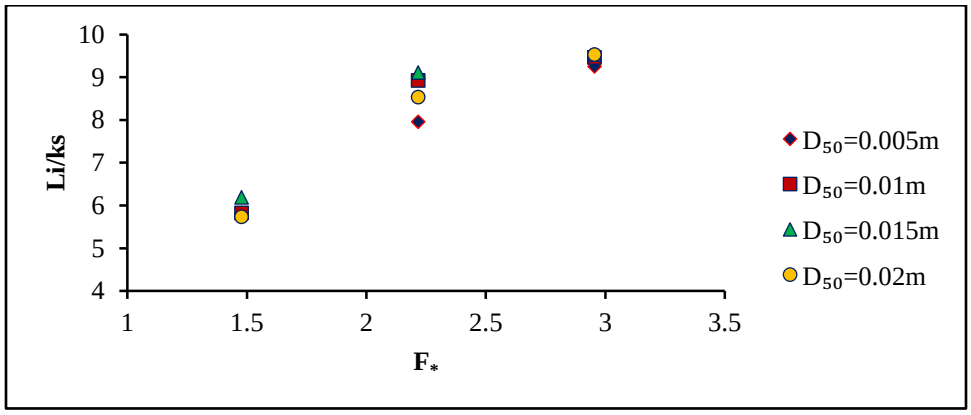

(c)

Figure 6.11 Computational results of the location of the free surface aeration with different D_{50} values on gabion stepped spillways for chute slopes: a) 1V:2H, b) 1V:2.5H and c) 1V:3H.

The results showed that both porosity and particle size can have a significant impact on the location of the inception point. The figures show that no specific trend can be obtained between the porosity and the location of the inception point. However, an initial finding of the computational results of high discharges revealed that when the particle size decreases the location of the inception point will move up towards the weir. Thus the length of the non-aerated zone will be shorter. Conversely, some cases might not follow the same trend due to the wavy free surface or to the humps of the water which can be observed over the gabion, as a result of the seepage flow inside the porous media. Seepage flow could be influenced by particle sizes and the porosity as well, therefore,

that effect could accelerate the intersection between the free surface and the turbulent boundary layer or it could delay it. In conclusion, both porosity and particle sizes can have more effect with high discharges rather than low discharges. Also, it is crucial to highlight that up to this point of this work, it is hard to determine whether there is a direct or inverse relationship between the porosity and the particle size with the length of the non-aerated zone. Consequently, a nonlinear multiple regression equation for the length of the non-aerated zone is suggested in the next section to determine what kind of relation can be obtained depending on the computational data.

In order to determine the location of the inception point and the length of the non-aerated zone, many past studies have developed nonlinear multiple regression equations to fit their results such as Chanson, (1996); Carosi and Chanson (2008); Meireles and Matos (2009), Hunt and Kadavy (2010) and Husain (2013). Therefore, the computational results of gabion stepped spillways which are presented in this work were used to develop new equations to determine the length of the non-aerated zone and the water depth at the inception point for gabion stepped spillways. For this purpose, the values of Li and the corresponding values of F_* collected from various step heights, chute slopes, gabion porosity, particle sizes and discharges tested in this work were used to obtain the Eq. 6.1. In developing Eq. 6.1, Chanson's (1994) equation (Eq. 6.2) which is developed for normal stepped spillways has been used initially to obtain the equation of gabion stepped spillways. Therefore, including extra terms to describe the parameters of the gabion boxes is significantly important to increase the accuracy of the equation. The coefficients of Eq. 6.1 have been estimated by using an iterative least squares estimation routine available in MATLAB.

$$\frac{Li}{ks} = 2.2281 * (\sin\theta)^{-0.3172} * (F_*)^{1.2486} * (p)^{-0.2831} * \left(\frac{D_{50}}{hs}\right)^{0.1537} \qquad (6.1)$$

It is important to mention that the numerical data, selected randomly, has been split into two groups; the first group which contains around 80% of the data has been used to find the coefficients of the equation. The remaining data (20%) has been used to test the equation. The value of the R^2 and the correlation factor were 0.9057 and 0.9517 respectively (Figure 6.12). The value of R^2 has been used to measure of how well the

regression line approximates the data. The value of R^2 for Eq. 6.1 is relatively good 0.9057 which gives an indication that the formula described the data well.

The regression indicates that porosity term has a negative power sign which reveals the reciprocal relationship between the porosity and the length of the non-aerated zone. The small value for the power, which is 0.28, suggests that porosity has less impact on the length of the non-aerated zone if compared with F_* and the bottom chute slope. Moreover, a positive sign for the particle size shows a direct relationship between the particle size and the length of the non-aerated regime and again the value is quite small: the impact of the particle size on the Li is low. These relationships represent the general trend for all the computational data. However, many individual points can be found in the database showing different relations to those mentioned here which can explain small magnitudes for porosity and particle size coefficients as there are no fixed relations for all the data.

A further comparison has been conducted against different empirical correlations which have been proposed by many researchers such as Chanson (1994), Carosi and Chanson (2008), Meireles and Matos (2009), Hunt and Kadavy (2011) and Hunt and Kadavy (2013) (Figure 6.13). The objective of this comparison is to assess whether the empirical correlations which are established for the normal stepped spillways can be used to find the location of the inception point over the gabion stepped spillways.

The empirical formulae are:

$$\frac{Li}{ks} = 9.8 * (\sin\theta)^{0.08} * (F_*)^{0.71} \quad \text{Chanson (1994)} \quad (6.2)$$

$$\frac{Li}{ks} = 1.05 + 5.11 * F_* \quad \text{Carosi and Chanson (2008)} \quad (6.3)$$

$$\frac{Li}{ks} = 5.25 (F_*)^{0.95} \quad \text{Meireles and Matos (2009)} \quad (6.4)$$

$$\frac{Li}{ks} = 6.1 * (\sin\theta)^{0.08} * (F_*)^{0.86} \quad \text{Hunt and Kadavy (2011)} \quad (6.5)$$

$$\frac{Li}{ks} = 5.19 * (F_*)^{0.89} \quad \text{Hunt and kadavy (2013)} \quad (6.6)$$

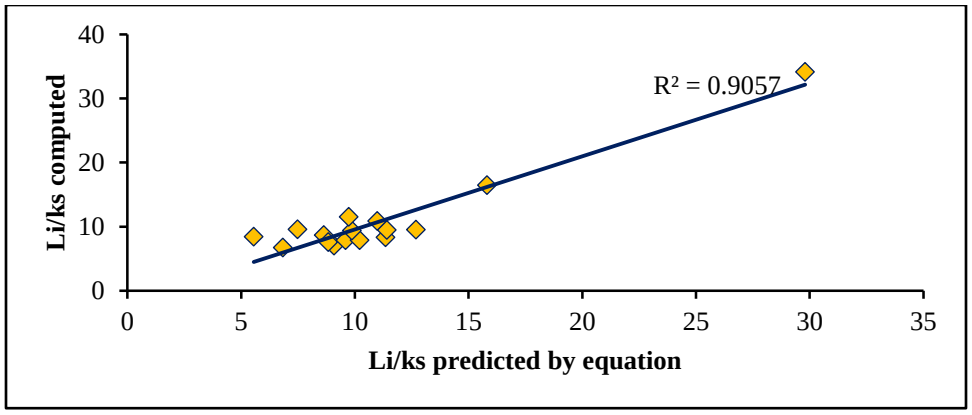

Figure 6.12 Comparison of Equation 6.1 to numerical data.

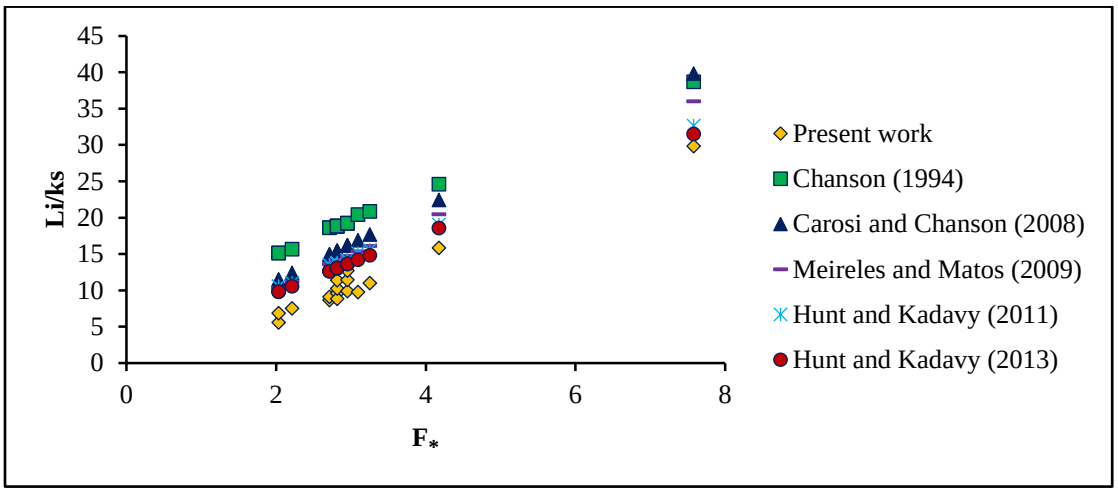

Figure 6.13 Comparison of Equation 6.1 with different correlations.

The results show that all correlations overestimated the location of the inception point, however, Hunt and Kadavy's (2013) equation showed the closest result to the present study. Also, the results reveal that using gabion boxes will increase the roughness of the surface and therefore accelerate the growth of the boundary layer thickness. Thus, that will reduce the length of the non-aerated zone. Overall, using porous media over the concrete steps likely to reduce the non-aerated length and then reduce the danger of having cavitation damages over the steps.

The computational results have been used to develop another equation that provides an estimate of the water depth at the inception point for gabion stepped spillways. The expression is given in Equation 6.7. The same procedure used for Equation 6.1 was

applied. The value of the RMSE, R^2 and the correlation factors were 0.056 0.9413, and 0.9702 respectively (Figure 6.14).

$$\frac{di}{ks} = 0.2569 * (\sin\theta)^{0.1175} * (F_*)^{0.7469} * (p)^{-0.1188} * \left(\frac{D_{50}}{hs}\right)^{-0.0091} \quad (6.7)$$

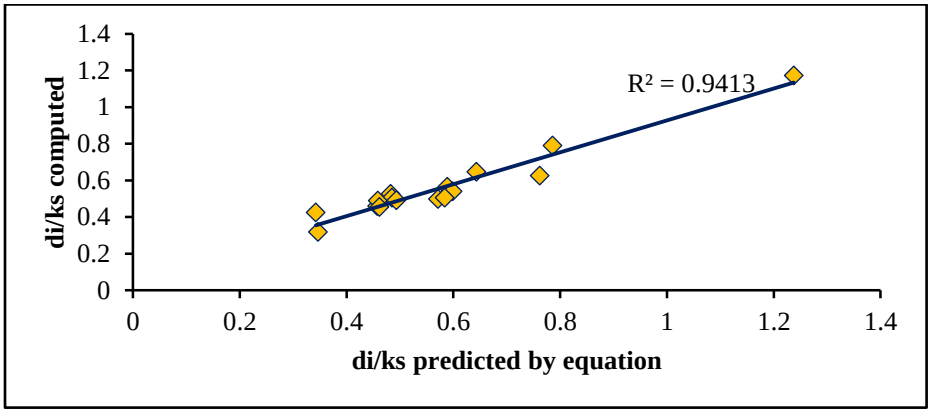

Figure 6.14 Comparison of Equation 6.7 to numerical data.

The results of the empirical correlation of the water depth at the inception point over gabion stepped spillway have been compared with the empirical formulae of Chanson (1994) and Meireles and Matos (2009) (Figure 6.15).

The empirical correlations are:

$$\frac{di}{ks} = \frac{0.4}{(\sin\theta)^{0.04}} * (F_*)^{0.64} \quad \text{Chanson (1994)} \quad (6.8)$$

$$\frac{di}{ks} = 0.28\,(F_*)^{0.68} \quad \text{Meireles and Matos (2009)} \quad (6.9)$$

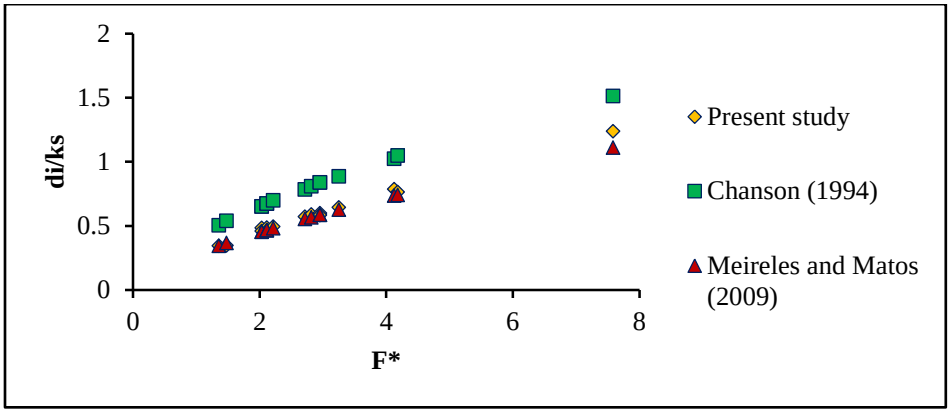

Figure 6.15 Comparison with different correlations.

Both equations were developed for normal stepped spillways, not for gabion stepped spillways. As can be seen in Figure 6.15, Chanson's formula (1994) consistently overestimates the water depth in comparison with the computational results of this study, whereas Meireles and Matos's formula (2009) slightly underestimates the water depth.

It should be noted that Equations 6.1 and 6.7 are valid for gabion stepped spillways. Both equations have been obtained from the computational results of different step heights 0.06, 0.09 and 0.12m ($0.832 \leq Yc/hs \leq 3.08$) and also by using different chute slopes 1V:2H, 1V:2.5H and 1V:3H. Moreover, these equations are applicable for porosity values from 0.25-0.40 and also for different values of D_{50} in the range 0.005m-0.02m. The maximum discharge used was $0.25m^2/s$. As ever with empirically derived formulae, application outside the parameter ranges used to find the regression is not recommended unless further tests are performed.

The location of the inception point can be significantly influenced by changing the step heights and the flow rates. However, some parameters such as the chute slope might have less impact on the length of the non-aerated zone. Velocity distributions and the energy rate will be investigated in details in the next chapter to optimise the design of gabion stepped spillways.

Chapter 7 : The Results and Discussion of Velocity Distribution and Energy Dissipation Rate

7.1. Introduction

Stepped spillways capability to dissipate energy during overtopping events can be considered as the most important benefit of using them. Therefore, more attention has been paid to the design of stepped spillways in the past studies (Chanson, 1994). Dissipating a high amount of energy rate is crucial as it can reduce the size of the stilling basin which normally constructs at the end of the spillway to dissipate the residual energy which the steps couldn't dissipate. Hence, calculating the energy dissipation rate over steps is significantly crucial in the design of stepped spillways. Two different ways can be used to estimate the energy dissipation over gabion stepped spillways;

- The first method using Bernoulli's equation: the flow depth and the velocity distribution are required in different sections in the non-aerated zone.
- The second method to estimate the energy dissipation using Turbulent Kinetic Energy (TKE). Turbulent kinetic energy is associated with eddies in the turbulent flow so there is a direct relation between the energy dissipation and TKE. For instance, when the eddy energy increases in turbulent flow due to one of the effective parameters such as fluid shear or friction, high values of TKE are expected, and that leads to an increase in the energy dissipation. The turbulent kinetic energy was computed directly from the instantaneous velocities over the whole domain. Hence, it represents the spatial or the average value of TKE at specific time.

The next section will evaluate the distribution of the velocity in the non-aerated zone over gabion stepped spillways and then the energy dissipation rate over gabion stepped spillways will be examined.

7.2. Velocity distribution

In this section, the properties of the velocity over gabion stepped spillways will be investigated for different flow rates typical of the skimming flow regime. Three different step heights 0.06m, 009m and 0.12m and various bottom chute slope 1V:2H, 1V:2.5H and 1V:3H will be included in this investigation (see Table 5.1). Furthermore, to examine the effect of the porosity and particle size of the gabion on velocity distributions over the pseudo-bottom, four values of porosity and particle sizes have been investigated for three bottom chute slopes with 0.12m step height. Figure 7.1 shows the velocity pattern over gabion stepped spillways of 0.06 m step height and unit discharge of q=0.25m^2/s over stepped spillways with slopes of 1V:2H, 1V:2.5H and 1V:3H. Conversely, Figure 7.2 displays the velocity pattern over gabion stepped spillways of 1V:2H chute slope with a flow rate of q=0.20m^2/s over step heights of 0.06m, 0.09m and 0.12m.

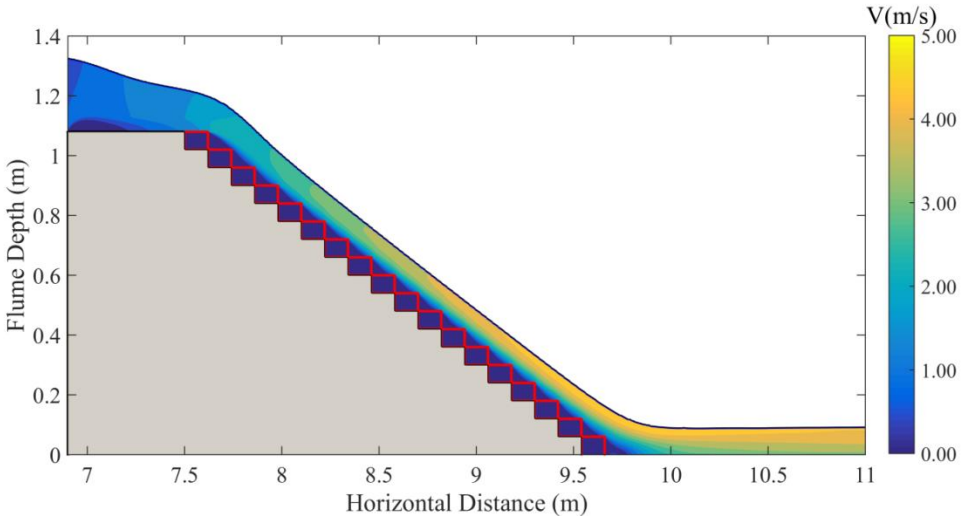

(a)

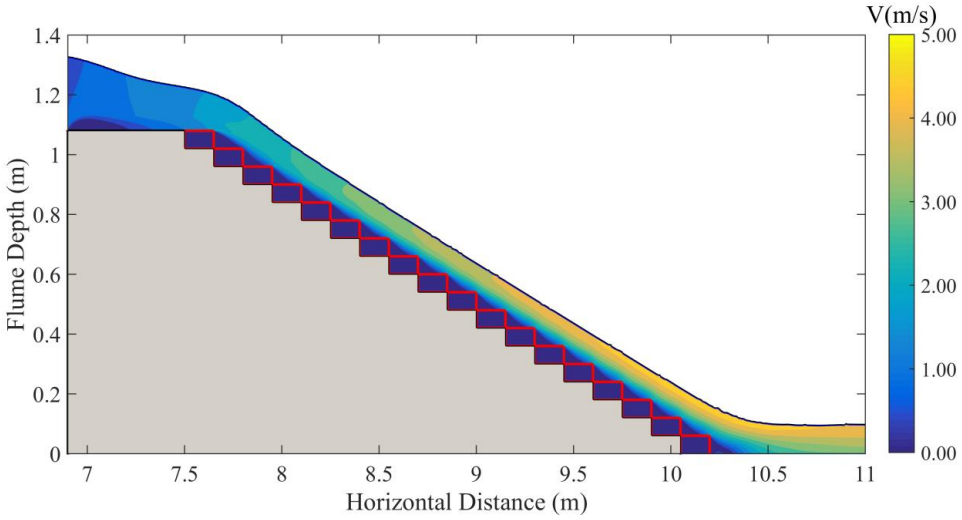

(b)

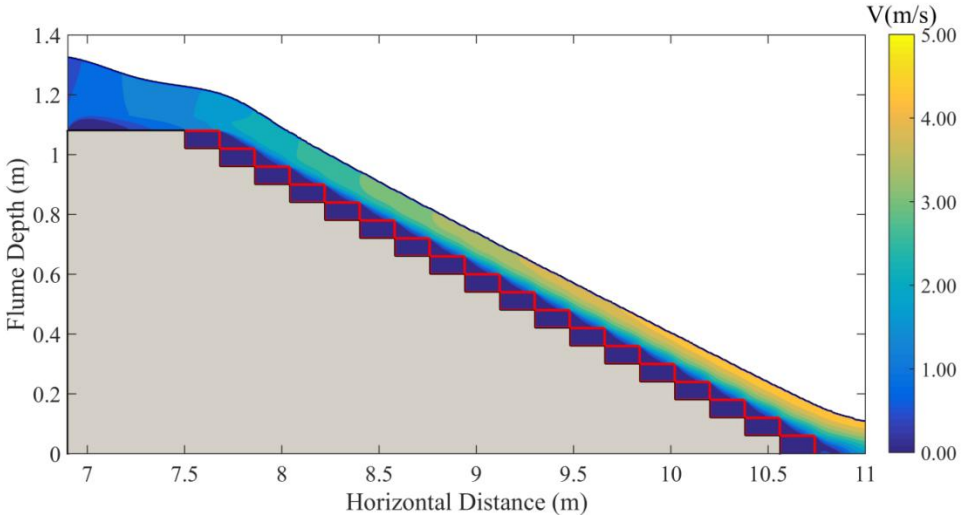

(c)

Figure 7.1 Velocity flow field for the unit discharge of q=0.25m^2/s along gabion stepped spillway with steps of height 0.06m and bottom slope: a) 1V:2H, b) 1V:2.5H and c) 1V:3H.

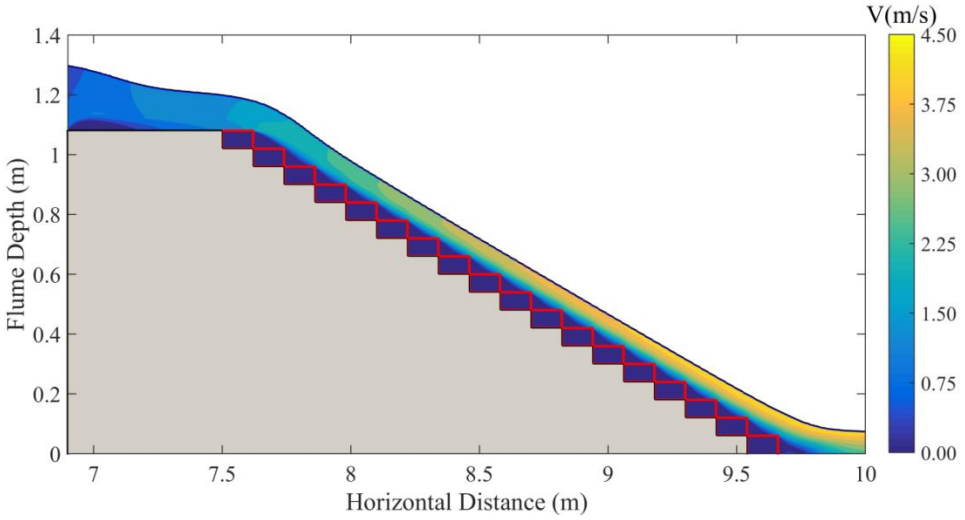
V(m/s)
4.50
3.75
3.00
2.25
1.50
0.75
0.00
Flume Depth (m)
1.4
1.2
1
0.8
0.6
0.4
0.2
0
7
7.5
8
8.5
9
9.5
10
Horizontal Distance (m)

(a)

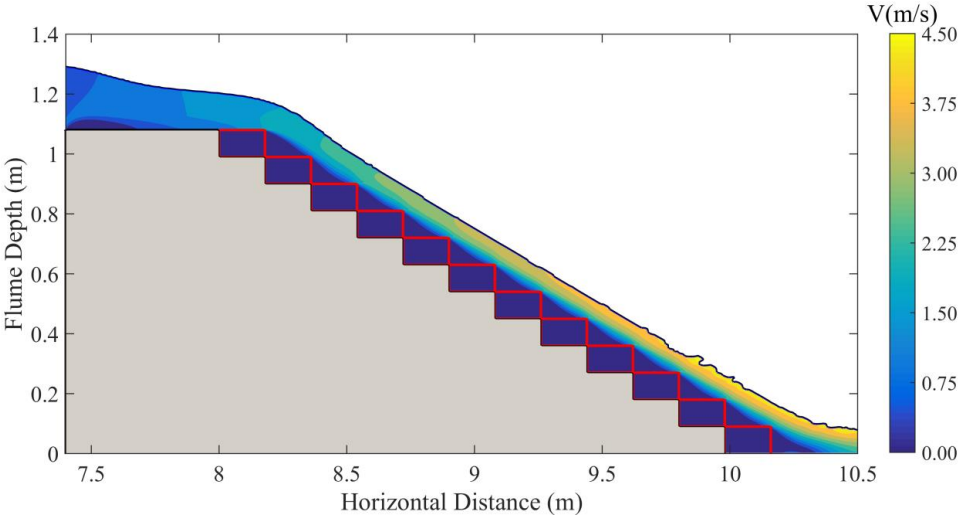
V(m/s)
4.50
3.75
3.00
2.25
1.50
0.75
0.00
Flume Depth (m)
1.4
1.2
1
0.8
0.6
0.4
0.2
0
7.5
8
8.5
9
9.5
10
10.5
Horizontal Distance (m)

(b)

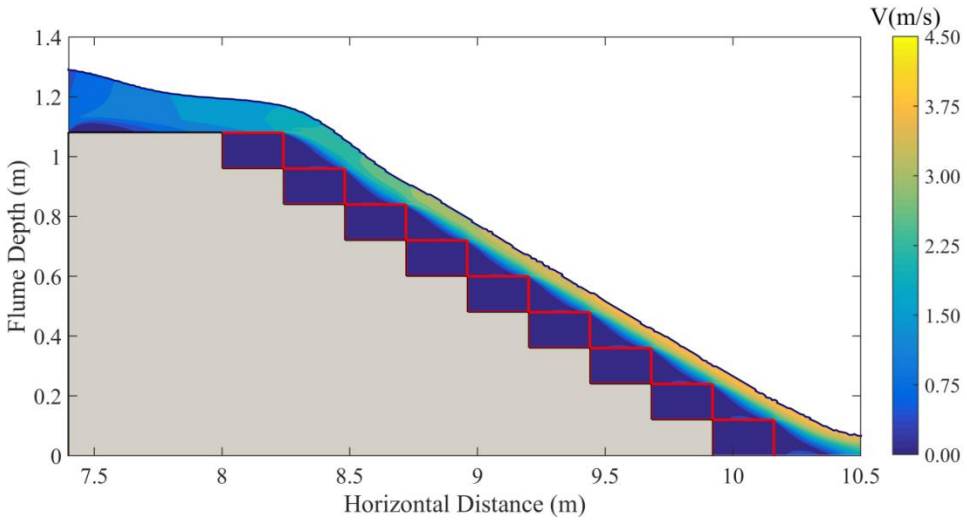

(c)

Figure 7.2 Velocity flow field for the unit discharge of q=0.20m^2/s along gabion stepped spillway with bottom slope 1V:2H and step heights: a) 0.06, b) 0.09 and c) 0.12m.

It is plain to see from these figures that the velocity trend is nearly identical apart from the peak values due to the differences in the flow rates. The velocity values over the gabion steps increase towards the downstream as a result of the increasing in the acceleration of the flow. The colour map of the velocity distributions over the pseudo-bottom showed some small differences. Therefore, the following section demonstrates and discusses the characteristics of the velocity profile on the gabion steps. To investigate the velocity performance in the non-aerated zone over gabion stepped spillways, velocity distributions are investigated in different positions. The velocity profile has been computed perpendicularly to the pseudo-bottom which represents a line passing through the outer edges of the steps. It is crucial to highlight that the velocity profile should be determined by using the parallel velocity to the chute slope which represents the resultant velocity of the horizontal and the vertical components.

Figure 7.3 shows the velocity profiles which are computed at the outer edge of number of steps in the non-aerated regime, for a unit discharge of q=0.2m^2/s. The velocity profiles have been calculated at different distances, L, normalized by the step roughness, ks. Three step heights of 0.06m, 0.09m and 0.12m and three chute slopes of 1V:2H, 1V:2.5H and 1V:3H have been selected and presented in this work to study the effect of the step

heights and the chute slopes on the velocity behaviour. In this figure, y represents the distance between the step outer edge and the point where the streamwise velocity V is computed, v represents the flow velocity at the section where the velocity profile is taken, ks is the roughness height and L is the distance between the downstream face of the first step and the outer edge of the step under consideration. Yc is the critical water depth and Vc is the critical water velocity over the crest of the spillways.

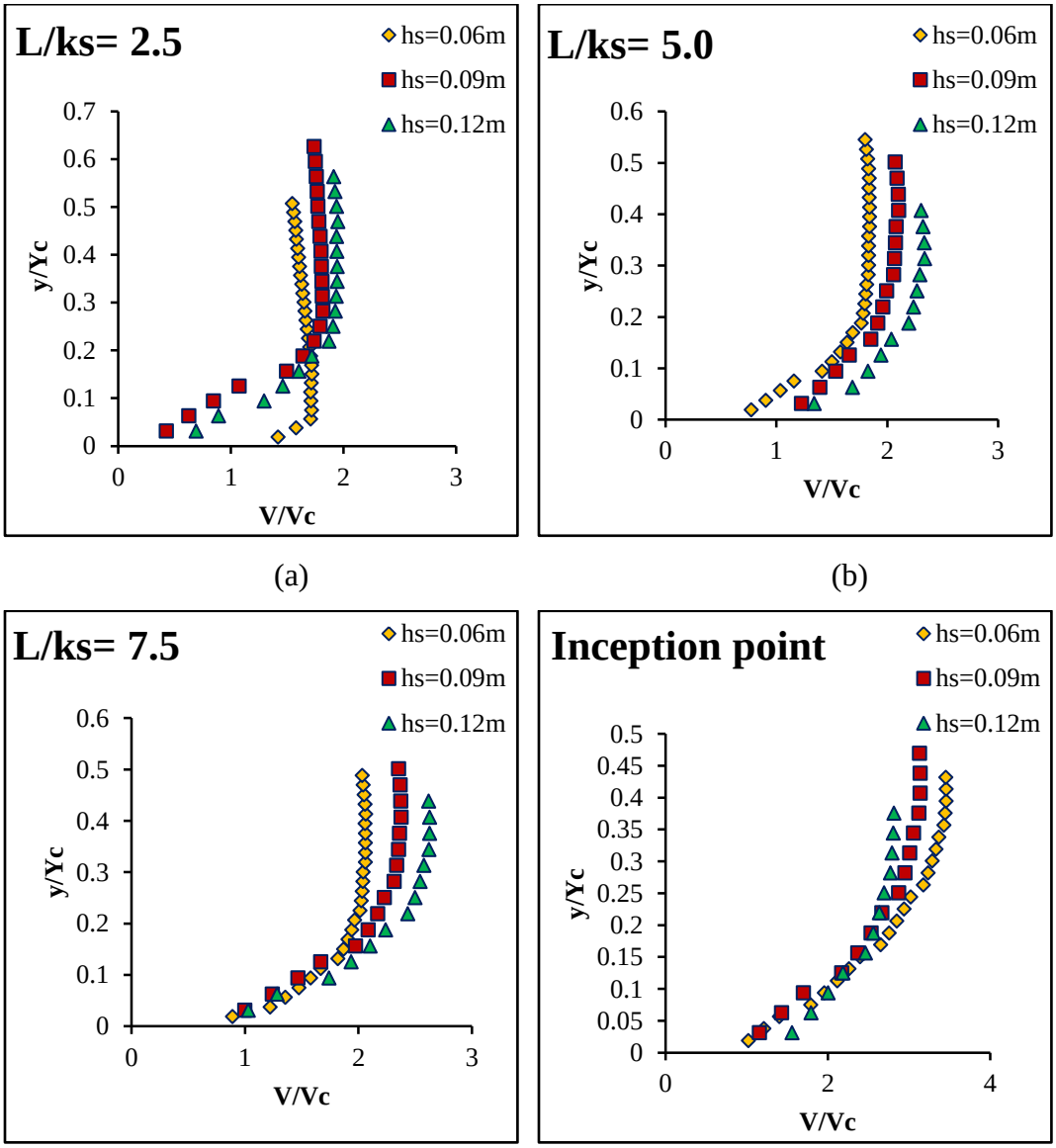

Figure 7.3 Velocity profile along the non-aerated flow region over the bottom stepped spillway slope of 1V:2H and step heights 0.06m, 0.09m and 0.12m, for a unit discharge $0.2m^2/s$.

The trend of the velocity profiles in the skimming flow is different along the non-aerated zone. The velocity values on the steps near to the weir crest are relatively small and almost uniformly distributed over the measured flow depth over the step outer edge. Then, the investigation carried out for the other steps towards the downstream side, it has been observed that the velocity magnitudes are increased. The uniformity of the velocity profiles begin to be gradually mitigated (Figure 7.3). The flow velocity reaches the peak value near the inception point location where the turbulent boundary layer thickness intersects with the free surface (Figures 7.4 and 7.5).

Furthermore, the velocity profiles over a particular step have been investigated. The results showed that the flow velocity increases towards the outer edge of the step until it reaches the maximum value at the outer edge of the steps. This is probably the reason for the high thickness of the turbulent boundary layer at the outer edges. The same characteristics of flow velocity are observed with the other chute slopes that tested in the present work.

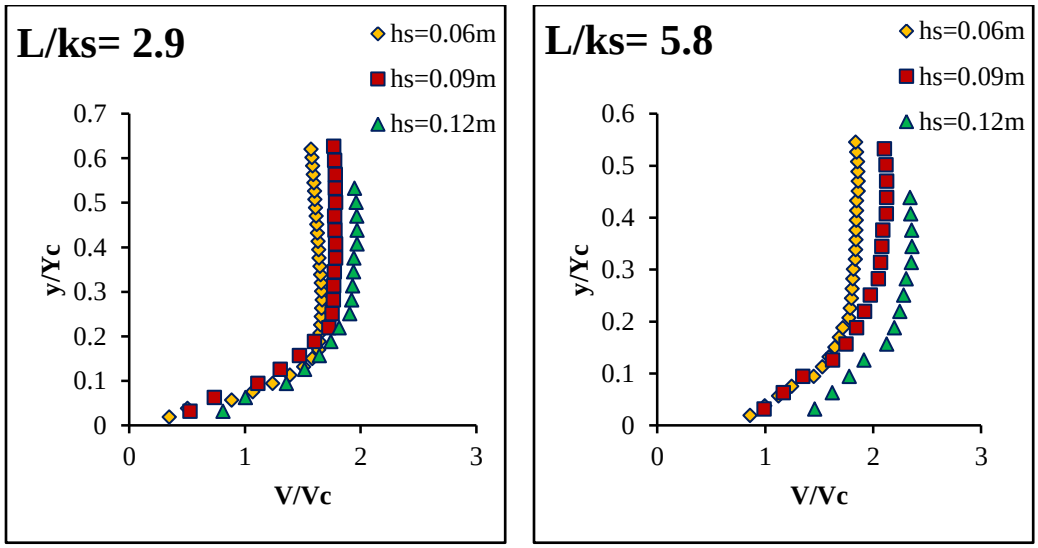

(a) (b)

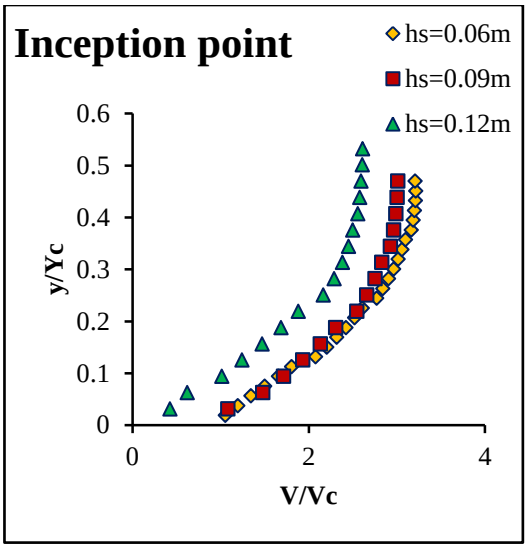

(c)

Figure 7.4 Velocity profile along the non-aerated flow region over the bottom stepped spillway slope of 1V:2.5H and step heights 0.06m, 0.09m and 0.12m, for a unit discharge $0.2m^2/s$.

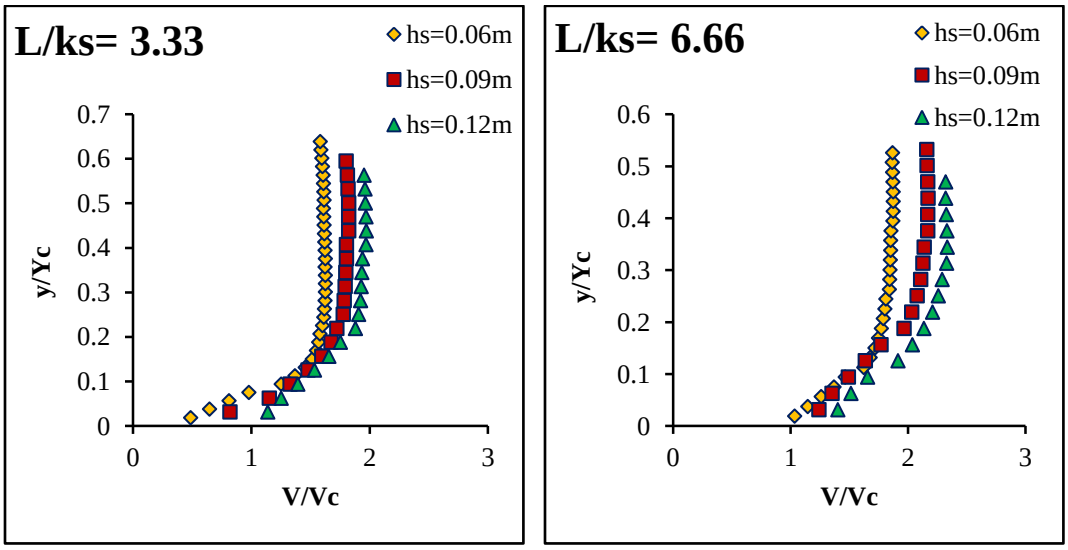

(a) (b)

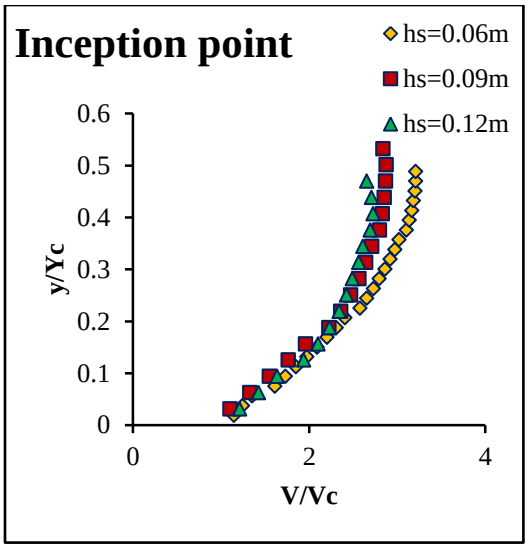

(c)

Figure 7.5 Velocity profile along the non-aerated flow region over the bottom stepped spillway slope of 1V:3.0H and step heights 0.06m, 0.09m and 0.12m, for a unit discharge $0.2m^2/s$.

For the same chute slope, the results in the non-aerated zone showed that the velocity of the water flow increases when 0.12m and 0.09m step heights are used instead of 0.06m step height. This could be due to the fact that increasing the step height may increase the recirculating area under the skimming layer inside the step cavity. However, the flow velocity has been reduced close the location of the inception point when the step height of 0.06m is replaced by 0.09m and 0.12m which is different from the trend of the velocity profiles over the non-aerated zone. That probably happened due to the air entrainment effect at the inception point which could impact the velocity distribution.

The same technique has been used to evaluate the velocity distribution over different values of porosity and particle sizes of the gabion. Figures 7.6 and 7.7 present the velocity profiles of gabion stepped spillways with 0.12m step height and with three different bottom chute slopes 1V:2H, 1V:2.5H and 1V:3H to cover different values for L/ks. Velocity profiles are plotted perpendicular to the pseudo-bottom at the outer edge of steps located at different distances measured from the downstream face of the weir crest along the non-aerated zone, for a unit discharge of $q=0.2m^2/s$. These figures clearly

illustrate that the velocity profiles along the non-aerated flow region have the same characteristics which have been mentioned and discussed earlier. Additionally, they reveal that for a given discharge and stepped spillway geometry, in terms of step height and chute slope, the velocity of the skimming flow in the non-aerated zone is not significantly influenced by porosity and particle size of the gabion.

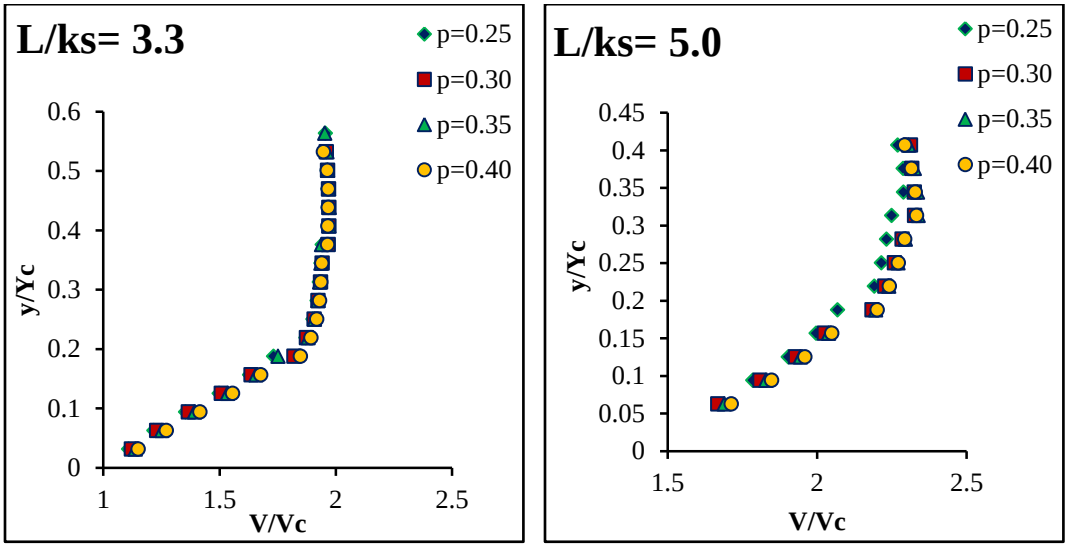

(a)

(b)

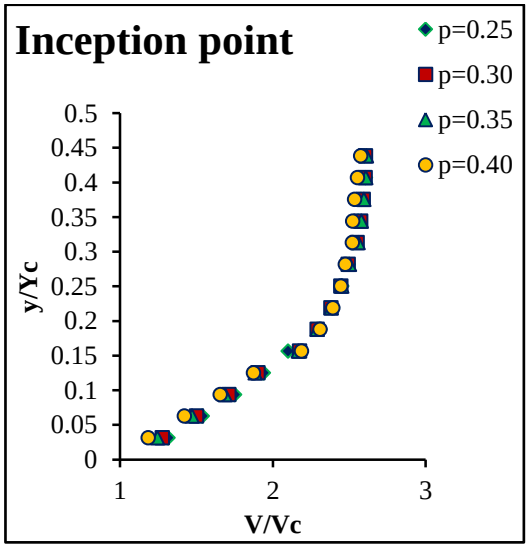

(c)

Figure 7.6 Velocity profile along the non-aerated flow region over the gabion stepped spillways of step height 0.12m and four porosities 0.25, 0.30, 0.35 and 0.40, with a unit discharge of q=0.2m^2/s of bottom chute slopes a)1V:3H, b)1V:2H and c)1V:2.5H.

As can be seen from Figures 7.6 and 7.7, both porosity and particle sizes can impact the gabion surface slightly so it can cause around 10% of reduction in the velocity values. That impact becomes smaller when it moves towards the free surface of the water; it could be less than 1% near the free surface of the water. Over different sections in the non-aerated zone, the results showed that the velocity value increases slightly with porosity and particle sizes increase. However, the general trend of the results at the inception point indicates that velocity decreases slightly when porosity increases and also, the velocity profile is decreased slightly when the particle size is decreased. This is absolutely agreed with the outcomes which mentioned in the previous chapter about the relations between the location of the inception point with the porosity and particle sizes. This is could be related to the seepage flow inside the gabion, for instance, water flow seeps inside the porous media easily when the porosity is large but it could be harder when the porosity is small. To sum up, there is no significant impact on the velocity distribution when the values of the porosity and the particle size are changing, however, in some cases, very minor differences can be observed near the bed surface.

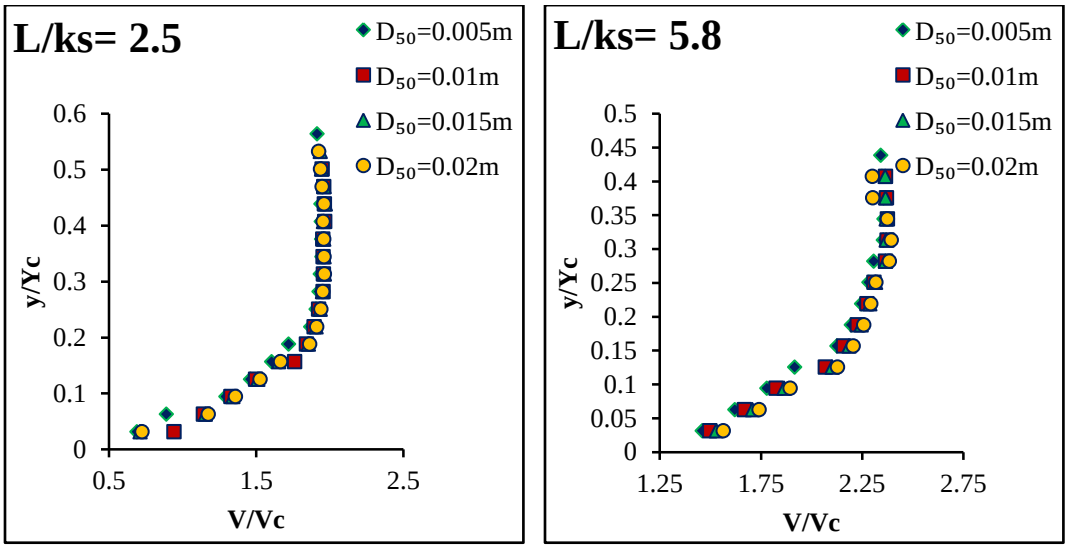

(a) (b)

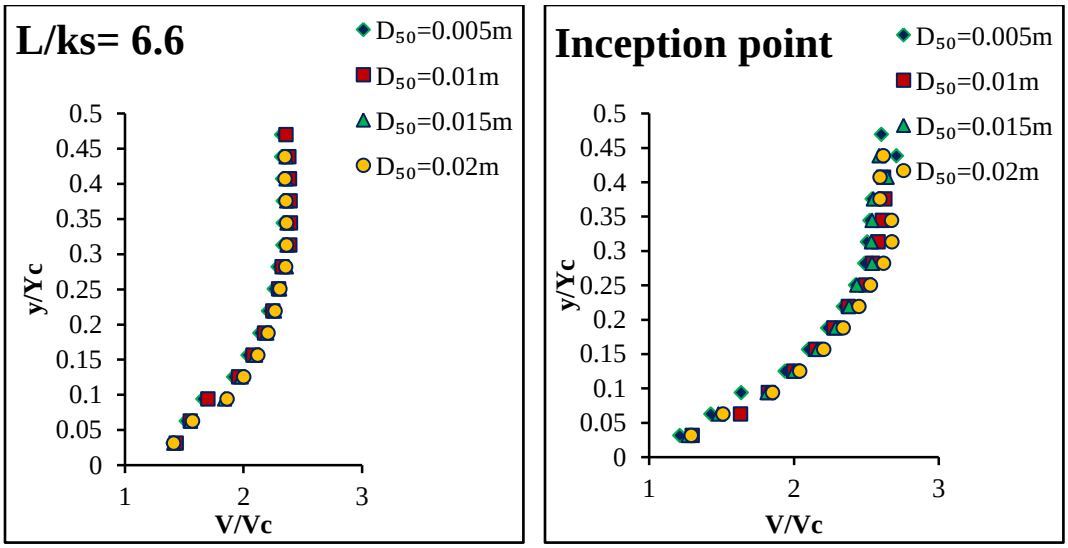

(c) (d)

Figure 7.7 Velocity profile along the non-aerated flow region over the gabion stepped spillways of step height 0.12m and four particle sizes 0.005, 0.01, 0.015 and 0.02m, with a unit discharge of q=0.2m^2/s of bottom chute slopes a)1V:2H, b)1V:2.5 H, c)1V:3H and d) 1V:3H.

In order to investigate how the velocity vectors perform inside and outside the porous media and to be able to observe the properties of vortices over the steps, three Figures 7.8, 7.9 and 7.10 have been plotted for different step heights and bottom chute slopes in the non-aerated zone.

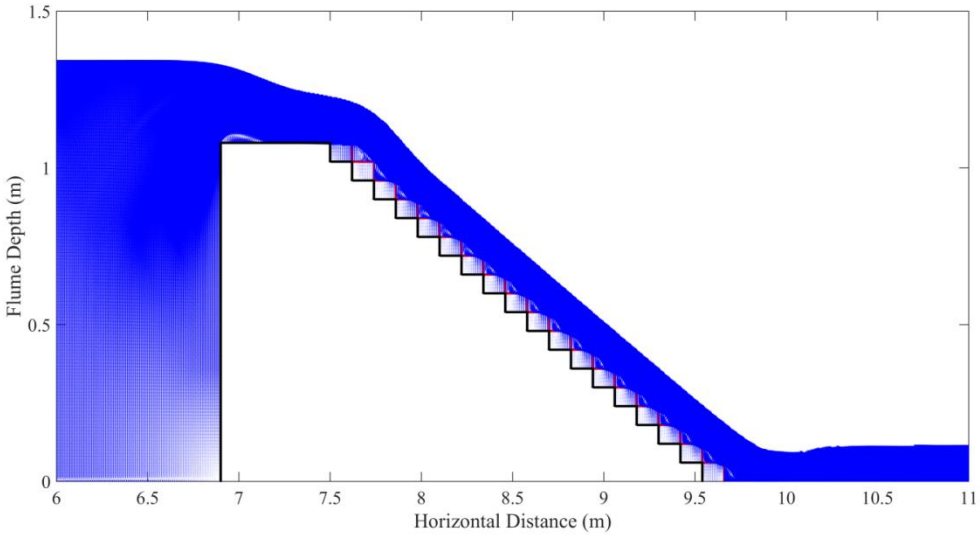

(a)

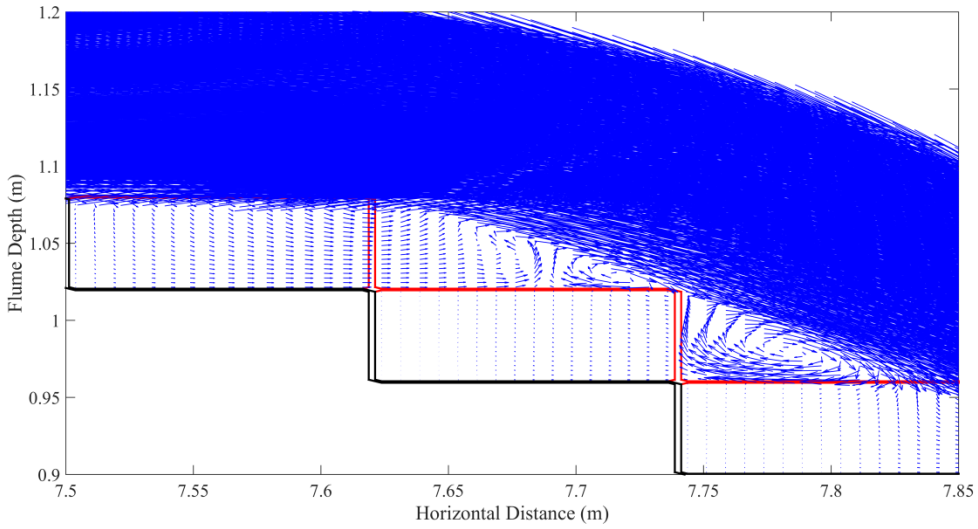

(b)

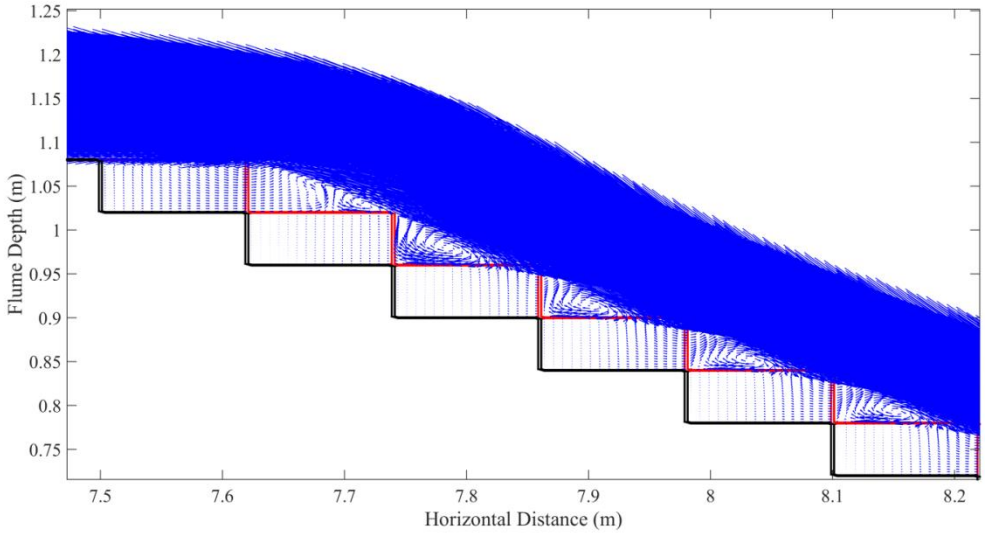

(c)

Figure 7.8 Velocity vectors over the gabion stepped spillways of step height 0.06m with a unit discharge of q=0.25m^2/s of bottom chute slope1V:2H a) full geometry, b) first three boxes and c) six boxes.

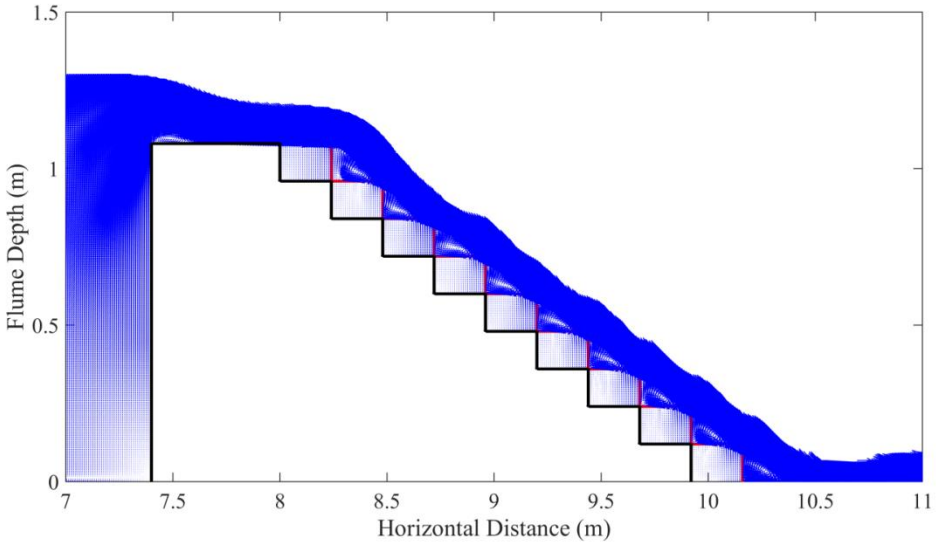

(a)

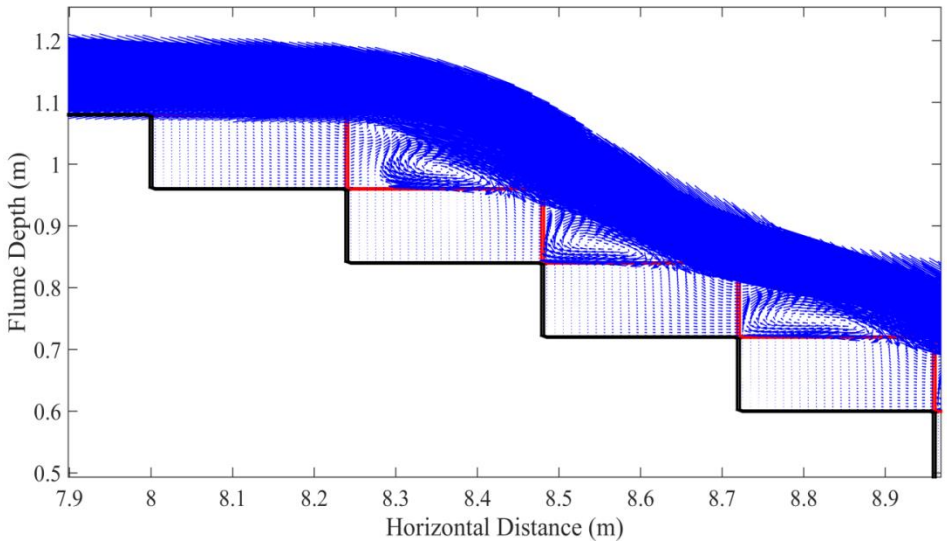

(b)

Figure 7.9 Velocity vectors over the gabion stepped spillways of step height 0.12m with a unit discharge of q=0.20m^2/s of bottom chute slope1V:2H a) full geometry and b) first three steps.

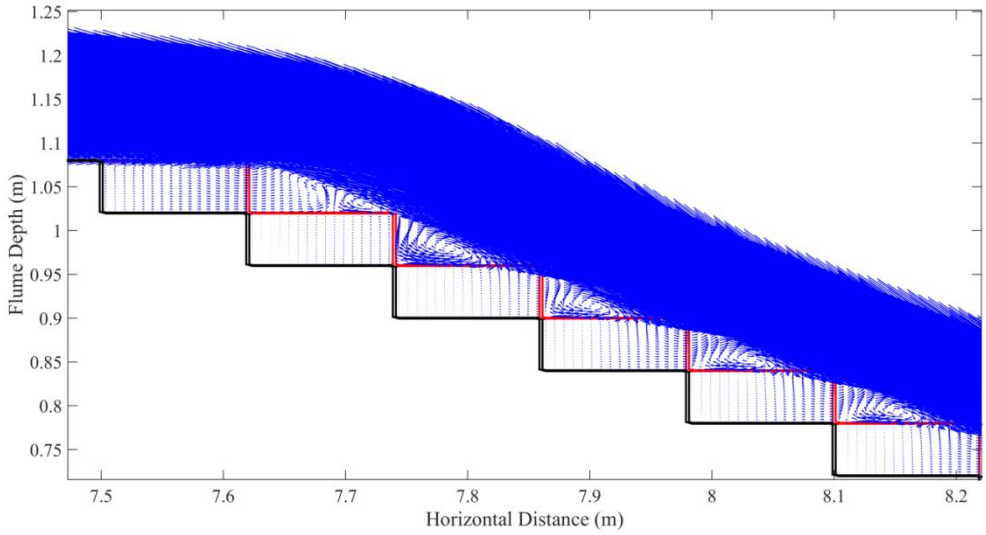
Flume Depth (m)
1.25
1.2
1.15
1.1
1.05
1
0.95
0.9
0.85
0.8
0.75
7.5
7.6
7.7
7.8
7.9
8
8.1
8.2
Horizontal Distance (m)

(a)

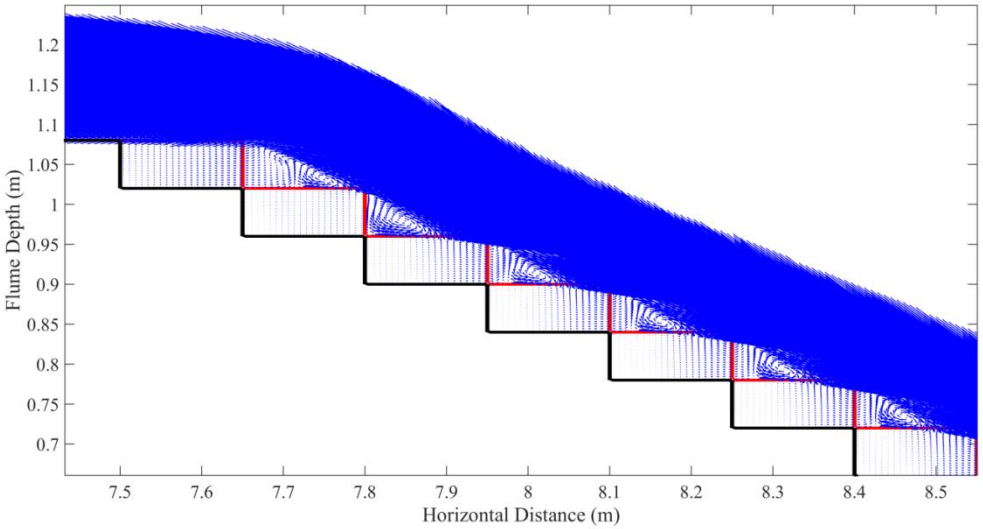
Flume Depth (m)
1.2
1.15
1.1
1.05
1
0.95
0.9
0.85
0.8
0.75
0.7
7.5
7.6
7.7
7.8
7.9
8
8.1
8.2
8.3
8.4
8.5
Horizontal Distance (m)

(b)

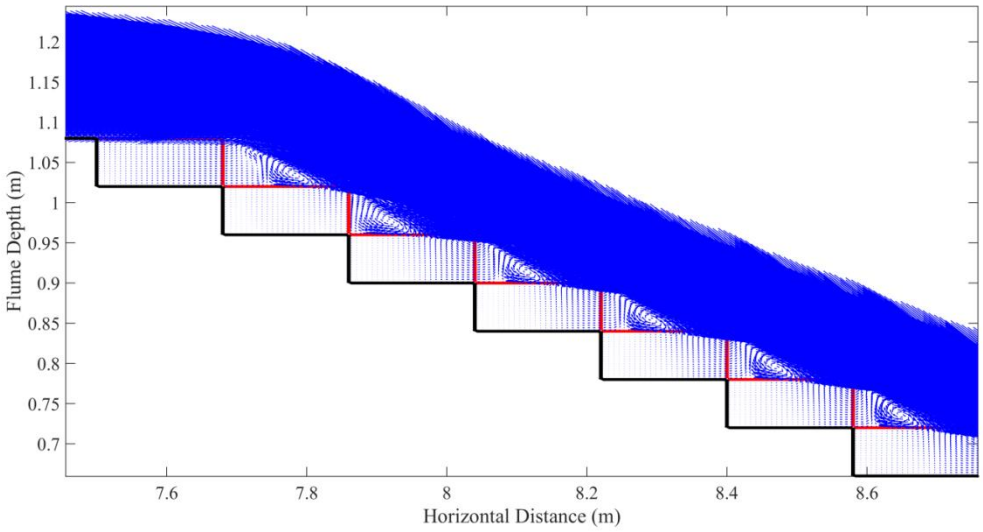

(c)

Figure 7.10 Velocity vectors in the non-aerated zone over the gabion stepped spillways of step height 0.06m with a unit discharge of q=0.25m^2/s of bottom chute slopes a)1V:2H, b)1V:2.5 H and c)1V:3H.

Figures 7.8-7.10 show that the flow inside the first box of the porous media is quite high over the entire box. For the other steps, the flow is only high around the last third of steps, which close to the outer edges. It is also low at the beginning of the steps near to the inner edge which is probably due to the water recirculation. The water at the end of the steps can have high amount of energy and relatively high values of velocity. Therefore, an increasing in the capability of flow can be observed and that can stimulate the water flow to go inside the porous media with high magnitudes of velocities.

Over the first step, it is noticed that the vortices of water recirculation take place initially in the second half of the step towards the outer edge then the vortices will move towards the inner side in step 2. After this, the vortices start to move a small distance towards the downstream side for the other steps. According to the observations, vortices will start their movement at a certain distance and it could be from 0.25 to 0.30 of ls, from the inner edge side. The same finding has been found by Wüthrich and Chanson (2014).

It is important to highlight that it would be harder to observe the movement of vortices with high step heights as the vortices would be stronger than those in small step heights due to the availability of the space. Having more space due to the step heights increasing can increase the power and the size of the vortices, therefore the area covered by the vortices will be longer; this makes it more difficult to observe the movement of the vortices. Moreover, the results revealed that bottom chute slopes cannot impact the performance of vortices and the water recirculation. Flow rates were found to have a direct relationship with the vortices power as increasing the discharge will increase the velocity of the vortices. It could be useful to highlight that the previous studies revealed that the power of vortices might play a crucial role in the next section where the energy dissipation will be investigated.

Figure 7.11 shows the velocity profiles inside gabion boxes in the non-aerated zone under skimming flow conditions. The velocity values at the end of the boxes are high due to the vortices and water recirculation over that location.

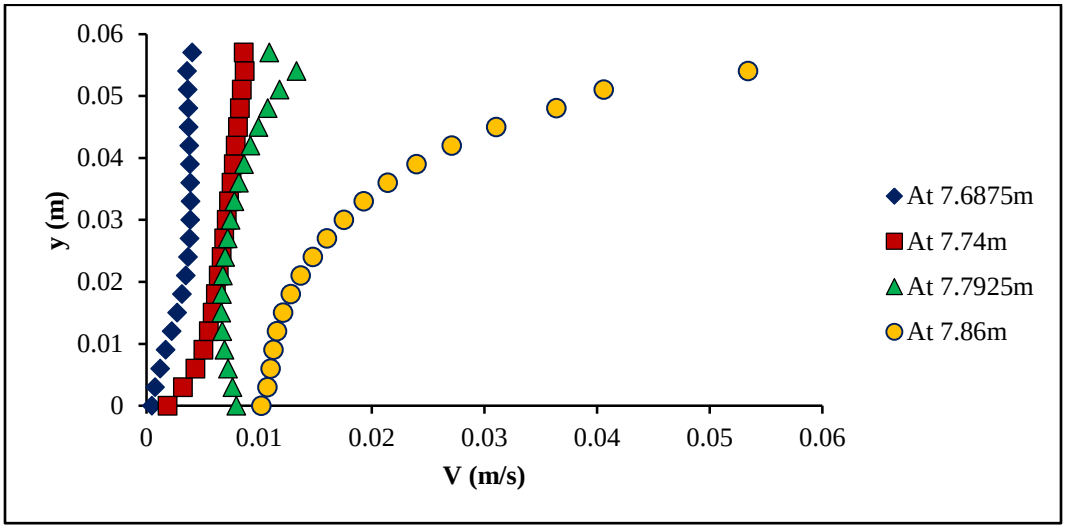

(a)

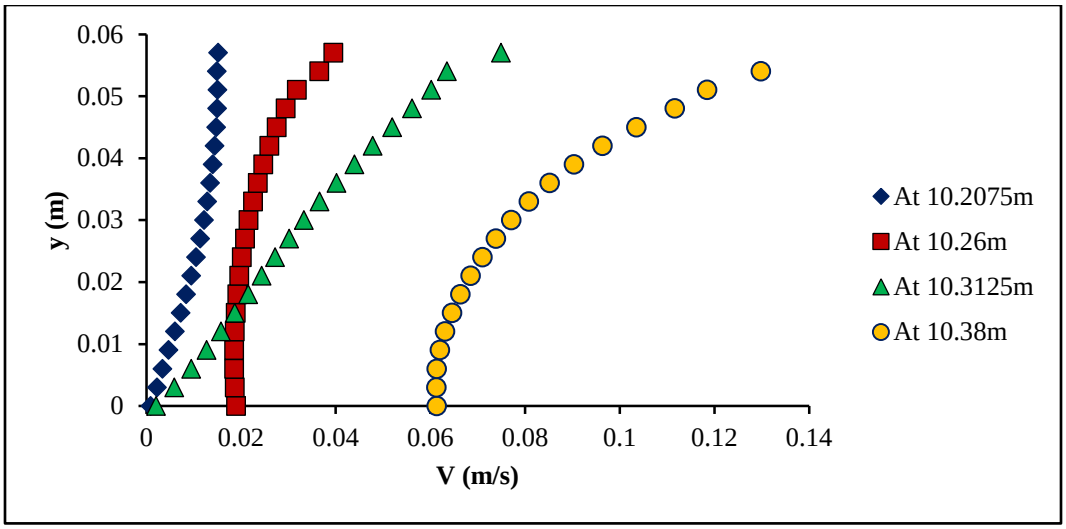

(b)

Figure 7.11 Velocity profiles inside the gabion in the non-aerated zone of step height 0.06m with a unit discharge of q=0.25m^2/s of bottom chute slope 1V:3H a) in the second box and b) box close to the inception point.

The velocity profiles inside the porous media have been plotted with different values of porosity and particle sizes, in order to demonstrate the influence of these parameters on the velocity profiles (Figure 7.12). The velocity profiles have been measured at the end of the second step of gabion stepped spillways of 0.12m step height and 1V:3H bottom chute slope with four different values for both porosity and particle sizes. All the velocity values have been measured with same discharge to be able to compare the results directly.

The results showed that both porosity and particle size can impact the velocity profiles inside the porous media. As shown in Figure 7.12, increasing the values of porosity and particle sizes will increase the magnitude of the velocity profiles. However, it is easy to notice that particle size has a significant impact on the velocity compared to the porosity. In other words, the maximum velocity with the maximum value of the porosity is 0.265m/s; however, it is 0.479m/s when the particle size is 0.02m. Therefore, an increase or decrease in the particle size will be more efficient than changing the porosity. This is because the voids between the particles will be much higher than the voids inside the

particles. Thus, the availability of the space between the particles will increase the amount of the seepage flow which can lead to high changes in the velocity values.

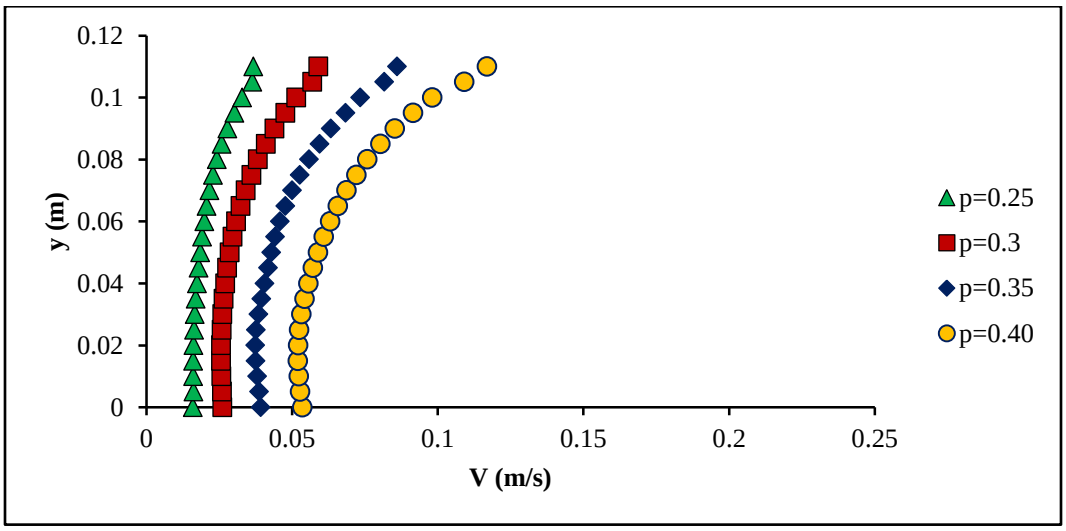

(a)

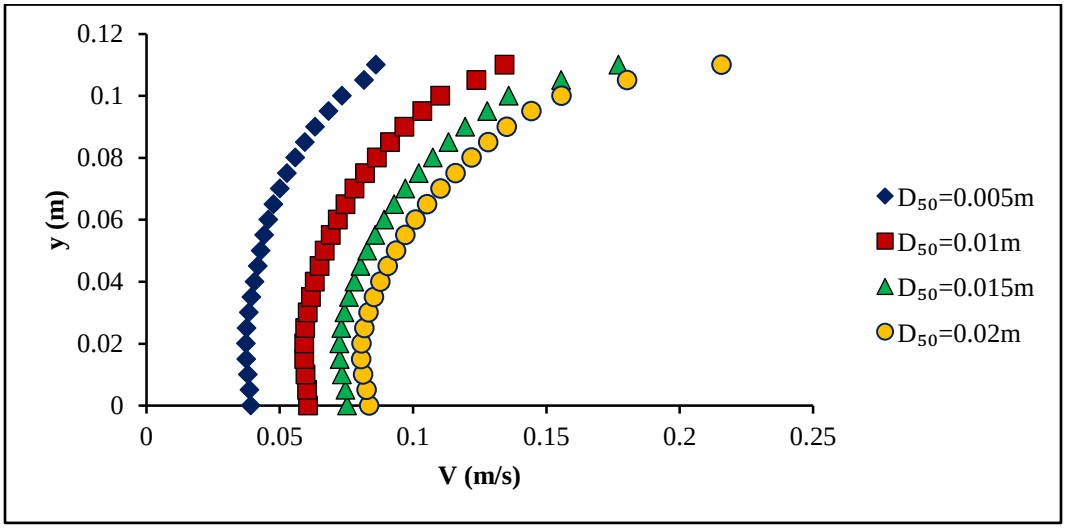

(b)

Figure 7.12 Velocity profile inside the porous media of gabion stepped spillways of step height 0.12m and 1V:3H bottom chute slope, with a unit discharge of q=0.2m^2/s of different values of a) porosity and b) particle sizes.

According to Chanson (2002), the velocity profile at any section in the non-aerated zone which is perpendicular to the pseudo-bottom can be represented by the power law equation:

$$\frac{V}{Vmax} = (\frac{y}{\delta})^{1/N} \quad (7.1)$$

where:

V is the time-averaged flow velocity at distance y that is measured perpendicular to the pseudo bottom originating at the outer edge of the steps, Vmax is the maximum flow velocity, N is a constant, δ is the whole thickness of the boundary layer, where the flow velocity is equal to 0.99Vmax.

Many past studies which were conducted experimentally and numerically showed that the value of the exponent N could depend on many parameters, however, it could be essentially depending on the chute slope and the section where the velocity distribution is observed. According to Meireles and Matos (2009), the results of the experimental study on 1V:2H stepped spillways revealed that the value of N exponent for a wide range of flow rates under skimming flow conditions could vary from 4.4 to 6.3 with an average value equal to 5.1, for $0.38 \leq L/Li \leq 1.00$. It might be useful to clarify that if the data point (L/Li) is less than 1.00 then it is in the non-aerated zone; equal to 1.00 at the inception point; greater than 1.00 in the aerated zone, thus, since this study investigate the non-aerated zone only, the maximum value for L/Li should be equal to 1. From the data analysis of the laser Doppler anemometer measurements, taken by Ohtsu and Yasuda (1997) on a 1V:2.9H stepped chute, for h=5cm and for a single discharge value $q=0.089m^2/s$, the value of the exponent N was equal to 5.0 (Chanson, 2002). In normal stepped spillways, the velocity profiles trend moves toward the one-sixth power law distribution for the steps which are located close to the inception point (Boes and Hager, 1998; Chanson, 2000).

Hunt and Kadavy (2009) investigated the power law distribution in their experimental study on a normal stepped spillway with 1V:4H chute slope and for a unit discharge of $0.28m^2/s$. They found that one-sixth power law distribution agrees more closely with the

velocity profile as it approaches the inception point. Smart et al. (2002) suggested that the N value of the power law could probably reduce from 6 to 2 for the channels that are subject to large-scale relative bed roughness. Therefore, low values for N are expected in the present study as gabion boxes are presented.

Cheng (2007) revealed that each individual value for the power number is only applicable for a limited range of Reynolds numbers. Especially, the exponent of 1/6 could be more suitable for Reynolds numbers usually observed in practical applications. Nevertheless, the exponent value could need significant adjustment for some extreme cases like in the presence of large-scale boundary roughness. With the purpose of obtaining the value of the exponent N, it is vital to explore the growth of the turbulent boundary layer in the non-aerated flow region over gabion stepped spillways. Although there is no specific mathematical or analytical expression to define the development of the boundary layer, it is highly affected by both the discharge and step height, and slightly influenced by the chute slope (Chanson, 2002).

Chanson (2002) suggested an equation to calculate the development of the boundary layer; the real numbers in the equation below are obtained from the analysis of a wide range of model prototypes velocity distributions.

$$\frac{\delta}{L} = 0.15 \left(\frac{L}{ks}\right)^{-0.37} \qquad (7.2)$$

where

δ the thickness of turbulent boundary layer,

L the length measured from the downstream face of the weir corner to the step outer edge,

ks the roughness height.

According to André's results (2004), the growth of the boundary layer can be varying for different step configurations; consequently, the development of the boundary layer over the particular arrangement of end sills and spaced blocks was faster when compared with the horizontal steps. The analysis of the experimental data on steeply stepped spillways

revealed that the growth of boundary layer is sensitive to the step height (Chamani and Rajaratnum, 2000).

In order to find an equation showing the growth of the boundary layer in the non-aerated zone over gabion stepped spillways, the thickness of the boundary layer was calculated at the outer edges of all steps which they located in the non-aerated regime by using the velocity profiles. Various discharges, step heights, particle sizes, porosity and chute slopes are used to develop the equation which can express turbulent boundary layer development along the non-aerated flow region of the moderate slope of gabion stepped spillways.

Chanson's equation for the development of the turbulent boundary layer has been modified in the present study in order to include the effects of the discharge, step height, chute slope, particle size of the gabion and gabion porosity. To achieve that, four dimensionless parameters Yc/hs, sinθ, p and D_{50}/hs have been added to Equation 7.2 to develop an expression to determine the thickness of the boundary layer on steps of gabion stepped spillways. In the present work, the non-linear multiple regressions have been established on these parameters and therefore the following formula is achieved:

$$\frac{\delta}{L} = 0.3115 \left(\frac{L}{ks}\right)^{-0.7794} * \left(\frac{Yc}{hs}\right)^{0.6918} * (\sin\theta)^{0.4177} * (p)^{-0.0542} * \left(\frac{D_{50}}{hs}\right)^{-0.0874} \quad (7.3)$$

This equation is valid for gabion stepped spillways with chute bottom slopes of 1V:2H, 1V:2.5H and 1V:3H within $0.832 \leq Yc/hs \leq 3.08$ and $2.214 \leq L/ks \leq 56.11$. The numerical data is split into two groups; the first which contains around 85% of the data and it is used to find the coefficients of the equation. The second group has the rest of the data which is around 15%, the data of the second group has been applied to test the equation. All the data has been selected randomly. The value of the R^2, RMSE and the correlation factor were 0.9526, 1.216 and 0.9757 respectively (Figure 7.13).

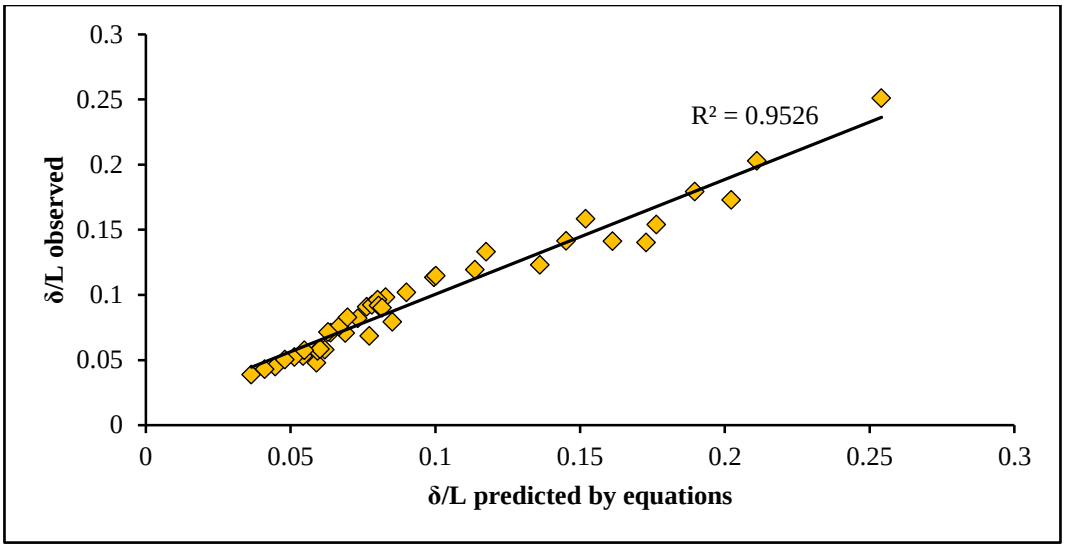

Figure 7.13 Comparison of Equation 8.3 to numerical data.

Equation 8.3 shows that the growth of the turbulent boundary layer along the non-aerated flow region on moderate gabion stepped spillways is highly affected by the discharge and step height due to the high value of the coefficient and this is well agreed with the previous work such as Chamani and Rajaratnam (2000) and Zhang and Chanson (2016b). However, chute slopes have less impact on the development of the turbulent boundary layer. Both porosity and particle sizes of the gabion steps can have a slight influence on the boundary development as the values of the power coefficient numbers for them are small.

A comparison with two extra equations for normal stepped spillways has been investigated in order to demonstrate the differences in turbulent boundary layer development between the gabion stepped spillways and the normal stepped spillways. The equations of the development of the turbulent boundary layer of normal stepped spillways are:

$$\frac{\delta}{L} = 0.218 \left(\frac{L}{ks}\right)^{-0.332} * \left(\frac{Yc}{hs}\right)^{-0.028} * (\sin\theta)^{0.557} \quad \text{Husain (2013)} \quad (7.4)$$

$$\frac{\delta}{L} = 0.15 \left(\frac{L}{ks}\right)^{-0.37} \quad \text{Chanson (2002)} \quad (7.5)$$

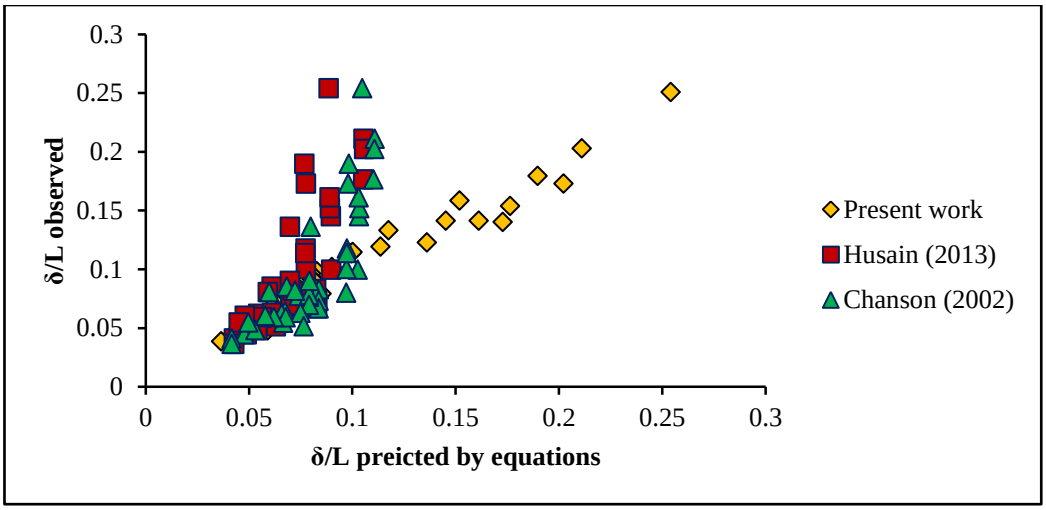

Figure 7.14 A comparison between Equation 8.3 with different previous equations.

As can be seen in Figure 8.14, both equations can describe the development of the boundary layer over gabion stepped spillways for the steps which are closed to the crest. However, that capability to describe the development of the turbulent boundary layer reduces when it moves towards the location of the inception point. This is related to the roughness of the gabion as it can change power law of flow resistance equations. That could lead to changes in the thickness of the turbulent boundary layer when it develops over more steps up to the location of the inception point.

In order to investigate the value of N in Equation 7.1, the velocity profiles over the gabion horizontal steps in the non-aerated zone are plotted and examined under skimming flow conditions for different values of discharge with step heights of 0.06m and 0.09m (Figures 7.15 and 7.16). The numerical results shown in these figures are obtained for different step heights, chute slopes and flow rates. The computational results are obtained at the outer edge of the steps starting from the outer edge of the first step up to the location of the inception point; hence it is covered the range of $0.116 \leq L/Li \leq 1.00$ for Figure 7.15. It is worth to highlight that it started from 0.116 as the values of the boundary layer thickness are very small when $L/Li < 0.1$; thus, following the previous studies, the results of that distance have been neglected. However, the range is slightly different for Figure 7.16 as it is located within $0.178 \leq L/Li \leq 1.00$ where L is the

distance from the downstream face of the weir to the outer edge of the step under investigation, and Li is the length to the inception point of air entrainment.

The values of the power law exponent N which are achieved for the gabion steps were varied from the linearity trend (N=1) for the steps that close to the weir crest to N=2 for the steps that close to the inception point. The current results agreed with the experimental results of Smart et al. (2002) who stated that the relative roughness bed could impact the exponent of power-law resistance equations. Therefore, the exponent of power-law resistance equations increases from 1/6 to more than 1/2 as relative roughness increases.

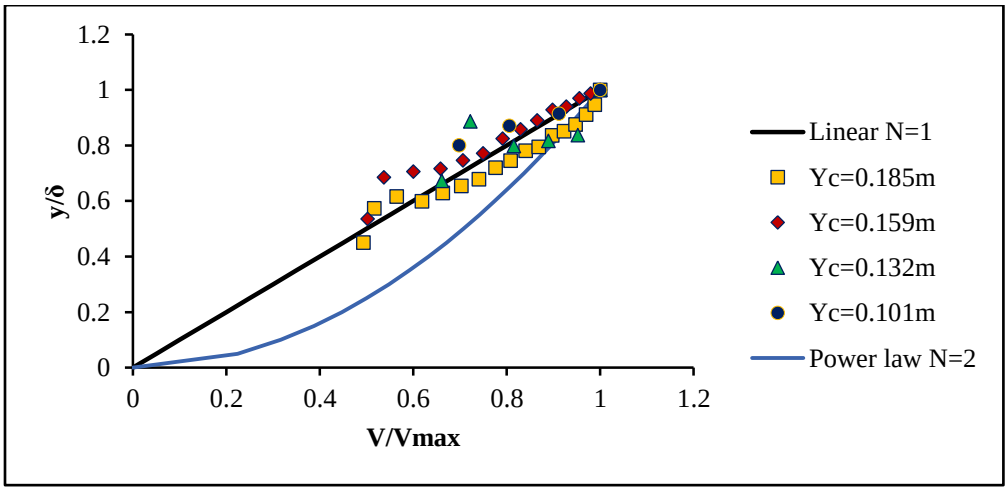

(a)

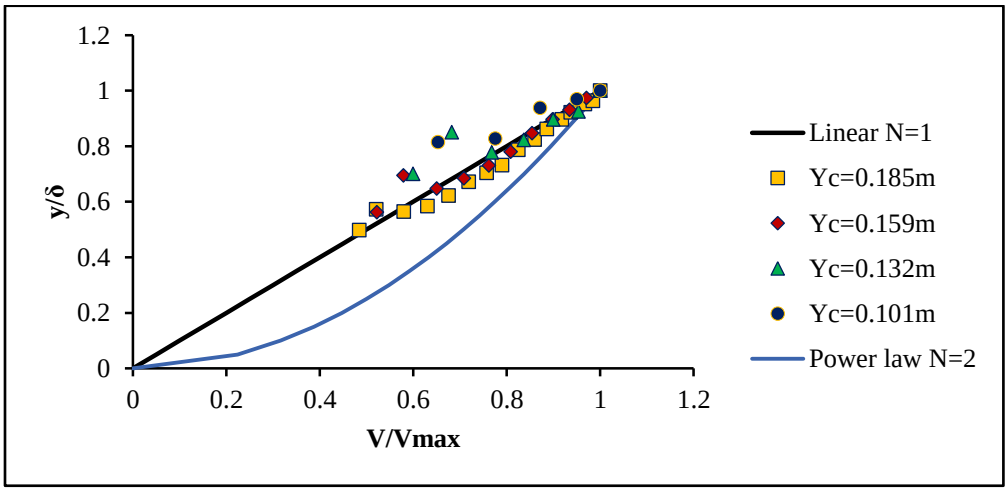

(b)

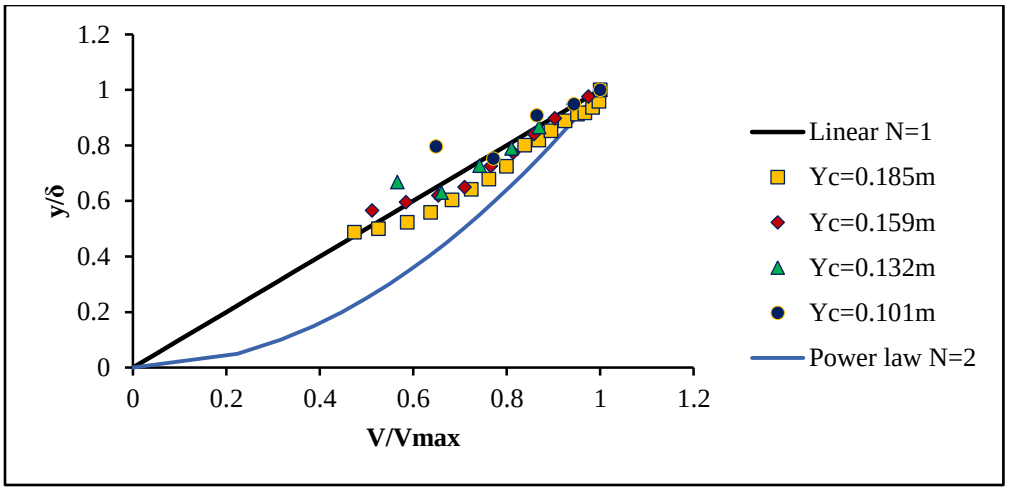

(c)

Figure 7.15 Velocity distribution in the non-aerated flow region over gabion steps of 0.06m step height versus the power law regression for slopes: a) 1V:2H, b) 1V:2.5H and 1V:3H.

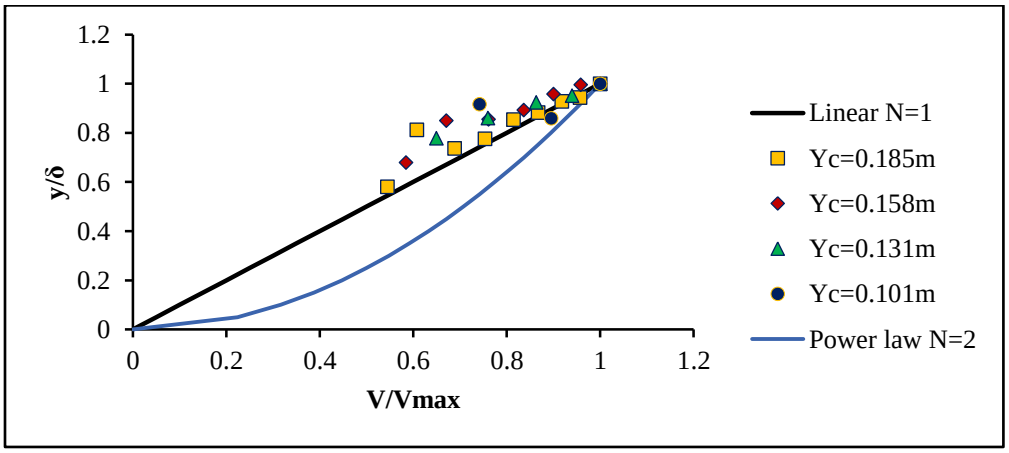

(a)

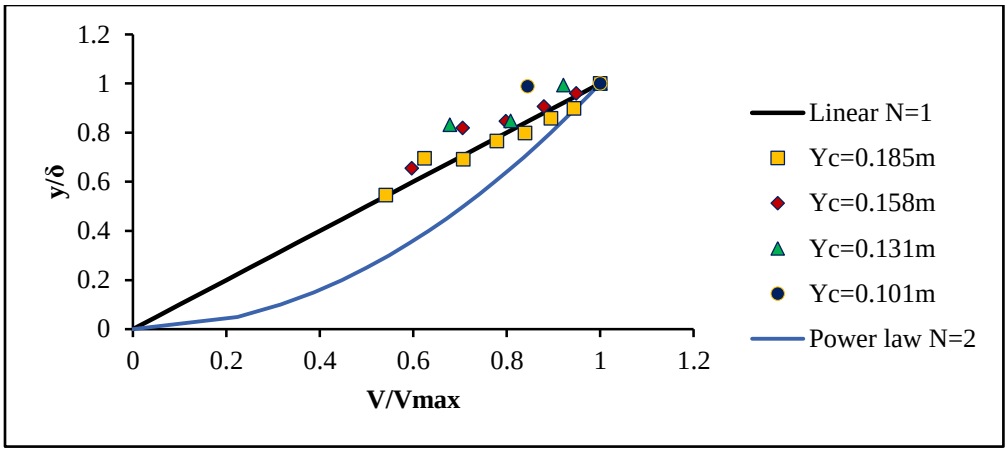

(b)

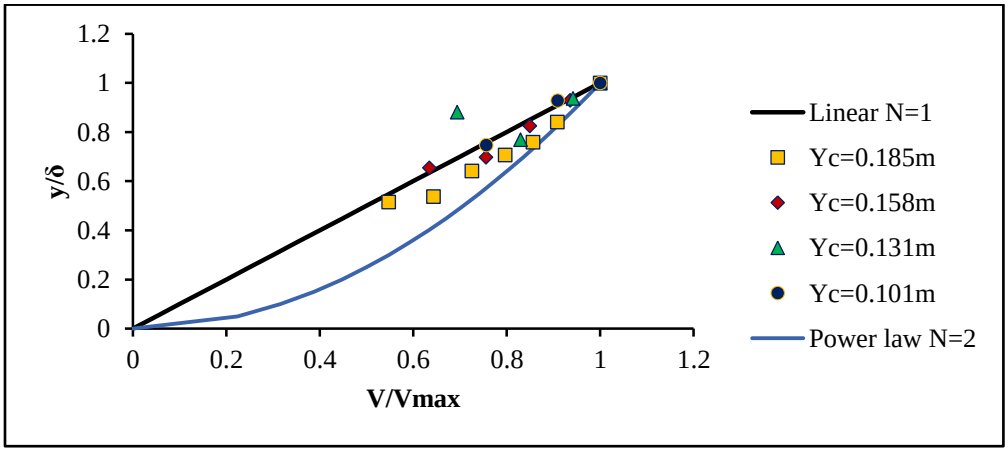

(c)

Figure 7.16 Velocity distribution in the non-aerated flow region over gabion steps of 0.09m step height versus the power law regression for slopes: a) 1V:2H, b) 1V:2.5H and 1V:3H.

7.3. Energy dissipation

The amount of the residual energy at the base of stepped spillways has attracted the attention of hydraulic designers as it can play a vital role in stilling basin design. Stilling basins have been used to increase the energy dissipation at the downstream of the spillway in order to protect that area from the scouring and the erosion issues. Estimating the amount of the residual energy at the toe of the spillway is essential in the design of the stilling basin in order to know the amount of the energy which needs to be dissipated through it. Chanson (2002) revealed that the steps in stepped spillways can generate a

high level of turbulence; thus, it could greatly enhance the energy dissipation mechanism, which represents the main benefit of using stepped spillways instead of smooth spillways. Because of the momentum transfer between the over-running flow and the recirculating fluid underneath, the energy dissipation takes place over the steps under the skimming flow conditions (Rajaratnam, 1990; Chanson, 2002). It is worth to highlight that the turbulence on stepped spillways generally includes the flow recirculating vortices which grow inside the cavity of each step and the internal transverse jet (Chanson, 1994; André, 2004).

As aforementioned, the present study focuses on the flow feature under the skimming flow conditions and in the non-aerated zone, therefore, the steps located on the upstream side of the inception point have been considered to estimate the residual energy.

Bernoulli's equation has been used to calculate the energy dissipation over gabion stepped spillways. Two points are required to determine the energy dissipation (ΔH):

The first point under consideration located in the non-aerated zone, H should be calculated by using

$$H=y\cos\theta+\frac{\alpha V^2}{2g} \tag{7.6}$$

where

y: the perpendicular depth of the water over a pseudo-bottom, (m)

θ: the bottom chute slope, (degree)

α: the energy coefficient, (unitless)

g: the gravitational acceleration, (m/s^2)

v: average velocity, (m/s)

The energy coefficient for non-uniform velocity distribution over stepped spillways can be estimated from the following expression (Chow, 1959):

$$\alpha\approx\frac{\sum v^3\Delta A}{V^3A}$$

where v is the flow velocity in the velocity distribution corresponding to the incremental area ΔA and A is the flow area. Assuming uniform flow across the channel width, then the area A can be replaced by the flow depth y.

The second point could be in the upstream of the weir or over the crest at the critical section

$$H°=Y° + \frac{V°^2}{2g} \quad (7.7)$$

where

Y°: flow depth above the horizontal surface of the step under consideration, (m)

v°: approach flow velocity, (m/s)

g: the gravitational acceleration, (m/s^2)

or

$$H°=P+Yc+\frac{V_c^2}{2g} \quad (7.8)$$

where

P: distance from the datum to the surface level of the crest (m),

Yc: flow depth above the critical section over the crest, (m)

V_C: critical flow velocity, (m/s)

g: the gravitational acceleration, (m/s^2)

Equation (7.8) can be written as

$H°=P+1.5Yc$

Therefore, the total dissipated energy with respect to the point under consideration is:

$\Delta H=H°-H$

Equations 7.6 to 7.7 have been used to determine the parameters required for evaluating the energy dissipation rates.

In this study, the value of the energy dissipation has been calculated using the point of the critical section in addition to the point at the edge of steps under consideration in the non-aerated zone. Energy coefficient values were changing over the steps in the non-aerated zone depending on the edge step that is chosen for the calculations, which is in good agreement with Meireles and Matos' results (2009).

There are two ways to present the energy dissipation over stepped spillways generally; firstly, by using the residual energy relative to the total flow energy H/H°. Secondly, using the total energy lost relative to the total energy flow ΔH/H°. The second method

ΔH/H° has been selected to estimate the energy dissipation rate along the non-aerated flow zone in the current work. The rate of energy dissipation has been investigated for the non-aerated zone starting where L/Li is equal to 0.13 and ending at the location of the inception point where L/Li=1. L represents the length measured from the downstream edge of the weir to the step under examination and Li is the length to the inception point of air entrainment.

It is worth to emphasise that all the results which will be presented now have been obtained from the computational outcomes. The main objective of this section is to demonstrate the development of the energy along the non-aerated zone over gabion stepped spillways with different values of bottom slopes, step heights, discharges, porosity and particle diameter by calculating the ΔH/H° as mentioned earlier or by obtaining the turbulent kinetic energy for the entire domain of the numerical flume.

Figures 7.17 and 7.18 show the variation of the relative energy dissipation rate ΔH/H° against L/Li on gabion steps with step heights of 0.06m and 0.09m over chute slopes of 1V:2H, 1V:2.5H and 1V:3H respectively, for different unit discharges.

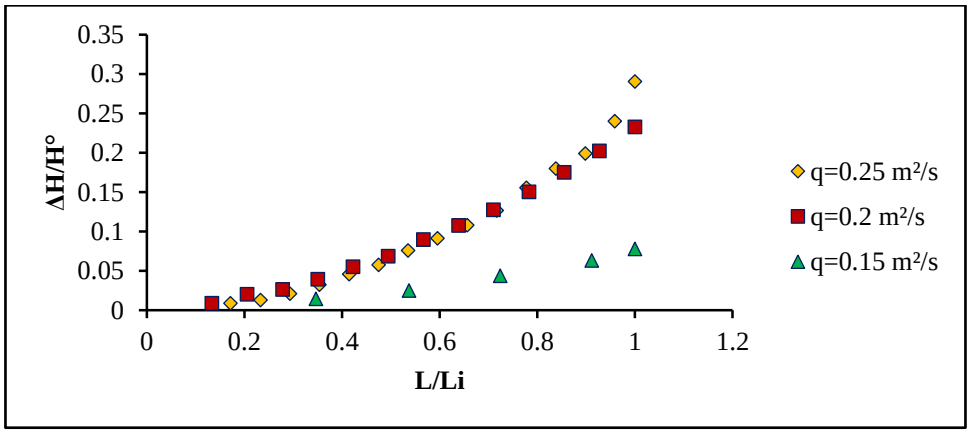

(a)

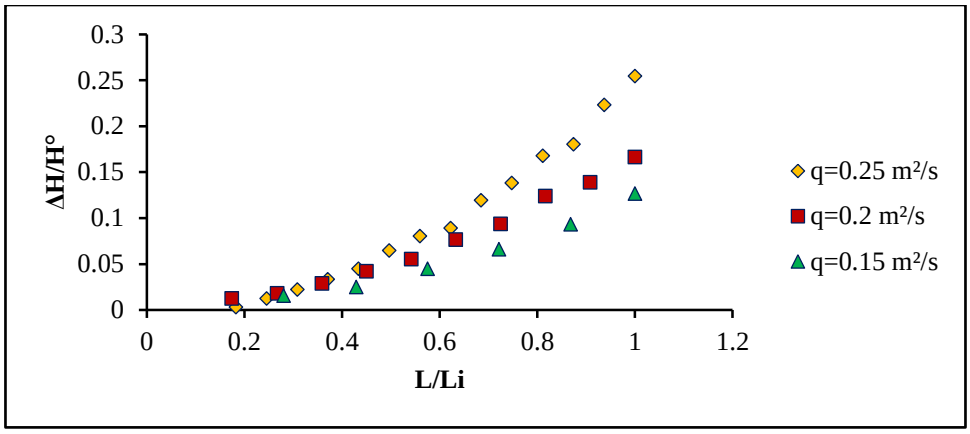

(b)

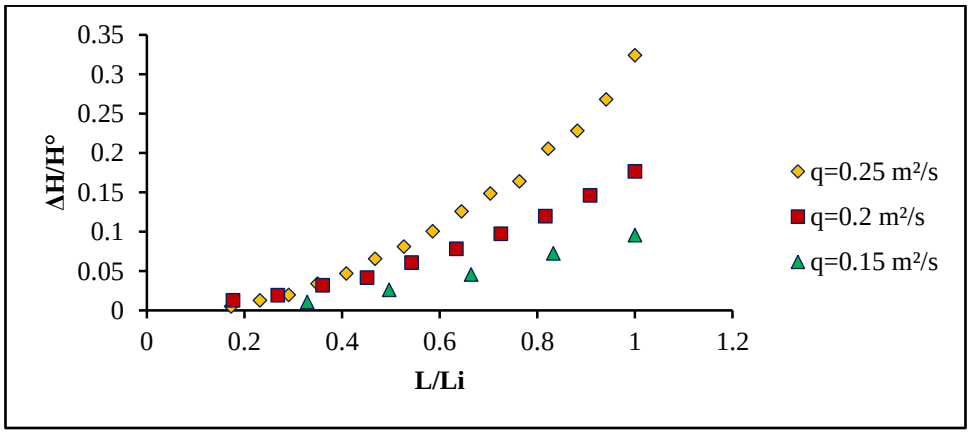

(c)

Figure 7.17 Variation of relative energy loss along the non-aerated flow region of gabion stepped spillways of step height 0.06m for three different discharges with bottom slopes of a)1V:2H, b) 1V:2.5H and c). 1V:3.0H.

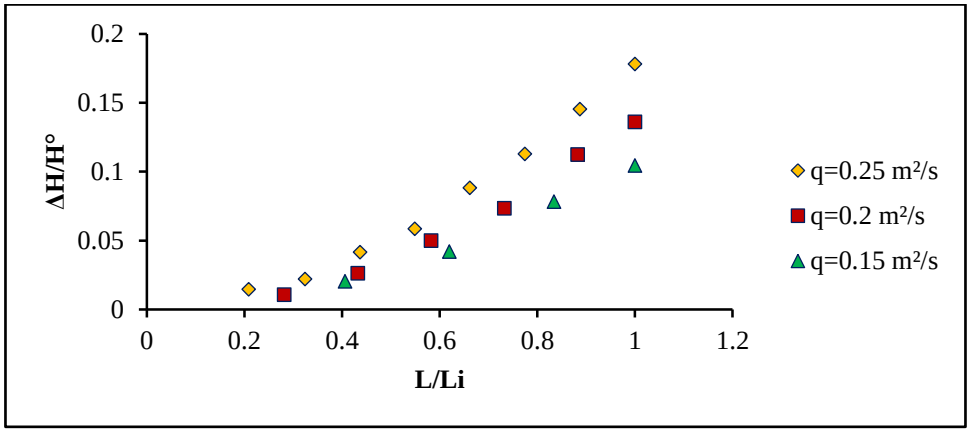

(a)

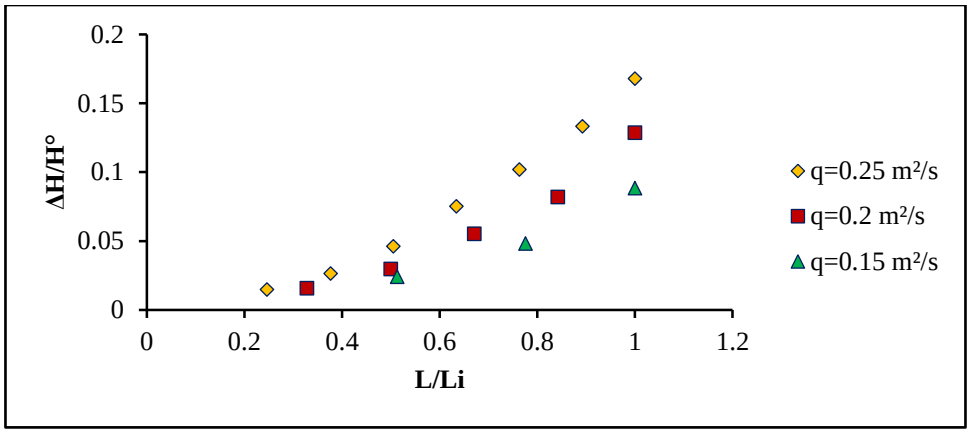

(b)

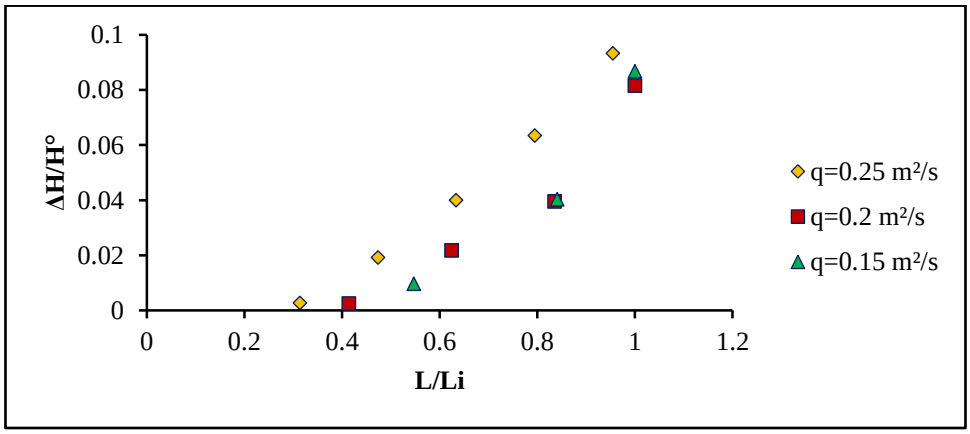

(c)

Figure 7.18 Variation of relative energy loss along the non-aerated flow region of gabion stepped spillways of step height 0.09m for three different discharges with bottom slopes of a)1V:2H, b) 1V:2.5H and c). 1V:3.0H.

It can be clearly seen from both figures that the rate of the relative energy dissipation has a direct relationship with discharges; therefore, when the discharge increases more energy dissipation will be expected. Also, for all discharges and chute slopes, the rate of energy dissipation is quite small at the steps close to the weir crest and then gradually increases downward, reaching its peak value at the inception point.

To study the effect of step heights on the energy dissipation over gabion stepped spillways, Figure 7.19 has plotted ΔH/H° versus L/Li for gabion stepped spillways of q=0.2m^2/s unit discharge for three bottom slopes of 1V:2H, 1V:2.5H and 1V:3.0H. The

results revealed that the energy dissipation rate has increased when the number of the steps increased. In other words, decrease the step height will increase the rate of the energy dissipation over gabion stepped spillways. Having more steps can increase the turbulence over the steps; thus, the energy dissipation will increase significantly. This result is in agreement with some previous studies such as Hunt and Kadavy (2009), Nohani et al. (2015), Karami (2012) and Felder and Chanson (2011). However, some previous studies such as Mohammad Rezapour Tabari and Tavakoli (2016), Ahadian and Aghamajidi (2014), Ab Ghani et al. (2010) and Patil and Jadhav (2017) found that increasing the number of the steps will reduce the energy dissipation.

It is worth to mention that Hunt and Kadavy (2009) obtained for a specific discharge that the relationship between the energy dissipation and the step heights could change over the steps. For instance, 38mm step height showed high energy dissipation compared to 76mm step height up to 3m over the steps, then, from 3.5m to 6m, 76mm step height showed better results. As a result of that, another way has been used to evaluate the energy dissipation over the steps with different steps height by using the Turbulent Kinetic Energy for the entire flume of the numerical model. Different runs have been conducted for three different slopes 1V:2H, 1V:2.5H and 1V:3H with the same initial conditions in order to examine the effect of the step height and the number of the steps on the energy dissipation over gabion stepped spillways.

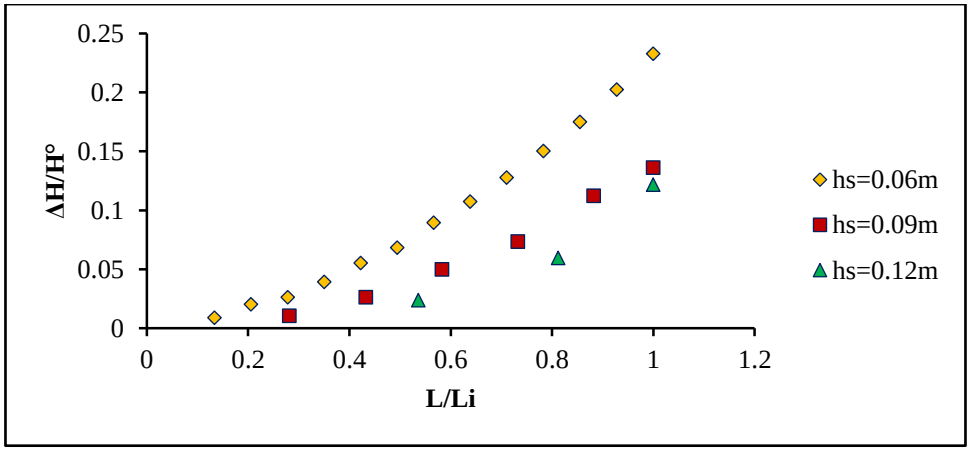

(a)

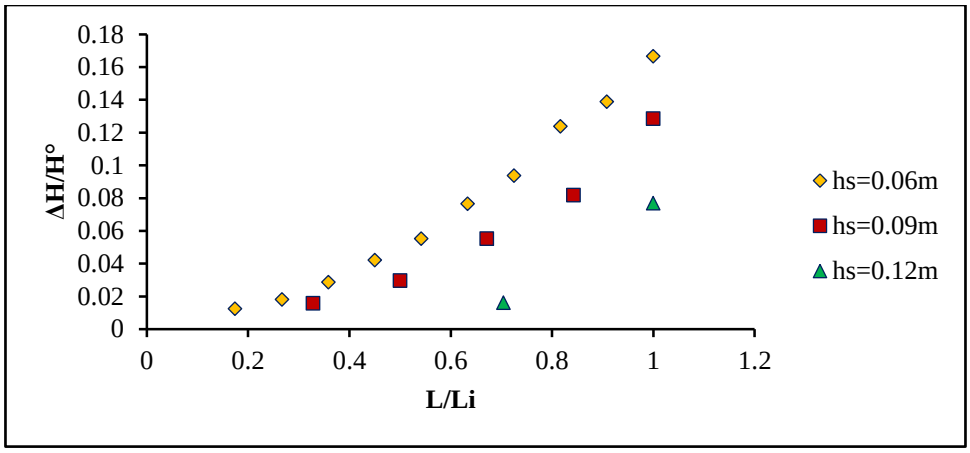

(b)

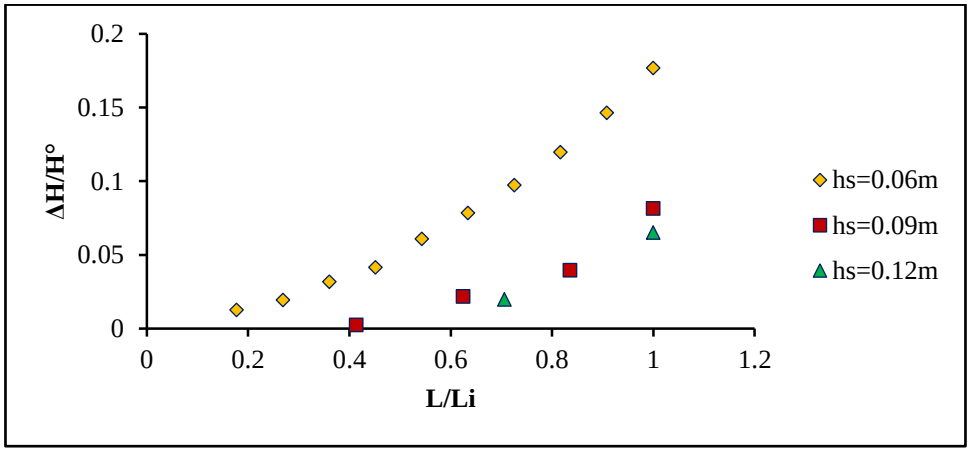

(c)

Figure 7.19 Variation of relative energy loss along the non-aerated flow region of gabion stepped spillways of q=0.2m^2/s unit discharge for bottom slopes of a) 1V:2H, b) 1V:2.5H and c). 1V:3.0H.

The results in Figure 7.20 showed that increasing the step heights increases the energy dissipation over gabion stepped spillways; this is opposite to the results from using Bernoulli's equation. It is obvious that there are many assumptions in the derivation of Bernoulli's equation such as the friction of the viscous forces is assumed to be negligible. Bernoulli's equation generally can be used for the steady and laminar flow and is valid with a streamline only, just between two points as different streamlines could probably have different Bernoulli's constant. However, TKE has been calculated by using Reynolds-averaged Navier Stokes equations which can take into account the viscosity, density, pressure and velocity with respect to time and space, in addition to include the

turbulence effect by using the k-ε model as mentioned in Chapter 3. It important to highlight that the rate of the energy dissipation in Figure 7.19 has been calculated using Bernoulli's equation and just over the edges of the steps which are located in the non-aerated zone, however in Figure 7.20, the TKE was estimated for all the numerical flume including the aerated zone as well, therefore, differences in the results would be expected. It is worth to highligth that using small step heights will increase the number of the steps. Moreover, considering an infinite number of infinitely small steps would produce stepped spillways similar to smooth spillways. The studies in Chapter 2 showed that stepped spillways can dissipate more energy than smooth spillways. Therefore, this is an indication that the result of the TKE more accurate compared to the Bernoulli's equation. This could be due to the assumptions in the derivation of Bernoulli's equation.

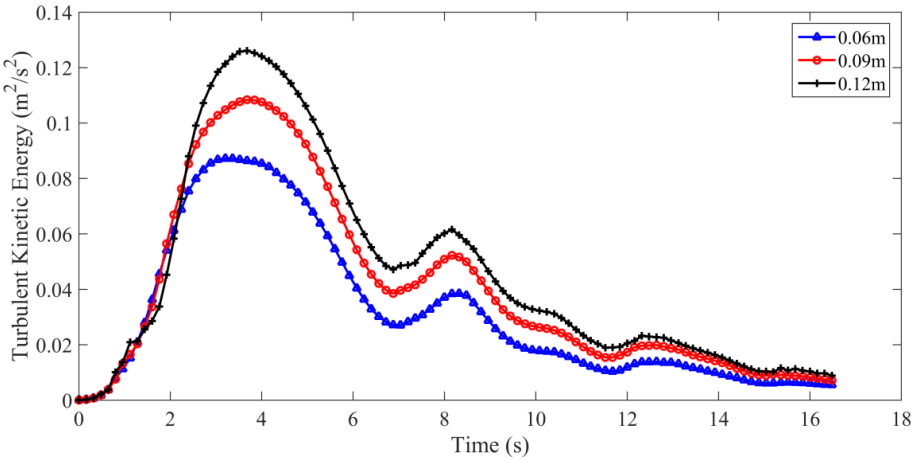

(a)

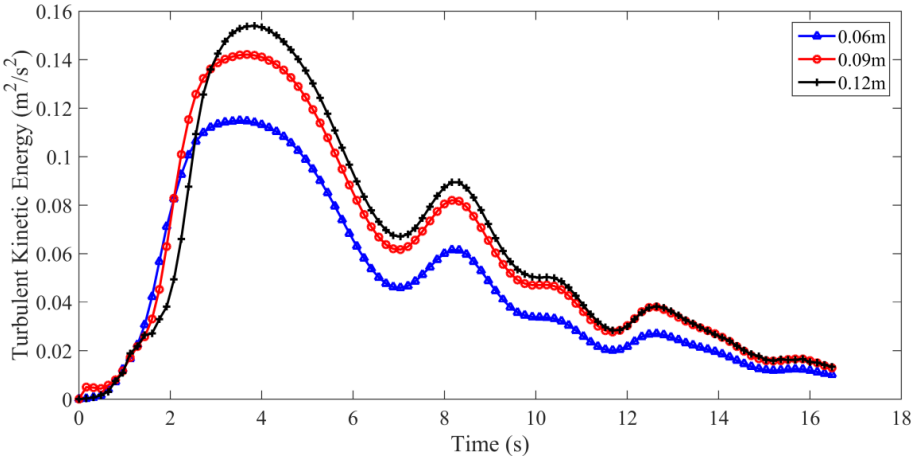

(b)

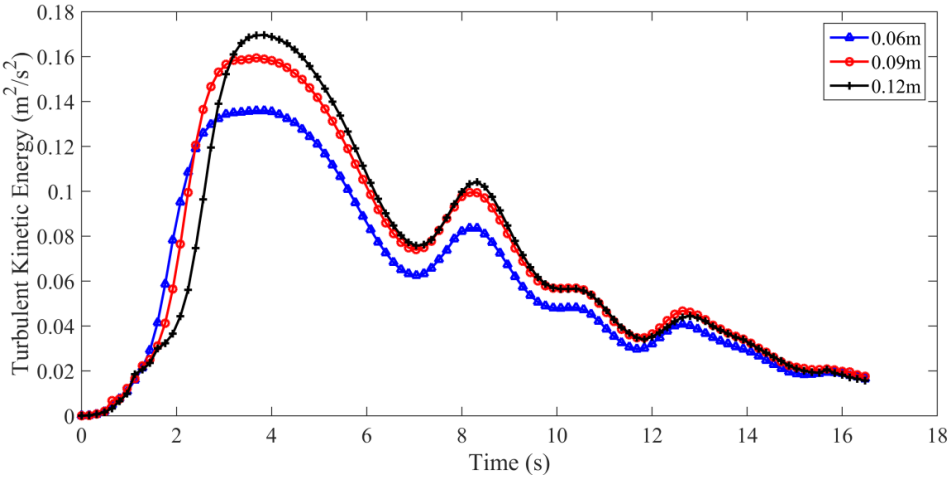

(c)

Figure 7.20 Variation of TKE along the whole domain of the flume of gabion stepped spillway for different step heights with bottom chute slopes of a) 1V:2H, b) 1V:2.5H and c) 1V:3.0H.

Figures 7.21 and 7.22 investigate the rate of energy dissipation over gabion stepped spillways when the slope of the bottom chutes variation with the same step height. The results have revealed that it is pretty hard to come up with one conclusion for all the cases as the performance of the energy dissipation keeps varying for every single case. For instance, as can be noted from Figure 7.21, when the step height equals 0.06m, 1V:3H slope has given the best results while the discharge equals to 0.25m^2/s. However, 1V:2.5H and 1V:2.0H have performed well when the discharge equals to 0.2m^2/s and 0.15m^2/s respectively.

On the other hand, the results were consistent when the step height set up to 0.09m as the 1V:2.0H slope has exposed the best results in terms of energy dissipation for the values of the tested discharges. This result has agreed with the outcome of Chinnarasri et al. (2008), however, it has not matched with the result of Peyras et al. (1992) who stated that although there are no significant changes in the energy dissipation rate, 1V:3.0H has shown better results compared to 1V:2.0H. Moreover, according to Salmasi et al. (2012), the energy dissipation rate might increase when the slope of gabion stepped spillways decreases which are opposite to the finding of Chinnarasri et al. (2008).

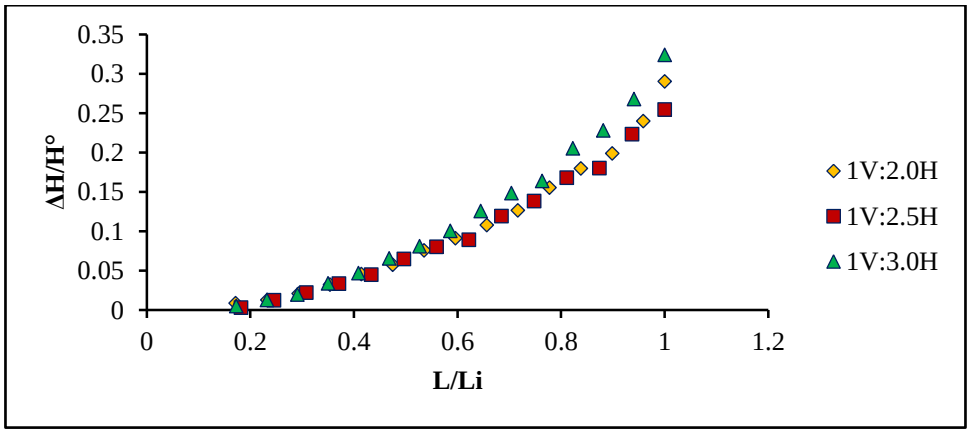

(a)

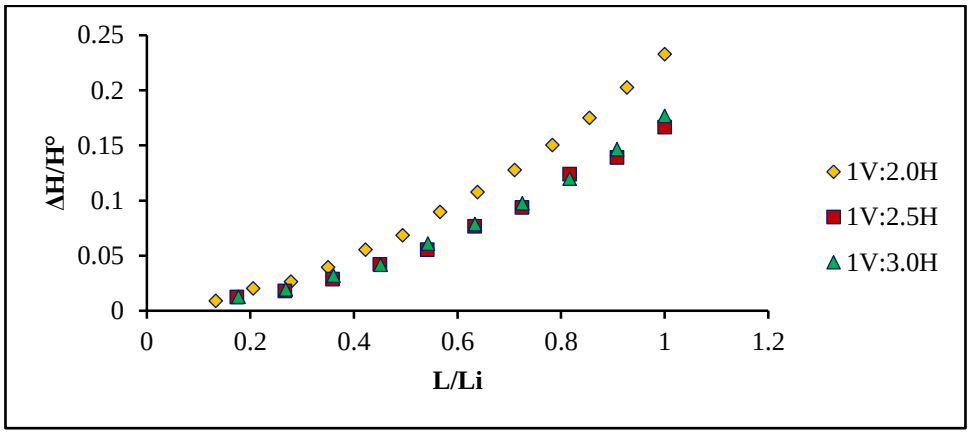

(b)

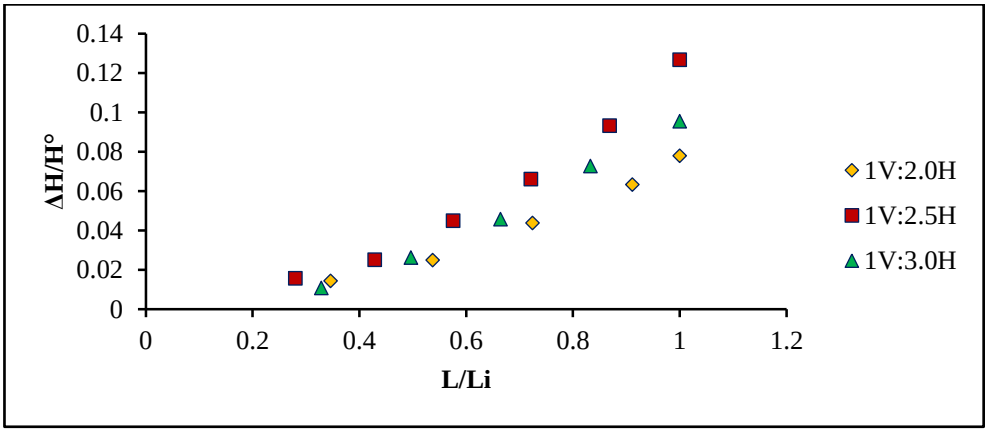

(c)

Figure 7.21 Variation of relative energy loss along the non-aerated flow region of gabion stepped spillways of step height 0.06m for different bottom slopes with unit discharges of a) $q=0.25m^2/s$, b) $q=0.2m^2/s$ and c). $q=0.15m^2/s$.

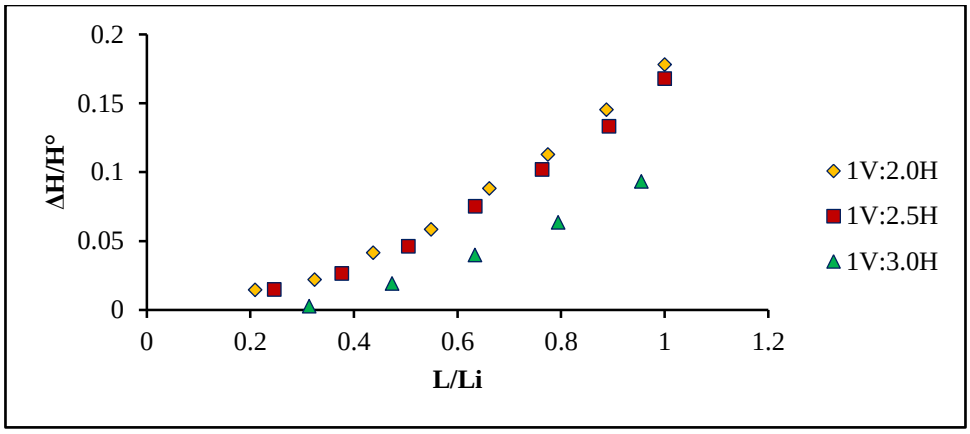

(a)

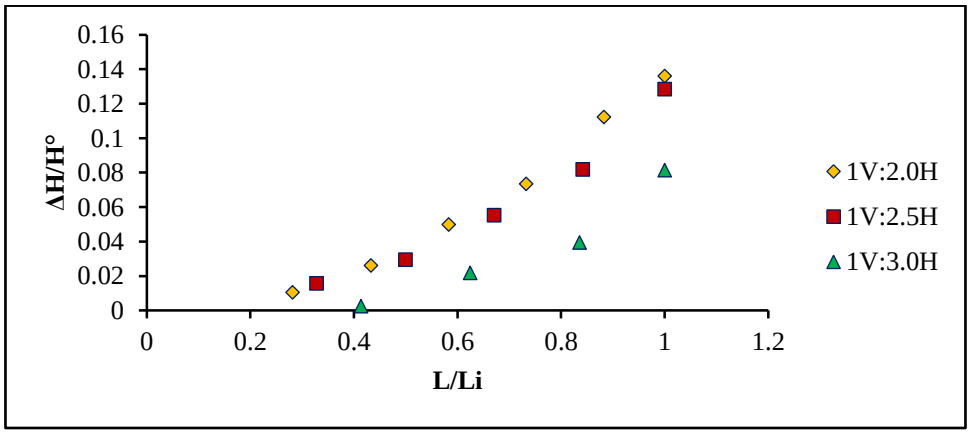

(b)

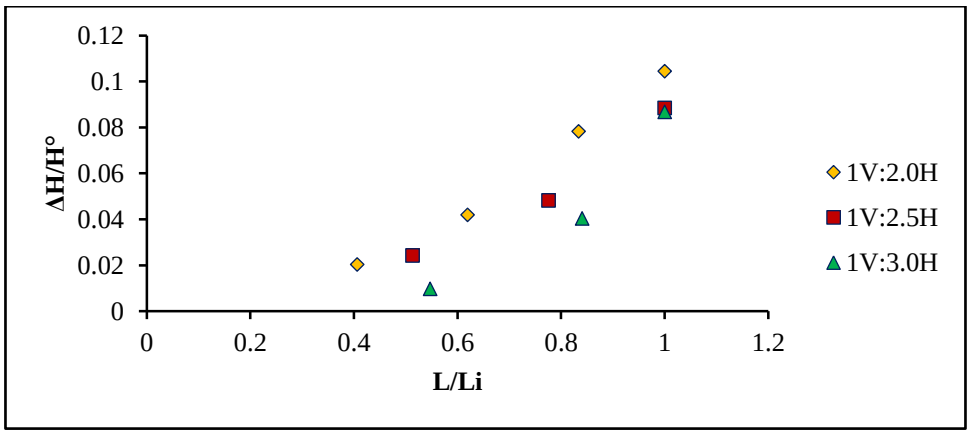

(c)

Figure 7.22 Variation of relative energy loss along the non-aerated flow region of gabion stepped spillways of step height 0.09m for different bottom slopes with unit discharges of a) $q=0.25m^2/s$, b) $q=0.2m^2/s$ and c). $q=0.15m^2/s$.

As a result of the disagreement between the previous papers, another evaluation was conducted to test the rate of the energy dissipation with different values of bottom chute slopes and step heights by using the Turbulent Kinetic Energy for the entire flume of the numerical model as mentioned earlier. Figure 7.23 shows the TKE of three-step heights 0.06m, 0.09m and 0.12m with three bottom chute slopes 1V:2H, 1V:2.5H and 1V:3H.

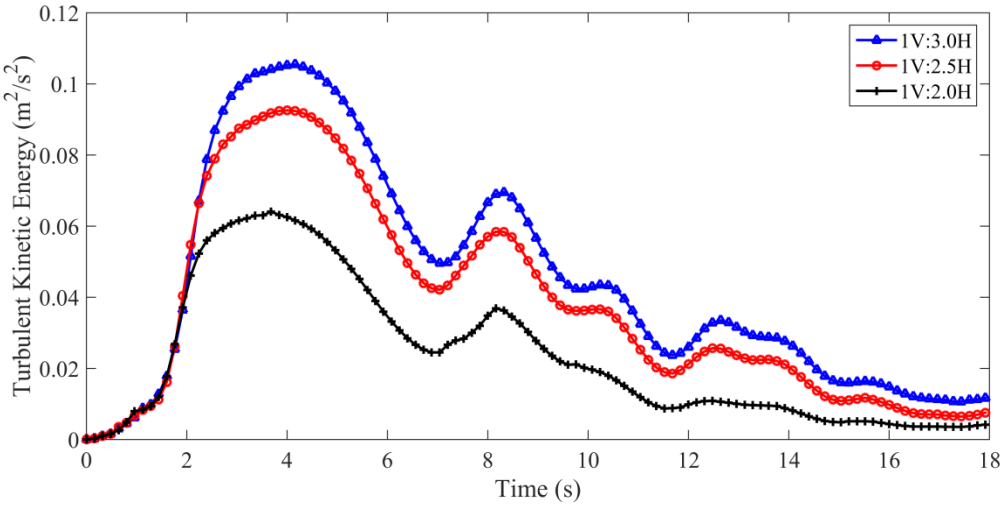

(a)

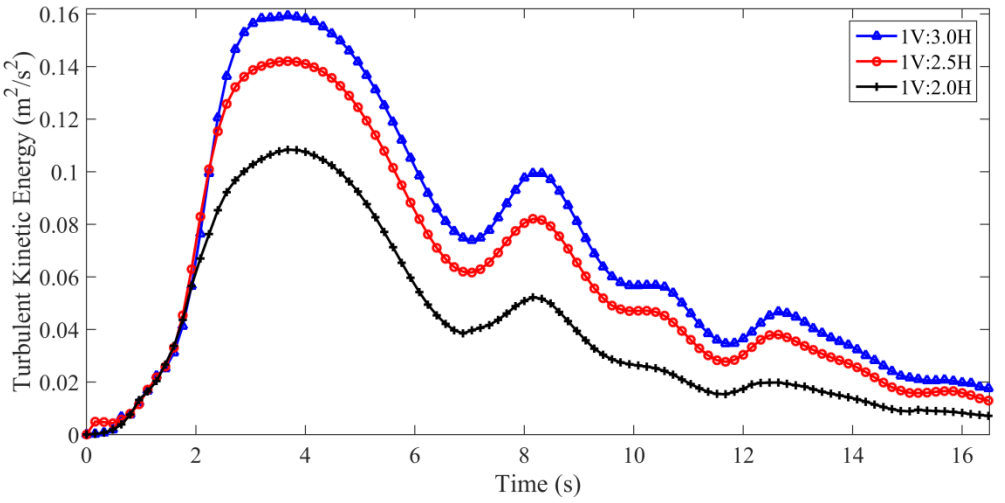

(b)

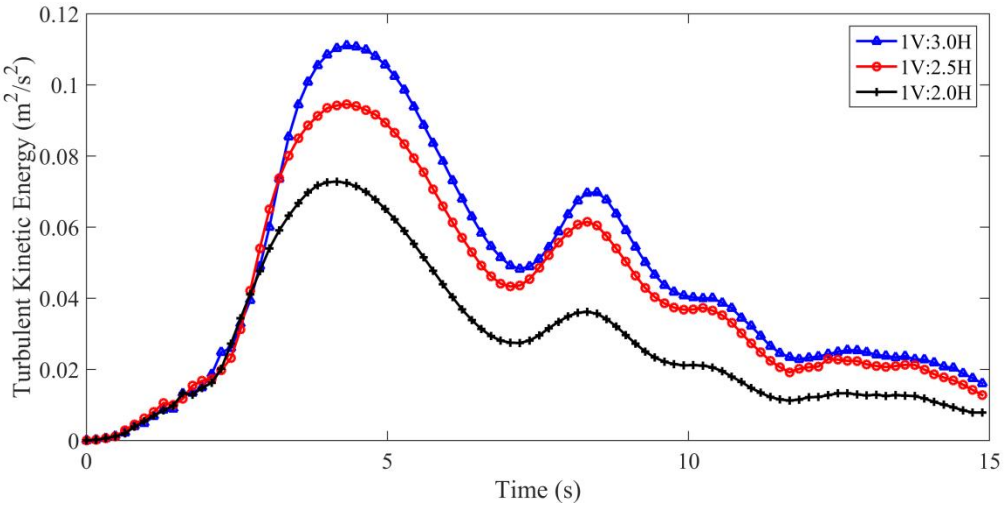

(c)

Figure 7.23 Variation of TKE along the whole domain of the flume of gabion stepped spillway for different bottom slopes with step heights of a) 0.06m, b) 0.09m and c) 0.12m.

The TKE results indicated that flat slopes can give better results compared to steep slopes for all the step heights which are opposite the finding of using Bernoulli's equation. It is very important to emphasise that the reasons for getting different results are the same which mentioned earlier in the step height investigation, which is mainly belong to how the energy dissipation is calculated and therefore discrepancies in the results would be expected. Following the result of the energy dissipation rate over different step heights which is revealed that TKE can give more accurate results compared to Bernoulli's equation results, the results of the TKE have been used as an outcome for this investigation. Therefore, flat slopes have the ability to dissipate more energy over the gabion steps compared to steep slopes.

In order to study the effect of the porosity and particle sizes on the rate of the energy dissipation, the TKE was plotted for three different chute slopes with 0.12m step height (Figures 7.24 and 7.25). The results indicated that the rate of energy dissipation increase when both porosity and particle sizes decrease. This is due to water flow as the flow needs more energy to seep between and inside the particles when the particle sizes and porosity are relatively small, thus that can lead to more dissipation in the energy rate.

Although the finding is counterintuitive, it is in agreement with the results of Wüthrich and Chanson (2014) which mentioned in Chapter 2. These results showed that under specific conditions normal stepped spillways can dissipate more energy compared to gabion stepped spillways; therefore, reducing the porosity and the particle size of the gabion has shown the best performance in terms of energy dissipation rates. It is important to mention that no significant changes in the rate of energy dissipation can be observed when both porosity and particle sizes change, which is also in agreement with the results of Chinnarasri et al. (2008).

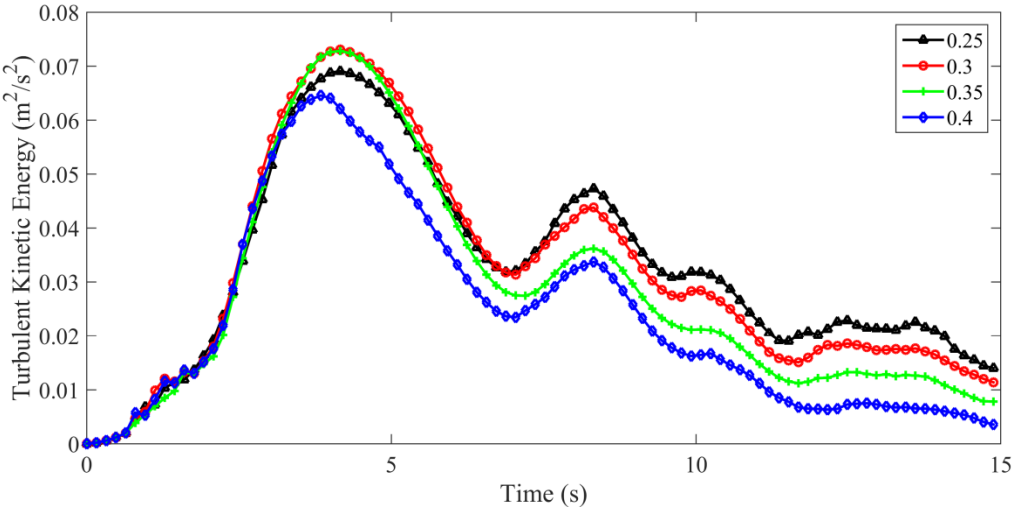

(a)

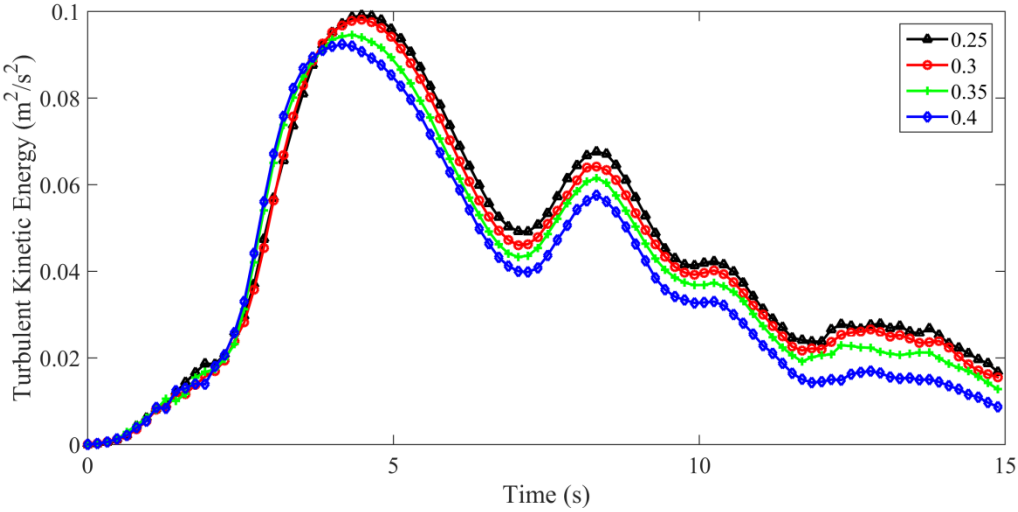

(b)

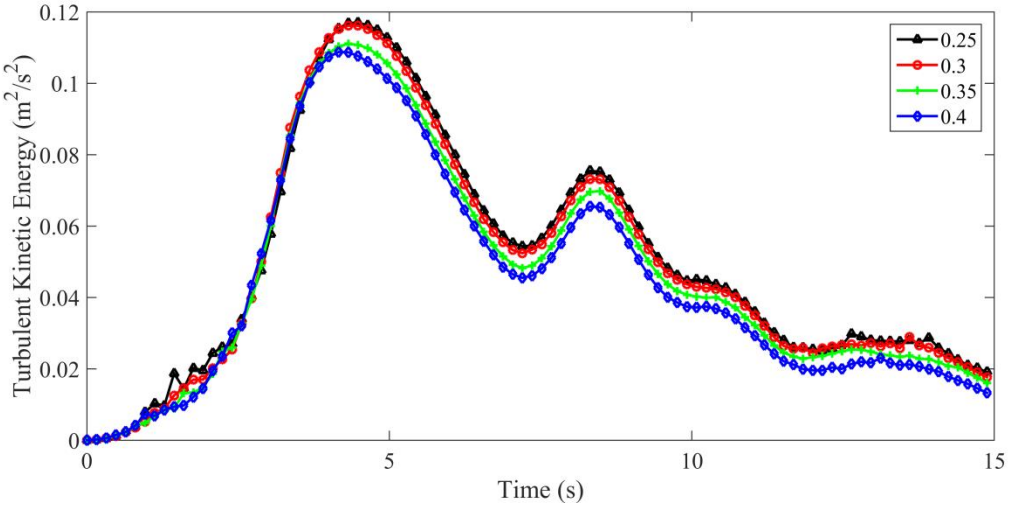

(c)

Figure 7.24 Variation of TKE along the whole domain of the flume with gabion stepped spillway of 0.12m step height for different porosities with bottom slopes of a) 1V:2H, b) 1V:2.5H and c) 1V:3H.

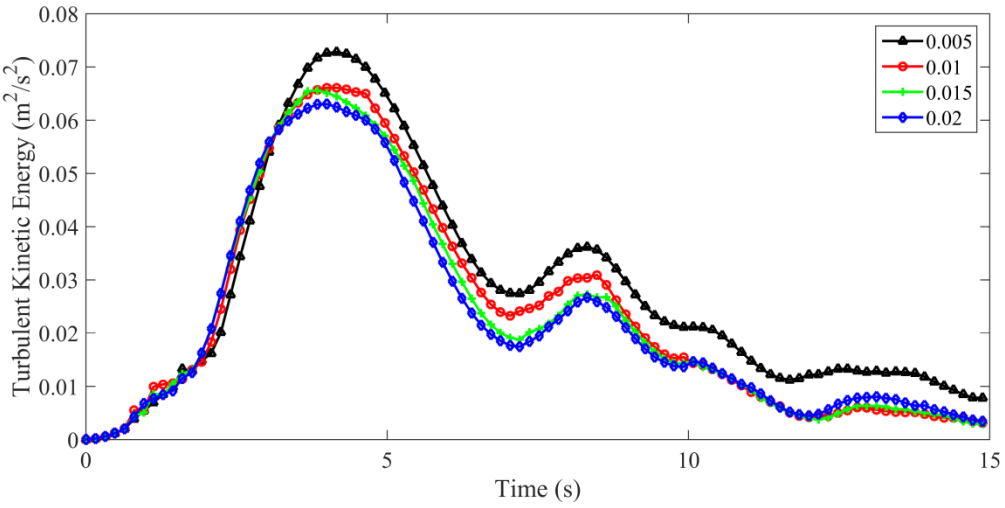

(a)

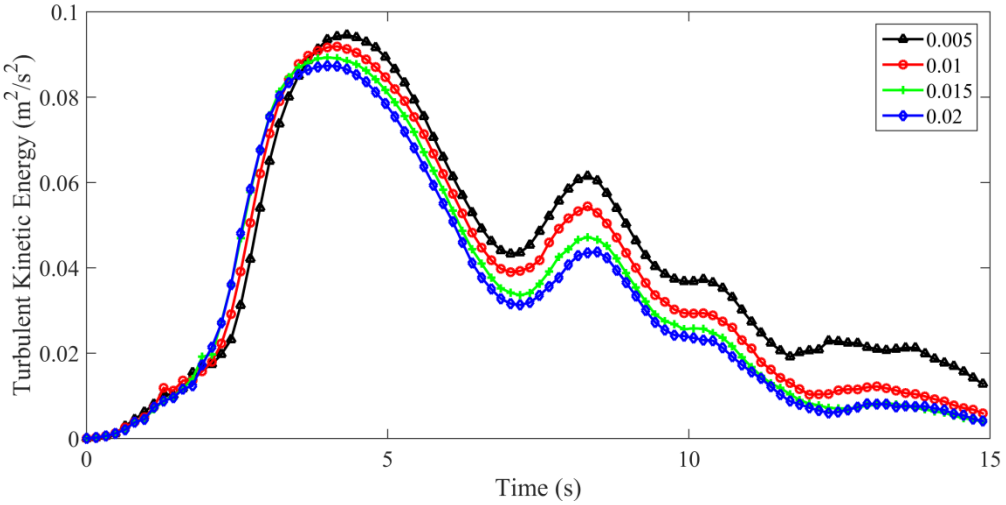

(b)

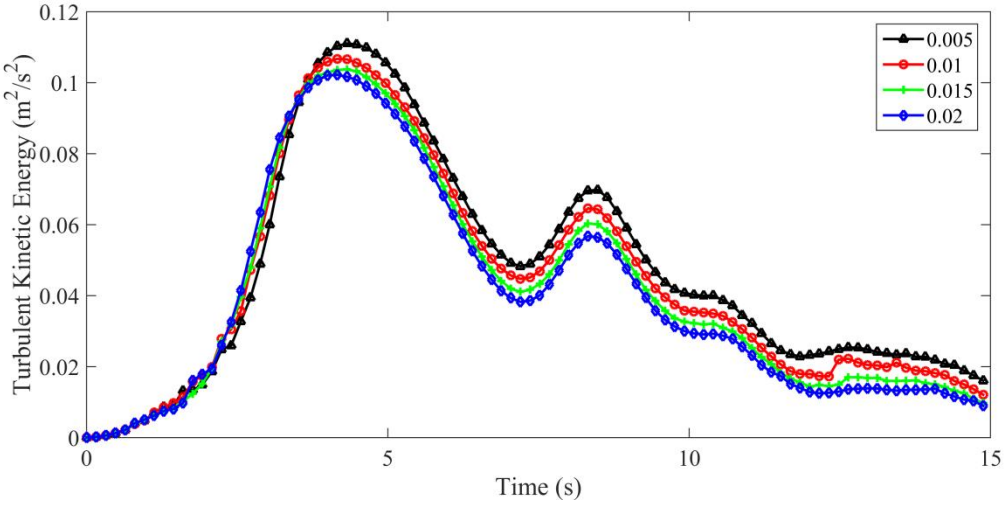

(c)

Figure 7.25 Variation of TKE along the whole domain of the flume with gabion stepped spillway of 0.12m step height for different particle sizes (m) with bottom slopes of a) 1V:2H, b) 1V:2.5H and c) 1V:3H.

In the present work, a new empirical equation has been suggested in order to estimate the energy coefficient in the non-aerated zone over gabion stepped spillways. The energy coefficient can be estimated based on velocity profiles of the computational results. This coefficient was computed as a function of L/Li as proposed by Meireles (2011), Meireles's Equation has been modified to develop a new equation for gabion stepped spillways as shown below

$$\alpha = 1 + (0.142 * \frac{L}{Li}^{0.3845}) \quad (7.9)$$

Around 10% of the data has been selected to assess the equation, while 90% of the data has been used to find the coefficient of the equation. The results showed that Equation 7.9 has the capability to show the development of the energy coefficient in the non-aerated zone over gabion stepped spillways with good accuracy as R^2 value is equal to 0.8312 (Figure 7.26). This equation is valid for gabion stepped spillways with chute bottom slopes of 1V:2H, 1V:2.5H and 1V:3H and for $0.832 \leq Yc/hs \leq 3.08$ and $0.13 \leq L/Li \leq 1.0$.

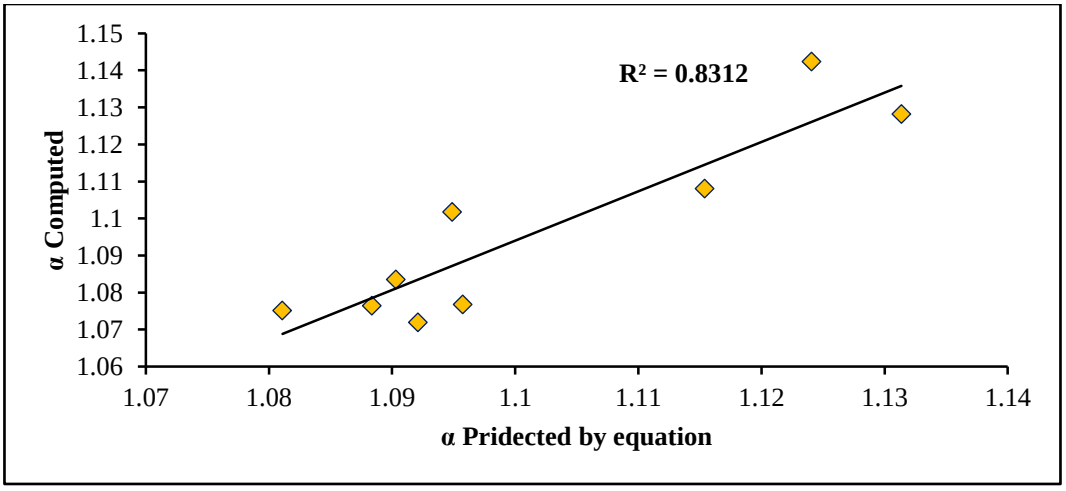

Figure 7.26 Comparison of Equation 7.9 to numerical data.

A comparison was conducted against another empirical correlation which is found by Meireles (2011). The main aim of this comparison is to check whether the empirical correlation which is established for the normal stepped spillways has the ability to find the values of the energy coefficient over gabion stepped spillways.

$$\alpha = 1 + (0.119 * (\frac{L}{Li})^{0.296}) \quad \text{Meireles (2011)} \quad (7.10)$$

The results showed that Meireles's equation has the ability to describe the energy coefficient for the steps which are close to the weir edge; however, this ability has reduced towards the location of the inception point (Figure 7.27).

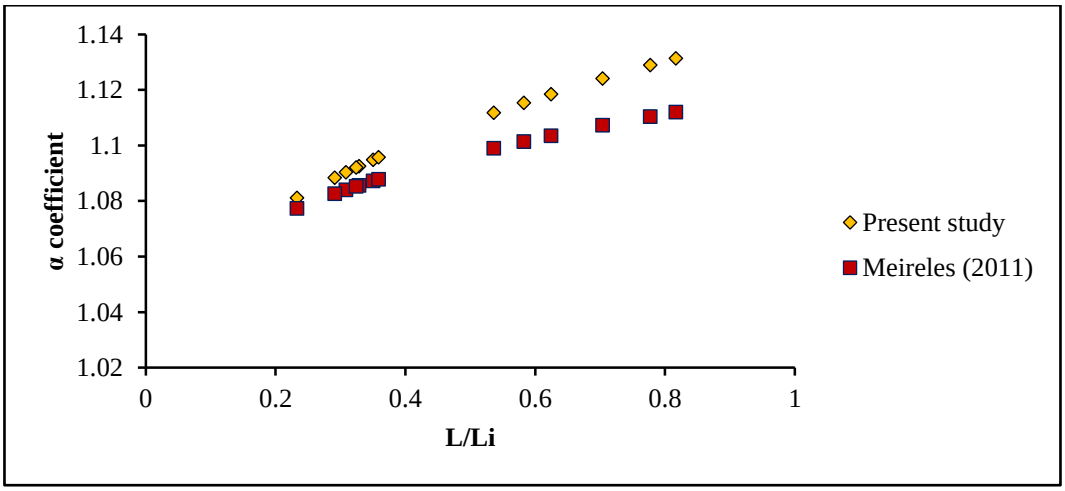

Figure 7.27 Comparison of Equation 7.9 to Equation 7.10.

Following Meireles and Matos (2009) a linear regression has established to find out the relationship between the relative energy loss ΔH/H° at the outer edge of steps situated in the non-aerated flow region over gabion stepped spillways, and the normalized distance between the downstream corner of the weir and the step under consideration, L/Li , as follows

$$\frac{\Delta H}{H^{\circ}} = A\frac{L}{Li} \qquad (7.11)$$

Meireles and Matos (2009) and Hunt and Kadavy (2010) showed that the value of A on chute slope of 1V:2H and 1V:4H of normal stepped spillways equal to 0.2 and 0.3 respectively. Moreover, Husain (2013) showed that the value of A is 0.23 based on the computational results.

In the present work, the results exposed that the value of A equals to 0.1418. The same procedure, which was used before to find equations, has also been applied in this part; therefore 10% of the data has been selected to test the equation and 90% of the data to find it (Figure 7.28). This equation is applicable for gabion stepped spillways of 0.06m, 0.09m and 0.12m step heights, with chute bottom slopes of 1V:2H, 1V:2.5H and 1V:3H and for $0.832 \leq Yc/hs \leq 3.08$ and $0.13 \leq L/Li \leq 1.0$.

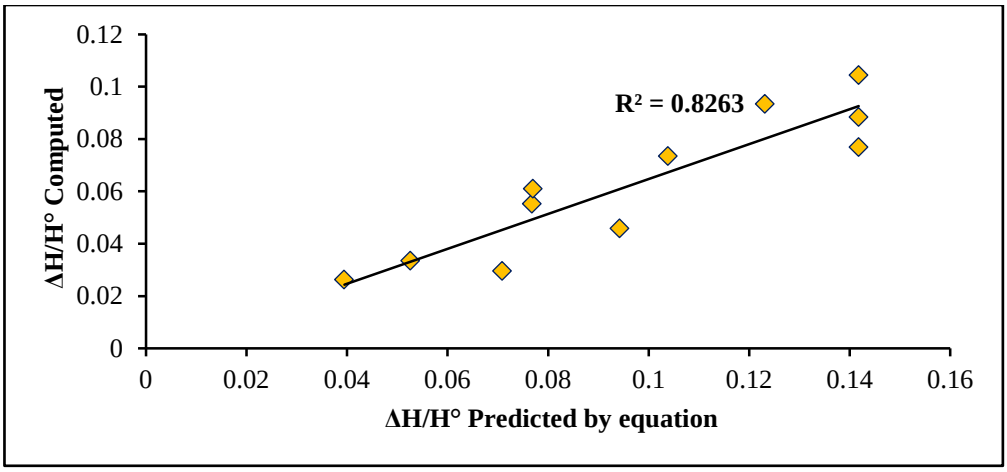

Figure 7.28 Comparison of Equation 7.11 to numerical data.

In Figure 7.29, a comparison has been made with the work of Meireles and Matos (2009), Hunt and Kadavy (2010) and Husain (2013), in order to investigate the trend of the energy dissipation over gabion stepped spillways and then compare it with normal stepped spillways. The results showed that gabion stepped spillways have the lowest rate of energy dissipation under the skimming flow condition. Although the finding is counterintuitive, it is in agreement with the results of Wüthrich and Chanson (2014) which mentioned in Chapter 2.

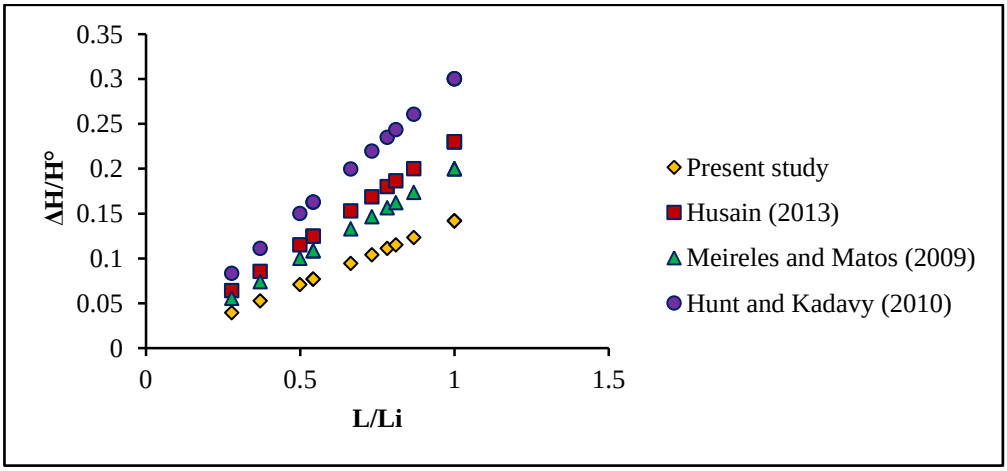

Figure 7.29 A comparison between the correlation of the present work with different previous equations.

Finally, it might be useful to demonstrate the turbulence intensity (k) distribution over horizontal and vertical faces of the gabion steps in the non-aerated zone in order to observe the position of the maximum and the minimum value of the intensity turbulence (Figure 7.30). As can be seen in Figure 7.31, the turbulence intensity values increase towards the location of the inception point. The maximum value of the turbulence intensity is observed between 10-35% distances from the inner side of each step. However, the minimum value is always at the outer edges of steps. Furthermore, Figure 7.32 shows the turbulence intensity distribution over the vertical faces of the gabion steps along the non-aerated zone. The maximum value of the turbulence intensity over the vertical faces located between 5-20% of the step height measured from the gabion horizontal face. At the outer edge of the vertical faces, the minimum values of the turbulence intensity could always be observed as a result of the vorticities which normally present at the corner area between the horizontal and the vertical faces of steps. Therefore, increasing the size and the power of the vorticities could lead to an increase in the turbulence intensity.

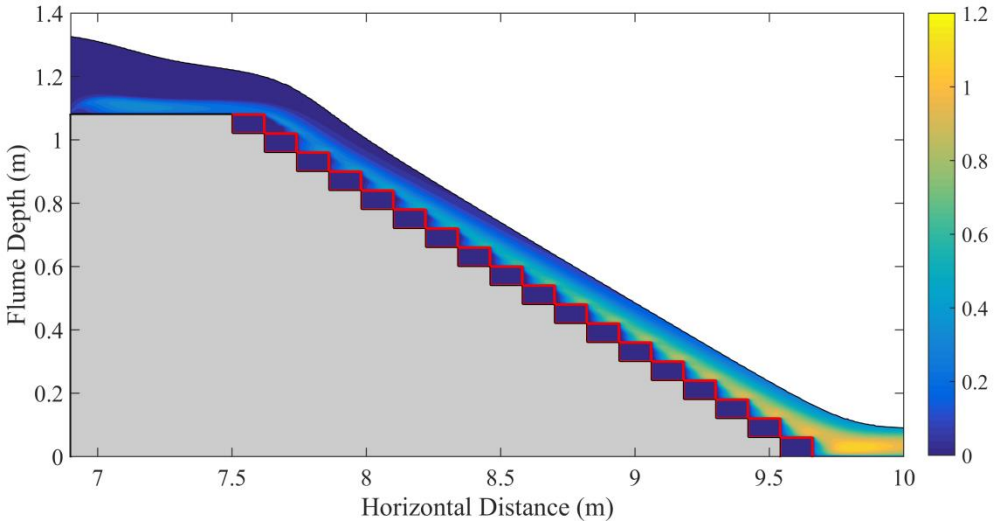

Figure 7.30 Turbulence intensity distribution along gabion stepped spillways with a step height of 0.06m and chute slope of 1V:2H for q=0.25m^2/s.

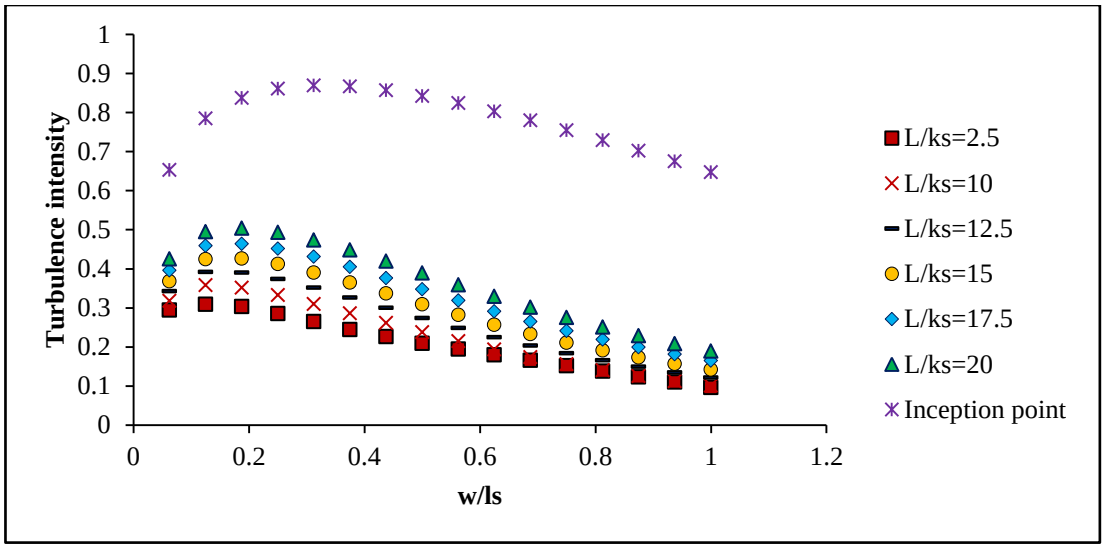

Figure 7.31 Turbulence intensity distribution along the horizontal gabion faces of step height 0.06m on chute slope of 1V:2H for q=0.25m^2/s.

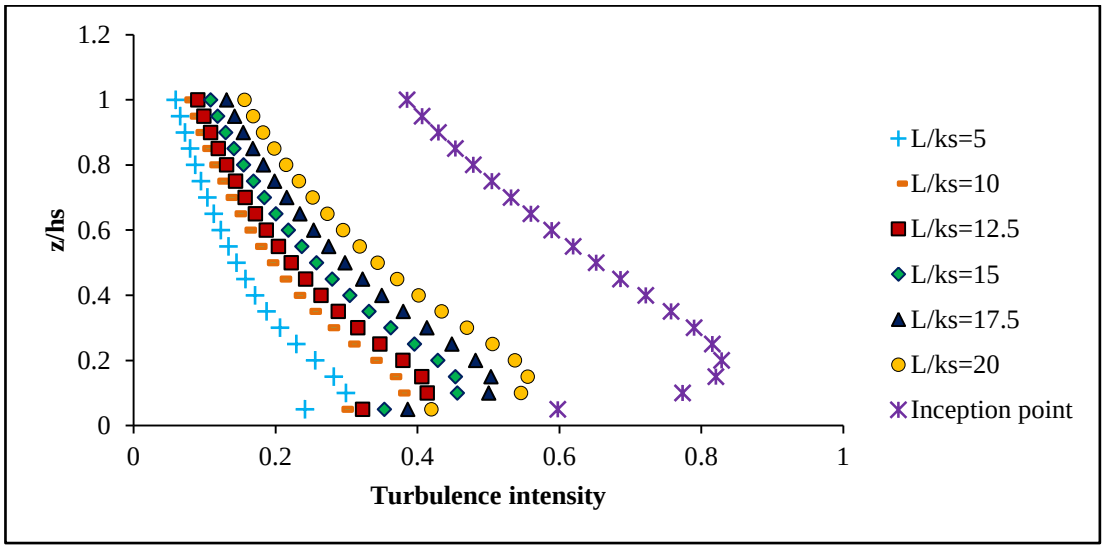

Figure 7.32 Turbulence intensity distribution along the vertical gabion faces of step height 0.06m on chute slope of 1V:2H for q=0.25m^2/s.

To summarise, the computational results showed that the energy dissipation rate can be influenced by many parameters like the step heights and the chute slopes. Pressure distributions over the vertical and the horizontal faces will be investigated in the next chapter. Also the cavitation damage in the non-aerated zone will be examined by using the cavitation index.

Chapter 8 : Results and Discussion of Pressure Distribution and Cavitation Damage

8.1. Introduction

Pressure distribution can be considered as one of the important parameters which can play a significant role in the design of the hydraulic structures. This is due to the formation of cavitation which represents the main concern for flows; especially for turbulent flows; cavitation can be achieved when the flow velocity is slightly high. The occurrence of the cavitation over stepped spillways is related to the pressure values over the steps as the pressure could drop to or below the vapour water pressure (Amador et al., 2006). According to Peterka (1953), the presence of air in the flow over stepped spillways between 5%-8% could mitigate the risk of having cavitation over the steps. Therefore, the risk of cavitation mainly occurs in non-aerated zones where the air is absent. The risk after the inception point would be low as the air starts to enter the flow naturally through the process of the self-aeration.

To summarise, the non-aerated regime is potentially at the risk of cavitation more than the aerated zone. This is essential because of two reasons:

- The flow velocity approaching its peak near to the location of the inception point so as a result of that, the pressure can fall to the lowest value.
- The air could insufficiently occur or be completely absent in the non-aerated zone.

It has been cited that there is a strong link between the location of the inception point, pressure values and cavitation damage over stepped spillways (Husain et al., 2013). As a result, all parameters which have been established as important parameters on the location of the inception point need to be considered in this section. This is due to their connections with the pressure and cavitation damage. In some cases, it may be observed

that all the steps located in the non-aerated zone, so damage can happen during high flood events when the discharge is extremely high.

The main objectives of this chapter are:

- Investigate the pressure distribution over the horizontal and vertical faces of steps over the gabion stepped spillways.
- Determine whether the cavitation damage can occur over gabion steps using the calculation of the cavitation index.

8.2. Pressure distribution

This section presents and discusses the characteristics of the pressure variation over the vertical and horizontal faces of gabion steps situated in the non-aerated zone under the skimming flow conditions. It also focuses on the effects of the step geometry and chute slope on the pressure behaviour. It is worth to mention that the investigation of the pressure distribution has been conducted for different values of step heights, chute slopes, porosity and particle sizes as mentioned in Table 5.1.

Figure 8.1 shows the pressure evolution over the non-aerated zone on the gabion steps of height 0.06m with three chute slopes of 1V:2H, 1V:2.5H and 1V:3H which are examined when the unit discharge equal to $q=0.25m^2/s$. Figure 8.2 displays the pressure field over the non-aerated zone of gabion stepped spillways of three different step heights over a chute slope of 1V:2H for flow rates of $q=0.2m^2/s$. As can be seen in these figures, smooth pressure flow fields have been detected by observing the computational results over gabion stepped spillways. This indicates that the pressure pattern is qualitatively similar, even though the dimensions of steps are different. However, the peak values of the pressure distribution are different, and they might be more sensitive to the many parameters such as the flow rates, chute slopes and step heights.

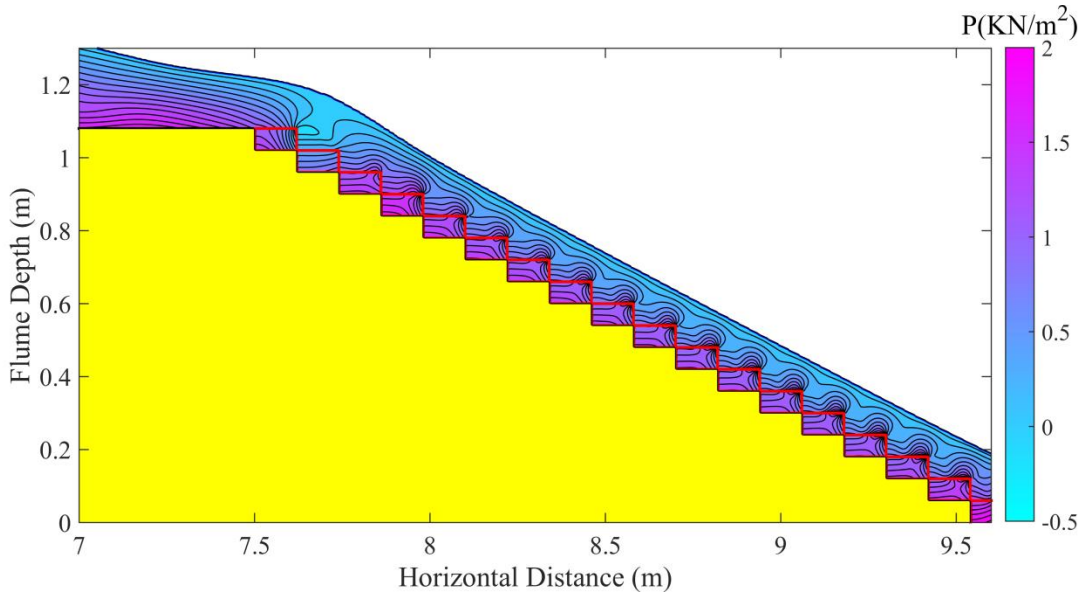
P(KN/m2)
Flume Depth (m)
Horizontal Distance (m)
1.2
1
0.8
0.6
0.4
0.2
0
7
7.5
8
8.5
9
9.5
2
1.5
1
0.5
0
-0.5

(a)

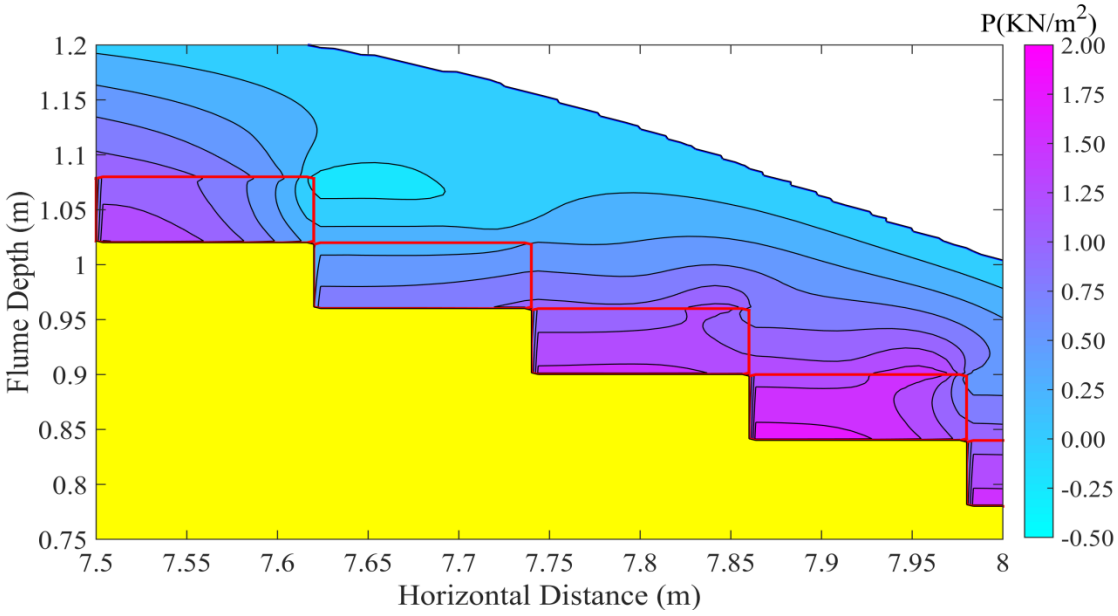
P(KN/m2)
Flume Depth (m)
Horizontal Distance (m)
1.2
1.15
1.1
1.05
1
0.95
0.9
0.85
0.8
0.75
7.5
7.55
7.6
7.65
7.7
7.75
7.8
7.85
7.9
7.95
8
2.00
1.75
1.50
1.25
1.00
0.75
0.50
0.25
0.00
-0.25
-0.50

(b)

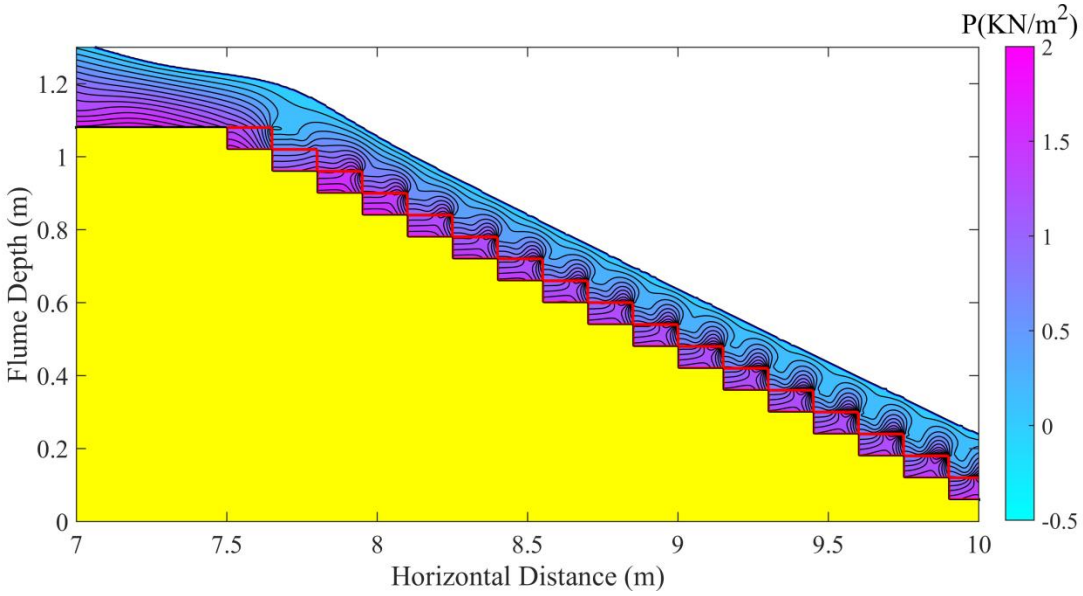

(c)

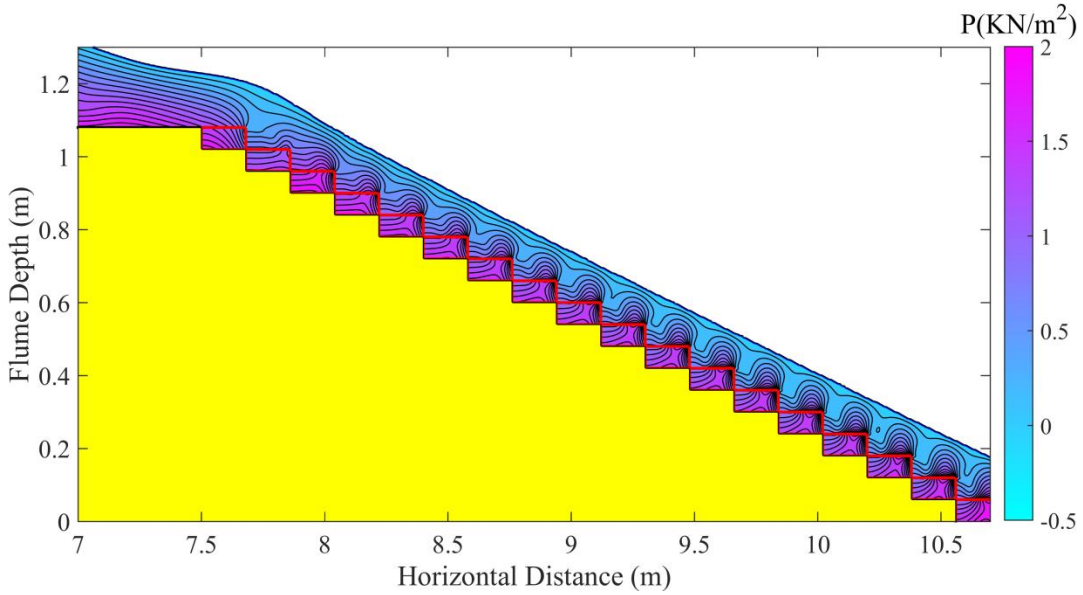

(d)

Figure 8.1 Pressure flow field along the non-aerated flow region for a unit discharge of $q=0.25m^2/s$, over gabion stepped spillways using steps with height 0.06m and slope of a) 1V:2H, b) zoom in at the first three steps of slope 1V:2H c) 1V:2.5H and d) 1V:3H.

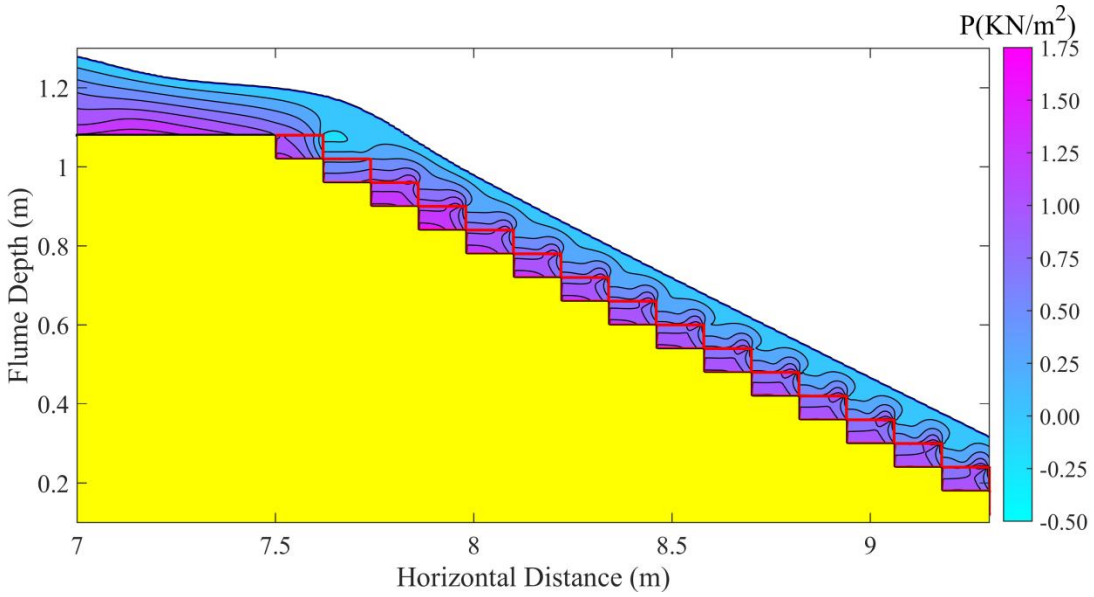
P(KN/m2)
1.75
1.50
1.25
1.00
0.75
0.50
0.25
0.00
-0.25
-0.50
Flume Depth (m)
1.2
1
0.8
0.6
0.4
0.2
7
7.5
8
8.5
9
Horizontal Distance (m)

(a)

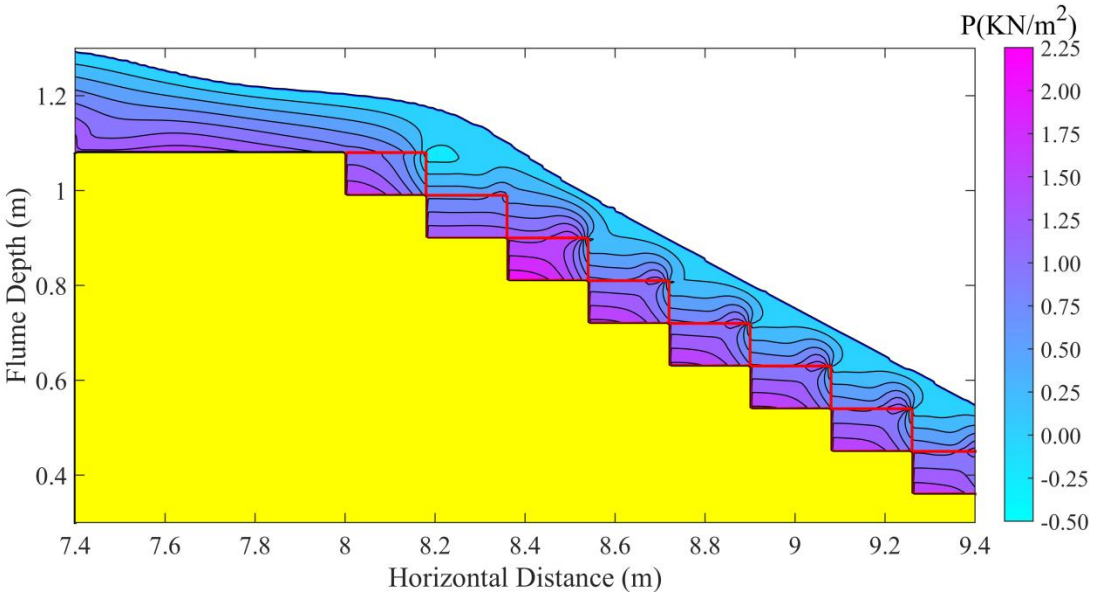
P(KN/m2)
2.25
2.00
1.75
1.50
1.25
1.00
0.75
0.50
0.25
0.00
-0.25
-0.50
Flume Depth (m)
1.2
1
0.8
0.6
0.4
7.4
7.6
7.8
8
8.2
8.4
8.6
8.8
9
9.2
9.4
Horizontal Distance (m)

(b)

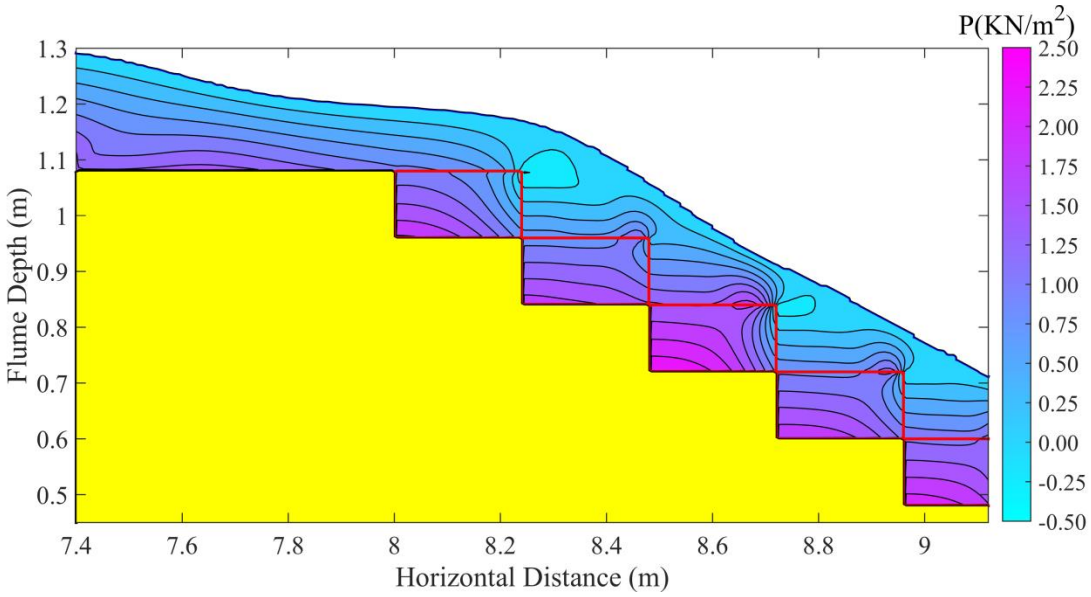

(c)

Figure 8.2 Pressure flow field along the non-aerated flow region for a unit discharge of q=0.20m^2/s, over gabion stepped spillways using steps with slope 1V:2H and height of a) 0.06, b) 0.09 and c) 0.12m.

8.2.1. Pressure distribution on the horizontal face of the gabion steps

Figures 8.3 and 8.4 show the pressure distribution on the horizontal face of the gabion steps of heights of 0.06m and 0.09m, located at different positions in the non-aerated zone along the chute of bottom slope 1V:2H. The normalised pressure values $\frac{P}{\rho * g * Yc}$ have been plotted against the dimensionless term w/ls.

where:

P is the pressure,

ρ is the fluid density,

g is the gravitational acceleration,

Yc is the critical flow depth on the weir crest,

ls is the step length,

w is the distance measured from the step inside edge to the point under the consideration,

L is the distance between the downstream face of the weir and the outer edge of the step in scope,

ks is the roughness height.

In Figure 8.3, three different unit discharges of 0.25, 0.2 and 0.15m^2/s have been investigated when the step height of the gabion stepped spillway is 0.06m. However, in Figure 8.4, only two discharges of 0.25 and 0.2m^2/s have been explored when the step height is 0.09m, as the non-aerated zone length has become shorter due to step height increase; hence, the non-aerated zone is along the first two steps only.

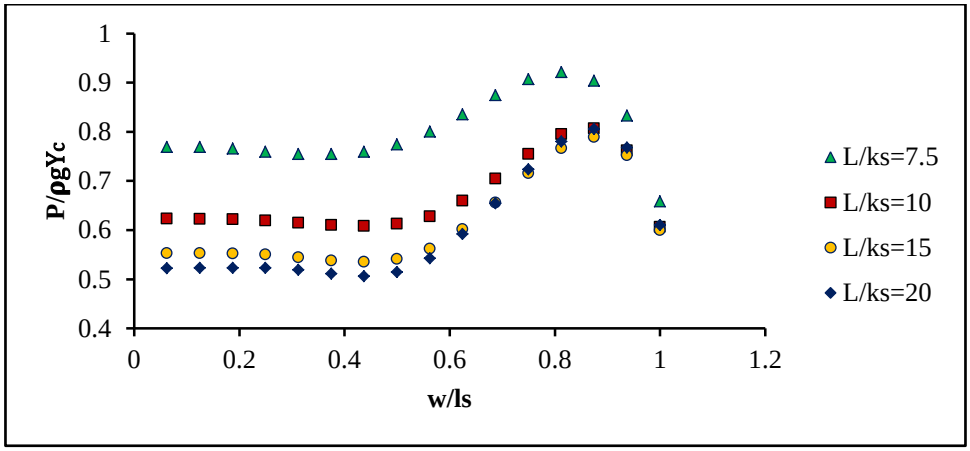

(a)

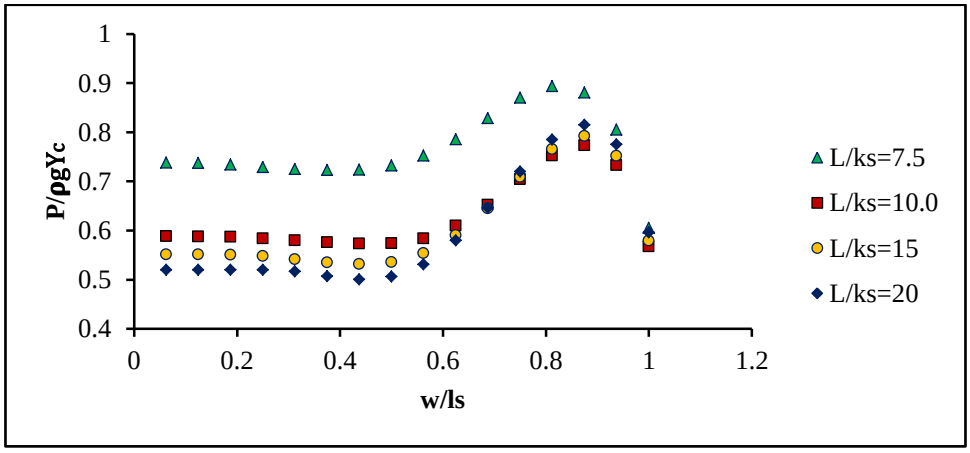

(b)

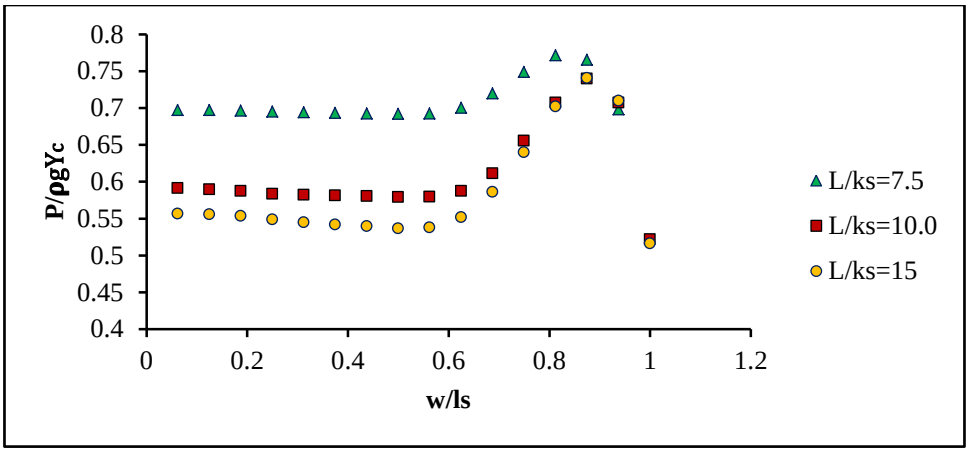

(c)

Figure 8.3 Pressure distribution along the gabion face of step height 0.06m on a chute slope of 1V:2H for a) q=0.25m^2/s, b) q=0.20m^2/s and c) q=0.15m^2/s.

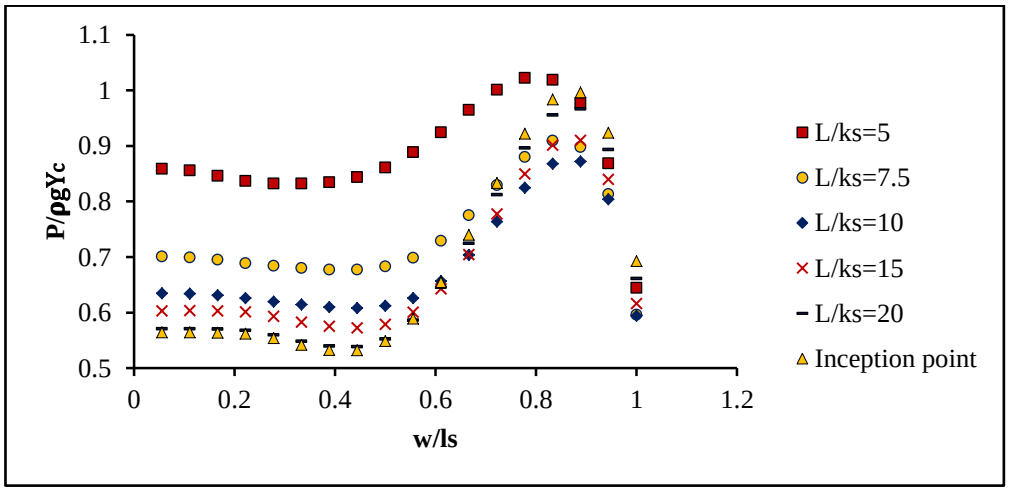

(a)

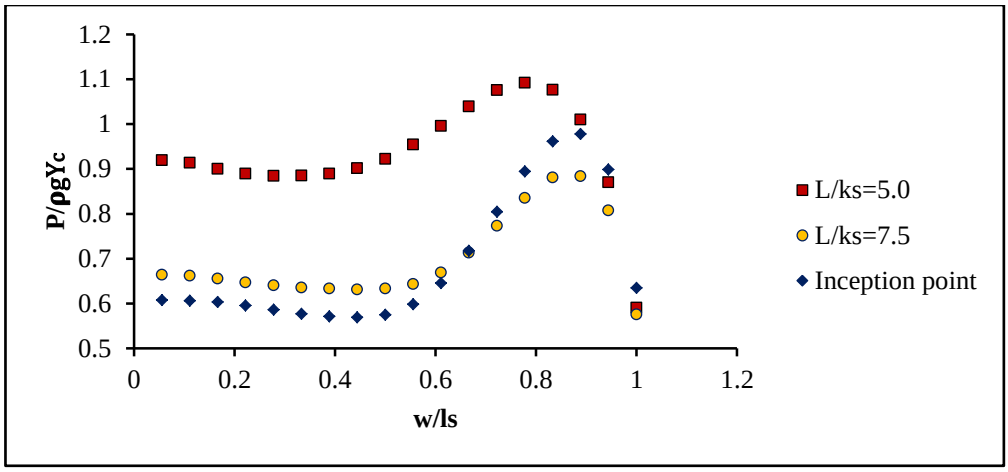

(b)

Figure 8.4 Pressure distribution along the gabion face of step height 0.09m on a chute slope of 1V:2H for a) q=0.25m^2/s and b) q=0.20m^2/s.

The computational results in both figures reveal that for different flow rates, the pressure distribution achieves the peak value at about 10% to 20% of the step length measured from the outer edge. A gradual decrease in the pressure values can be observed towards the inner edge of steps inside the step cavity until it reaches the minimum peak value at the middle of the steps. The maximum pressure value on the gabion face may possibly be achieved as an impact of the skimming flow on the tread of the step. The minimum pressure values might be observed due to the eddy formation inside the step cavity. Similar explanations were concluded for the normal stepped spillways by Amador et al. (2009) and Husain et al. (2013). Husain et al. (2013) concluded that the peak value of the pressure was from 22% to 25% of the step length from its outer edge. The computational results of the current work revealed that the pressure values over the non-aerated zone decrease towards the location of the inception point. High-pressure values might be expected in the first three steps; a graduated decrease can then be observed until reaching the minimum value at the inception point where the velocity is normally high as mentioned and explained before in Chapter 7. Low values for the pressure should be anticipated because of the inverse relationship between velocity and pressure. Figure 8.5 shows the pressure distribution inside the gabion boxes over the concrete steps. The results showed that the maximum value of the pressure is found close to the inner edge. Then, the pressure values stay very close to the maximum value until the middle of the

steps where a graduated decrease starts up from the outer edge of the steps where the lowest value of the pressure has been captured.

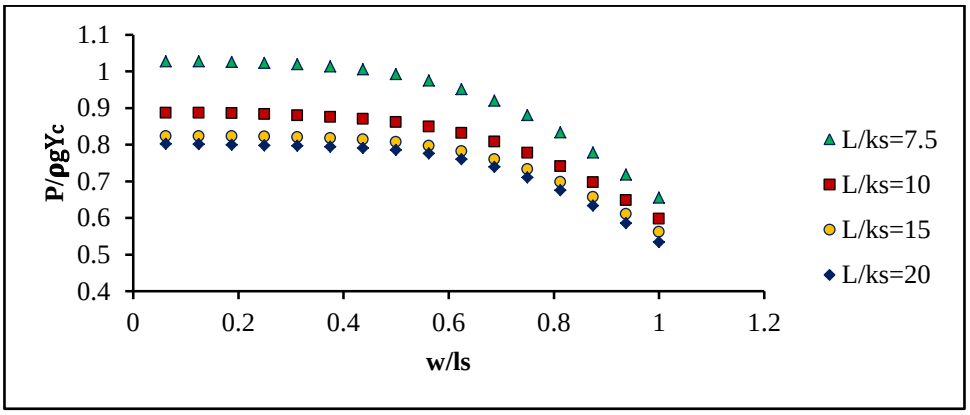

(a)

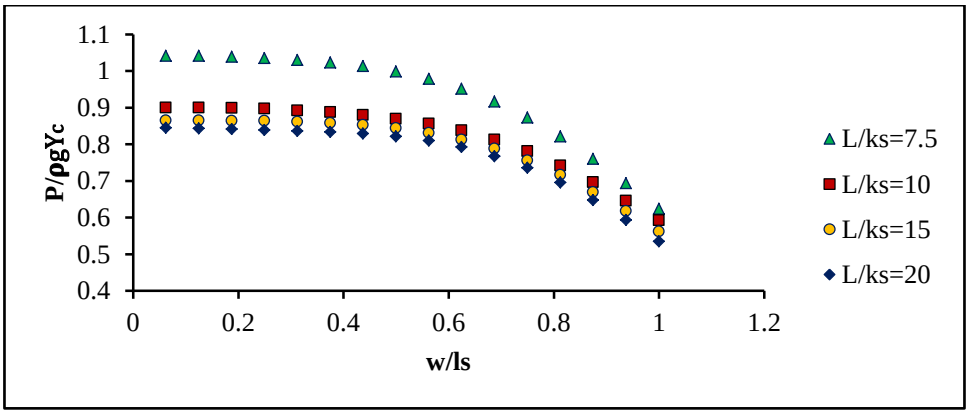

(b)

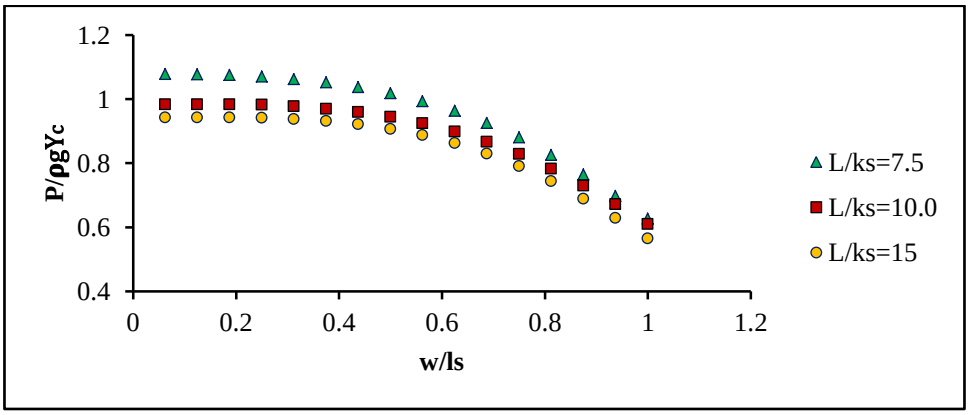

(c)

Figure 8.5 Pressure distribution inside the gabion along the horizontal face of step height 0.06m on a chute slope of 1V:2H for a) $q=0.25m^2/s$, b) $q=0.20m^2/s$ and c) $q=0.15m^2/s$.

Figure 8.6 shows the distribution of the pressure over the gabion steps at L/ks=7.5 which is located at a distance from the weir crest along the non-aerated zone and also at the inception point of air entrainment. The pressure distribution over the chute slope of 1V:2H for a flow rate of q=0.20m^2/s with different step heights have been presented in order to investigate the effect of step heights on the pressure variation over the stepped gabion.

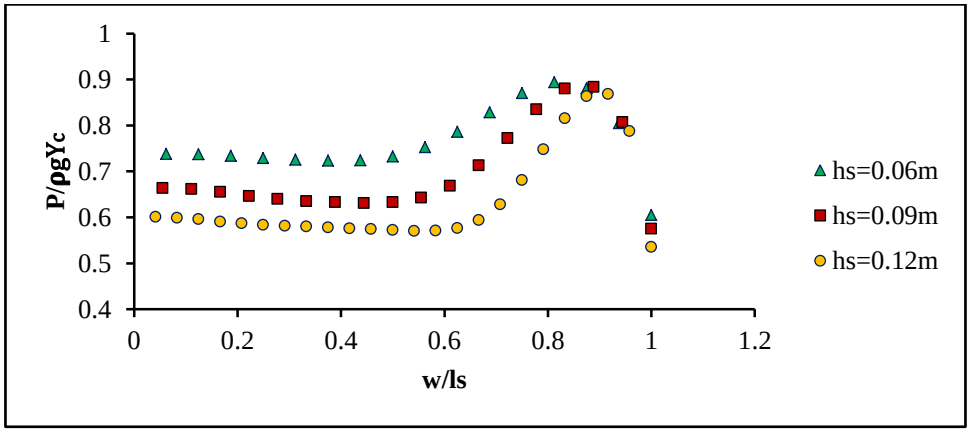

(a)

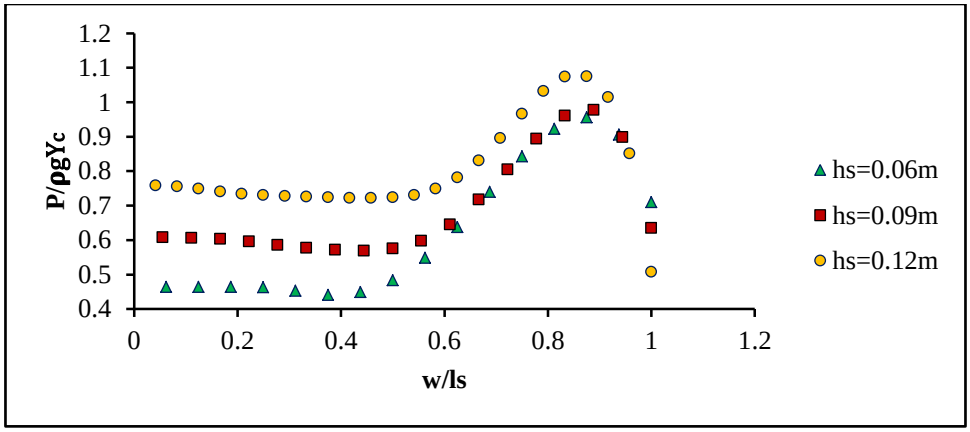

(b)

Figure 8.6 Pressure distribution along the gabion face of horizontal steps over the chute slope of 1V:2H for the unit discharge of q=0.20m^2/s at a) L/ks=7.5 and b) inception point.

The computational results revealed that over the non-aerated zone no significant differences could be observed in terms of the pressure distribution characteristics along

the gabion steps with the change of the step heights. However, the pressure values were sensitive to the step height variation. In the non-aerated zone, the pressure values decreased when the step height increased, conversely, the pressure values increased at the inception point when the step heights changed from 0.06 to 0.12m. It is clear that the behaviour of the pressure may vary over the non-aerated zone up to the inception point. This is well agreed with the velocity results in Chapter 7 which showed that velocity profile values at the inception point were much higher when the step height has changed from 0.12 to 0.06m due to the inverse relationship between the pressure and velocity. Consequently, high pressure values at the inception point have been achieved when the step height equals to 0.12m.

To recognise how the pressure distributes in the non-aerated zone over gabion steps, Figures 8.7 to 8.9 plot the pressure distribution along the chute of bottom slopes 1V:2H, 1V:2.5H and 1V:3H respectively. As can be clearly seen from the three figures, the maximum pressure value might move slightly towards the inner edge by 10% when the slope of the bottom chute becomes flatter. However, there were no differences in terms of the distribution. Flat gabion stepped spillway has gained high-pressure values compared to the steep slopes. This is might be related to the length of the width, as having more length that possibly can increase the opportunity to reduce the vorticities and make the water calmer, so that can lead to a reduction in the velocity values and increase the pressure values. Moreover, it is crucial to highlight that for all flow rates and step configurations which have been tested in the present work, the pressure values that act on the gabion faces are positive, consequently, cavitation is unlikely to effect the gabion steps.

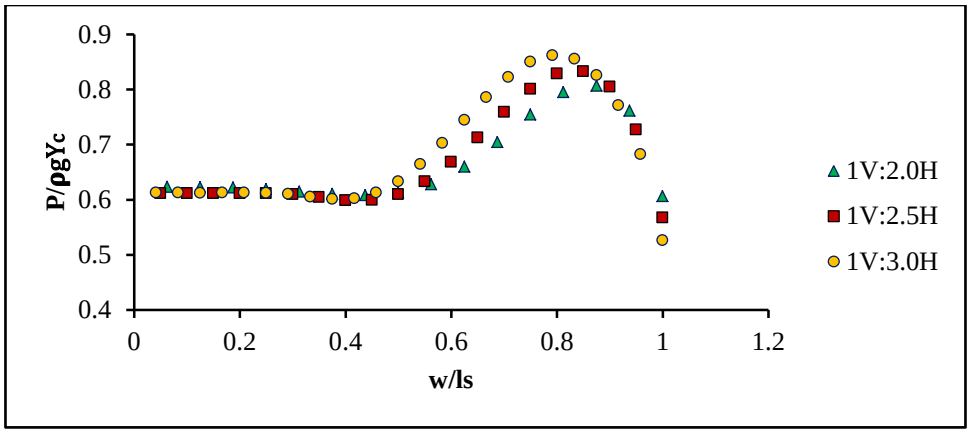

Figure 8.7 Pressure distribution along the gabion face of steps height 0.06m over different chute slopes for the unit discharge of q=0.25m^2/s at the fourth step.

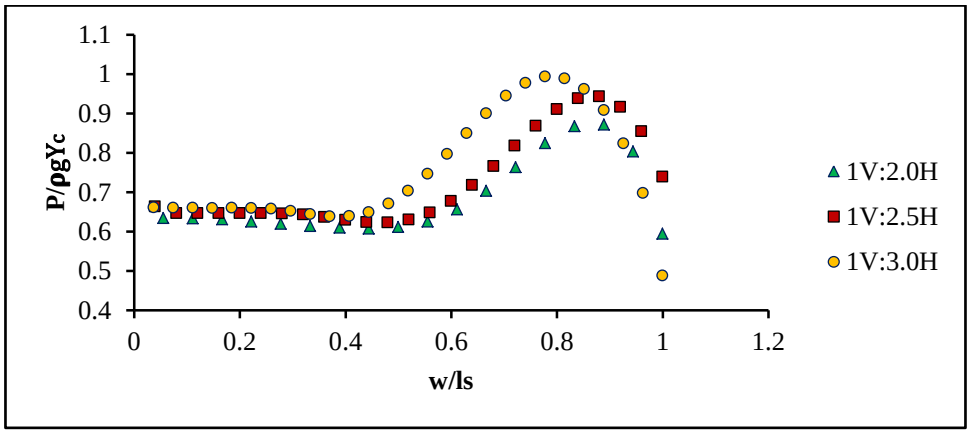

Figure 8.8 Pressure distribution along the gabion face of steps height 0.09m over different chute slopes for the unit discharge of q=0.25m^2/s at the fourth step.

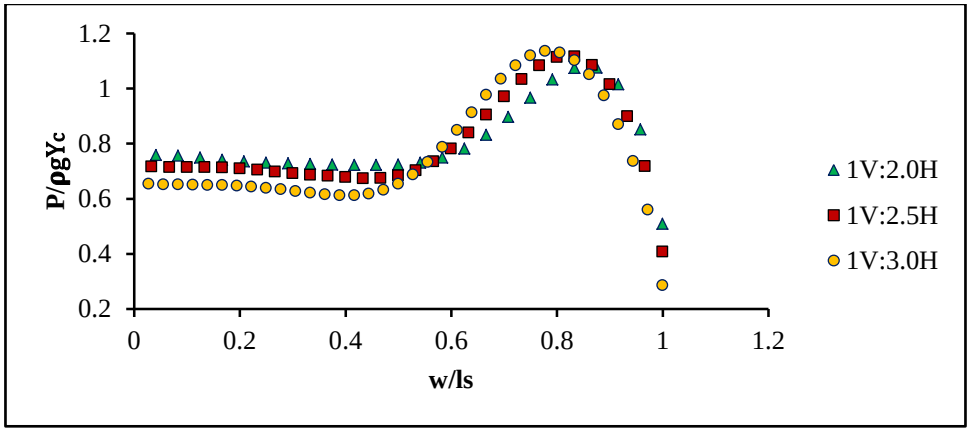

Figure 8.9 Pressure distribution along the gabion face of steps height 0.12m over different chute slopes for the unit discharge of q=0.20m^2/s at the fourth step.

The effect of the gabion porosity and particle sizes on the pressure distribution over the horizontal face of the gabion steps has been thoroughly investigated. Figures 8.10 to 8.15 show the effect of both porosity and particle sizes over the non-aerated zone up to the location of the inception point with three different slopes 1V:2H, 1V:2.5H and 1V:3H, for a flow rate of $0.2m^2/s$ and 0.12m step height.

The computational results showed that both porosity and particle sizes can affect the value of the peak pressure and slightly its location as well. However, similarly to the chute slopes, no crucial changes have been observed for the pressure distribution. The general trend of the results reveals that the pressure value decreases when both porosity and particle sizes increase along the non-aerated zone and at the inception point. This is because the flow needs more pressure to seep inside the gabion and to flow over it.

Furthermore, the pressure is more affected by the porosity and the diameter sizes at the inception point compared to different positions in the non-aerated zone; in some cases, it could reach over 25% fluctuating for the value of the peak pressure. As can be seen in the below figures, in most cases, the changes due to the porosity and particle sizes start at around 0.6 from the inner edge of the steps and its continued towards the outer edge of the steps. That can depend on many parameters like the position in the non-aerated zone, flow rates, chute slopes and step heights.

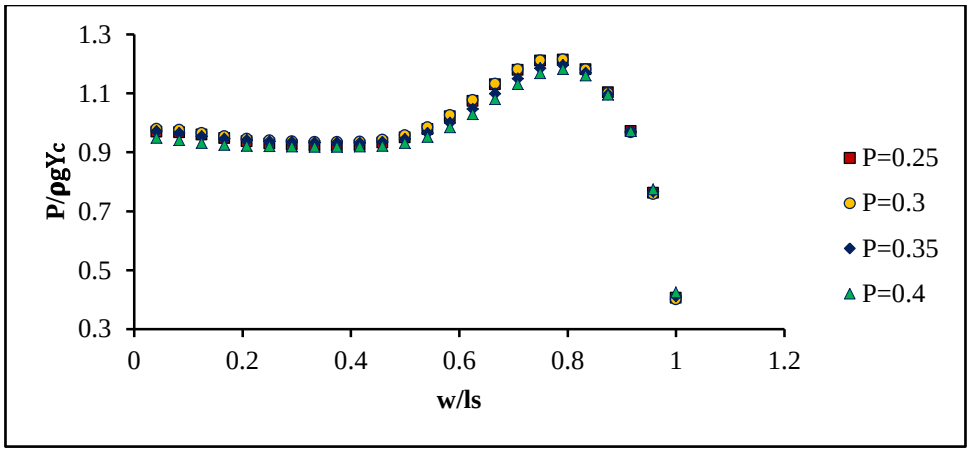

(a)

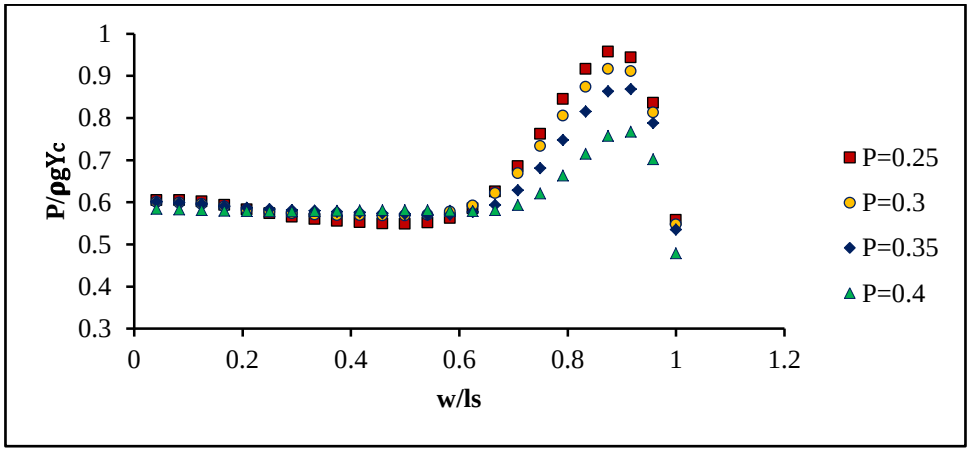

(b)

Figure 8.10 Pressure distribution of different values of porosity along the gabion face of horizontal steps over the chute slope of 1V:2H for the unit discharge of q=0.20m^2/s at a) L/ks=5.0 and b) inception point.

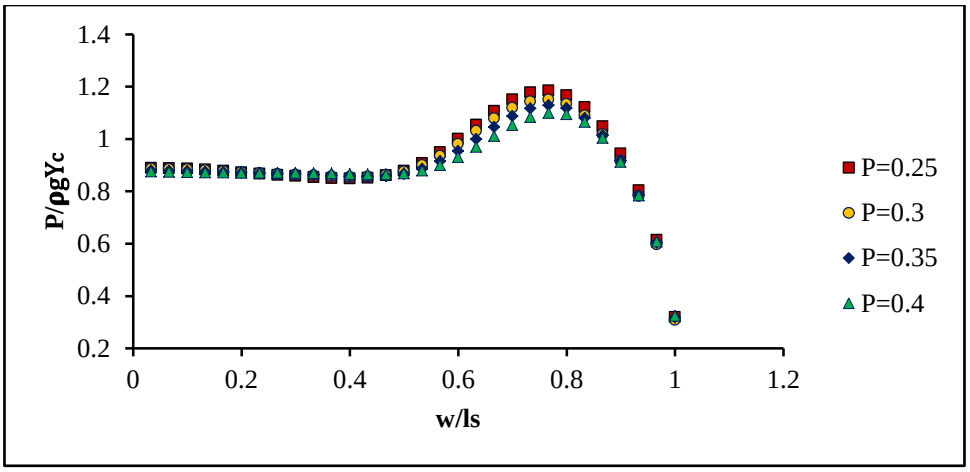

(a)

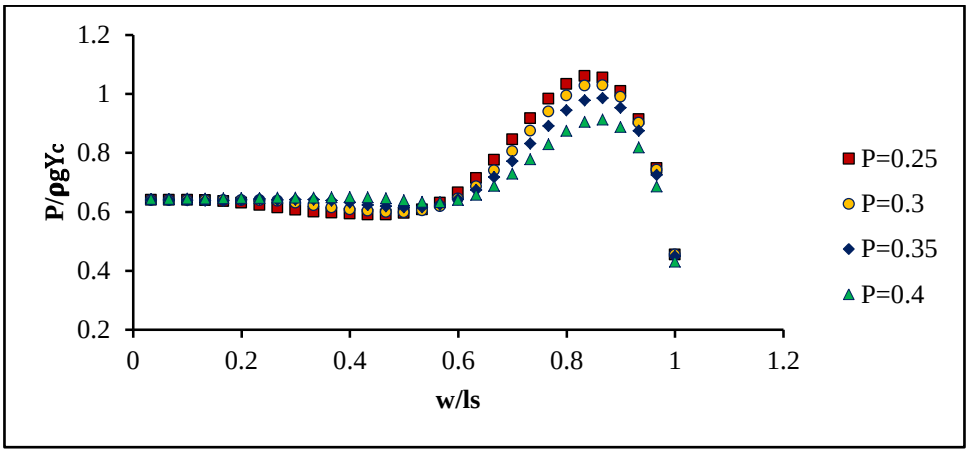

(b)

Figure 8.11 Pressure distribution of different values of porosity along the gabion face of horizontal steps over the chute slope of 1V:2.5H for the unit discharge of q=0.20m^2/s at a) L/ks=5.8 and b) inception point.

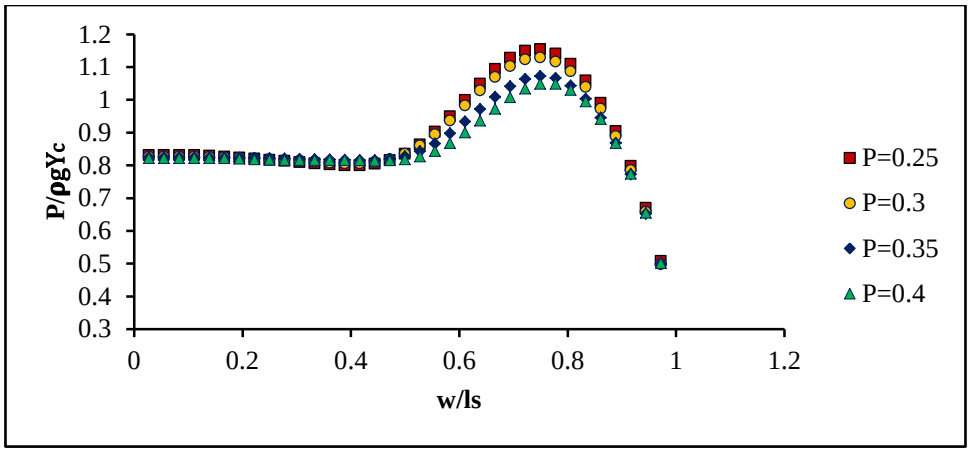

(a)

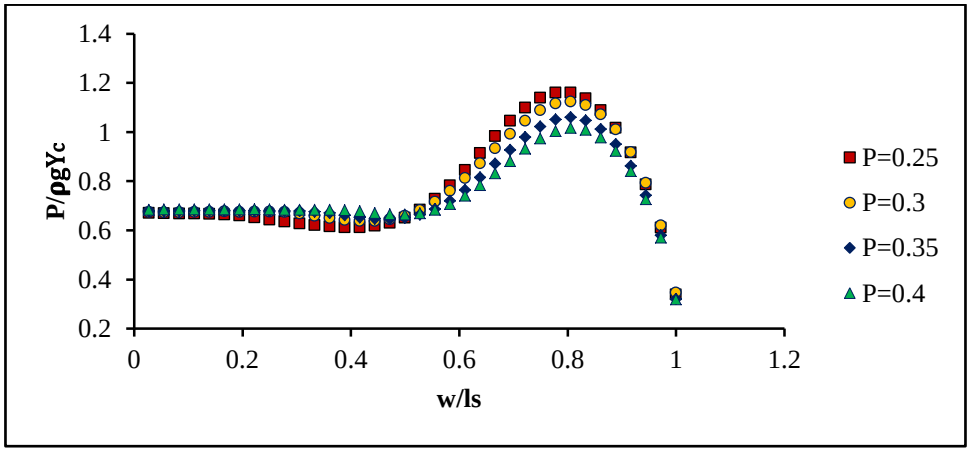

(b)

Figure 8.12 Pressure distribution of different values of porosity along the gabion face of horizontal steps over the chute slope of 1V:3.0H for the unit discharge of q=0.20m^2/s at a) L/ks=6.6667 and b) inception point.

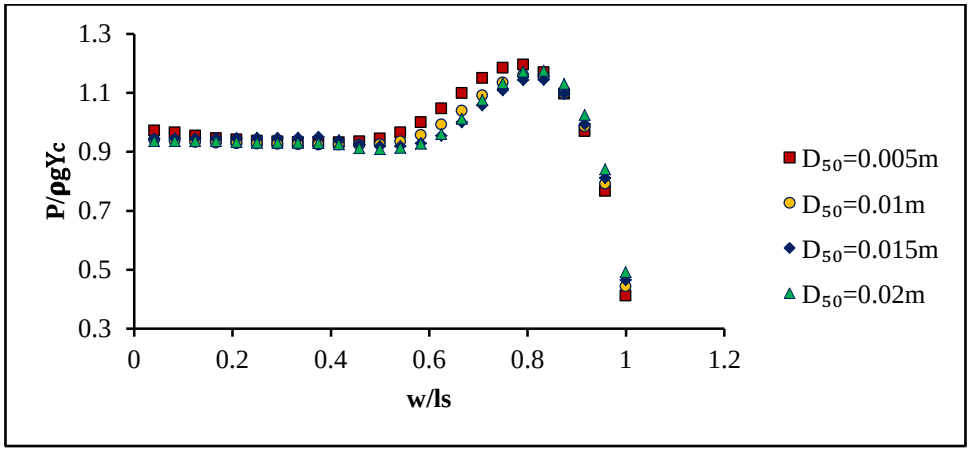

(a)

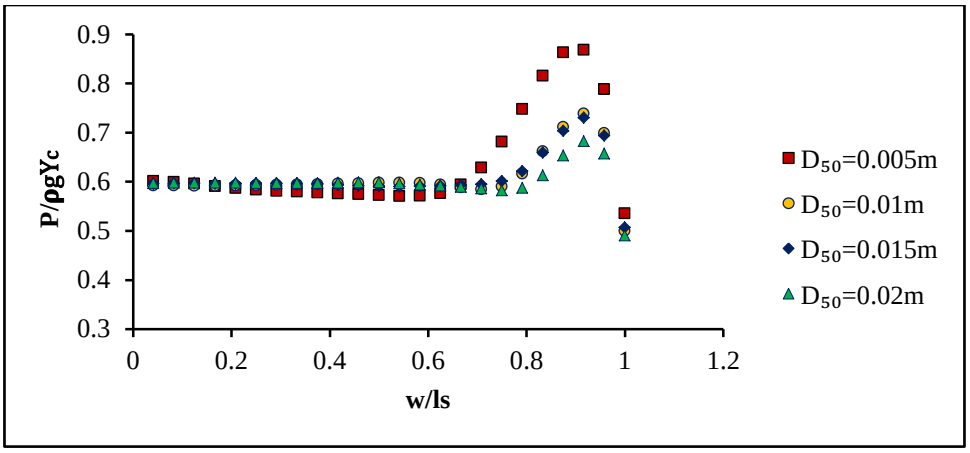

(b)

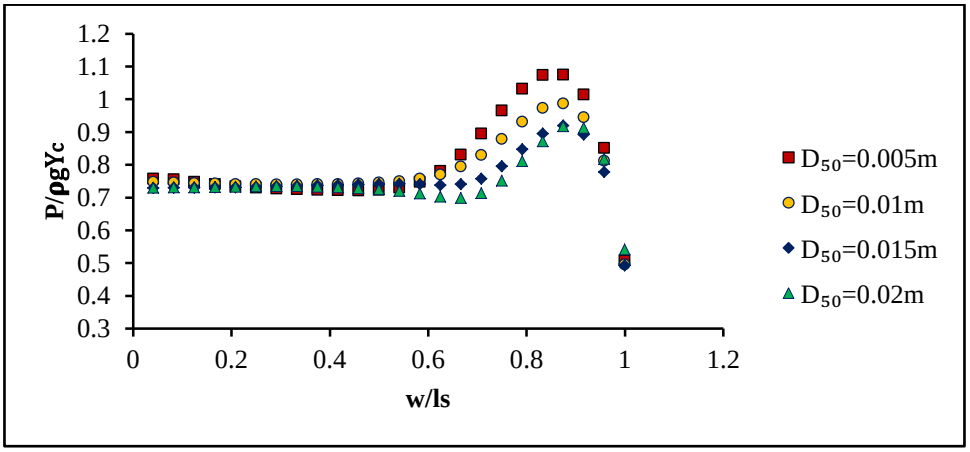

(c)

Figure 8.13 Pressure distribution of different values of particle sizes along the gabion face of horizontal steps over the chute slope of 1V:2.0H for the unit discharge of q=0.20m^2/s at a) L/ks=5.0, b) L/ks=7.5 and c) inception point.

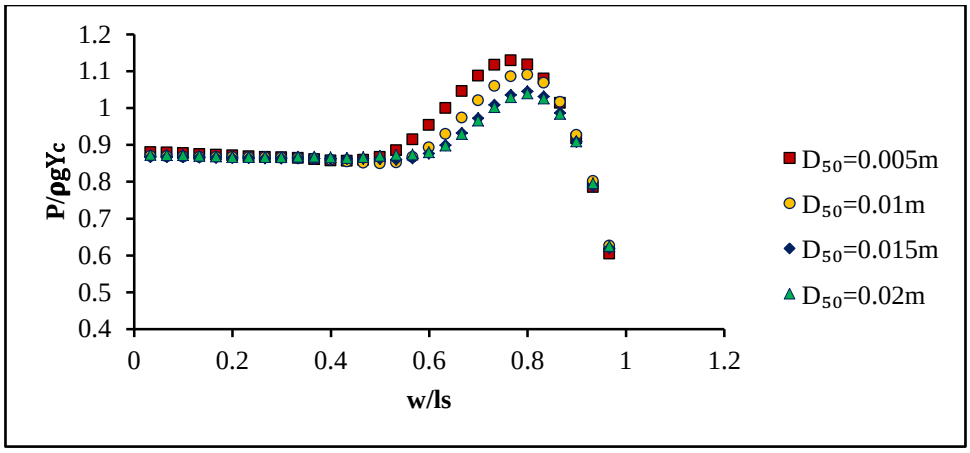

(a)

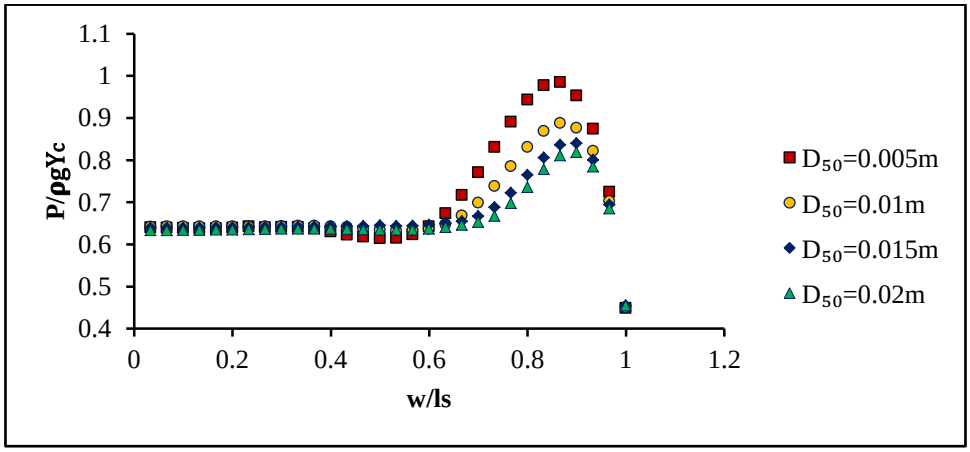

(b)

Figure 8.14 Pressure distribution of different values of particle sizes along the gabion face of horizontal steps over the chute slope of 1V:2.5H for the unit discharge of $q=0.20m^2/s$ at a) L/ks=5.8 and b) inception point.

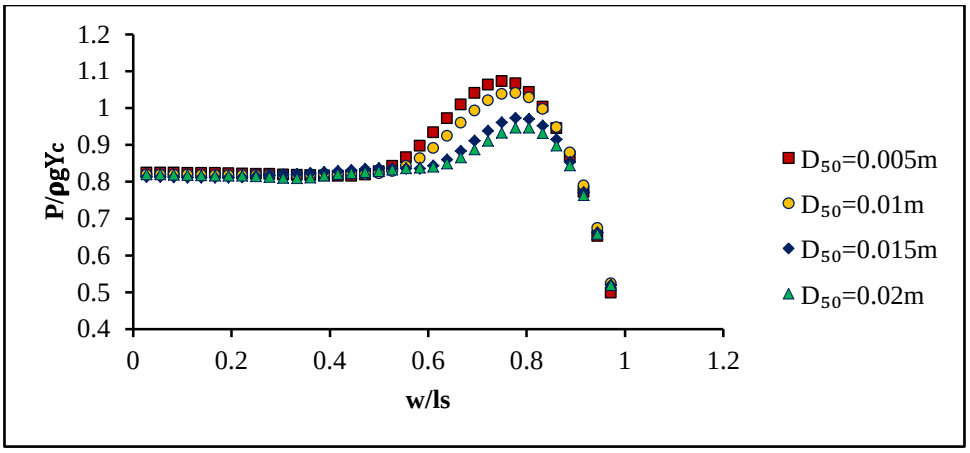

(a)

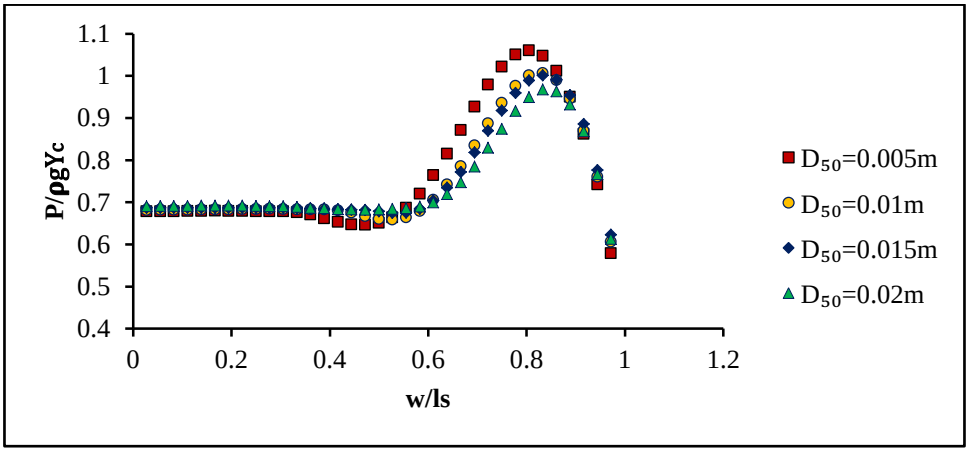

(b)

Figure 8.15 Pressure distribution of different values of particle sizes along the gabion face of horizontal steps over the chute slope of 1V:3.0H for unit discharge of q=0.20m^2/s at a) L/ks=6.6667 and b) inception point.

8.2.2. Pressure distribution on the vertical face of the gabion steps

The pressure distribution over the vertical faces of gabion steps is investigated in this section of the current work, in order to demonstrate the shape of the pressure variation along the gabion face and to observe the negative values of the pressure in the non-aerated zone where the cavitation damage might occur. Therefore, the pressure distribution of three different discharges with gabion step height of 0.06m and chute

slope 1V:2H, located at different distances along the non-aerated zone is shown in Figure 8.16.

The normalized pressure values P/ρgYc have been calculated and plotted in Figure 8.16 against the values of the dimensionless term z/hs, for different values of L/ks, where P is the pressure, ρ is the fluid density, g is the gravitational acceleration, Yc is the critical water depth, hs is the step height, z is the distance measured from the step outer edge to the point under the consideration along the vertical face, L is the distance between the downstream face of the weir and the outer edge of the step in scope, and ks is the roughness height.

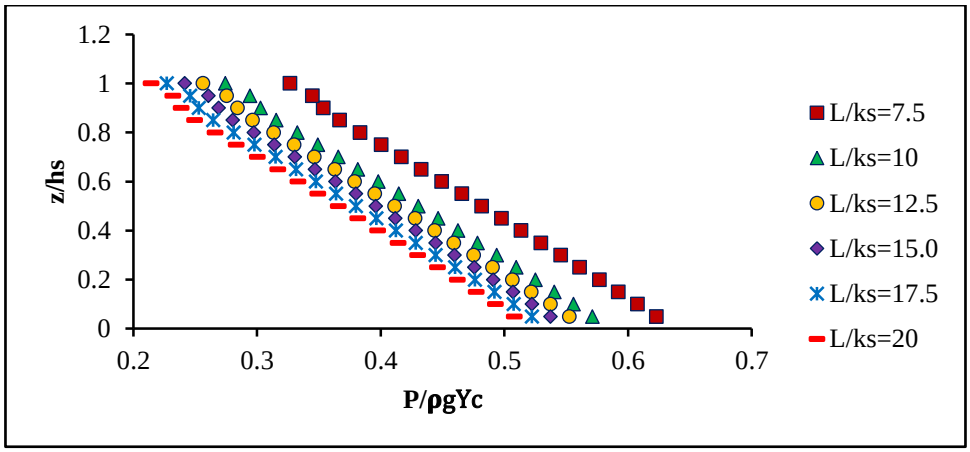

(a)

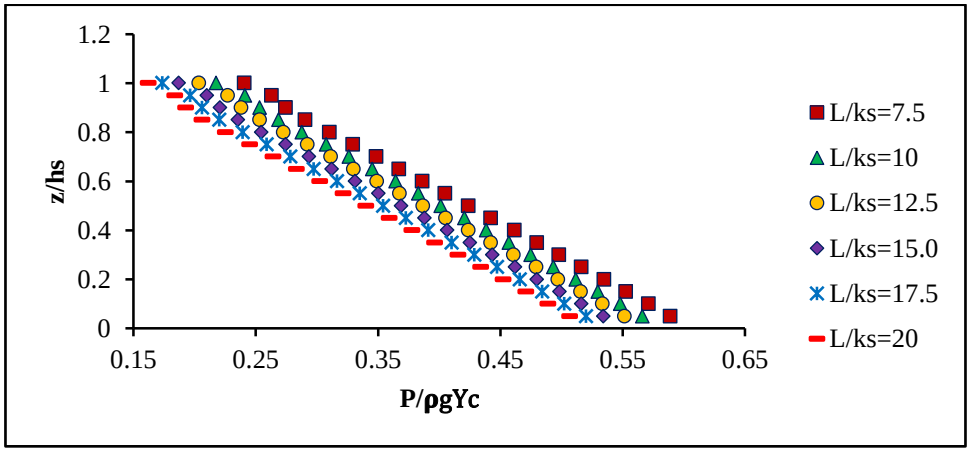

(b)

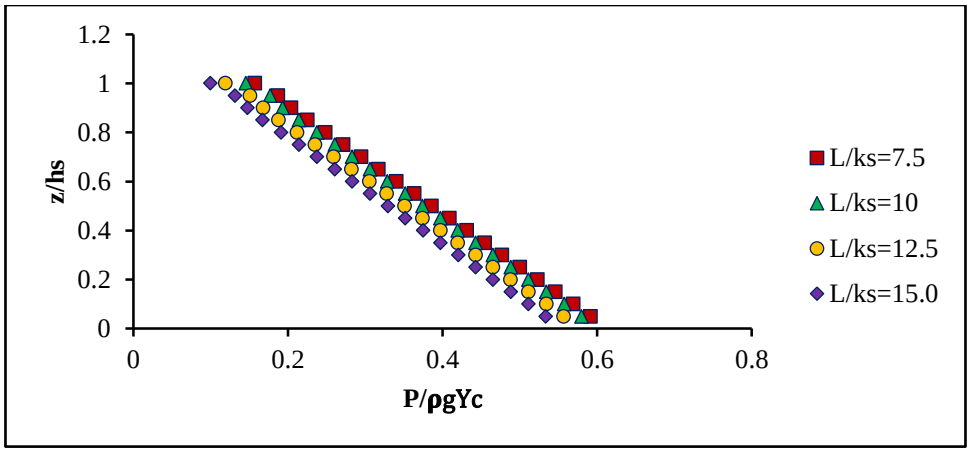

(c)

Figure 8.16 Pressure distribution on the vertical face of gabion steps of height 0.06m and chute slope 1V:2H, for unit discharges: a) $q=0.25m^2/s$, b) $q=0.20m^2/s$ and c) $q=0.15m^2/s$.

Although the maximum value of the unit discharge is tested in Figure 8.16, no negative values of pressure were observed along the gabion vertical face where all the values are positive. The computational results have shown that the minimum value of the pressure could be observed at the step outer edge. The pressure distribution increased gradually towards the step corner where the maximum value can be achieved. The same variation in pressure is observed for the normal stepped spillways when the gabion steps were not applied (Husain et al., 2013).

Husain et al. (2013) revealed that the minimum pressure value observed in this region is possibly due to the separation between the streamlines of the skimming layer and the main flow when passing over the vertical face. However, the formation of the rotating vortices inside the step cavity may have led to increase the pressure towards the corner. The results showed that for all discharges the minimum pressure values have been achieved at the outer edge of steps that are located close to the inception point. This can probably be related to the mean flow velocity as it reaches the peak value close to the inception point of air entrainment. Thus, the pressure normally drops to low values as a result of the flow velocity increases.

Figure 8.17 shows the pressure distribution along the vertical faces of the impervious steps, inside the gabion box, in order to demonstrate the differences between the pressure distribution inside and over gabion boxes. The results showed that the same distribution and the same positions for the maximum and minimum values have been observed for the pressure variation over the vertical faces. All the results which have been established for the pressure distribution over the vertical faces of the gabion have gained inside the gabion.

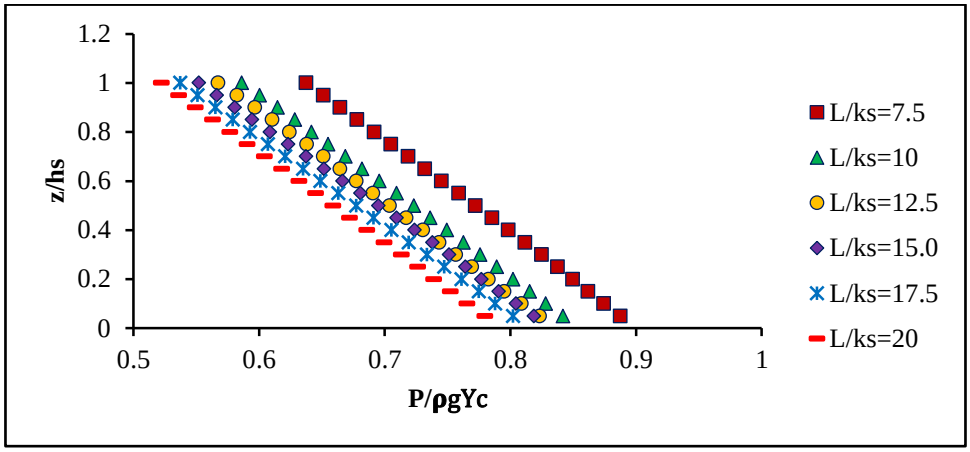

(a)

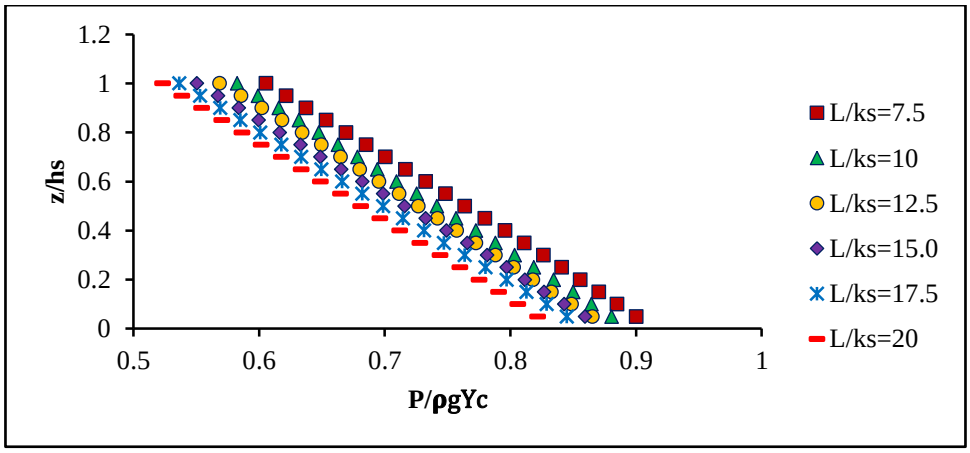

(b)

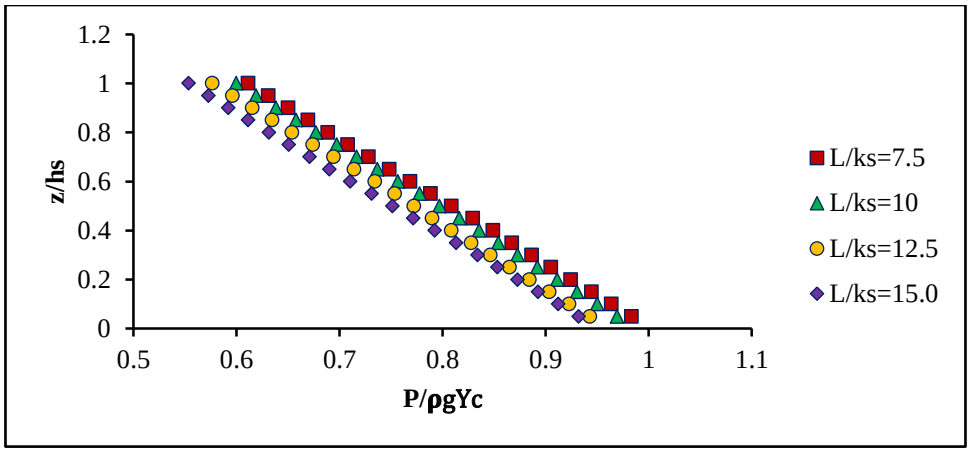

(c)

Figure 8.17 Pressure distribution on the vertical face of the impervious steps (inside the gabion) of height 0.06m and chute slope 1V:2H, for unit discharges: a) $q=0.25m^2/s$, b) $q=0.20m^2/s$ and c) $q=0.15m^2/s$.

In order to explore the influence of the step height on the pressure distribution of the vertical faces over the gabion steps, Figure 8.18 shows the pressure distribution on the vertical face in the non-aerated zone at L/ks=7.5 and also at the closer step to the inception point of air entrainment for a chute slope of 1V:2H and 0.06m step height.

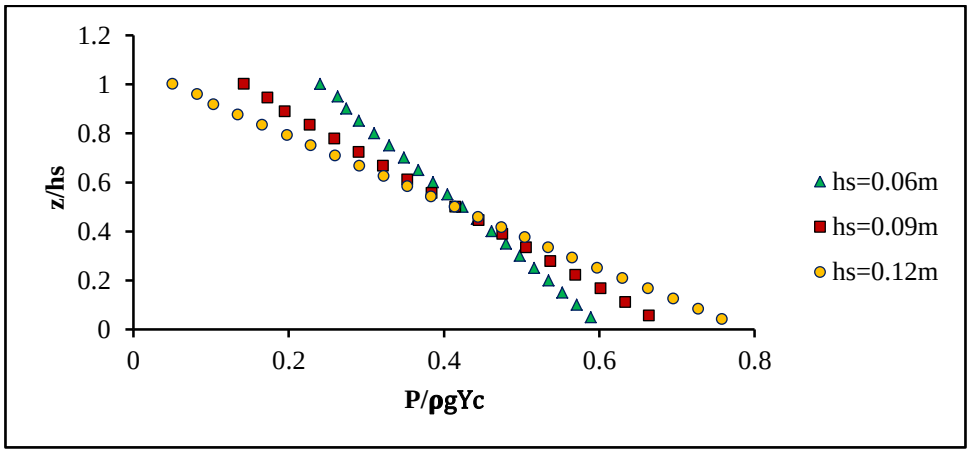

(a)

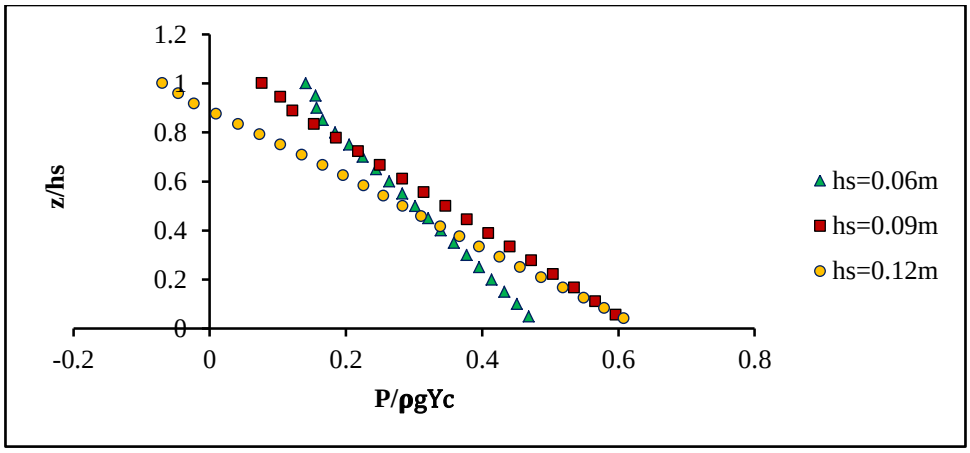

(b)

Figure 8.18 Pressure distribution along the vertical face of the gabion steps over the chute slope of 1V:2H for the unit discharge of q=0.20m^2/s and 0.06m step height at a) L/ks=7.5 and b) inception point.

It is been noted that the step height of 0.12m delivered lower pressure values at the step outer edge for both positions, and it is more prone to cavitation damage compared to the other step heights. Although the 0.12m step height presented the highest values of the pressure near the inner corner, it is still considered riskier compared to the step heights 0.06m and 0.09m. This is due to the lowest values achieved near the step outer edge at L/ks=7.5, in addition to the negative values of the pressure which is obtained near the inception point. As aforementioned, the step height of 0.12m is more effective in decelerating the flow velocity at the inception point compared with the step heights 0.06m and 0.09m. This may clarify why the pressure on the vertical step face of height 0.12m is relatively lower than the step heights 0.09m and 0.06m at the inception point.

Figure 8.19 displays the pressure distribution over the vertical step faces of gabion stepped spillways in the non-aerated zone with respect to the chute slope. The results illustrate that when the step height is 0.06m, the flatter the chute slope the higher the pressure on the step outer edge of vertical face and therefore the possibility of getting cavitation will be lower. However, a contrary conclusion has been achieved when the step height equals to 0.12m; flatter chute slopes produced lower-pressure values.

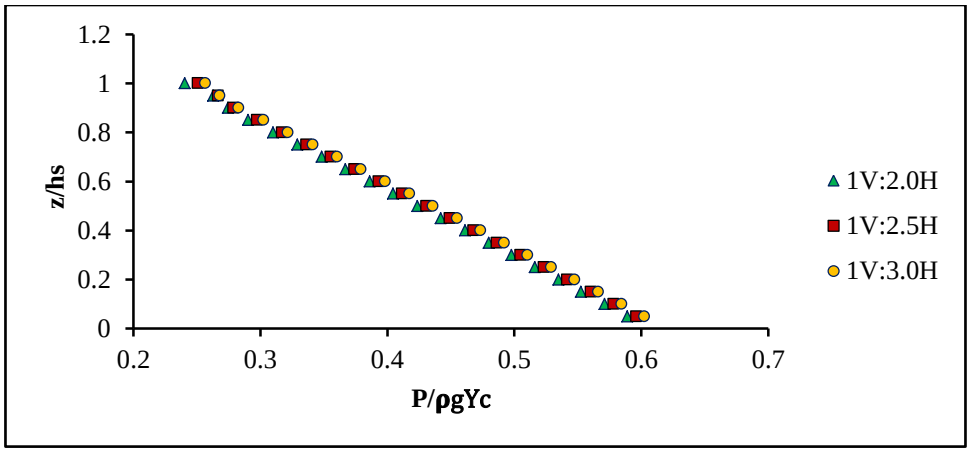

(a)

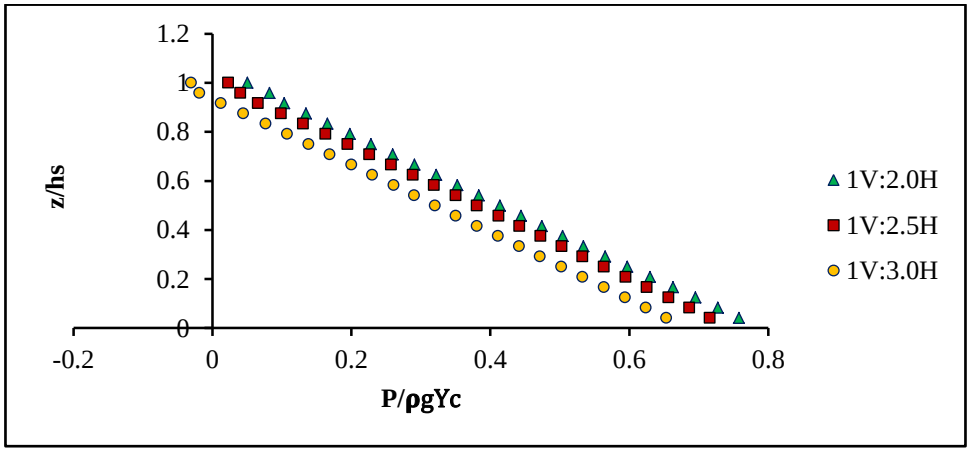

(b)

Figure 8.19 Pressure distribution along the vertical gabion face of steps over different chute slopes for the unit discharge of q=0.20m^2/s at the third step with step heights of a) 0.06m and b) 0.12m.

Figures 8.20 and 8.21 investigate the pressure distribution over the vertical step faces of gabion stepped spillways in the non-aerated zone with different values of porosity and particle size which represent the main parameters of the gabion. These figures were plotted to demonstrate the porosity and the particle size effect on the normalised pressure along the vertical step face in the non-aerated zone where L/ks=6.66 and at the closer step to the location of the inception point.

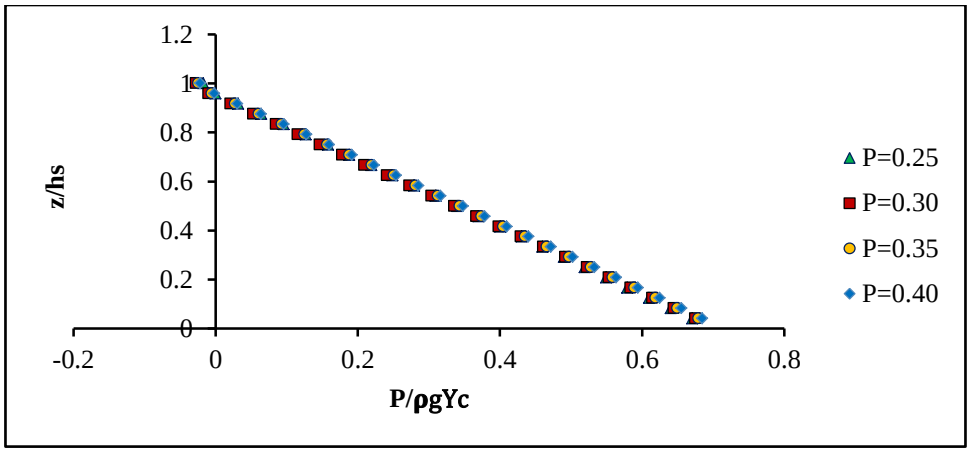

(a)

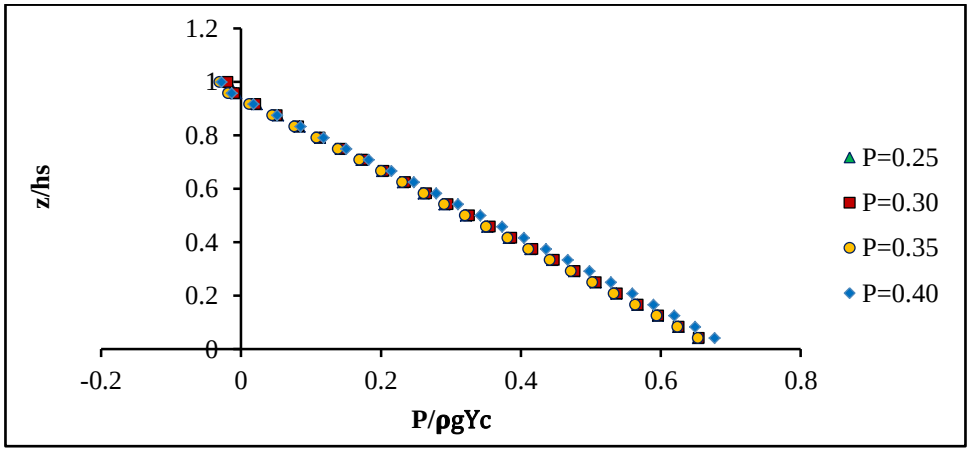

(b)

Figure 8.20 Pressure distribution of different values of porosity along the vertical gabion face of step height of 0.12m over the chute slope of 1V:3.0H for a unit discharge of q=0.20m^2/s at a) L/ks=6.66, and b) inception point.

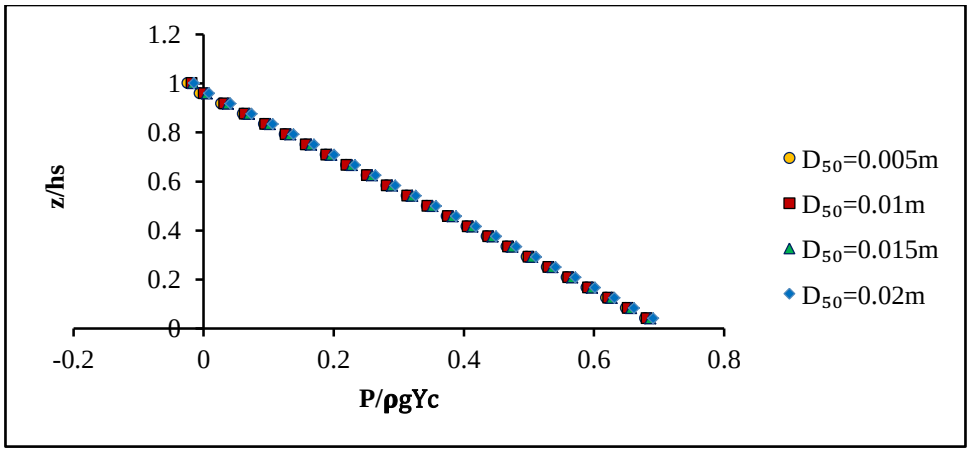

(a)

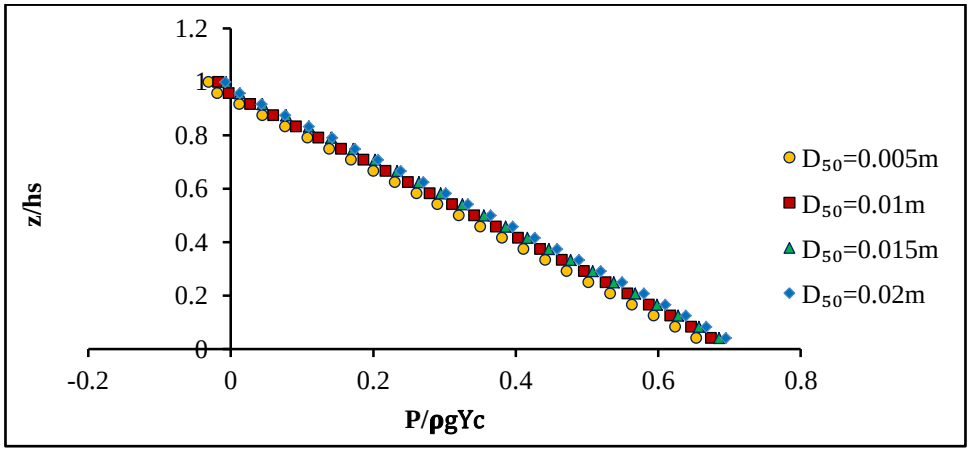

(b)

Figure 8.21 Pressure distribution of different values of particle sizes along the vertical gabion face of step height 0.12m over the chute slope of 1V:3.0H for a unit discharge of q=0.20m^2/s at a) L/ks=6.66, and b) inception point.

The results revealed that both porosity and particle sizes could not change the pressure distribution over the vertical step faces significantly and that probably achieved due to the complexity of the flow at that area where the eddies can be noticed easily and also due to the interaction between the mainstream flow and the eddies especially at the outer edge of the steps. Additionally, the computational results showed that with a step height of 0.12m and bottom chute slopes of 1V:2.0H, 1V:2.5H and 1V:3.0H, the pressure values increased with an increase in both the porosity and particle sizes, although the changes in the pressure distribution profile are small. This could be due to the spaces between the

particles or inside the particles as bigger spaces can lead to a reduction in the flow velocity and that might increase the water pressure.

8.3. Assessment of cavitation potential

The cavitation phenomenon could occur in many hydraulic structures as it is one of the major issues in the high-velocity channels (Chanson, 2004). It is established when the local pressure in flowing water drops below the vapour pressure, and also when the air bubbles or air pockets may form locally inside the flow. Cavitation bubbles are collapsed when it reaches an area with higher local pressure. Hence, if that collapse happens close to the concrete surface, holes might be observed over the concrete surface, known as cavitation pitting. This damage is due to the extremely high pressure which could be possibly generated due to the bubbles collapsing. As a result of that action on small areas and after a period of time, serious damages could be observed in the concrete surfaces. Spillways are at the risk of cavitation damage. Cavitation damages were observed on the Danjiangkou Dam (China) stepped spillway for a unit discharge of q=120m^2/s (Lin and Han 2001; Wang et al. 2014). The cavitation index number which is used before by Falvey (1990) will be used in the current work, in order to test whether cavitation could be occurred on moderate slopes of gabion stepped spillways.

$$\sigma = \frac{2(P_{atm}+P_0-P_v)}{\rho V_0^2} \quad (8.2)$$

where σ is the cavitation index, P_{atm} is the atmospheric pressure, P_o and P_v are respectively the reference pressure and the vapour pressure of water at a given temperature, ρ is the density of water and V_o is the reference velocity. The cavitation index equation shows that the possibility of cavitation formation over stepped spillways would be higher when cavitation index value is lowered. This mainly occurs when the pressure values are low and the flow velocity is high.

Frizell and Renna (2011) experimented on stepped spillways with mild slopes of 1V:2.48H; they found that cavitation was established when the critical cavitation index number was between 0.6 and 0.7. However, Frizell et al. (2013) performed an experimental study to assess the cavitation potential on stepped spillways with two-step

angles θ=21.8° and θ=68.2°, with two step heights each. Various discharges have tested for each configuration. A critical cavitation index of 0.60–0.65 was obtained for θ=68.2° and 0.30–0.40 for θ=21.8°.It is crucial to highlight that these values of the critical cavitation index cannot be used as an indication for the onset of cavitation; however, they could represent the point from which a large increase in cavitation activity might be observed. Although the lower values of critical cavitation index is achieved with θ=21.8°, the shear layer impact on the steps proposes that milder slope stepped chutes could be more prone to cavitation damages compared to steeper slopes where the shear layer is mostly above the pseudo-bottom.

In the current work, the cavitation index number of 0.3 is selected as the minimum cavitation index number below which cavitation could occur. As discussed earlier, the computational results revealed that the lowest values of the vertical pressure and the highest values of the flow velocity can achieve at the end of the non-aerated zone close to the inception point. In other words, low-pressure values together with high velocities occur typically along the chute of a spillway, so the risk of cavitation increases.

In order to use the equation of the cavitation index and avoid the scale effects, all the variables need to be converted to the prototype scale. Therefore, all the stepped spillways which are modelled and examined in this study have been converted using the scale ratio of 1:10, based on the hypothesis of Boes and Hager (2003) regarding the scale ratios of stepped spillways. The value of the vapour water pressure is assumed to be 2.34KN/m^2 in the current work and that based on a water temperature of 20^{o}C.

A drop in the pressure value has been observed to either close to the water vapour pressure or below atmospheric pressure at the outer edge of the vertical face of the gabion steps, which can lead to cavitation developing especially when the mean flow velocity in the tested section is relatively high. It is worth to mention that

- The minimum pressure value that achieved on the vertical face has been used in this study to determine the cavitation index number.

- The critical cavitation index number would be 0.3, which was established experimentally by Frizell et al. (2013).
- Froude similitude is applied in this study, as both the gravity and inertia forces are dominant factors governing the free surface flow.
- The results of the cavitation index values and flow rates that obtained in the present study are applied on prototype stepped spillways using the scale ratio of 1:10.

Having established the velocity and minimum pressure values on the vertical face of step heights of 0.06, 0.09 and 0.12m, close to the inception point of air entrainment due to the maximum flow rates over the chute slopes of 1V:2H, 1V:2.5H and 1V:3H, the minimum cavitation index number would be 1.52. This is an indication that cavitation is unlikely to occur with the aforementioned flow conditions.

Overall, the results showed that the cavitation damage unlikely to occur over the non-aerated zone of gabion stepped spillways under the conditions of this study; therefore, it needs to be considered during the design of gabion stepped spillways for high flow rates. Different configurations and geometries of gabion stepped spillways will be investigated in the next chapter in order to assess their impact on the energy dissipation rate.

Chapter 9 : Testing Different Configurations and Geometries of Gabion Stepped Spillways

9.1. Different configurations of gabion stepped spillways

The validated computational model was used to investigate the performance of different spillways configurations. Different shapes for gabion stepped spillways have been suggested, these shapes are normal gabions, overlapping gabions, inclined gabions and pooled gabions (Figure 9.1). All the configurations of the gabion steps have been installed over impervious steps of concrete. The same initial conditions have been applied for all configurations in order to discover differences in terms of the time taken to establish skimming flow, the location of the inception point, velocity distribution, pressures distribution and energy dissipation.

The stepped spillway was placed at distance 8m from the boundary edge, while the weir was positioned at distance 7.4m with length 0.6m. The initial water depth was 1.58m, so the area of the upstream tank was 7.4m*1.58m which is sufficient to achieve the required discharge. The total time for the simulation was 15s with an initial time step of 0.001s to meet the Courant stability criterion. The mesh size in the x-direction and in the y-direction was equal to 0.01m and 0.005m respectively, all of the boundary conditions were closed except the right boundary which was an open boundary condition to allow the water to exit the flume.

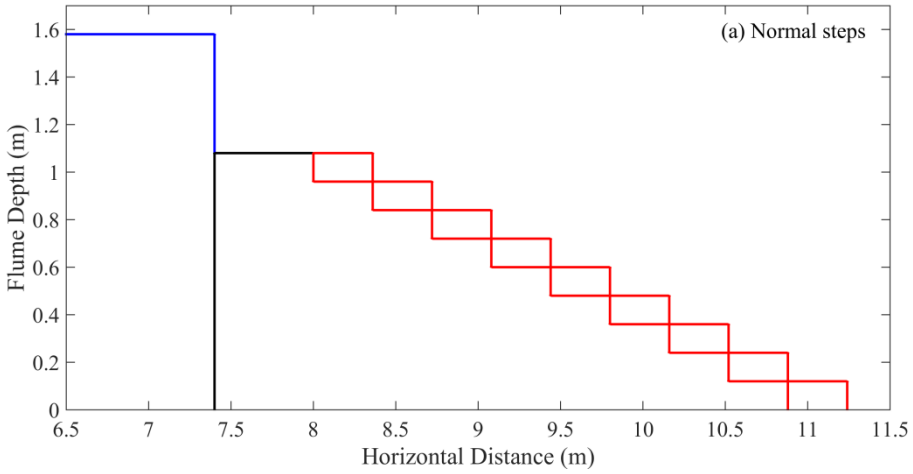
(a) Normal steps
Flume Depth (m)
Horizontal Distance (m)
0
0.2
0.4
0.6
0.8
1
1.2
1.4
1.6
6.5
7
7.5
8
8.5
9
9.5
10
10.5
11
11.5

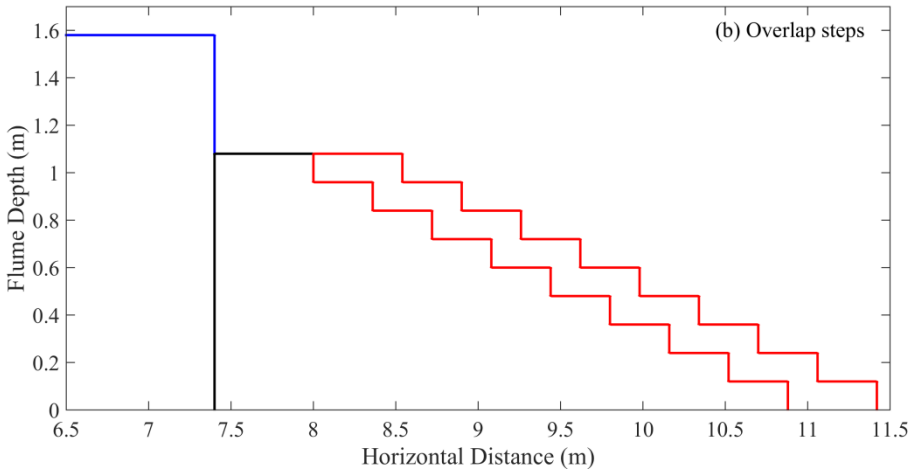
(b) Overlap steps
Flume Depth (m)
Horizontal Distance (m)
0
0.2
0.4
0.6
0.8
1
1.2
1.4
1.6
6.5
7
7.5
8
8.5
9
9.5
10
10.5
11
11.5

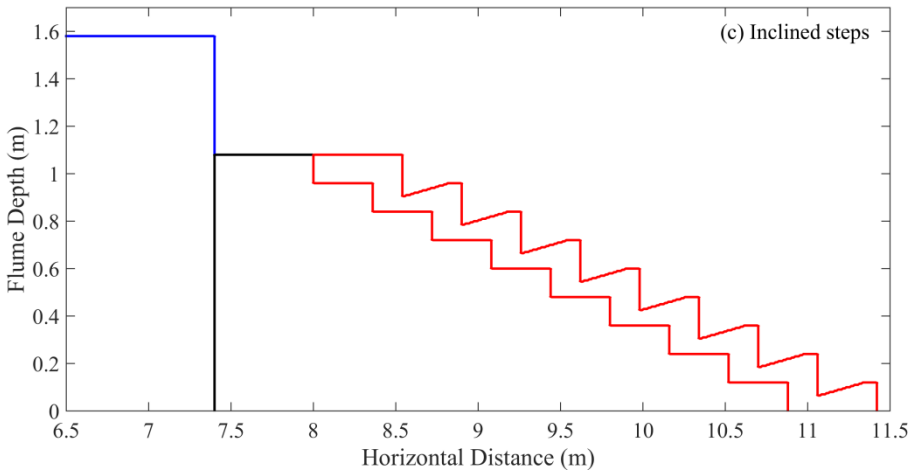
(c) Inclined steps
Flume Depth (m)
Horizontal Distance (m)
0
0.2
0.4
0.6
0.8
1
1.2
1.4
1.6
6.5
7
7.5
8
8.5
9
9.5
10
10.5
11
11.5

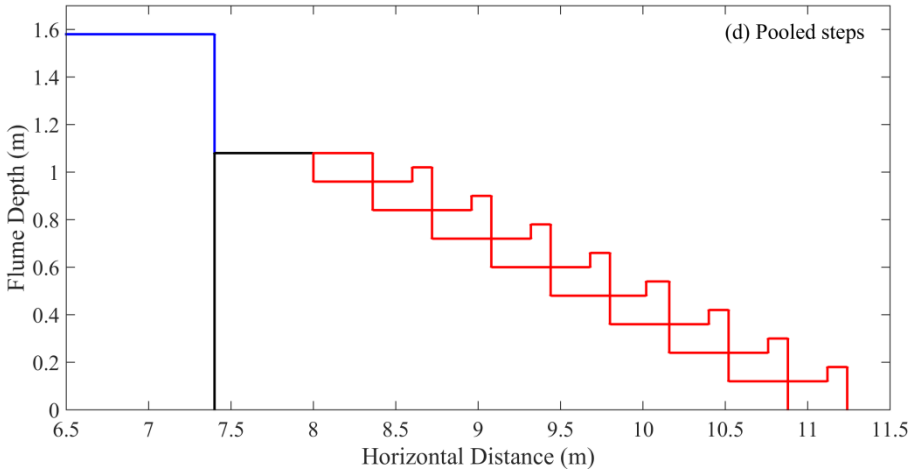

Figure 9.1 Different steps configuration: a) normal steps, b) overlap steps, c) inclined steps and d) pooled steps.

The same initial conditions were applied for all types of gabion stepped spillway to be able to make comparisons between them and also all the comparisons were conducted for a particular discharge at skimming flow stage.

The discharge was calculated by the same way which is conducted previously for the validation at the critical section over the broad crested weir, the critical section was located by testing Froude Number, so if the Froude Number equal to one, corresponding location represent the critical section over the broad crested weir. The width of the broad crested weir was selected to be 0.6m in order to localise the critical section of the required discharges in this study.

9.1.1. Time to establish skimming flow

Skimming flow is established when all of the air pockets inside and outside the gabions under the water free surface have disappeared. A comparison between the different configurations of gabion steps is shown in Table 9.1. The results reveal that the pooled gabion spillway needs more time to achieve skimming flow (4.91s) than the normal gabion which required just 3.18s to catch the skimming condition. Therefore, in terms of required time to attach the skimming flow, pooled gabion spillway reported the best result. It is worth to mention that skimming flow could be more dangerous than nappe

flow and transition flow. Consequently, it would be better to make the skimming flow late as possible and that clearly happened in the other types as shown in Table 9.1.

Table 9.1 Time to attach skimming flow for the different types of gabion stepped spillway.

Experiment Number	Type of gabion spillway	Time to achieve skimming flow in seconds
1	Normal gabion steps	3.18
2	Overlap gabion steps	3.63
3	Inclined gabion steps	4.22
4	Pooled gabion steps	4.91

9.1.2. Pressure distribution and velocity distribution

Some studies reported that over stepped spillways, pressure variation can consider as a vital parameter in the non-aerated zone under skimming flow conditions because of the significant relationship between the pressure and the formation of cavitation (Husain, 2013). Cavitation might cause damage which could occur due to the entrained air bubbles in the non-aerated zone. Many studies revealed that there is a high probability of having cavitation damage in the non-aerated zone as the absence of the air entrainment (Husain, 2013). A comparison of the pressure value at a certain place in the non-aerated zone has been conducted for different configurations of gabion stepped spillways. The results showed that normal steps have the lowest value for the pressure while pooled steps achieved the highest value with 2.317 $KN.m^{-2}$ (Table 9.2).

The pressure distribution over the horizontal faces of the steps in the non-aerated zone has been tested for the four configurations. Figure 9.2 shows that the pressure values over the non-aerated zone of gabion stepped spillways for normal gabion steps achieved the lowest values; however, overlap gabion steps had the highest values with a small difference from inclined gabion steps. Generally, the trend of the pressure distribution along the steps is quite similar for all four types. The variation in the pressure values

along the non-aerated zone is related to the location of the measured point over a particular step as the pressure value basically varies over each step depending on the distance from the step edges. Although, high pressure value can be observed near the outer edges, low pressure values might be observed near to the inner edges.

Table 9.2 Pressures values of different types of gabion stepped spillways.

Experiment Number	Gabion type	At 9.98m (near to the inception points)
1	Normal gabion steps	2.057 KN.m^{-2}
2	Overlap gabion steps	2.286 KN.m^{-2}
3	Inclined gabion steps	2.212 KN.m^{-2}
4	Pooled gabion steps	2.317 KN.m^{-2}

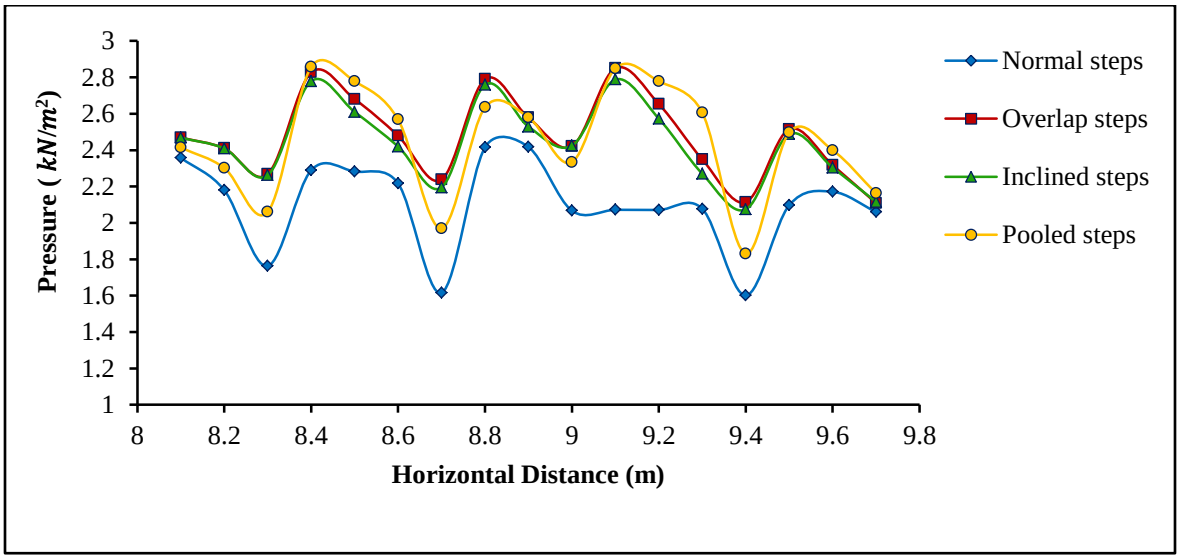

Figure 9.2 Pressure distribution for q=0.20m^2/s over few steps.

Furthermore, the comparison has moved onto velocities and velocity profile. The velocity distribution can play an important role in the design of gabion stepped spillways. Therefore, under the same flow rate q=0.2m^2/s, a comparison of water velocity was established for three different places in the non-aerated zone and for all types of the gabion spillway. The results indicated that the highest value for all places is observed for the normal gabion stepped spillway; however, the lowest value for the velocities is

attached with the overlap gabion spillway (Table 9.3). Figure 9.3 shows the velocity distribution at one point for four different types of spillways. At 9.25m, it can be noticed that normal steps have the largest velocities. The results revealed that there is no significant difference near the surface of the gabion, conversely, clear differences have been observed near the free surface of the water. Also, it is clear that both the overlap steps and the inclined steps have almost the same velocity distribution.

Table 9.3 Velocities at different locations of the different types of the gabion stepped spillways.

Experiment Number	Gabion type	At 8.5m	At 9m	At 9.5m
1	Normal gabion steps	1.847	2.637	3.264
2	Overlap gabion steps	1.707	2.379	2.985
3	Inclined gabion steps	1.707	2.386	2.988
4	Pooled gabion steps	1.806	2.377	3.059

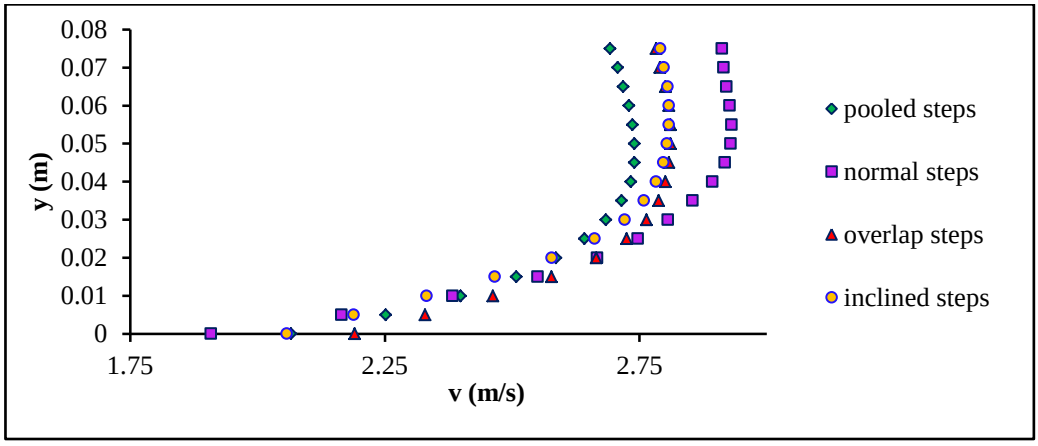

Figure 9.3 Velocity distribution of q=0.20m^2/s at 9.25m.

9.1.3. Energy dissipation

Energy dissipation can be considered the most important parameters from the hydraulic point of view for the designers; therefore, Bernoulli's equation has been used to calculate the energy dissipation for each of the gabion configurations. In brief, two points are

required to determine the energy dissipation (ΔH) (Figure 9.4), at the first point (under consideration in the non-aerated zone) H is calculated by using

$$H=y\cos\theta+\frac{\alpha V^2}{2g} \quad (9.1)$$

where

y: the perpendicular depth of the water over a pseudo-bottom, (m)

θ: the bottom chute slope, (degree)

α: the energy coefficient, (unitless)

g: the gravitational acceleration, (m/s^2)

V: average velocity, (m/s)

The second point is the upstream of the weir and the head is calculated as

$$H°=Y°+\frac{V°^2}{2g} \quad (9.2)$$

where

Y°: flow depth above the horizontal surface of the step under consideration, (m)

V°: approach flow velocity, (m/s)

g: the gravitational acceleration, (m/s^2)

Hence, the total dissipated energy with respect the point under consideration is:

ΔH=H°-H

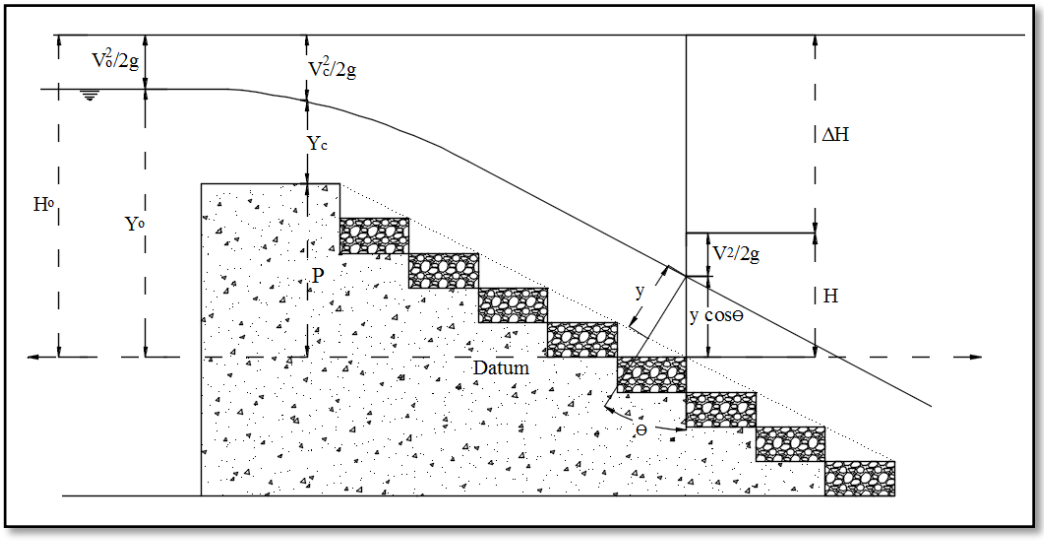

Figure 9.4 2D schematic view of a stepped spillway showing the parameters required to estimate the residual energy at the outer edge of steps.

Table 9.4 Energy dissipation of different types of the gabion stepped spillway.

Experiment Number	Gabion type	At 9.44m
1	Normal gabion steps	0.0994 m
2	Overlap gabion steps	0.0759 m
3	Inclined gabion steps	0.0688 m
4	Pooled gabion steps	0.0457 m

The results in Table 9.4 show that normal gabions have the best performance in terms of energy dissipation while the pooled spillway presents the worst performance which is probably related to the pressure. Usually, when the pressure is high, then less energy dissipation will be expected.

Moreover, another comparison has been conducted for the normal, overlap, inclined and pool steps in terms of turbulent kinetic energy. Turbulent kinetic energy (TKE) is associated with eddies in turbulent flow so there is a direct relation between the energy dissipation and TKE. Also, turbulent kinetic energy is the kinetic energy per unit mass of the turbulent fluctuations in a turbulent flow. For instance, when the eddy energy increases in turbulent flow due to one of the effective parameters such as fluid shear or friction, high values of TKE are expected and that could lead to an increase in the energy dissipation. The turbulent kinetic energy was computed directly from the instantaneous velocities over the whole domain (see Figure 9.5).

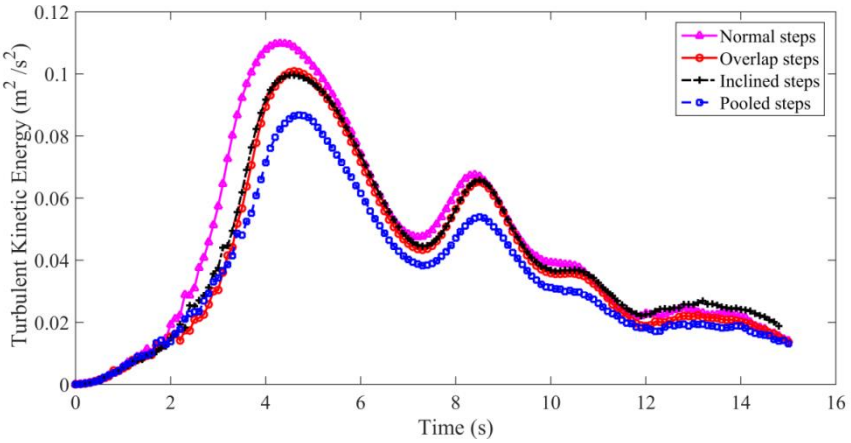

Figure 9.5 Turbulent kinetic energy of different gabion steps shape.

The plot shows the same morphology for the four configurations: from being initially at rest the fluid gradually accelerates down the spillway resulting in a rise in the TKE (Turbulent Kinetic Energy). There are some fluctuations in TKE as skimming flow establishes and it gradually reduces as the head in the upstream tank falls towards the level of the weir. Based on the TKE, the results revealed that the normal steps can dissipate more energy than the other shapes and clearly it is the same conclusion which achieved for the normal energy dissipation through the hand calculation above. For all types, there is an increasing in the energy at the ninth second and the reason for that related to increasing the discharge at this time due to the wavy movement of water in the upstream tank.

Finally, in order to ensure that normal steps can dissipate more energy compared to the other shapes, the total energy dissipation is plotted for the four configurations. Figure 9.6 illustrates that the normal steps have the best performance in terms of energy dissipation. This is due to the direct relationship between the turbulent kinetic energy and the energy dissipation rate. Therefore, the TKE can be used to indicate the energy dissipation over different configurations of gabion stepped spillways.

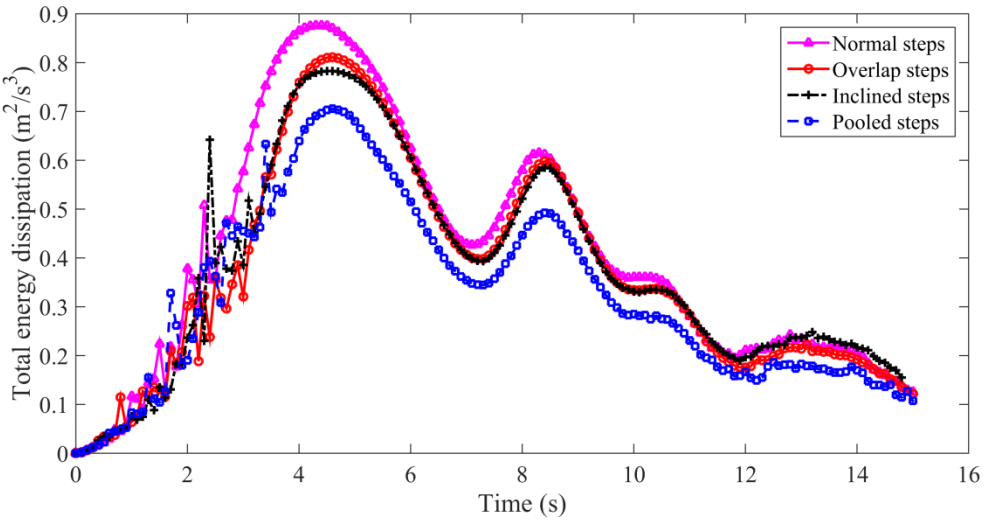

Figure 9.6 Total energy dissipation of different gabion steps shape.

It is worth to mention that the results of this section are contradictory to the previous results which have been obtained by the previous researchers as mentioned and discussed in Chapter 2. These results stated that pooled steps, adverse inclined steps and end sill steps can increase the energy dissipation rate compared to the plain steps (normal steps). It is clearly that the outcomes of the previous research have been based on the results of normal stepped spillways. Therefore, using the porous media steps might impact the performance of the steps. Also, the flow conditions may impact the results as under the nappe flow conditions some steps will perform in a different way compared to the skimming flow conditions.

9.1.4. Inception point location

The definition of the inception point was applied to determine its location (Figure 9.7), similar to the method which stated previously in the validation with Wüthrich and Chanson (2014). In Table 9.5, the results showed that the non-aerated zone for the normal gabion is smaller than the other types while the longest non-aerated zone has been observed for pooled gabion. Also, the results revealed that there is a small difference between the overlap gabion and the inclined gabion in terms of inception point location.

Table 9.5 Inception point location of different types of gabion stepped spillways.

Experiment Number	Gabion type	Inception point location (m)
1	Normal gabion steps	9.75
2	Overlap gabion steps	10.16
3	Inclined gabion steps	10.20
4	Pooled gabion steps	10.32

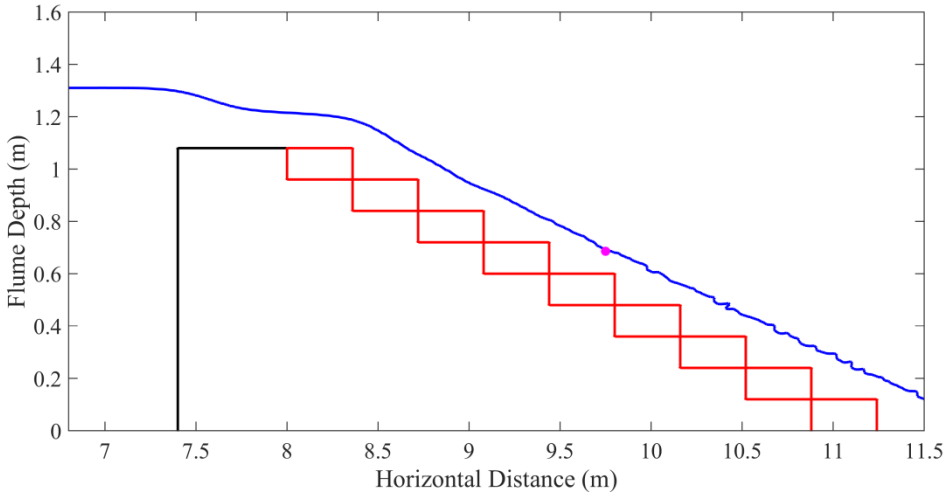

Figure 9.7 Inception point location for normal gabion steps.

After testing the four configurations, normal steps demonstrated the best results in terms of energy dissipation and the location of inception point; therefore, normal steps will be used to conduct further investigations about important hydraulic parameters such as energy dissipation, pressure distribution over the vertical and horizontal faces in the non-aerated zone and the location of the inception point with different porosity for the gabion and different grain size (D_{50}). As mentioned earlier, gabion stepped spillways have two types of flow: seepage flow through the porous media and flow over the porous media. It is worth mentioning that Wüthrich and Chanson (2014) revealed that some bubbles could be observed during the nappe flow conditions inside the gabion box. Once the flow rate increases, gabion boxes will start to be completely saturated so all bubbles will start to disappear. Also, Wüthrich and Chanson (2014) highlighted two main points, firstly, the inception point is clearly observed for the skimming flow regime, secondly, many differences arise due to seepage flow effect. Therefore, a series of experiments have been conducted with different values for the porosity and grain size to study the influence of porous parameters on hydraulic parameters.

9.2. Different geometries

In this section, different configurations of gabion stepped spillways will be investigated numerically in terms of energy dissipation, in order to understand how the energy can dissipate over the gabion steps and to obtain the optimal efficiency as the energy issue represents the main problem which might be achieved over stepped spillways generally.

Many solutions have been suggested to use the same conditions that can be observed in the mountain streams, as it has shown good efficiency of energy dissipating for the torrents naturally. This is due to the random distribution of the rock boulders which have different spacing and particle sizes. Canovaro et al. (2003) revealed that random distribution of the high gradient gravel bed can produce greater values of flow drag forces that may persuade shear stresses. Moreover, Sorensen (1985) revealed that the energy dissipation in stepped spillways depends on many functions like discharge, the slope of spillway and geometry of steps. Based on the literature, three different configurations for the steps have been suggested:

1) Install one or two blocks over the gabion steps

2) Change the crest's sharp edge of stepped spillways to a circular edge, and also that changing might include the shape of the slope beneath the gabion steps, where the slopes could be an inclined line of concrete or concrete steps.

3) Increase the number of the gabion layers over the concrete steps

Investigating these different configurations can increase the understanding of the energy dissipation over gabion stepped spillways and also might lead to increase the required time to attach the skimming flow under the dam break conditions as the skimming flow may represent the worst case which always needs to be avoided. Moreover, demonstrating how those configurations can affect the flow characteristics over the gabion steps.

9.2.1. Blocks fixed on the steps

Few studies have focused on the effect of the macro-roughness elements on the energy dissipation over stepped spillways (André, 2004). However, Peruginelli and Pagliara (2000) conducted an experimental study to investigate the influence of the carpet plastic grass over the steps and also steps endsills on the energy dissipation over the steps. They used the same chute slope 1V:2H with the same number of steps to observe how the energy dissipation can change because of the endsills and plastic grass. The results showed that, within the nappe flow conditions, both the endsills and the carpet can increase the energy dissipation rate by almost the same order. However, for the skimming flow, no effect can be observed on the rate of the energy dissipation due to the endsills or the carpet. In the present study, two cases have been conducted numerically with the same initial conditions in order to demonstrate the difference between using one block and two blocks in terms of energy dissipation rate over gabion steps, and then comparing both cases with the normal one, without any block.

The gabion stepped spillway was installed 8 m from the boundary edge, while the weir was set up at 7.4m from the edge, with a length of 0.6m. The initial water depth is 1.58m, which means the area of the upstream tank is 7.4m*1.58m and that should be enough to achieve the required discharge. The total time for the simulation has set up to 15s with 0.001s initial time step for the stability purposes. The mesh size in the x-direction and in the y-direction equal to 0.01m and 0.005m respectively, all of the boundary conditions were closed except the right boundary which has set to be an open boundary to let the water go out of the flume (Figure 9.8).

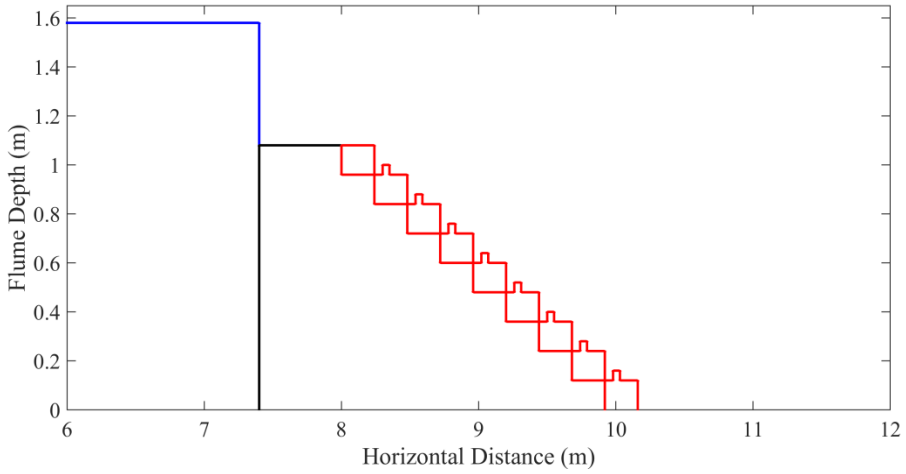

(a)

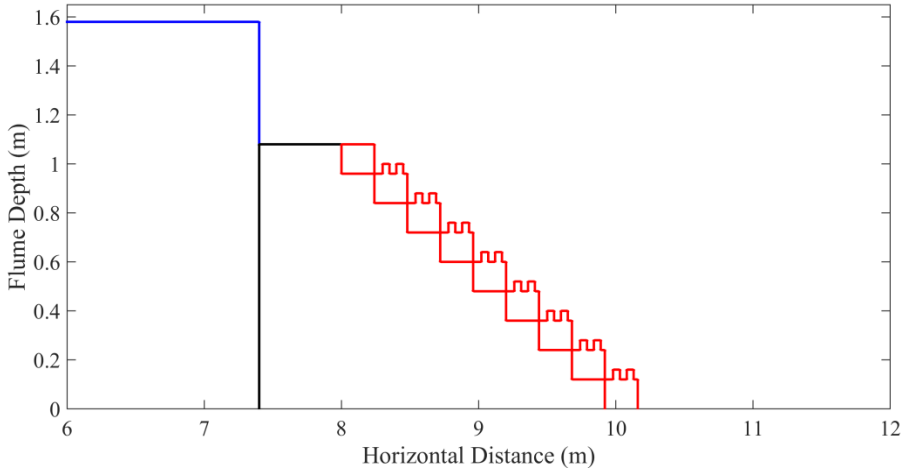

(b)

Figure 9.8 Blocks inserting over gabion steps: a) one block and b) two blocks.

Testing these configurations under the dam break condition can lead to unexpected results. At the beginning of the run, nappe flow is observed over the gabion steps, then after a certain time, the skimming flow starts. The necessary time to establish skimming flow is affected by the block configuration.

The results of the energy dissipation showed that the blocks can reduce the maximum value of the turbulent kinetic energy (TKE) and especially in the case of one block

(Figure 9.9). However, there are no significant changes between the two blocks case compared to the normal case without blocks. During the experiments, most of the time was under the skimming flow conditions where the blocks might not have a vital role in terms of energy dissipation rate. This is well agreed with the results of Peruginelli and Pagliara (2000), although gabion steps and gabion blocks have been used in the current work.

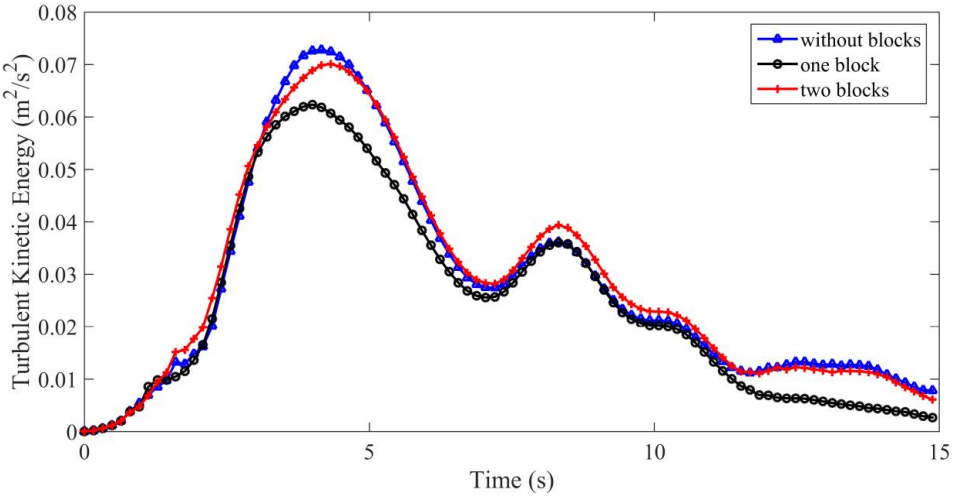

Figure 9.9 TKE over gabion stepped spillways with and without blocks.

As can be noted in Figure 9.9, the single block has reduced the TKE during the period 4-7s, and then it started to agree with the normal case for more than 4 seconds, and then it started to be less than the normal one. Therefore, having one or two blocks could be useful in terms of increasing the required time to attach the skimming flow by a very small rate. However, it would not be useful in terms of energy dissipation rate.

9.2.2 Different steps geometries

The purpose of this section is to investigate the effect of the round edges combined with the steps on the energy dissipation over gabion stepped spillways, and also to compare the turbulent kinetic energy when impermeable steps may use under the gabion steps or an impermeable inclined slope (Figure 9.10). From a practical point of view, using the inclined slopes beneath the gabion steps can lead to stability issues for the gabion steps,

especially during flooding events. However, these types of geometry might be able to provide good rates of energy dissipation.

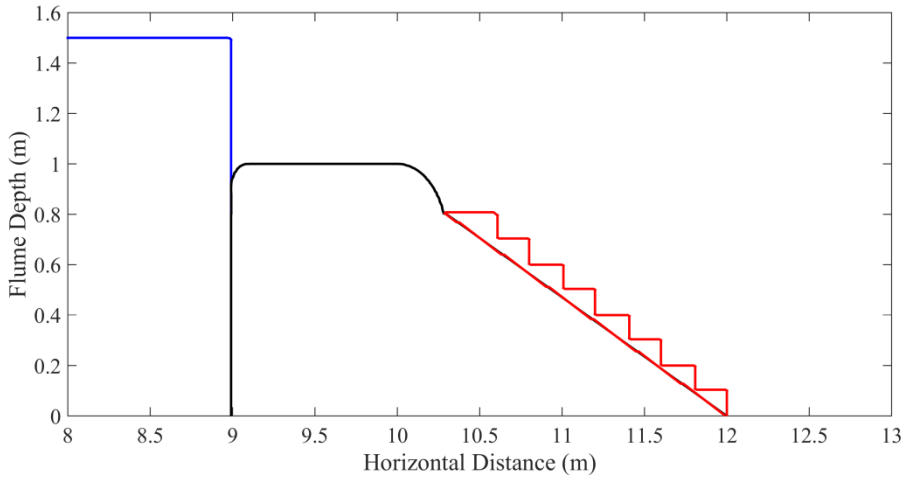

(a)

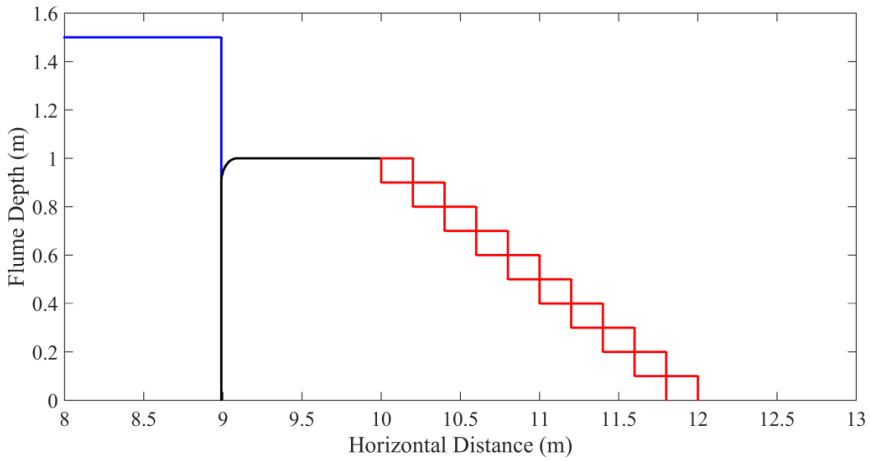

(b)

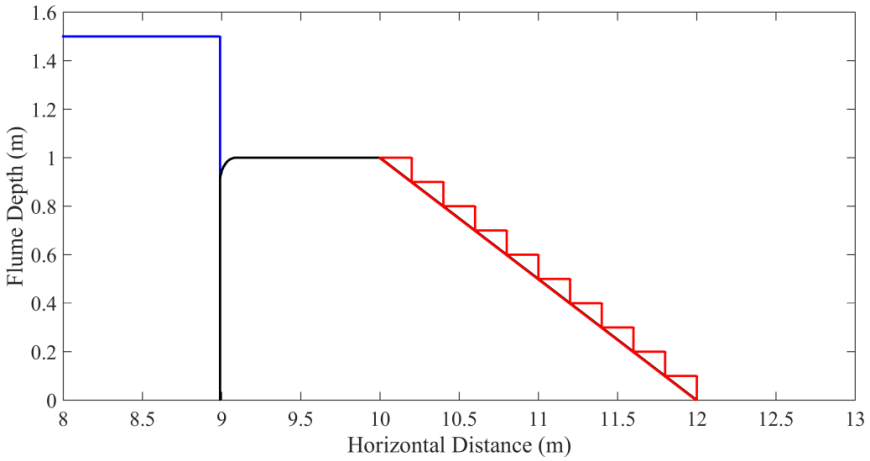

(c)

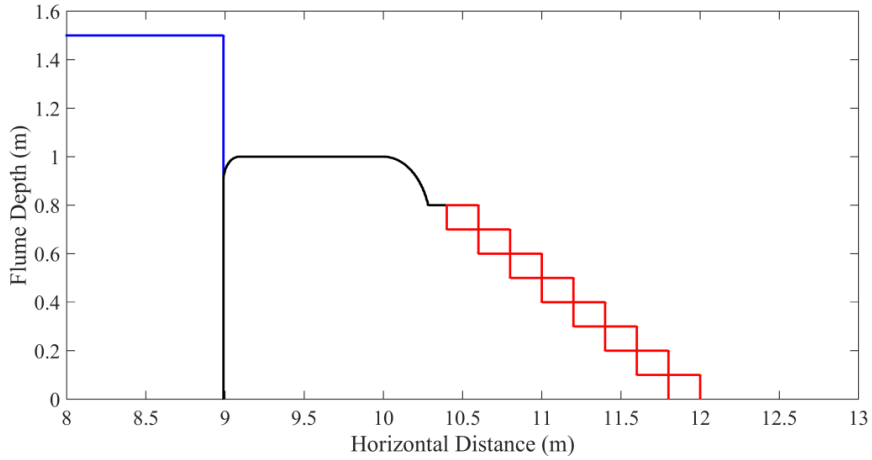

(d)

Figure 9.10 Different steps geometry: a) round edge with impermeable slope, b) sharp edge with impermeable steps, c) sharp edge with impermeable slope, and d) round edge with impermeable steps.

All the cases have been conducted numerically with the same initial conditions in order to compare the results in terms of energy dissipation rate over gabion steps. The gabion stepped spillway is fixed at 10m from the boundary edge, while the weir was set up at 9m from the edge with 1.0m length. The initial water depth is 1.50m, which means the area of the upstream tank is 9.0m*1.50m. The total time for the simulation has set up to 16s with 0.001s initial time step for the stability purposes. The mesh size in the x-direction

and in the y-direction has set up to 0.01m and 0.005m respectively for three cases, excluding the case which has the round edge with impermeable slope. In this case, the mesh size has increased to 0.016m in the x-direction and to 0.008m in the y-direction due to the stability issues. Similar to the previous tests, the boundary conditions have been applied which can present the dam break conditions.

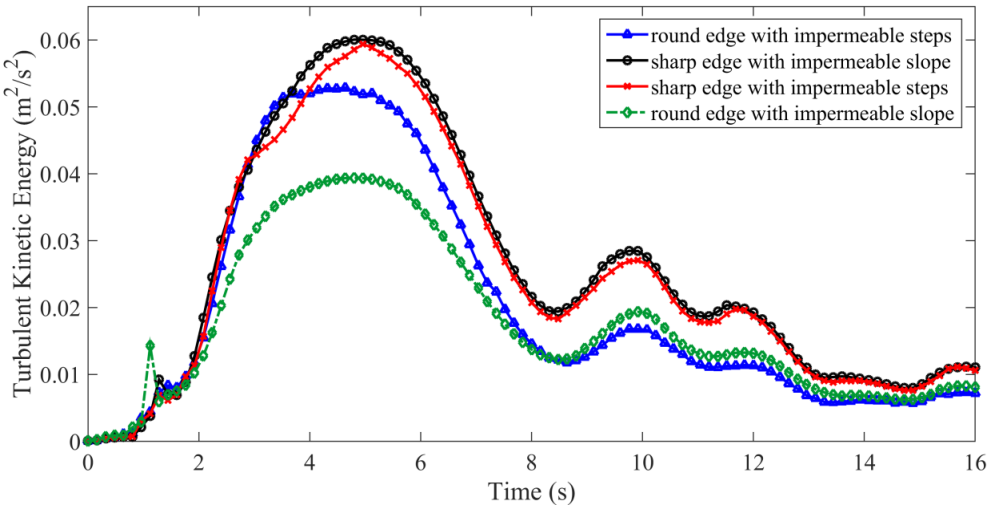

Figure 9.11 TKE over gabion stepped spillways with different geometry shapes.

As can be seen in Figure 9.11, using the round edge will generally reduce the rate of the turbulent kinetic energy. This can support the benefits from using stepped spillways instead of the other types such as ogee spillways as the steps have the ability to dissipate more energy. The impermeable layer beneath the gabion steps has shown an important impact on the turbulent kinetic energy. In other words, the geometry shape of the impermeable layer can affect the energy dissipation rate significantly. The impermeable steps, which are located under the gabion steps, of the sharp edge case showed nearly similar results to the impermeable inclined slopes of the sharp edge case. However, it is quite different to the round edge case where the impermeable steps showed more dissipation compared to the impermeable slope case. Generally, the impermeable steps can probably provide more stability for the gabion; this can also make the construction process easier compared to the inclined slope case.

9.2.3. Increase the gabion layers

Increasing the area of porous media generally could be very useful as that will increase the required time to attach the skimming flow. Wüthrich and Chanson (2014) revealed that the porous media might not have a significant impact on the rate of the energy dissipation under the skimming flow conditions; however, it could have a vital role within the nappe flow conditions. Therefore, increasing the time of having nappe flow would be valuable. Beside to the single layer of the porous media, two cases with 2 and 3 layers have been added to the current work in order to investigate the relationship between the rate of the energy dissipation and the number of layers of porous media numerically (Figure 9.12). Three bottom chute slopes 1V:2.0H, 1V:2.5H and 1V:3.0H have been tested with same initial conditions to compare the results.

All gabion stepped spillways were placed at distance 8m from the boundary edge, while the weir is positioned at distance 7.4m from the edge with 0.6m length. The initial water depth was 0.5 m over the crest level, so the area of the water over the crest is 7.4m*0.5m. For the stability requirements, the initial time step was set up to be 0.001; however, the total time for the simulation equals to 15s. The mesh size in the x-direction and in the y-direction was equal to 0.01m and 0.005m respectively, all of the boundary conditions were closed except the right boundary which has set to open boundary condition to let the water go out of the flume.

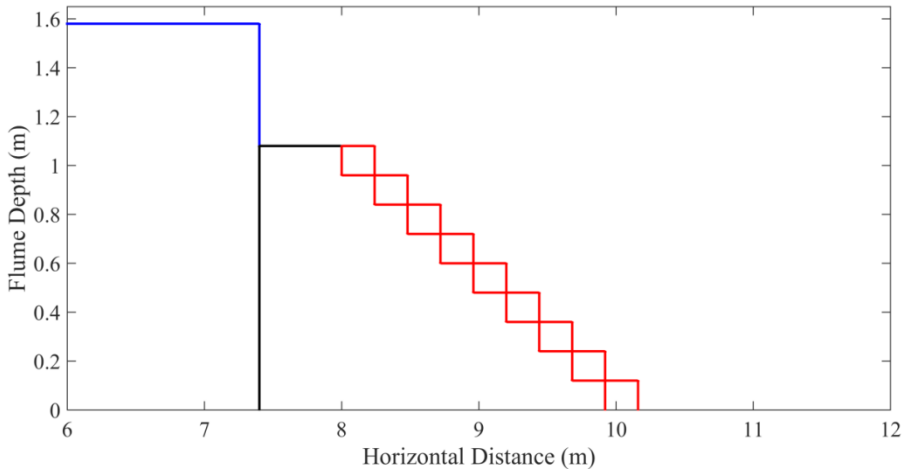

(a)

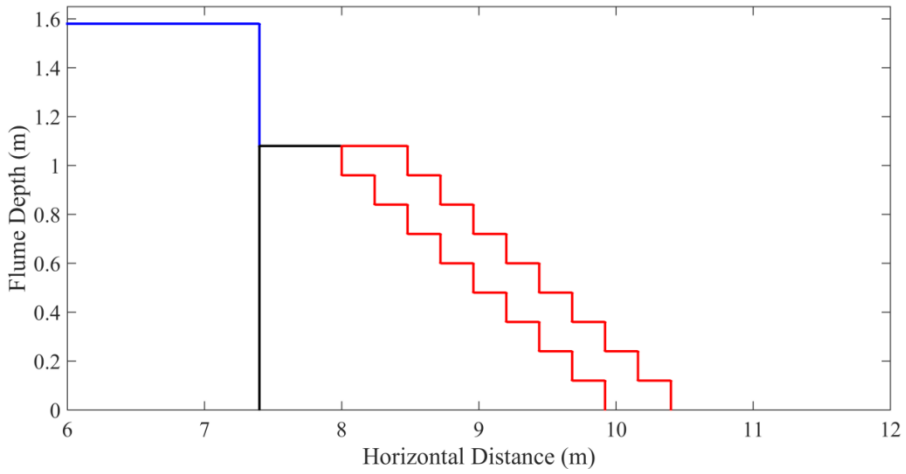

(b)

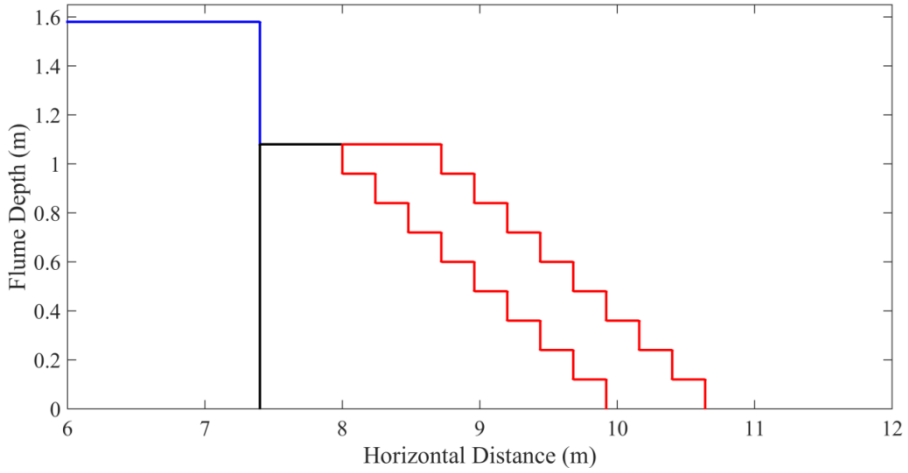

(c)

Figure 9.12 Different numbers of porous media over steppes spillways: a) single layer, b) two layers and c) three layers.

As can be seen in Figure 9.13, all the chute slopes showed the same trend in terms of turbulent kinetic energy behaviour. The results revealed that for the single layer test, the energy may start to dissipate earlier compared to the other cases which have 2 and 3 layers. The results also showed that the highest value has been observed for the single layer case.

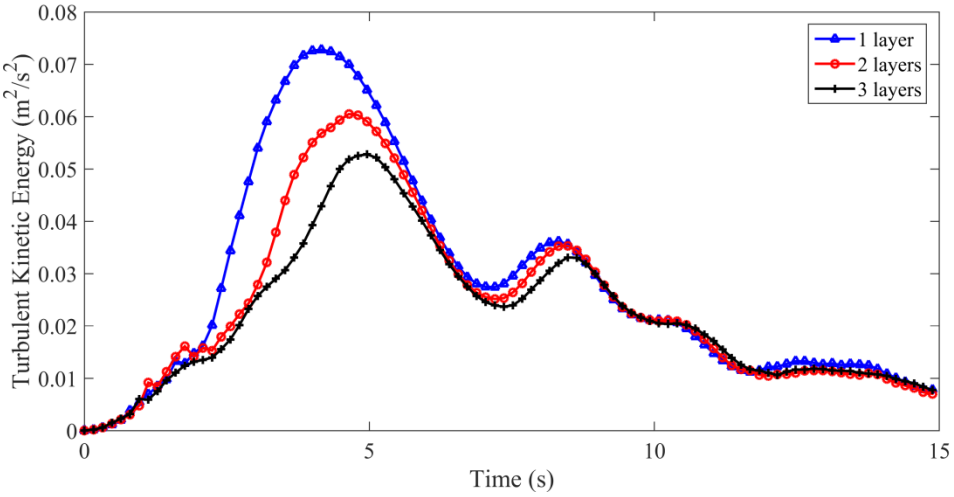

(a)

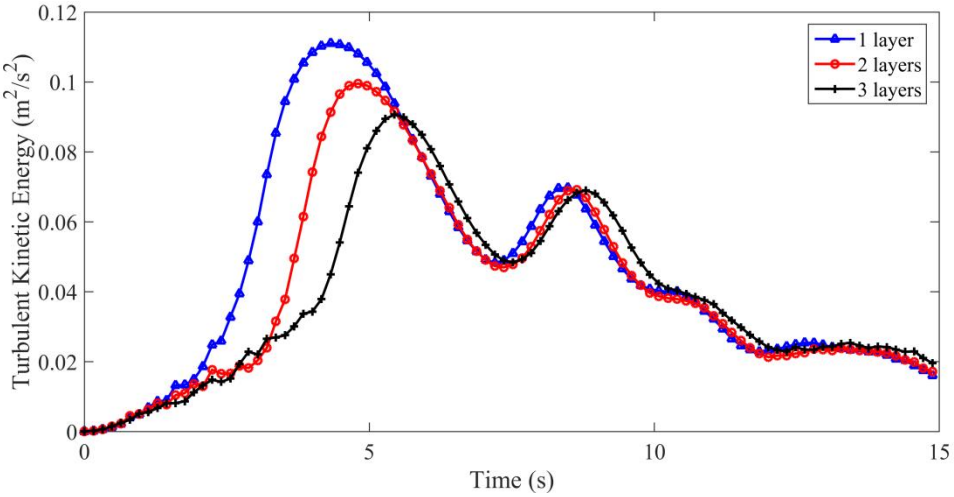

(b)

Figure 9.13 Turbulent kinetic energy distribution through 15s over gabion steppes spillways: a) 1V:2.0H and b) 1V:3.0H.

According to the computational results, any increase in the number of the gabion layers can be very useful as it can increase the time to attach skimming flow by varied percentages depending on the initial water depth. However, using more layers has caused an opposite effect to the energy dissipation rate over the gabion steps and that was counterintuitive (Figure 9.13). It can be concluded that increasing the number of layers

leads to a reduction in the energy dissipation rate over the gabion steps due to the turbulence reduction as the water would flow inside the porous media calmly without producing turbulence.

Chapter 10 : Conclusions and Recommendations for Future work

10.1. Introduction

The present research was conducted numerically to investigate skimming flow conditions over moderate slopes of gabion stepped spillways. The attention was specifically on the properties of the skimming flow over the non-aerated flow region. All previous studies on gabion stepped spillways have been carried out experimentally. For this reason, the 2D numerical model NEWFLUME was applied. The study explored the impacts of step height and chute slope on the characteristics of the skimming flow along the non-aerated zone over gabion stepped spillways. It also sought the gabion parameters like the porosity of the gravels, in addition to gravels particle sizes. Furthermore, the research investigated the potential for cavitation formation on moderate slopes of gabion stepped spillways.

Understanding the features of the skimming flow regime in the non-aerated flow region is significantly crucial to develop the design of gabion stepped spillways, and also the downstream slope of small embankment dams. This study aimed to answer the following key research questions:

1- Are the numerical codes capable to simulate the flow over and inside gabion stepped spillways?
2- What effects do the step height, chute slope and steps shape have on the main elements of the design of this type of hydraulic structure? These main elements include the location of the inception point, the growth of the turbulent boundary layer, pressure on both step faces and the energy dissipation rate.
3- Is it possible to observe cavitation over gabion stepped spillways?
4- How the energy dissipation can be affected when different configurations of the gabion steps are used?

This chapter initially presents the main findings that have been achieved in the current work and then highlights the main implications and limitations of the current study. Finally, some suggestions will be presented for directions and areas of future works.

10.2. Synthesis of research findings

This section synthesizes the main outcomes that have been achieved and also answers the research questions which are raised in this study. The first research question was about the capability of the numerical codes to simulate the flow over gabion stepped spillways and also the seepage flow inside the gabion. For this purpose, the numerical 2D NEWFLUME code was applied. The computational code was calibrated and validated against the experimental data that collected from experiments conducted previously. These laboratory data are

- The flow over broad-crested weirs carried out by Hager and Schwalt (1994),
- The skimming flow over moderate slope stepped spillways conducted by Meireles and Matos (2009).

Then, the validation process was extended to two more sets of experimental data that conducted by Chanson and Toombes (2002) and Hunt and Kadavy (2013). The extension in the validation process was taken place as the three cases of stepped spillways were different in terms of the discharge values and the spillway geometry which includes the slope and number of the steps. Since the previous validations were applied for normal stepped spillways, another validation for gabion stepped spillways was conducted using the experimental data of Wüthrich and Chanson (2014). Furthermore, the numerical code was compared with the experimental results of normal stepped spillways and gabion stepped spillways that conducted in the present work. The PIV technique was used to measure the velocity distribution over both spillways.

Generally, the comparisons between the computational and experimental results were made in order to verify the accuracy and efficiency of the numerical model that has been used in the current study. The agreement between the computational results and the measured data for all cases was fairly good. This shows that the numerical model can be

used to simulate the flow over both normal stepped spillways and gabion stepped spillways.

The computational code was then applied to examine twenty-seven cases of gabion stepped spillways with different step heights, slopes, diameter sizes and porosity. These tests have been set to investigate the position of water surface level, the location of the inception point, velocity distribution, pressure distribution, and energy dissipation. Also, to assess the cavitation over gabion stepped spillways.

The second research question in this study was about the step geometry impact on the characteristics of the skimming flow conditions over gabion stepped spillways. Initially, the free surface of the water flow over gabion stepped spillways was investigated with different cases. Then, the length of the non-aerated region was the next parameter that needed to be demonstrated. The length of the non-aerated zone was determined by using the definition of the inception point which states that it represents the intersection point between the free surface of the water and the turbulent boundary layer thickness. Based on the computational results of this study, an equation was developed to determine the location of the inception point over gabion stepped spillways. Also, another equation was developed to estimate the water depth at the inception point. These equations showed that in addition to the unit discharge; the step height and chute slope are two important factors that must also be considered in determining the inception point location over gabion stepped spillways.

The accuracy of these equations was examined by comparing their results with the previous correlations which are developed on moderate slope stepped spillways. Some discrepancies were observed between the computational results obtained in this study and those correlations of past experimental works. This is because all of the previous equations were developed for normal stepped spillways rather than gabion stepped spillways. Therefore, gabion occurrence needs to be considered since it can affect the lactation of the inception point significantly.

This investigation has also highlighted the influences of the step geometry and chute slope on the growth of the turbulent boundary layer. The numerical results obtained in this study showed that boundary layer growth could be associated with step height.

However, chute slope has less impact on the development of the turbulent boundary layer. Gabion porosity and gabion particle sizes might have a slight effect on the boundary growth. The outcomes attained in the current work showed that flow conditions and geometry conditions can impact the growth of the boundary layer, and that was in agreement with what has been observed by other researchers on normal stepped spillways. Nevertheless, there is no definite equation to assess the growth of the boundary layer on stepped spillways. Using the computational results from various step heights, chute slopes, porosity, particle sizes and discharges, an equation was developed to calculate the thickness of the turbulent boundary layer in the non-aerated flow zone over gabion stepped spillways.

Additionally, the effect of step geometry on characteristics of the velocity distribution for different flow rates was addressed. To do so, the velocity profiles at the outer edges of a number of steps, located at different distances from the weir crest over the non-aerated zone, were computed for different flow rates. The numerical results exposed that for the same chute slope using large step height can decrease the mean flow velocity close to the inception point. It was also found that both porosity and particle sizes can have a minor impact on the velocity distribution.

The effect of the discharge and step geometry on the energy dissipation rate in the non-aerated flow region over gabion stepped spillways was one of the elements that investigated in the current research. The computational results revealed that the energy dissipation rate is affected by the unit discharge, step height and chute slope. Based on the computational results achieved in this study, an equation to examine the energy dissipation rate at any section along the non-aerated flow zone was obtained.

Furthermore, the influence of step geometry and unit discharge on the pressure distribution along the non-aerated regime was investigated in the current work. The pressure distribution acting on the vertical and horizontal faces of a number of steps was considered. These steps were positioned at different distances from the downstream face of the weir crest. This can give the opportunity to observe whether the pressure near to these faces is enough to cause cavitation damages on the steps. It was observed that for a given chute slope and unit discharge the pressure values along both steps faces increase

as the step height is increased. Also, the results revealed that for a given step height and unit discharge the pressure values acting on both steps faces increase as the chute slope is decreased. Gabion porosity and gabion particle sizes can impact the pressure distribution over both faces in the non-aerated zone.

These demonstrate that cavitation might occur over gabion stepped spillways when small step heights and steep chute slopes are used as these are more subject to such kind of damage than larger step heights and flatter chute slopes.

The third research question in the current investigation asked whether cavitation is capable to occur on moderate slopes of gabion stepped spillways, and what the maximum velocity is that can be passed safely over gabion stepped spillways. This is because no attention has been paid to cavitation formation on the moderate slopes of gabion stepped spillways, and also the maximum velocity above which such damage can occur. In order to achieve that, the critical cavitation index number was determined from experiments that have done previously. It is important to highlight that the cavitation index which used in this study has been established for moderate slope stepped spillways. The mean flow velocity and minimum pressure at different sections along the non-aerated flow region were considered in the calculations. The computational results showed that there is no risk to have cavitation damage under the conditions which are conducted in the current work.

To answer the last research question, the validated code was applied to test different configurations of steps geometry in terms of energy dissipation. The results showed that the normal steps can dissipate more energy compared to the other types. Also, inserting blocks over the steps might not significantly affect the rate of the energy dissipation. Moreover, increasing the number of the gabion layers could be useful to delay the skimming flow under the dam break conditions. However, it has a negative impact on the energy dissipation rate as increasing the number of the gabion layers can lead to reducing the energy dissipation over gabion stepped spillways.

10.3. Implications and limitations of this study

The current study delivers more insight into the skimming flow properties over gabion stepped spillways. The contribution of this work may be represented by extending the current knowledge of the non-aerated zone by suggesting a number of equations which could be used in establishing the design elements of the downstream slope of embankment dams subject to overtopping during times of peak flow.

These elements include:

1- The location of the inception point and the water depth at it. This element is significantly essential in the design of gabion stepped spillways as it can show whether the self-aeration mechanism will occur over the structure or not. Two equations were proposed in this study in order to predict the location of the inception point and the water depth at it over gabion stepped spillways. These equations cannot be applied for gabion stepped spillways when the slopes are steeper than 1V:2H or flatter than 1V:3H. These equations are valid only with step heights between 0.30m and 1.2m. These equations can be applied when the roughness Froude numbers less than 11.

2- Energy dissipation rate. This parameter has crucial effects on the design of the stilling basin which can be located at the end of the downstream, in order to avoid the scouring and the erosion at that place. The stilling basin has the ability to dissipate more energy, especially when the downstream length of the gabion stepped spillway is relatively small, thus the self-aeration mechanism might not occur.

10.4. Suggestions for future research

The following extra investigations need to be conducted to recognise the properties of the flow over gabion stepped spillways:

1- In this study, a single phase flow model is used to characterise the skimming flow properties over gabion stepped spillways, known as the non-aerated flow region,

where air content entirely absent. The detailed information regarding the skimming flow properties over the aerated flow region is still lacking. Therefore, it would be interesting to apply a two-phase flow, water and air, to estimate the global energy dissipation rate over gabion stepped spillways.

2- This work provides new insights into the skimming flow condition over gabion stepped spillways. The behaviour of the nappe and transition flow regimes has not yet been investigated numerically. It would, therefore, be interesting to conduct further research to give more definitions of the hydraulic details of the flow over gabion steps.

3- Using 3D models with different numerous techniques to investigate the energy dissipation mainly and all other design parameters over gabion stepped spillways. Also, it would be attractive to demonstrate the seepage flow inside the porous media in the non-aerated by using 3D models to compare it with the results of the 2D models.

4- Investigate the performance of the computation SPH particle-based method, in simulating the flow over and inside gabion stepped spillways in both non-aerated and aerated zones.

5- Examine the differences in the results of the numerical models when prototype scales apply instead of the model scales.

References

Ab Ghani, a., Sarkardeh, H., Pahlavan, H., Azamathulla, H. M., Marosi, M. and Roshan, R. (2010). Hydraulics of stepped spillways with different numbers of steps. *Dams and Reservoirs*, *20*(3), pp. 131–136. http://doi.org/10.1680/dare.2010.20.3.131.

Abbasi, S. and Kamanbedast, A. (2012). Investigation of Effect of Changes in Dimension and Hydraulic of Stepped Spillways for Maximization Energy Dissipation. *World Applied Sciences Journal*, 18(2), pp.261-267.

Ahadian, J. and Aghamajidi, R. (2014). Investigation of Geometric Effect of Steps on energy dissipation on Stepped Spillway. *International Journal of Engineering & Technology*, *2*(2), pp. 491–503. http://doi.org/10.14419/ijet.v3i4.3561.

Alghazali, N. and Jasim, S. (2014). Experimental Study on the Limits of Flow Regimes for Different Configurations of Stepped Spillway. *Civil and Environmental Research*, 6(6).

Amador, A, Van der Graaf, G., Sanchez-Juny, M., Dolz, J., Sanchez-Tembleque, F. and Puertas, J., (2004). Characterization of the flow field in a stepped spillway by PIV. 12th Int Symp on the Application of laser anemometry to fluid mechanics, Lisbon, Portugal.

Amador, A., Sánchez-Juny, M. and Dolz, J. (2009). Developing Flow Region and Pressure Fluctuations on Steeply Sloping Stepped Spillways. *Journal of Hydraulic Engineering*, 135(12), pp. 1092-1100.

Amador, A., Sanchez-Juny, M. and Dolz, J. 2006. Characterization of the Nonaerated Flow Region in a Stepped Spillway by PIV. *Jl of Fluids Engineering*, ASME, Vol. 128, No. 6, pp. 1266-1273.

Amador, A., Van der Graaf, G., Sánchez-Juny, M., Dolz, J., Sanchez-Tembleque, F., Puertas, J., and Girona, C. J. (2004). Characterization of the flow field in a stepped spillway by PIV. In *Proc. 12th Symp. Applications Laser to Fluid Mechanics* (pp. 12-15).

André, S. (2004). High velocity aerated flows on stepped-chutes with macro-roughness elements. *Communication 20.* Lausanne, Switzerland: Laboratorie de Constructions Hydrauliques Ecole Polytechnique Federale de Lausanne;.ISSN: 1661–1179.

André, S., and Schleiss, A. (2004). *High velocity aerated flows on stepped chutes with macro-roughness elements* (No. LCH-BOOK-2008-020). EPFL-LCH.

André, S., Boillat, J. L., Schleiss, A. J., and Matos, J. (2004). Energy dissipation and hydrodynamic forces of aerated flow over macro-roughness linings for overtopped embankment dams. In *Hydraulics of Dams and River Structures: Proceedings of the International Conference, Tehran, Iran, 26-28 April 2004* (p. 189). CRC Press.

André, S., Matos, J., Boillat, J.-L., and Schleiss, A. (2004). Energy Dissipation and Hydrodynamic Forces of Aerated Flow over Macro-roughness Linings for Overtopped Embankment Dams.

Atencio, B., 2011. *Measurements and Prediction of Laminar-Turbulent Transition at High Free-Stream Turbulence in Boundary Layers with Pressure Gradients*, Sweden: Chalmers University of Technology.

Barani, G.A., Rahnama, M.B. and Sohrabipoor, N. (2005). Investigation of flow energy dissipation over different stepped spillways. *American Journal of Applied Sciences*, 2(6) pp. 1101-1105.

Beitz, E., and Lawless, M. (1992). Hydraulic model study for dam on GHFL 3791 Isaac River at Burton Gorge. *Water Resources Commission Report*, Brisbane, Australia.

Bindo, M., Gautier, J. and Lacroix, F. (1993). The Stepped Spillway of M'Bali Dam. *Intl Water Power and Dam Construction*, Vol. 45, No. 1, pp. 35-36.

Boes, R. and Minor, H. E. (2002). Hydraulic design of stepped spillways for RCC dams. *International Journal on Hydropower and Dams*, 9(3): pp.87-91.

Boes, R. M. (1999). Physical model study on two-phase cascade flow. In *Proc. 28th IAHR Congress*. Graz, Austria.

Boes, R. M. and Hager, W. H. (2003). Hydraulic design of stepped spillways. *Journal of Hydraulic Engineering*, 129(9): pp.671-679.

Boes, R. M., and Hager, W. H. (1998). Fiber-optical experimentation in two-phase cascade flow. In *Proc. Intl. RCC Dams Seminar*. Denver Colorado, Schabel Engineering.

Boes, R.M. (1999). Physical model study on two-phase cascade flow. In *Proc. 28th IAHR Congress*. Graz, Austria.

Calitz, J. A. (2015). *Investigation of air concentration and pressures of a stepped spillway equipped with a crest pier* (Doctoral dissertation, Stellenbosch: Stellenbosch University).

Canovaro, F., Paris, E. and Solari, L. (2003). Analysis of resistance of flow over macro-scale roughness: first results, *XXX IAHR Congress on water Engineering and research in*

a learning society: Modern Development and Traditional Concepts, Vol. Theme C: Hydraulic Resistance, IAHR, Thessaloniki, Greece, pp.1-8.

Carosi, G. and Chanson, H. (2008). Turbulence characteristics in skimming flows on stepped spillways. *Canadian Journal of Civil Engineering*, 35(9): 865-880.

Chakib, B. (2013). Numerical Computation of Inception Point Location for Flat-sloped Stepped Spillway. *International Journal of Hydraulic Engineering*, *2*(3), 47–52. http://doi.org/10.5923/j.ijhe.20130203.03.

Chamani, M. R. (2000). Air inception in skimming flow regime over stepped spillways. In. H. E. Minor e W. H. Hager (Ed.) International Workshop on Hydraulics of Stepped Spillways, Zürich, Switzerland: 61-67. Balkema.

Chamani, M. R. (2000). Air inception in skimming flow regime over stepped spillways. In *Proc., Int. Workshop on Hydraulics of Stepped Spillways* (pp. 61-67). Balkema, Rotterdam, The Netherlands.

Chamani, M. R. and Rajaratnam. N. (2000). Onset of skimming flow on stepped spillways. *Journal of Hydraulic Engineering*, 125: 969-971.

Chamani, M. R., and Rajaratnam, N. (1999). Characteristics of skimming flow over stepped spillways. *Journal of Hydraulic Engineering*, *125*(4), 361-368.

Chamani, M.R. (2000). Air Inception in Skimming Flow Regime over Stepped Spillways. *proc. Intl Workshop on Hydraulics of Stepped Spillways*, Zürich, Switzerland, Balkema Publ., pp. 61-67.

Chanson, H. (1993). Stepped spillway flows and air entrainment. *Canadian Journal of Civil Engineering*, 20: 422-435.

Chanson, H. (1994). Hydraulics of skimming flows over stepped channels and spillways. *Journal of Hydraulic Research*,32(3),pp.445–460.

Chanson, H. (1995). *Air bubble entrainment in free-surface turbulent flows: Experimental investigations*, Report CH46/95, Dept. of Civil Engineering, University of Queensland, Australia, June, 368 pages.

Chanson, H. (1995). History of stepped channels and spillways: a rediscovery of the 'wheel'. *Canadian Journal of Civil Engineering*, 22(2): pp.247-259.

Chanson, H. (1996). Prediction of the transition nappe/skimming flow on a stepped channel. *Journal of Hydraulic Research*, IAHR, 34(3): pp.421-429.

Chanson, H. (1997). *Air bubble entrainment in free-surface turbulent shear flows*. Academic press, London.

Chanson, H. (2000a). Characteristics of Skimming Flow over Stepped Spillways. *Journal of Hydraulic Engineering*, 126(11): pp.862-865.

Chanson, H. (2000b). Embankment overflow stepped spillways and Earth dam spillways with precast concrete blocks. *Internet Resource*, 1-1.

Chanson, H. (2002). *Hydraulics of stepped chutes and spillways*. CRC Press.

Chanson, H. (2004). *The hydraulics of open channel flow: an introduction*, 2nd edition. Butterworth-Heinemann, Oxford, UK.

Chanson, H. (2005). Discussion of "hydraulic design of stepped spillways" by Robert M. Boes and Willi H. Hager. *Journal of Hydraulic Engineering*, 131: 521- 524.

Chanson, H. (2006). Hydraulics of skimming flows on stepped chutes: The effects of inflow conditions?. *Journal of Hydraulic Research*, 44: 51-60.

Chanson, H. (2007). "Embankment overflow protection systems and earth dam spillways" "In: dams: Impacts, stability and design", Nova Science Publishers, Hauppauge NY, USA, Ed. W.P. Hayes and M.C. Barnes, Chapter 4, pp. 101-132.

Chanson, H. and Gonzales, C.A. (2004). Stepped Spillways for Embankment Dams. Review, Progress and Development in Overflow Hydraulics. Hydraulics of Dams and River Structures, Yazdandoost and Attari (eds), Taylor and Francis Group, London.

Chanson, H. and Gonzalez, C. (2005). Physical modelling and scale effects of air- water flows on stepped spillways. *Journal of Zhejiang University-Science*, A 6(3): 243-250.

Chanson, H. and Toombes, L. (2004). Hydraulics of stepped chutes: The transition flow/ L'hydraulique des chutes en marches d'escalier: L'ecoulement de transition. *Journal of Hydraulic Research*, 42: 43-54.

Chanson, H. and Toombes, L. (1997). *Flow aeration at stepped cascades*. Brisbane, Australia, Univ. of Queensland.

Chanson, H. and Toombes, L. (2002). Experimental study of gas-liquid interfacial properties in a stepped cascade flow. *Environmental Fluid Mechanics*, 2(3): 241-263.

Chanson, H. and Toombes, L. (2003). Strong interactions between free-surface aeration and turbulence in an open channel flow. *Experimental Thermal and Fluid Science*, 27(5): 525-535.

Chanson, H., and Gonzalez, C. A. (2004). Stepped spillways for embankment dams: Review, progress and development in overflow hydraulics. In *Hydraulics of Dams and River Structures* (pp. 287-294).

Chanson, H., and Tommbes, L. (2002). Experimental Investigation of Air Entrainment in Transition and Skimming flows down a stepped Chute. *Can J Civil Eng*,29, pp.145-156.

Chanson, H., and Toombes, L. (1997). *Flow aeration at stepped cascades* (No. CE155). University of Queensland.

Chanson, H., Yasuda, Y. and Ohtsu I. (2002), Flow resistance in skimming flows and its modelling, *Can. J. Civ. Eng*. 29 (6), pp. 809–819.

Chanson, H., Yasuda, Y. and Ohtsu, I. (2000). Flow Resistance in Skimming Flow: A Critical Review. *Proc. Int. Workshop on Hydraulics of Stepped Spillways*, VAW, ETH Zurich, Minor, H.E., and Hager, W.H., (eds). Balkema, Rotterdam, pp. 95-102.

Chanson, H., Yasuda, Y. and Othsu, I. (2002). Flow resistance in skimming flows in stepped spillways and its modelling. *Canadian Journal of Civil Engineering*, 29(6): 809-819.

Chatila, J. G. and Jurdi, B. R. (2004). Stepped spillway as an energy dissipater. *Canadian Water Resources Journal*, 29: pp. 147-158.

Chen, S. (2015). *Hydraulic structures*. Berlin Heidelberg: Springer-Verlag. http://doi.org/10.1007/978-3-662-47331-3.

Cheng, N. S. (2007). Power-law index for velocity profiles in open channel flows. *Advances in water Resources*, *30*(8), pp. 1775-1784.

Chinnarasri, C. (2002). Assessing the Flow Resistance of Skimming Flow on the Step Faces of Stepped Spillways. *Dam Eng.*, 12, pp. 303–321.

Chinnarasri, C. and Wongwises, S. (2004). Flow regimes and energy loss on chutes with upward inclined steps. *Canadian Journal of Civil Engineering*, 31(5), pp. 870-879.

Chinnarasri, C., Donjadee, S. and Israngkura, U. (2008). Hydraulic characteristics of gabion-stepped weirs. *J. Hydra. Engrg.*, ASCE, Vol. 134, No. 8, pp. 1147-1152.

Chinnarasri, C., Donjadee, S. and Israngkura, U. (2008). Hydraulic Characteristics of Gabion-Stepped Weirs. *Journal of Hydraulic Engineering*, *134*(August), 1147–1152. http://doi.org/10.1061/(ASCE)0733-9429(2008)134:8(1147).

Chow V. T. (1959). Open channel hydraulics. McGraw-Hill, New York, USA,680p.

Christodoulou, G. C. (1993). Energy dissipation on stepped spillways. *Journal of Hydraulic Engineering*, 119(5): 644-650.

Dong, Z. Y. and Lee, J. H. (2006). Numerical simulation of skimming flow over mild stepped channel*. *Journal of Hydrodynamics*, 18(3): 367-371.

Elviro, V. and Mateos, C. (1995). Spanish research into stepped spillways. *The International Journal on Hydropower and Dams*, September, pp. 61-65.

Falvey, H. T. (1990). *Cavitation in chutes and spillways*. Engineering Monograph 42, Bureau of Reclamation, Denver.

Falvey, H. T. (1990). *Cavitation in chutes and spillways*. In United States Bureau of Reclamation, editor, Engineering monographs 42. U.S. Dept. of the Interior, Denver, Colorado.

Felder, S. and Chanson, H. (2011). Energy Dissipation down a Stepped Spillway with Non- Uniform Step Heights. *Journal of Hydraulic Engineering*, Vol. 137, No. 11, pp. 1543-1548.

Felder, S. and Chanson, H. (2013). Air-water flow measurements in a flat slope pooled stepped waterway. *NRC Reseaech Press, 372*(October 2012), pp. 361–372.

Felder, S., and Chanson, H. (2013). Air entrainment and energy dissipation on porous pooled stepped spillways. In *International Workshop on Hydraulic Design of Low-Head Structures (IWLHS 2013)* (pp. 87-97). Bundesanstalt fur Wasserbau (BAW).

Fratino, U. and Piccinni, A. (2000). Dissipation Efficiency of Stepped Spillways, in H.-E. Minor and W. Hager, *Proceeding of the International Workshop on Hydraulics of Stepped Spillways*, IAHR,A.A. Balkema/Rottersam/Brookfield, Zurich, Switzerland.

Freeman, G. E., and Fischenich, J. C. (2000). *Gabions for streambank erosion control* (No. ERDC-EMRRP-SR-22). ARMY ENGINEER WATERWAYS EXPERIMENT STATION VICKSBURG MS ENGINEER RESEARCH AND DEVELOPMENT CENTER.

Frizell, K. H. (1992, February). Hydraulics of stepped spillways for RCC dams and dam rehabilitations. In *Roller Compacted Concrete III* (pp. 423-439). ASCE.

Frizell, K. H., and Mefford, B. W. (1991). Designing spillways to prevent cavitation damage. *Concrete International*, *13*(5), pp. 58-64.

Frizell, K. W., and Renna, F. M. (2011). Laboratory studies on the cavitation potential of stepped spillways. In *Proceedings of the 34th World Congress of the International Association for Hydro-Environment Research and Engineering: 33rd Hydrology and*

Water Resources Symposium and 10th Conference on Hydraulics in Water Engineering (p. 2420). Engineers Australia.

Frizell, K. W., Renna, F. M. and Matos, J. (2013). Cavitation Potential of Flow on Stepped Spillways. *Journal of Hydraulic Engineering*, *139*(6), pp. 630–636. http://doi.org/10.1061/(ASCE)HY.1943-7900.0000715.

Frizell, K.H. 1992. Hydraulics of Stepped Spillways for RCC Dams and Dam Rehabilitations. *Proc. 3rd Specialty Conf. on Roller Compacted Concrete*, ASCE, San Diego CA, USA, pp. 423-439.

Frizell, K.W., Renna, F. and Matos, J. (2015). Closure to "Cavitation potential of flow on stepped spillways". *Journal of Hydraulic Engineering*, 141(8):07015009.

Gonzalez, C. A. and Chanson, H. (2007), Experiment Measurements of Velocity and Pressure Distributions on a Large Broad-Crester Weir. *Flow Measurement and Instrumentation*, Vol.18, pp.107-113.

Gonzalez, C.A. (2005). *An Experimental Study of Free-Surface Aeration on Embankment Stepped Chutes*. Ph.D. thesis, Department of Civil Engineering, The University of Queensland, Brisbane, Australia, 240 pages.

Hager, W.H. and Schwalt, M. (1994). Broad crested weir. *Journal of Irrigation Drain Eng*; 120(1), pp.13-26.

Hirt, C.W. and Nichols, B. D. (1981). Volume of Fluid (VOF) method for the dynamics of free boundaries. *Journal of Computational Physics*, 39:pp. 201-225.

Hunt, S. L. and Kadavy, K. C. (2009). The Effect of the Step Height on Energy Dissipation in Stepped Spillways. *World Environmental and Water Resources Congress*. http://doi.org/10.1007/s13369-013-0900-y.

Hunt, S. L. and Kadavy, K. C. (2010). Energy dissipation on flat-sloped stepped spillways: Part 2. Downstream of the inception point. *Trans. ASABE* 53(1), pp. 111-118.

Hunt, S. L. and Kadavy, K. C. (2013). Inception Point for Embankment Dam Stepped Spillway. *Journal of Hydraulic Engineering*,139(1), pp.60-64.

Hunt, S.L. and Kadavy, K.C. (2011). Inception Point Relationship for Flat-slopped Stepped Spillways. *Journal of Hydraulic Engineering*, ASCE, Vol. 137, No. 2, pp. 262-266.

Husain, S. M. (2013). *Computational Investigation of Skimming Flow on Stepped Spillways Using The Smoothed Particle Hydrodynamics Method*. PhD thesis. Swansea University.

Husain, S.M., Muhammed, J.R., Karunarathna, H.U. and Reeve, D.E. (2013). Investigation of pressure variation over stepped spillways using smooth particle hydrodynamic. *Advances in Water Resources*, (66), pp.52-69.

James, C., Comnino, M. and Palmer, M.W. (1999). Effects of slope and step size on the hydraulics of stepped chutes. *J. South African Inst. Civil Engrg*., 41(2), pp. 1-6.

Jumaily, K. K. E. L., Khudair, M. and Lami, A. (2009). Study of Conveniency of Using Stepped Spillway in Roller Compacted Concrete Dams (RCCD). *Eng. and Tech. Journal*, *27*(16).

Kálal, Z., Jahoda, M. and Fořt, I. (2014). Modelling of the bubble size distribution in an aerated stirred tank: Theoretical and numerical comparison of different breakup models. *Chemical and Process Engineering - Inzynieria Chemiczna I Procesowa*, *35*(3), pp. 331–348. http://doi.org/10.2478/cpe-2014-0025.

Kálal, Z., Jahoda, M., and Fořt, I., (2014). CFD Prediction of gas-liquid flow in an aerated stirred vessel using the population balance model, *Chemical and Process Engineering*, 35 (1), pp. 55-73.

Karami, M. (2012). Investigation the effect of number of steps on energy dissipation of stepped spillways based on new design approach. *Life Science Journal*, *9*(4).

Kavianpour, M. R. and Masoumi, H. R. (2008). Technical Note : New Approach for Estimating of Energy Dissipation over Stepped Spillways. *International Journal of Civil Engineerng*, *6*(3), 2–9.

Keller, R. J., and Rastogi, A. K. (1977). Design chart for predicting critical point on spillways. *Journal of the Hydraulics Division*, *103*(12), 1417-1429.

Kells, J. A. (1994). Energy dissipation at a gabion weir with throughflow and overflow. In *Ann. Conference Can. Soc. Civ. Engrg., Winnipeg, Canada, June* (pp. 1-4).

Khademi, U. and Shirvani, M. (2014), Hydrodynamic modeling of flow over different type of stepped spillway. *Indian Journal of fundamental & applied life sciences*, Vol.4, pp. 1290-1296.

Kobus, H. (1984). 'Local air entrainment and detrainment.' *Proc., Symp. on Scale Effects in Modelling Hydraulic Structures*, H. Kobus, ed., Esslingen, Germany, Vol. 4.10, pp. 1–10.

Kositgittiwong, D. (2012). *Validation of Numerical Model of the Flow Behaviour through Smooth and Stepped Spillways using Large-scale Physical Model* (Degree of Doctor of Philosophy). King Mongkut's University of Technology Thonburi. http://doi.org/10.1007/s13398-014-0173-7.2

Kositgittiwong, D., Chinnarasri, C. and Julien, P. Y. (2013). Numerical simulation of flow velocity profiles along a stepped spillway. *Proceedings of the Institution of Mechanical Engineers, Part E: Journal of Process Mechanical Engineering*, *227*(4), pp. 327-335. http://doi.org/10.1177/0954408912472172.

Kothe, D.B., Mjolsness, R.C. and Torrey, M.D. (1991). *RIPPLE: A Computer Program for Incompressible Flows with Free Surface*. Rep. LA-12007-MS, Los Alamos National Laboratory, Los Alamos, U.S.

Lin, K., and Han, L. (2001). Stepped spillway for Dachaoshan RCC dam. In *SS2 Key Hydraulics Issues of Huge Water Projects, Proc. 29th IAHR Congress, Special Seminar, Beijing, China* (pp. 88-93).

Lin, P. and Liu, P.L.-F. (1998). A Numerical Study of Breaking Waves in the Surf Zone. *J. Fluid Mech.* 359, pp.239–264.

Lin, P. and Xu, W. (2006). NEWFLUME: a numerical water flume for two two-dimensional turbulent free surface flow. *Journal of Hydraulic Research*, 44(1), pp.60-64.

Liu, P. L. F., Lin, P., Chang, K. A., and Sakakiyama, T. (1999). Numerical modeling of wave interaction with porous structures. *Journal of waterway, port, coastal, and ocean engineering*, *125*(6), pp. 322-330.

Lobosco, R. J., Schulz, H. E., Bortoloti, A. and Oliveira, F. De. (2011). Numerical Simulation of Stepped Spillway Flow, 1–4.

Losada, I. J., Losada, M. A. and Martin, F. L. (1995). Experimental study of wave-induced flow in a porous structure. *Coast. Engng*., 26, pp. 77-89.

Losada, I. J., Silva, R. and Losada, M. A. (1996). 3-D non-breaking regular wave interaction with submerged breakwaters. *Coast. Engng*., 28, pp. 229-248.

Manes, C., D. Pokrajac, I. McEwan, and V. Nikora (2009). Turbulence structure of open channel flows over permeable and impermeable beds: A comparative study, *Phys. Fluids*, 21, 125109.

Matos, J. (2000). Hydraulic Design of Stepped Spillways over RCC Dams. In *Intl Workshop on Hydraulics of Stepped Spillways*, Zürich, Switzerland, H.E. Minor & W.H. Hager Editors, Balkema Publ., pp. 187-194.

Matos, J. (2000). Hydraulic design of stepped spillways over RCC dams. *Proc. of Intern. Workshop on Hydraulics of stepped spillways*, Zurich, Ed. Balkema, Rotterdam: 187-194.

Matos, J. (2000, March). Hydraulic design of stepped spillways over RCC dams. In *Intl Workshop on Hydraulics of Stepped Spillways* (pp. 187-194). Balkema Publ.

Mehdi, A. (1997). *The hydraulics of flow on stepped ogee-profile spillways*. PhD thesis. Faculty of Engineering, University of Ottawa, Ottawa, Canada.

Meireles, I. (2011). *Hydraulics of Stepped Chutes: Experimental-numerical-theoretical Study*, Ph.D. thesis, University of Aveiro, Aveiro, Portugal.

Meireles, I. and Matos, J. (2009). Skimming flow in the non-aerated region of stepped spillways over embankment dams. *Journal of Hydraulic Engeneering*,135(8),pp.685–9.

Mohammad Rezapour Tabari, M. and Tavakoli, S. (2016). Effects of Stepped Spillway Geometry on Flow Pattern and Energy Dissipation. *Arabian Journal for Science and Engineering*, *41*(4), pp. 1215–1224. http://doi.org/10.1007/s13369-015-1874-8.

Murillo-Munoz, R. E. (2006). *Experimental Study of the Development Flow Region On Stepped Chutes*. PhD Thesis. University of Manitoba, Canada.

Nezu, I. and Sanjou, M. (2011). PIV and PTV measurements in hydro-sciences with focus on turbulent open-channel flows. *Journal of Hydro-Environment Research*, *5*(4), pp. 215–230. http://doi.org/10.1016/j.jher.2011.05.004.

Nohani, E., Bahadoribirgani, B., Jalili, D., and Mirazizi, S. (2015). Study The Effect Of The Number Of Steps On Energy Dissipation Of Stepped Spillways In Non- Nappe Or Skimming Flow. *Journal of Novel Applied Sciences*, pp. 932-939.

Novak, P., Guinot, V., Jeffrey, A. and Reeve, D. (2010). *Hydraulic Modelling - An Introduction*. Spon Press, Abingdon, UK, 599p.

Novak, P., Mofatt, A.I.B., Nalluri, C. and Narayanan, R., (2001). *Hydraulic Structures (4st ed)*. London and NewYork: Taylor and Francis.

Ohtsu, I. and Yasuda, Y. (1997). Characteristics of Flow Conditions on Stepped Channels. In *Proceedings of 27th IAHR Congress*, 10-15 August, San Francisco, USA.

Ohtsu, I., and Yasuda, Y. (1997). Characteristics of flow conditions on stepped channels. In *Energy and Water: Sustainable Development* (pp. 583-588). ASCE.

Ohtsu, I., Yasuda, Y. and Takahashi, M. (2004). Flow Characteristics of Skimming Flows in Stepped Channels. *Journal of Hydraulic Engineering*, 130 (9), pp. 860-869.

Ohyama, T. and Nadaoka, K. (1991). Development of a Numerical Wave Tank for Analysis of Nonlinear and IrregularWave Field. *Fluid Dyn. Res*. 8, pp. 231-251.

Patil, L. G. and Jadhav, S. (2017). Performance Evaluation of Stepped Spillway under Nappe Flow Condition. *Iarjset*, *4*(1), pp. 111–114. http://doi.org/10.17148/IARJSET.2017.4126.

Pegram, G., Officer, A. and Mottram, S. (1999). Hydraulics of skimming flow on modelled stepped spillways. *Journal of Hydraulic Engineering,* ASCE, 125(4):361-368.

Peruginelli, A., and Pagliara, S. (2000). Energy Dissipation Comparison among Stepped Channel, Drop and Ramp Structures. *Proc. Intl Workshop on Hydraulics of Stepped Spillways*, Zürich, Switzerland, Balkema Publ., pp. 111-118.

Peterka, A. J. (1953). The effect of entrained air on cavitation pitting. *In Proceedings of the 5th IAHR/ASCE congress*, Vol. Joint meeting paper, Minneapolis, USA, pp.507-518.

Peyras, L. A., Royet, P., and Degoutte, G. (1992). Flow and energy dissipation over stepped gabion weirs. *Journal of Hydraulic Engineering*, *118*(5), pp. 707-717.

Pinto, N. D. S. (1984). Model evaluation of aerators in shooting flow. *Scale effects in modelling hydraulic structures*, *4*, 1-6.

Rajaratnam, N. (1990). Skimming flow in stepped spillways. *Journal of Hydraulic Engineering*, *116*(4), pp. 587-591.

Rassaei, M. and Rahbar, S. (2014). Study and comparison of the rate of energy dissipation in stepped overflows before and after hydraulic jump using laboratory model. *Journal of Engineering (IOSRJEN)*, *4*(6), pp. 30-33.

Rutschmann, P. (1988). 'Belüftung Einbauten in Schussrinnen.' PhD thesis, VAW, ETH Zurich, Switzerland (in German).

Salmasi, F., Chamani, M. R. and Zadeh, D. F. (2012). Stepped Gabion Spillways With Low Heights. *IJST, Transactions of Civil Engineering*, *36*, pp. 253-264.

Salmasi, F., Chamani, M. R., and Zadeh, D. F. (2012). Experimental study of energy dissipation over stepped gabion spillways with low heights. *Iranian Journal of Science and Technology. Transactions of Civil Engineering*, *36*(C2), 253.

Salmasi, F., Sattari, M. and Pal, M. (2012). Application of data mining on evaluation of energy dissipation over low gabion-stepped weir. *Turk J Agric For*, 36, pp.95-106.

Sanches Juny, M. S., Pomares, J., and Dolz, J. (2000). Pressure field in skimming flow over a stepped spillway. In *Proceedings of the International Workshop on Hydraulics of Stepped Spillways, Zurich. Edited by HE Minor and WH Hager. AA Balkema, Rotterdam* (pp. 137-146).

Sanches Juny, M., Pomares, J. and Dolz, J. (2000). Pressure field in skimming flow over a stepped spillway. *... on Hydraulics of Stepped Spillways, ...*, 1–9. Retrieved from http://www.flumen.upc.edu/admin/files/63.pdf

Sarfaraz, M., Attari, J. and Pfister, M. (2012). Numerical Computation of Inception Point Location for Steeply Sloping Stepped Spillways. *In 9th International Congress on Civil Engineering*. Isfahan University of Technology (IUT), Isfahan, Iran.

Schlichting, H. (1979), Boundary Layer Theory, McGraw-Hill. New York.

Shafai-Bejestan, M., and Kazemi-Nasaban, G. (2011). Experimental Study on Gabion Stepped Spillway. In *Experimental Methods in Hydraulic Research* (pp. 267-274). Springer Berlin Heidelberg.

Shoja, F., Nikpour, M. and Sadeghi, H. (2013). Determination of Energy Dissipation in Stepped Spillways Using Finite Element and Finite Volume Methods. *Journal of Civil Engineering and Urbanism*, 3(4), pp.150-155.

Smart, G. M., Duncan, M. J. and Walsh, J. M. (2002). Relatively Rough Flow Resistance Equations. *Journal of Hydraulic Engineering*, 128(6), pp. 568-578. http://doi.org/10.1061/(ASCE)0733-9429(2002)128:6(568).

Sorensen, R.M. (1985). Stepped spillway hydraulic model investigation. *J. Hydraulic Eng.*, ASCE;111(12):1461-72.

Speerli, J. (1999). 'Strömungsprozesse in Grundablass Stollen.' PhD thesis, VAW, ETH Zurich, Switzerland (in German).

Stephenson, D. (1979). Gabion energy dissipators. *13th International Congress on Large Dams*, New Delhi, India, Q. 50, R. 3, pp. 33-43.

Stephenson, D. (1979). Rock fill in hydraulic engineering. Elsevier scientific publishing Co., Oxford, UK. 215P.

Tabbara, M., Chatila, J. and Awwad, R. (2005). Computational simulation of flow over stepped spillways. *Computers & Structures*, 83(27), pp. 2215-2224. doi:10.1016/j.compstruc.2005.04.005.

Te Chow, V. (1959). *Open channel hydraulics*. McGraw-Hill Book Company, Inc; New York.

Toombes, A. (2002). *Experimental Study of Air-Water Flow Properties on Low Gradient Stepped Cascades*. PhD thesis. Faculty of Engineering, Physical Sciences and Architecture. University of Queensland, Brisbane, Australia.

Tozzi, M. J. (1994). Residual energy in stepped spillways. *International water power and dam construction*, *46*(5), 32-34.

Unami, K., Kawachi, T., Babar, M. M. and Itagaki, H. (1999). Two-dimensional numerical model of spillway flow. *Journal of Hydraulic Engineering*, ASCE, 125(4), pp. 369-375.

Vischer, D., Volkart, P., and Sigenthaler, A. (1982). Hydraulic modelling of air slots in open chute spillways. In *Int. Conf. on Hydraulic Modelling, BHRA Fluid Engineering, Coventry, England*.

Vosoughifar, H. R., Dolatshah, A., Shokouhi, S. K. S. and Nezhad, S. R. H. (2013). Evaluation of Fluid Flow over Stepped Spillways Using the Finite Volume Method as a Novel Approach. *Journal of Mechanical Engineering*, *59*, pp. 301-310. http://doi.org/10.5545/sv-jme.2012.669.

Vosoughifar, H., Dolatshah, A., Shokouhi, S. and Nezhad, S. (2013). Evaluation of Fluid Flow over Stepped Spillways Using the Finite Volume Method as a Novel Approach. Strojniški vestnik. *Journal of Mechanical Engineering*, 59(5), pp. 301-310.

Wang, H., Murzyn, F. and Chanson, H. (2014). Total pressure fluctuations and two-phase flow turbulence in hydraulic jumps. *Experiments in Fluids*, Vol. 55, No. 11, Paper 1847, 16 pages (DOI: 10.1007/s00348-014-1847-9).

Wang, S. Y., Hou, D. M. and Wang, C. H. (2012). Aerator of stepped chute in Murum Hydropower Station. *In 2012 International Conference on Modern Hydraulic Engineering*, 28, pp. 803-807, Nanjing, China. Elsevier Procedia.

Webber, N., 1979. *Fluid mechanics for civil engineers.* London: Chapman and Hall.

WOOD, I.R., ACKERS, P. and LOVELESS, J. (1983). General Method for Critical Point on Spillways. *Journal of Hydraulic Engineering*, ASCE, Vol. 109, No. 2, pp. 308-312.

Wüthrich, D. and Chanson, H. (2014). Hydraulics, Air Entrainment, and Energy Dissipation on a Gabion Stepped Weir. *Journal of Hydraulic Engineering*, *140*(9), 04014046. doi:10.1061/(asce)hy.1943-7900.0000919.

Yasuda, Y. and Ohtsu, I. (1999). Flow resistance of skimming flow in stepped channels. In *Proc. 28th IAHR Congress*. Graz, Austria.

Yasuda, Y. and Othsu. I. (1999). Flow resistance in skimming flow in stepped channels. In *Proceedings, 28th IAHR congress*, Graz, Australia.

Yasuda, Y. Takahashi, M. and Ohtsu, I. (2001). Energy Dissipation of Skimming Flows on Stepped-channel Chutes. In *Proceedings of the 29th IAHR Congress*, 16-21 September, Beijing, China.

Yazdandoost, F., and Attari, J. (Eds.). (2004). *Hydraulics of Dams and River Structures: Proceedings of the International Conference, Tehran, Iran, 26-28 April 2004*. CRC Press.

Zhang, G. (2017). *Free-Surface Aeration, Turbulence, and Energy Dissipation on Stepped Chutes with Triangular Steps, Chamfered Steps, and partially Blocked Step Cavities*. PhD thesis. The University of Queensland.

Zhang, G. and Chanson, H. (2016a). Hydraulics of the developing flow region of stepped spillways. Part I: physical modelling and boundary layer development. *Journal of Hydraulic Engineering*, ASCE, Vol. 142, No. 7, 8 pages (DOI: 10.1061/(ASCE)HY.1943- 7900.0001138)

Zhang, G., and Chanson, H. (2014). Step cavity and gabion aeration on a gabion stepped spillway. *Proc. of 5th IAHR International Symposium on Hydraulic Structures*, Brisbane, Australia, 25-27 June 2014, 8 pages.

Zhang, G., and Chanson, H. (2014). Step cavity and gabion aeration on a gabion stepped spillway. In *11th National Conference on Hydraulics in Civil Engineering & 5th International Symposium on Hydraulic Structures: Hydraulic Structures and Society-Engineering Challenges and Extremes* (p. 207). Engineers Australia.

Zhang, G., and Chanson, H. (2014). Two-phase flow on a gabion stepped spillway: cavity and seepage air-water motion. *Proc. of 19th Australasian Fluid Mechanics Conference*, Melbourne, Australia, Paper 119, 4 pages.

Zhang, G., and Chanson, H. (2016b). Gabion stepped spillway: interactions between free-surface, cavity and seepage flows. *Journal of Hydraulic Engineering*, ASCE, Vol. 142, No. 5, 5 pages (DOI: 10.1061/(ASCE)HY.1943-7900.0001120)

Zhang, G., Chanson, H. and Wang, H. (2016). Total pressure fluctuations and two-phase flow turbulence in self-aerated stepped chute flows. *Flow Measurement and Instrumentation*, Vol. 51, pp. 8-20 (DOI: 10.1016/j.flowmeasinst.2016.08.007)

Zindovic, B., Savic, L., Kapor, R. and Mladenovic, N. (2014). Stepped spillway flow: Comparison of numerical and scale models. *FME Transaction*, *42*(3), pp. 218-223. http://doi.org/10.5937/fmet1403218z.

Zuhaira, A.A., Karunarathna, H.U. and Reeve, D.E. (2017). Numerical Investigation of Step Dimensions Impact over Gabion Stepped Spillways. In *Proceedings of the 37th IAHR World Congress*,13-18 August, Kuala Lumpur, Malaysia.